Universidade de Lisboa

Faculdade de Ciências

Departamento de Química e Bioquímica

Molecular characterisation of the poorly differentiated and undifferentiated thyroid carcinomas using genome-wide approaches

Jaime Miguel Gomes Pita

Doutoramento em Bioquímica

Especialidade em Genética Molecular

2013

Universidade de Lisboa

Faculdade de Ciências

Departamento de Química e Bioquímica

Molecular characterisation of the poorly differentiated and undifferentiated thyroid carcinomas using genome-wide approaches

Jaime Miguel Gomes Pita

Tese orientada pelo

Professor Doutor Valeriano Alberto Leite

(Instituto Português de Oncologia de Lisboa, Francisco Gentil)

e Professora Doutora Maria Luísa Cyrne

(Faculdade de Ciências da Universidade de Lisboa)

especialmente elaborada para a obtenção do grau de doutor

em Bioquímica, especialidade em Genética Molecular

2013

A presente dissertação foi redigida de acordo com o disposto no artigo 45.º do Despacho n.º 4624/2012 do Diário da República 2.ª série - N.º 65 - 30 de Março de 2012

*** * ***

As opiniões expressas nesta publicação são da exclusiva responsabilidade do seu autor.

(...)

Eles não sabem que o sonho
é vinho, é espuma, é fermento,
bichinho álacre e sedento,
de focinho pontiagudo,
que fossa através de tudo
num perpétuo movimento.

(...)

Eles não sabem, nem sonham,
que o sonho comanda a vida.
Que sempre que um homem sonha
o mundo pula e avança
como bola colorida
entre as mãos de uma criança.

António Gedeão, *Pedra Filosofal in* '*Movimento Perpétuo*' (1956)

'The deeper we search the more we find there is to know,
and as long as human life exists, I believe it will always be so.'

Albert Einstein

Agradecimentos

Na presente tese de doutoramento são apresentados os resultados do trabalho de investigação realizado no Grupo de Endocrinologia Molecular da Unidade de Investigação de Patobiologia Molecular (UIPM) no Instituto Português de Oncologia de Lisboa, Francisco Gentil (IPOLFG) entre Janeiro de 2009 e Dezembro de 2012, sob a orientação do Professor Doutor Valeriano Alberto Leite e co-orientação da Doutora Branca Maria Cavaco. Entre Janeiro de 2011 e Abril de 2012, o trabalho foi realizado no laboratório de Endocrinologia do "Institut de Recherche Interdisciplinaire en Biologie Humaine et Moléculaire" (IRIBHM) na "Université Libre de Bruxelles", sob a co-orientação do Professor Doutor Jacques Emile Dumont. O trabalho esteve sob a orientação interna da Professora Doutora Maria Luísa Cyrne da Faculdade de Ciências da Universidade de Lisboa.

O trabalho de investigação teve o seu início durante o estágio curricular em Outubro de 2006, ao qual seguiu-se uma bolsa de investigação científica e o projecto de doutoramento. Assim, esta dissertação é fruto da colaboração e empenho de variadíssimas pessoas ao longo destes anos, as quais dedico o mais profundo apreço e gratidão.

Em primeiro lugar, agradeço ao Professor Doutor Valeriano Leite e à Doutora Branca Cavaco pelo acolhimento no seu grupo e pela oportunidade para despertar e contribuir para a Ciência. Agradeço a ambos, toda a contínua confiança e consideração que depuseram em mim. Ainda ao Doutor Valeriano, pelo estímulo científico, por toda a dedicação ao meu trabalho e pela amizade, bem como, pela oportunidade no laboratório do Professor Dumont. À Doutora Branca, um agradecimento especial pelo apoio, dedicação e disponibilidade constantes na minha aprendizagem e no rigor do trabalho científico. Também por toda a sua amizade, conhecimento científico, cultural e gastronómico, que com prazer partilhou.

À Professora Doutora Luísa Cyrne agradeço ter aceite a orientação do Doutoramento e pelo apoio e interesse despendidos para a concretização deste.

Ao Professor Dumont, por quem tenho grande admiração e respeito, por me ter recebido no seu grupo e partilhado a sua sabedoria, por todo o seu apoio, jovialidade e por ser um exemplo de dedicação à Ciência e à Endocrinologia.

A todos os membros que pertencem e aos que já passaram pelo grupo de Endocrinologia e pelos vários grupos de trabalho do UIPM, os quais me acompanharam e contribuíram para o agradável e simpático ambiente de trabalho. Ao antigo director do UIPM, o Doutor Sérgio Dias, por ter proporcionado todas as condições de trabalho necessárias, pelos conselhos, disponibilidade e simpatia. À Ana Banito, por me ter iniciado no mundo dos "microarrays", por todo o apoio e amizade. À Inês Figueiredo, por todo o árduo trabalho e dedicação, sem os quais, esta tese perderia grande parte do seu valor. Agradeço também todo o apoio, amizade e simpatia e desejo-lhe muito sucesso na vida

profissional. À Doutora Lúcia Roque do grupo de Citogenética, pela constante simpatia e por facultar as 'preciosas' linhas celulares. Às quatro meninas LHOs, que fizeram do nosso laboratório, um lugar sempre limpo, organizado, e claro, cheio de muita boa disposição. À Fátima e à Joaquina, pela amabilidade e carinho que sempre deram e por manterem o laboratório limpo e organizado. Ao Pedro Baptista, à Carla Espadinha, à Margarida Moura e à Ana Luísa Silva, pela vossa amizade e por estarem sempre prontos a ajudar. Em especial, às futuras Doutoras Rute Tomaz e "Jo" Costa, à Rita Domingues, à "maninha" Sofia Fragoso e à Cristiana Teixeira pela grande amizade e carinho que partilhamos dentro e fora do laboratório, bem como pela paciência para me "aturar".

Agradeço ainda aos membros dos serviços do IPOLFG de Endocrinologia, de Cirurgia de Cabeça e Pescoço e de Anatomia Patológica, pela identificação, recolha, conservação e cedência dos casos clínicos, sem os quais, este trabalho de investigação não seria possível.

Aos membros do grupo de Endocrinologia do IRIBHM em Bruxelas, agradeço o caloroso acolhimento e a simpatia que todos ofereceram para me sentir em casa. Infelizmente, não poderei mencionar todos individualmente. À Professora Carine Maenhaut, investigadora principal do grupo, por todo o apoio e simpatia durante o tempo em que estive em Bruxelas. À Post-doc Soazig Le Pennec, que igualmente longe de casa partilhou o mesmo sentimento de saudade, agradeço toda a amizade, companheirismo e ajuda. Um agradecimento em especial, ao Sébastien Floor, pelo seu árduo trabalho e dedicação ao nosso projecto em conjunto, bem como, desde o primeiro momento, ter sido um verdadeiro amigo, sempre bem-disposto e altruísta.

Este trabalho não seria possível sem o imprescindível apoio financeiro da Fundação Calouste Gulbenkian, do Centro de Estudos de Doenças Crónicas (CEDOC) e da Sociedade Portuguesa de Endocrinologia, Diabetes e Metabolismo (SPEDM), as quais quero agradecer. Ainda, à Fundação para a Ciência e Tecnologia por me ter concedido a bolsa de Doutoramento (SFRH/BD/46096/2008).

Agradeço às minhas sempre grandes amigas de Faculdade "Burrólicas", Andreia Freire, Rita Carilho, Sandra Brasil e Catarina Ramos, que apesar da vida nos ter separado, continuamos a nos encontrar e a nutrir um grande carinho.

Não posso deixar de agradecer à minha família. À minha madrinha Rosália por toda a esperança que deposita em mim, à minha mãe por acreditar sempre que serei o melhor, e à minha avó que apesar de não entender aquilo que faço, possui um orgulho inabalável em mim.

Por último, quero agradecer à minha futura esposa, pelo terno amor, carinho e paciência que me dedicou e continua a oferecer todos os dias. Obrigado por todo o apoio incondicional e por ter sempre acreditado em mim. Espero poder retribuir todo o afecto que dela recebo.

Dedico esta tese a quem encaminhou a minha vida, o meu pai...

Acknowledgements

This thesis presents the results of the experimental work performed at the Molecular Endocrinology lab in the Unidade de Investigação de Patobiologia Molecular (UIPM) at the Instituto Português de Oncologia de Lisboa, Francisco Gentil (IPOLFG), from January 2009 to December 2012, under the supervison of Professor Valeriano Alberto Leite and co-supervision of Dr. Branca Maria Cavaco. Between January 2011 and April 2012, the research work was undertaken at the Endocrinology lab in the "Institut de Recherche Interdisciplinaire en Biologie Humaine et Moléculaire" (IRIBHM) at the "Université Libre de Bruxelles", under the co-supervision of Professor Jacques Emile Dumont. The work was supervised by Professor Maria Luísa Cyrne from the Faculty of Science of the Universidade de Lisboa.

The research work was initiated during the undergraduate internship in October 2006, followed by a research fellowship and the PhD project. This thesis is thus, the result of the collaboration of several people, along these years, who I devote all my gratitude.

Firstly, I thank Professor Valeriano Leite and Dr. Branca Cavaco for accepting me at their laboratory and for the opportunity to growth and contribute to Science. I am grateful to both, for all the confidence and consideration they have placed in me. To Professor Valeriano, for all the knowledge, support and friendship, as well as, for arranging the opportunity to be at Professor Dumont's laboratory. To Dr. Branca, I express my deep gratitude for all the support, guidance and availability during my thesis. Also, for all the friendship and for the scientific, cultural and gastronomic knowledge that enthusiastically shared.

To Professor Luísa Cyrne, for accepting to supervise my PhD project and for all the support and interest in my work.

To Professor Dumont, who I deeply admire and respect, for receiving me in his research group and for sharing his wisdom, for all his support, joviality and for being an example of dedication to Science and Endocrinology.

To all former and current members of the Endocrinology group and research groups of UIPM, who contributed to the pleasant and friendly work environment. To Dr. Sérgio Dias, former director of UIPM, for providing all the work conditions, for the advices, availability and kindness. To Ana Banito, for introducing me to the microarray's world, for all the help and friendship. To Inês Figueiredo, for all the hardworking and dedication. Her work was of crucial value to this thesis. I also thank all her friendship and kindness, and wish her a huge success in her career. To Dr. Lúcia Roque of the Cytogenetic group, for her gentleness and for providing the cell lines. To the Haematology group that always maintained our laboratory, a clean, organized and cheerful place. To Fátima e Joaquina for caring and maintaining the institute in proper conditions. To Pedro Baptista, Carla

Espadinha, Margarida Moura and Ana Luísa Silva, for your friendship and assistance. To Rute Tomaz, Joana Costa, Rita Domingues, Sofia Fragoso and Cristiana Teixeira, a special appreciation for the deep friendship that we share inside and outside the lab, and also, for putting up with me.

I would like to acknowledge all the members of the Endocrinology, Surgery and Pathology services from IPOLFG, for the identification, collection, preservation and providing of the clinical cases, which were essential for this research work.

To the members of the Endocrinology group at IRIBHM in Brussels, I am sincerely grateful for your warm welcome and all your kindness. Please, forgive me for not being able to mention each and every one of you. I thank Professor Carine Maenhaut, Principal Investigator of the group, for the huge support and kindness during my stay in Brussels. To Postdoc Soazig Le Pennec, who was also far from home, I thank her for all the friendship, help and support she gave me. A special gratitude to my colleague Sébastien Floor, for his work and devotion to our research project, as well as, for being from the first moment, a truly great friend, always joyful and generous.

I would like to gratefully acknowledge the Calouste Gulbenkian Foundation, the Chronic Disease Research Centre and the Portuguese Society of Endocrinology, Diabetes and Metabolism for the financial support. Also, the Fundação para a Ciência e Tecnologia for awarding me, a PhD fellowship (SFRH/BD/46096/2008).

I thank to my dear friends from the time of faculty, who have taken separate ways, but still, find time to meet each other again.

I must also express my gratitude to my family. To my godmother for all the hope that she has in me, to my mother for always believing in my capabilities, and to my grandmother for all her proudness despite not understanding what I do.

Last but not least, I thank to my future wife, all the love, tenderness and patience that she has given and continues to give me. Also for all the unconditional support and for always believing in me.

This thesis is dedicated to the one who outlined my life, my father…

Sumário

O cancro da tiróide constitui a neoplasia mais comum do sistema endócrino (van der Zwan *et al.*, 2012), representando nos homens e nas mulheres respectivamente, cerca de 1 e 3% dos casos de cancro, estimados em Portugal (Ferlay *et al.*, 2010a) e no mundo (Ferlay *et al.*, 2010b).

Os tumores com origem no epitélio folicular representam 90 a 95% das neoplasias da tiróide (Nikiforov and Nikiforova, 2011), e de acordo com as características morfológicas e clínicas, os tumores foliculares malignos são subdivididos em carcinomas bem-diferenciados (WDTC), carcinomas pouco diferenciados (PDTC) e carcinomas indiferenciados ou anaplásicos (ATC). Os tumores foliculares da tiróide representam assim, um modelo clássico do processo tumoral pelo qual uma célula epitelial possui potencial para originar diferentes tipos de tumores, cada um com características patológicas distintas.

Nos WDTC incluem-se os carcinomas papilares (PTC) e os carcinomas foliculares (FTC), sendo os PTC os mais frequentes, representando cerca de 80 a 90% dos casos (Kondo *et al.*, 2006; Nikiforov and Nikiforova, 2011). Os WDTC são, em geral, tratados eficazmente com cirurgia e iodo radioactivo, e cerca de 90% dos doentes com menos de 45 anos ficam curados (DeLellis *et al.*, 2004). Por outro lado, os PDTC e os ATC apresentam escassa diferenciação folicular e comportam-se de forma altamente agressiva. Em particular, os ATC apresentam uma progressão clínica muito rápida, e em geral, manifestam no diagnóstico inicial, uma extensa invasão dos tecidos adjacentes e metástases à distância, nomeadamente pulmonares, ósseas ou cerebrais (Muro-Cacho and Ku, 2000; DeLellis *et al.*, 2004). Apesar dos ATC contribuírem apenas para 1 a 2% dos tumores da tiróide (Kondo *et al.*, 2006; Nikiforov and Nikiforova, 2011), são responsáveis por 14 a 50% das mortes relacionadas com cancro da tiróide. Estão associados a uma sobrevivência média de 3 a 5 meses (DeLellis *et al.*, 2004; Nagaiah *et al.*, 2011), representando assim uma das neoplasias mais letais. Os PDTC apresentam características morfológicas e clínicas intermédias entre os WDTC e ATC (Lam *et al.*, 2000; Volante *et al.*, 2004; Sanders *et al.*, 2007; Nambiar *et al.*, 2011). A taxa média de sobrevida aos 5 anos, dos doentes com PDTC é de cerca de 50% e a mortalidade deve-se sobretudo a metástases pulmonares e ósseas (DeLellis *et al.*, 2004; Nambiar *et al.*, 2011). Os PDTC e em especial, os ATC, são refractários às formas convencionais de tratamento (cirurgia e iodo radioactivo). Na maioria dos casos, a ressecção dos tumores não é viável e a quimio- e a radioterapia demonstram um efeito reduzido na sobrevivência dos doentes (Sanders *et al.*, 2007; Smallridge *et al.*, 2009; Abate and Smallridge, 2011). Assim, é de

extrema importância a implementação de novas modalidades terapêuticas que sejam eficazes nestas neoplasias.

A transformação do epitélio folicular da tiróide resulta tipicamente de alterações genéticas que envolvem componentes das vias de sinalização MAPK-ERK e PI3K-AKT, essenciais na regulação da proliferação e homeostasia celular. Nos PTC detectam-se, de forma mutuamente exclusiva (Kimura *et al.*, 2003; Nikiforov and Nikiforova, 2011), mutações activantes nos genes que codificam a cinase de serina/treonina BRAF e as GTPases H-, K- e NRAS, sendo a mutação do gene *BRAF* a alteração mais frequente (Kimura *et al.*, 2003; Fugazzola *et al.*, 2006). Entre os WDTC, as mutações nos genes *RAS* estão associadas a tumores com morfologia folicular, sendo detectadas na variante folicular dos PTC e em FTC (Vasko *et al.*, 2003; Zhu *et al.*, 2003; Di Cristofaro *et al.*, 2006).

As características clínicas e histológicas dos carcinomas da tiróide sugerem uma contínua perda da diferenciação celular (um processo de desdiferenciação) pelo qual ocorre um aumento progressivo da agressividade. Considera-se que os PDTC e ATC possam surgir directamente a partir da célula folicular ou derivarem de tumores pré-existentes. Este último modelo é apoiado pela frequente detecção de áreas bem-diferenciadas em casos de PDTC e ATC (Nikiforova *et al.*, 2003a; DeLellis *et al.*, 2004; Quiros *et al.*, 2005; Takano *et al.*, 2007a; Wang *et al.*, 2007a; Santarpia *et al.*, 2008; Ricarte-Filho *et al.*, 2009). Várias evidências moleculares sugerem, de igual modo, que os WDTC podem progredir para PDTC e para ATC. A detecção dos oncogenes *RAS* e *BRAF* em casos de PDTC e ATC (Garcia-Rostan *et al.*, 2003; Smallridge *et al.*, 2009; Volante *et al.*, 2009) e a presença destas mutações em componentes diferenciadas e indiferenciadas de um mesmo tumor (Oyama *et al.*, 1995; Nikiforova *et al.*, 2003a; Begum *et al.*, 2004; Cohen *et al.*, 2004; Takano *et al.*, 2007a; Costa *et al.*, 2008; Schwertheim *et al.*, 2009), sugerem um processo de progressão a partir de WDTC. Além disso, estas mutações podem coexistir com alterações no gene supressor de tumores *TP53* (Lam *et al*., 2000; Quiros *et al*., 2005; Wang *et al*., 2007), no gene *CTNNB1* que codifica o efector β-catenina da via WNT (Garcia-Rostan *et al*., 2001) e no *PIK3CA* que codifica a subunidade catalítica da cinase PI3K da via PI3K-AKT (Lam *et al.*, 2000; Garcia-Rostan *et al.*, 2001; Garcia-Rostan *et al.*, 2005; Quiros *et al.*, 2005; Hou *et al.*, 2007a; Wang *et al.*, 2007a; Liu *et al.*, 2008; Santarpia *et al.*, 2008; Ricarte-Filho *et al.*, 2009). Estas alterações, que são detectadas exclusivamente, ou com maior frequência em PDTC e ATC, demonstram, assim, a acumulação e a cooperação de eventos específicos durante a desdiferenciação.

Os microRNA (miRNA), que com frequência se encontram desregulados no processo oncogénico (Calin and Croce, 2006), podem apresentar padrões de expressão anómalos nos tumores da tiróide (Nikiforova *et al.*, 2009). Cada um destes RNA, que são não-codificantes, pode estar envolvido na regulação de centenas de transcriptos-alvo, mediando a sua degradação ou a repressão da translacção proteica (Carthew and Sontheimer, 2009). Assim, os miRNA podem constituir potenciais agentes terapêuticos, na medida em que afectam simultaneamente várias vias de sinalização, impedindo os mecanismos compensatórios das células tumorais (Lujambio and Lowe, 2012). Os níveis de expressão dos miRNA numa célula são o resultado tanto da sua biossíntese como da sua degradação. Enquanto que a via de biossíntese se encontra bem caracterizada (Cullen, 2006), o processo de degradação e o tempo de semi-vida dos miRNA, são relativamente desconhecidos. A determinação da estabilidade e a caracterização dos factores que influenciam a degradação destas moléculas, representam, portanto, áreas importantes para a investigação da potencial utilidade terapêutica dos miRNA.

A análise de expressão génica global no campo da oncologia demonstrou ser vantajosa no prognóstico e classificação dos tumores, assim como, na identificação de potenciais alvos terapêuticos (Chung *et al.*, 2002; Nevins and Potti, 2007). Esta metodologia tem sido extensivamente utilizada na tiróide, especialmente no estudo dos diferentes subtipos de WDTC (Griffith *et al.*, 2006; Riesco-Eizaguirre and Santisteban, 2007). No caso dos PDTC e ATC, a análise da expressão génica global em tumores primários encontra-se restrita a poucos estudos. A comparação dos perfis de expressão de ATC e PDTC com WDTC e tecido tiroideu normal (TN) permitiu identificar assinaturas moleculares relacionadas com a proliferação e ciclo celular, instabilidade cromossómica, adesão, motilidade celular e perda da função tiróidea (Salvatore *et al.*, 2007; Montero-Conde *et al.*, 2008; Hébrant *et al.*, 2012).

Com o objectivo de elucidar os mecanismos envolvidos na progressão e na agressividade dos PDTC e ATC e identificar novos alvos para o tratamento destes tumores, compararam-se os perfis de expressão génica globais de amostras de TN e de WDTC com PDTC e ATC. Tendo em conta os resultados obtidos, procedeu-se a uma extensa pesquisa de mutações em genes envolvidos em processos celulares desregulados nos PDTC e ATC, e correlacionaram-se os dados obtidos com os aspectos clínico-patológicos dos doentes. Por fim, o estudo do turnover de RNA através da marcação com um análogo da uridina (4-tiouridina), foi usado para determinar os tempos de semi-vida de miRNA numa linha celular de carcinoma desdiferenciado da tiróide.

A comparação da expressão génica global entre 5 PDTC, 19 WDTC e 3 TN, e entre 5 ATC e 4 TN revelou que os PDTC e ATC exibem, em comum, genes desregulados com

expressão aumentada associados ao ciclo celular, proliferação celular, segregação cromossómica e ao "checkpoint" do fuso mitótico, enquanto que, os genes sub-expressos estavam principalmente relacionados com a adesão celular. Os ATC apresentaram como eventos específicos (ausentes na análise dos PDTC), o aumento de expressão de componentes da via do TGF-β e a sub-expressão de genes associados à função e metabolismo tiroideu, à morfologia epitelial e às junções celulares. A análise não-supervisionada da semelhança génica entre as amostras e a correlação com a pesquisa de alterações do *RAS* e *BRAF*, demonstrou que as variantes foliculares de PTC são os precursores mais prováveis dos PDTC com mutação no gene *RAS*. Por outro lado, a comparação dos genes diferencialmente expressos em cada tipo de tumor em relação ao tecido normal, permitiu avaliar que os ATC partilhavam maior número de genes com os PTC clássicos do que com os restantes tumores, o qual suporta a provável origem dos ATC a partir dos PTC clássicos. A análise dos genes diferencialmente expressos entre cada tipo de tumor e o TN revelou que 307 de 494 (60%) dos genes eram sobre-expressos em PTC, enquanto que 137 de 171 (80%) estavam sub-expressos em FTC, 92 de 107 (86%) estavam sub-expressos em PDTC e 983 de 1333 (74%) estavam com expressão diminuída nos ATC.

Validaram-se por RT-PCR quantitativo em grupos independentes de tumores, o gene *UHRF1*, associado à proliferação e identificado como sobre-expressos nos PDTC em relação ao tecido normal e o gene *ITIH5*, relacionado com a adesão celular e sub-expresso nos PDTC em relação ao tecido normal. Adicionalmente, caracterizou-se o gene *CDKN3*, o qual codifica um inibidor das cinases dependentes de ciclina (CDK) que foi identificado, na análise de expressão, como o gene mais sobre-expresso nos ATC, tendo-se confirmado a sua expressão aumentada em ATC, bem como em PDTC relativamente ao TN. De acordo com a sua função supressora de tumor, observou-se uma expressão significativa de formas de splicing aberrantes apenas nos ATC. Devido ao papel importante que a activação da via do TGF-β apresenta na promoção da transição epitelial-mesenquimal (EMT) (Huber *et al.*, 2005), validou-se a expressão do gene *SNAI2*, regulador do EMT, e cuja expressão é induzida por esta via (Xu *et al.*, 2009). Confirmou-se assim, a sobre-expressão específica deste gene em ATC.

Tendo em conta os resultados obtidos nos estudos de expressão génica global dos PDTC e ATC, procedeu-se a uma extensa análise mutacional em genes envolvidos na regulação do ciclo celular como os inibidores de CDK [*CDKN1A* ($p21^{CIP1}$), *CDKN1B* ($p27^{KIP1}$), *CDKN2A* ($p14^{ARF}$, $p16^{INK4A}$), *CDKN2B* ($p15^{INK4B}$) e *CDKN2C* ($p18^{INK4C}$)], genes envolvidos na adesão celular (*AXIN1*, que codifica um regulador negativo da via WNT) e genes cujo envolvimento

nestes tumores fora previamente descrito (*H-*, *K-*, *NRAS*, *BRAF*, *PIK3CA*, *TP53* e *CTNNB1*). A pesquisa de alterações patogénicas em 26 ATC e 22 PDTC revelou que as mutações dos genes *TP53* (presentes em 42% dos ATC e 27% dos PDTC) e *RAS* (presentes em 31% dos ATC e 18% dos PDTC) são as mais frequentes nestes tumores. As mutações nestes genes apresentaram mútua exclusividade (P=0,0354) e a sua presença estava associada a um menor tempo de sobrevida global dos doentes com PDTC e ATC (P=0,0383). No caso dos inibidores de CDK identificou-se, pela primeira vez, que alterações nos genes *CDKN2A* e *CDKN2B* podem estar envolvidos em cerca de 25% dos PDTC. Por outro lado, as mutações previamente descritas como frequentes em ATC, tais como *BRAF*, *PIK3CA*, *AXIN1* ou *CTNNB1* (Smallridge *et al.*, 2009), foram identificadas em menos de 8% dos casos.

O método não-disruptivo de marcação de RNA com 4-tiouridina, foi optimizado e utlizado, pela primeira vez, no estudo da estabilidade dos miRNA. A incubação de uma linha celular de tumor desdiferenciado da tiróide (BCPAP), com 200 μM 4-tiouridina durante 24 horas, revelou não ser tóxico para as células, não afectar a expressão dos miRNA e permitiu marcar, purificar e quantificar os miRNA de forma precisa. Recorrendo a "arrays" de expressão de miRNA, obtiveram-se os tempos de semi-vida para 249 miRNA, cujo tempo médio foi de 2,5 dias, variando desde 22 horas (miR-208a e miR-107) até mais de 5,5 dias (miR-1321 e miR-320d). Estes dados revelam que os miRNA apresentam uma maior estabilidade que os RNA mensageiros (Yang *et al.*, 2003; Friedel *et al.*, 2009), sendo comparável à estabilidade proteica (Boisvert *et al.*, 2012). O nosso estudo encontra-se em desenvolvimento mas, pretende-se identificar os factores determinantes para a degradação de miRNA. Em especial, a comparação destes dados com tempos de semi-vida determinados em células normais da tiróide, permitirá identificar miRNA cuja estabilidade se encontra desregulada no processo oncogénico.

Em suma, no presente trabalho identificaram-se várias vias e genes que poderão representar alvos para intervenção terapêutica, com impacto no seguimento clínico e na sobrevivência de doentes com tumores agressivos, como são os PDTC e ATC.

Palavras-chave

Carcinoma pouco diferenciado da tiróide; Carcinoma indiferenciado ou anaplásico da tiróide; Desdiferenciação; Expressão génica global; Mutações somáticas; Estabilidade dos microRNA

Abstract

Poorly differentiated (PDTC) and anaplastic thyroid carcinomas (ATC) are highly malignant tumours composed by dedifferentiated cells, for which current therapeutic options have been ineffective.

In the present project, the molecular signatures and genetic alterations associated with these tumours were elucidated, by using genome-wide expression analysis as first assessment. The role of the microRNA stability in thyroid tumourigenesis was also evaluated.

The comparison of the expression profiles between PDTC, well-differentiated thyroid carcinomas and normal thyroid tissues, and between ATC and normal thyroid tissues, revealed that PDTC and ATC have common deregulated signatures, indicative of cell adhesion impairment and increased cell cycle, proliferation and chromosomal instability. Additionally, ATC were specifically characterized by loss of epithelial and thyroid-related functions and activation of components from TGF-β pathway. The gene expression data suggested that follicular variants of papillary carcinomas were possible precursors of PDTC, whereas, ATC were more similar to classical papillary carcinomas. Validation by quantitative RT-PCR in independent sample sets, allowed to confirm the significant over-expression of *UHRF1* (associated to proliferation) and downregulation of *ITIH5* (associated to cell adhesion and invasion) in PDTC relatively to normal tissues. Moreover, *CDKN3* gene, which encodes a cyclin-dependent kinase inhibitor, was shown to be significantly upregulated in PDTC and ATC relatively to normal thyroid, and in accordance with its suppressive function, *CDKN3* was aberrantly spliced in ATC samples. The over-expression of the epithelial-to-mesenchymal transition factor *SNAI2*, which is induced by TGF-β, was significant in ATC.

Attending to the deregulated pathways identified, a mutational screening was undertaken in 26 ATC and 22 PDTC, which included the hot-spot regions of *RAS*, *BRAF*, *TP53*, *CTNNB1* (β-catenin) and *PIK3CA* genes, and, for the first time, a comprehensive mutational analysis of cell cycle [*CDKN1A* ($p21^{CIP1}$); *CDKN1B* ($p27^{KIP1}$); *CDKN2A* ($p14^{ARF}$, $p16^{INK4A}$); *CDKN2B* ($p15^{INK4B}$); *CDKN2C* ($p18^{INK4C}$)], and cell adhesion regulators (*AXIN1*). Most mutations were identified in *TP53* (42% of ATC; 27% of PDTC) and in *RAS* (31% of ATC; 18% of PDTC). The alterations in these genes were mutually exclusive (P=0.0354), and were associated with a lower patient survival (P=0.0383). *CDKN2A* and *CDKN2B* were found to be mutated, for the first time, in up to 25% of PDTC. Other known recurrent mutations in ATC (in *BRAF*,

PIK3CA, *CTNNB1* and *AXIN1* genes) were rarely detected, undermining their role in ATC development.

The study of the microRNA stability in thyroid tumourigenesis is still ongoing. Turnover rates were determined in a dedifferentiated thyroid carcinoma cell line (BCPAP), under standard conditions. A non-disruptive pulse-labelling method was applied and the decrease in microRNA expression along the time was quantified by two-colour arrays. These results represent the first report for an atlas of human microRNA half-lives. The determined average half-life for 249 microRNA was 2.5 days, a stability time more comparable to proteins than to mRNA. The comparison of these data with decay rates in normal thyroid cells will probably uncover miRNA for which stability is deregulated.

In conclusion, this project presents several genes and molecular events that were found deregulated in PDTC and ATC. More importantly, these represent potential therapeutic targets that can be used for the treatment of these highly aggressive tumours, in the near future.

Keywords

Poorly differentiated thyroid carcinoma; Anaplastic or undifferentiated thyroid carcinoma; Dedifferentiation; Genome-wide expression; Somatic mutations; microRNA stability

Table of contents

List of figures and tables

Conventions

Human gene names and symbols are in accordance with the Human Genome Organization (HUGO) Gene Nomenclature Committee. Human protein names, shown at the first appearance in the text, are in accordance with the Universal Protein Resource (UniProt) and symbols match the corresponding gene symbol. Exceptions to these conventions are shown at the list of abbreviations. Gene names are presented at the first appearance in the text, inside quotation marks. Human gene symbols are italicised and all letters are in uppercase. Symbols not italicised refer to human proteins. Symbols with the first letter in uppercase and the remaining letters in lowercase indicate mouse/rat genes (in italics) and proteins (not italicised).

List of abbreviations

3'	Downstream
4sU	4-thiouridine
5'	Upstream
A	Adenosine
ATC	Anaplastic (or undifferentiated) thyroid carcinoma
C	Cytidine
cAMP	3'-5'-cyclic adenosine monophosphate
CDK	Cyclin-dependent kinase
CDKN	Cyclin-dependent kinase inhibitor
cDNA	Complementary DNA
CGH	Comparative genomic hybridisation
CIP/KIP	Cyclin-dependent kinase interacting protein/kinase inhibitory protein
CpG	Cytosine and guanine joined by phoshodiester bond
cPTC	Classical variant of papillary thyroid carcinoma
del	Deletion
DNA	Deoxyribonucleic acid
E	Glutamic acid or glutamate
E-cadherin	Cadherin-1
EDTA	Ethylenediaminetetraacetic acid
EMT	Epithelial-to-mesenchymal transition

ERK	Extracellular signal-regulated kinase
FDR	False discovery rate
FFPE	Formalin-fixed paraffin embedded
FNAB	Fine-needle aspiration biopsy
fs	Frameshift
FTA	Follicular thyroid adenoma
FTC	Follicular thyroid carcinoma
fvPTC	Folicular variant of papillary thyroid carcinoma
FWER	Family wise-error rate
G	Glycine
G	Guanosine
G-protein	Guanine nucleotide-binding protein
G1 phase	Gap 1 phase of cell cycle
GDP	Guanosine 5'-diphosphate
Gq	Guanine nucleotide-binding protein G(q)
GSEA	Gene set enrichment analysis
Gsα	Guanine nucleotide-binding protein G(s) subunit alpha
GTP	Guanosine 5'-triphosphate
GTPase	Guanosine 5'-triphosphatase
HEPES	4-(2-hydroxyethyl)-1-piperazineethanesulfonic acid
INK4	Inhibitors of CDK4
K	Lysine
kDa	Kilodalton
Log	Logarithm
MAPK	Mitogen-activated protein kinase
miRISC	miRNA-induced silencing complex
miRNA	MicroRNA
mRNA	Messenger RNA
n	Number of samples
NADPH	Nicotinamide adenine dinucleotide phosphate reduced
p	Shorter arm of chromosome
p53	Cellular tumor antigen p53
PBS	Phosphate-buffered saline
PCA	Principal components analysis
PCR	Polymerase chain reaction

PDTC	Poorly differentiated thyroid carcinoma
PI3K	Phosphatidylinositol 3-kinase
PIP3	Phosphatidylinositol-3,4,5-trisphosphate
Pol	RNA polymerase
pre-	Precursor
pri-	Primary
PTC	Papillary thyroid carcinoma
q	Longer arm of chromosome
Q	Glutamine
R	Arginine
RET/PTC	Chromosomal rearrangements involving *RET* gene
RNA	Ribonucleic acid
RNAse	Ribonuclease
rRNA	Ribosomal RNA
RT-PCR	Reverse-transcriptase PCR
S phase	Synthesis phase of cell cycle
SEM	Standard error of the mean
T	Thymidine
T_3	Triiodothyronine
T_4	Thyroxine
TGF-β	Transforming growth factor beta
TRH	Thyrotropin-releasing hormone
Tris	Tris(hydroxymethyl)aminomethane
TRK	Chromosomal rearrangements involving *NTRK1* gene
TSH	Thyrotropin or thyroid-stimulating hormone
UV	Ultraviolet
V	Valine
v/v	Volume per volume
WDTC	Well-differentiated thyroid carcinoma
wt	Wild-type
X	Termination codon
β-catenin	Catenin, beta-1

CHAPTER I

General Introduction

1. Molecular aspects of the carcinogenic process

Described since ancient times, the concept and research of cancer has greatly evolved over the centuries. The oncology field, along with the prolific scientific progression, has drastically changed over the last 200 years. One of the first pioneering steps was Rudolph Virchow's concept over microscopic examination of tissues that permitted the general acceptance of cells being formed through division of pre-existing cells. Furthermore, Virchow deduced the origin of neoplasia, as growth of new tissue in the course of a pathological process through abnormal division of cells (Virchow, 1859/1863). Later on, the genetic basis of the disease was remarkably noticed by Theodor Boveri in 1914, who proposed that tumours were derived from cells that acquired chromosomal abnormalities (Boveri, 1914/2008). Among the environmental causes for tumour development (hormones, chemical carcinogens, radiation), viral-induced tumours played an extremely important role in cancer research. The first such virus (later on, named Rous sarcoma virus), was discovered in 1911 by Peyton Rous, who reported that cell-free filtrates from avian tumours (containing a "filterable agent"), could transmit the disease to other chickens (Martin, 2004). Research on this avian RNA tumour virus led to the identification of the first retroviral oncogene *src* (Martin, 1970; Bernstein *et al.*, 1976; Wang *et al.*, 1976), which had a functional cellular precursor (Stehelin *et al.*, 1976; Spector *et al.*, 1978) and protein (Collett *et al.*, 1979; Oppermann *et al.*, 1979) present in several vertebrates, including humans. These meant that normal components of human cells, proto-oncogenes like "v-src sarcoma (Schmidt-Ruppin A-2) viral oncogene homolog (avian)" (*SRC*), could become mutated and subsequently induce cancer formation/progression. This would set off the search for these cellular genes, culminating in the identification (Der *et al.*, 1982; Parada *et al.*, 1982; Santos *et al.*, 1982) of the first human oncogene, "v-Ha-ras Harvey rat sarcoma viral oncogene homolog" (*HRAS*), altered by a single point mutation (Reddy *et al.*, 1982; Tabin *et al.*, 1982; Taparowsky *et al.*, 1982). Since then, all three members of RAS family have been found mutated in several types of human cancers and are established as main regulators of the tumorigenesis process (Malumbres and Barbacid, 2003). Oncogenes have been found as excessively or inappropriately activated, promoting ultimately, unrestrained cell proliferation and neoplastic advantage. Oncogene alterations show a dominant trait normally affecting a single allele, and usually involve amplifications, missense mutations and chromosomal rearrangements. Epigenetic events (inheritance of information on gene expression levels by other means than DNA sequence modification) that include DNA methylation, histone modifications,

nucleosome remodeling and small non-coding regulatory RNAs, can also be involved in abnormal gene expression. Furthermore, not only mutations at genes controlling these mechanisms can induce epigenetic deregulation, but epigenetic changes of certain genes (like DNA repair genes) can lead to new somatic mutations (You and Jones, 2012).

By 1980s, another class of genes involved in tumorigenesis would be recognised. "retinoblastoma 1" (*RB1*) and "tumor protein p53" (*TP53*) were the first two identified tumour suppressor genes, as both alleles were frequently found inactivated in primary tumours (Cavenee *et al.*, 1983; Friend *et al.*, 1986; Fung *et al.*, 1987; Lee *et al.*, 1987; Baker *et al.*, 1989), and wild-type (wt) genes were capable of supressing neoplastic transformation (Huang *et al.*, 1988; Finlay *et al.*, 1989; Baker *et al.*, 1990). Moreover, the findings for *RB1* gene confirmed the model previously formulated by Alfred Knudson, based on a two-hit hypothesis (Knudson, 1971), which proposed that retinoblastoma disease was caused by two mutational events. Thus, inactivation of both alleles of a tumour suppressor gene is normally required for tumorigenesis (contrarily to the dominant trait of oncogenes). The Knudson model would explain the mechanism of most tumour suppressor genes, especially in hereditary forms of cancer (Knudson, 2001). The recessive, loss-of-function alterations affecting tumour suppressors genes (responsible for keeping a normal cell proliferation and cell behaviour), includes large chromosomal deletions, missense or nonsense mutations and base insertions and/or deletions. DNA methylation at gene promoters is also recognized as a frequent inactivation mechanism (Jones and Laird, 1999).

Human cancer is believed to derive from a cell that through a multistep acquisition of different alterations is sequentially selected and expanded originating more malignant subclones. This model was initially proposed in 1976 (Nowell, 1976) and later on, was mechanistically applied to colorectal cancer (Fearon and Vogelstein, 1990). The availability of the human genome sequence (Lander *et al.*, 2001; Venter *et al.*, 2001) has allowed the generalization and confirmation of the tumorigenesis model by large-scale sequencing, by DNA copy number analysis and more recently, by next-generation sequencing. Tumours frequently present thousands of mutations and copy number changes (Stephens *et al.*, 2005; Sjoblom *et al.*, 2006; Wood *et al.*, 2007; Parsons *et al.*, 2008; Mardis *et al.*, 2009; Shah *et al.*, 2009; Kan *et al.*, 2010; Lee *et al.*, 2010; Pleasance *et al.*, 2010; Stephens *et al.*, 2012) and show coexistence of diferent cell subclones (Campbell *et al.*, 2008; Anderson *et al.*, 2011; Navin *et al.*, 2011; Notta *et al.*, 2011; Nik-Zainal *et al.*, 2012; Shah *et al.*, 2012), sometimes with convergent phenotypic evolution (Gerlinger *et al.*, 2012), validating cancer as a truly

product of Darwinian evolution. The differential selection of each of these clones, as shown to greatly contribute for intra-tumour genetic heterogeneity (Navin *et al.*, 2010; Gerlinger *et al.*, 2012), chemoresistance (Jones *et al.*, 2010; Diaz *et al.*, 2012; Ding *et al.*, 2012; Gerlinger *et al.*, 2012; Misale *et al.*, 2012), relapse (Hunter *et al.*, 2006; Ley *et al.*, 2008; Mullighan *et al.*, 2008; Ding *et al.*, 2012) and metastasis (Shah *et al.*, 2009; Campbell *et al.*, 2010; Ding *et al.*, 2010; Yachida *et al.*, 2010). Among the somatic variants randomly acquired throughout the genome, the majority ("passenger mutations") do not influence the neoplastic process and thus, are not under selective pressure (Davies *et al.*, 2005; Greenman *et al.*, 2007; Mardis *et al.*, 2009). However, other mutations confer advantage to the neoplastic clone and are termed "driver mutations" (Stratton, 2011). These are responsible for the defects in the regulatory circuits controlling normal cellular properties, providing the means that allow cancer cells to survive, proliferate, and disseminate.

The "hallmarks" of cancer cells necessary for malignancy have been summarized (Figure I.1) (Hanahan and Weinberg, 2000; Hanahan and Weinberg, 2011), although these properties are widely interconnected and not all might be needed for a fully developed tumour. They may be transiently present over time and over different regions of the tumour and not necessary expressed by all neoplastic cells (Floor *et al.*, 2012). For instance, tumour-associated stromal cells are normal cells but can greatly contribute for tumorigenesis. Cancer cells are thus accepted to acquire molecular changes in order to: constantly stimulate proliferation and gain independence from external growth stimuli; override the anti-proliferative cellular mechanisms, which is required to maintain the continuous proliferation; evade apoptosis, which is a major cellular response to neoplastic events (*e.g.*, DNA damage, oncogene signals, insufficient survival factors, hypoxia and loss of adherence); confer limitless replicative potential (immortalization) by upregulation of telomerase; induce and sustain new blood vessels, for oxygen and nutrients supply; invade adjacent tissues, spread and colonize distant sites; reprogramme energy metabolism, mainly to support high glycolytic rates, which allows rapid generation of nucleosides and amino acids; and avoid elimination by immune cells.

Two mechanisms have been proposed as major inducers of the cancer hallmarks: Genomic/chromosomal instability and tumour-promoting inflammation. The former is acquired upon alterations of components involved in DNA damage repair, in genomic integrity surveillance or in chromosomal segregation, and leads to increased mutational rates, which fuels the neoplastic clones evolution to acquire new malignant properties.

Inflammation is a recent accepted enhancer of tumorigenesis, given that immune cells are capable of fostering angiogenesis, cell proliferation, and invasiveness, by supplying several survival, proangiogenic and growth factors.

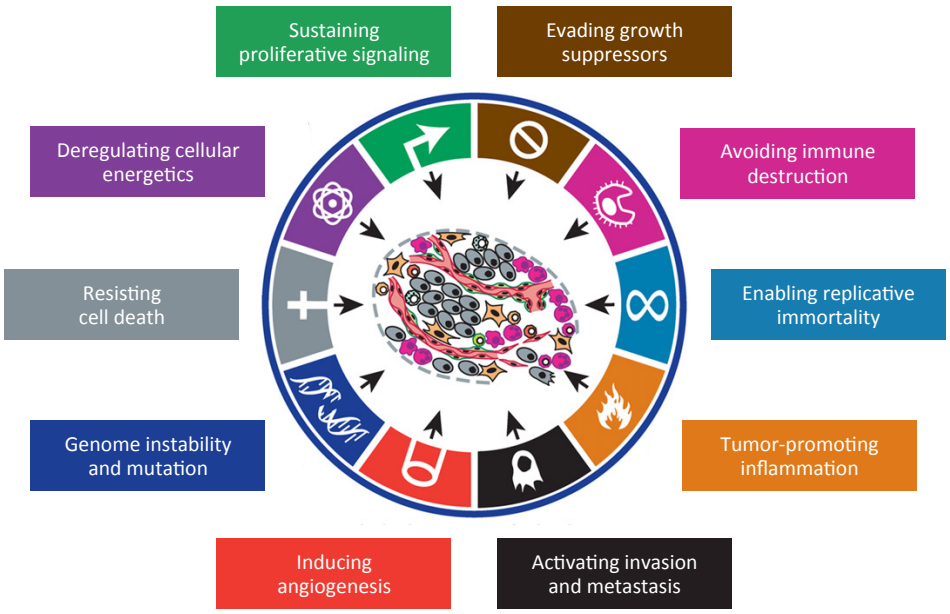

Figure I.1 - The hallmarks and enabling characteristics of cancer (adapted from Hanahan and Weinberg, 2011).

2. The thyroid gland

The thyroid gland is the largest endocrine organ in humans. It is located in the front of the trachea, below the cricoid cartilage and is composed of two lobes joined by a thin isthmus (Muro-Cacho and Ku, 2000). The gland is supplied by major arteries (Camacho *et al.*, 2011) and displays a rich lymphatic network, which drains into several lymphatic nodes (Muro-Cacho and Ku, 2000). The main function of this endocrine gland is the production of thyroid hormones that are crucial for development and regulation of the body metabolism and homeostasis.

2.1. Organogenesis and differentiation

The embryonic endoderm is involved in the lining of two structures within the body, the digestive and the respiratory tubes. These share a common chamber in the anterior region of the embryo, the pharynx. Epithelial outpockets from these structure give rise to the thyroid, thymus, and parathyroid glands (Gilbert, 2000).

During human embryonic days 20 to 22, thyroid morphogenesis is initiated by a thickening of the endodermal epithelium in the primitive pharyngeal floor, know as thyroid anlage. The expansion, proliferation and migration of this structure originate the embryonic thyroid in the correct anatomical position and bilobed shape, at embryonic days 45 to 50. The migrated cells give rise to the most numerous cell population in the gland, the thyroid follicular cells. Progenitors from an embryologic structure derived from the neural crest (neuroectodermal origin) that fuses with the primordial thyroid, originate another distinct thyroid cell, the parafollicular or C cells, responsible for calcitonin production (De Felice and Di Lauro, 2004; Fagman and Nilsson, 2010; Braverman and Cooper, 2012).

Thyroid functional differentiation, involves onset of follicle formation, critical structures for storage and regulation of thyroid hormones, around embryonic day 70. For this, thyroid-specific genes (involved in thyrocytes function and thyroid hormone metabolism) are expressed in concerted timing (Szinnai *et al.*, 2007). Iodine uptake and thyroxine hormone (T_4) production occur by the tenth to the fourteenth gestational week, during the final stages of follicles formation (Braverman and Cooper, 2012).

2.2. Molecular basis of thyroid morphogenesis

Thyroid follicular cell commitment is already hallmarked, at the molecular level, during the formation of the thyroid anlage. Despite being expressed by other embryonic tissues, only thyroid anlage and the derived thyroid primordium express simultaneously 4 transcription factors: homeobox protein NKX-2.1 (NKX2-1), formerly called TTF-1 for thyroid transcription factor-1 (Civitareale *et al.*, 1989; Francis-Lang *et al.*, 1990; Guazzi *et al.*, 1990; Lazzaro *et al.*, 1991); forkhead box protein E1 (FOXE1), formerly known as TTF-2 for thyroid transcription factor-2 (Sinclair *et al.*, 1990; Francis-Lang *et al.*, 1992a; Zannini *et al.*, 1997); paired box protein Pax-8 (PAX8) (Plachov *et al.*, 1990; Poleev *et al.*, 1992); and hematopoietically-expressed homeobox protein HHEX (HHEX) (Bedford *et al.*, 1993; Thomas *et al.*, 1998). The study of knockout mice has demonstrated the crucial role of these factors in the survival and migration of the thyroid cells precursors during embryogenesis (De Felice and Di Lauro, 2004; Fagman *et al.*, 2011). Besides being required during early stages, presence of these factors is a specific and essential feature of adult mature follicular cells, for proper thyroid-specific expressions and functions (Zannini *et al.*, 1992; Damante and Di Lauro, 1994; Pellizzari *et al.*, 2000; De Felice and Di Lauro, 2011).

The hormone released by pituitary, thyrotropin or thyroid-stimulating hormone (TSH), is the main regulator of thyrocytes. However is not involved in early thyroid development and in agreement, TSH is only detectable in the serum approximately at the twelfth gestational week (Thorpe-Beeston *et al.*, 1991). The thyrotropin receptor (TSHR) is a member of G-protein-coupled receptors, with 7 transmembrane domains (Parmentier *et al.*, 1989), whose mice mRNA expression is first detected following migration and before follicles formation. TSH signalling during embryogenesis is only required for proper functional differentiation of cells, since mutant mice and human infants with impaired TSHR exhibit a properly localized gland, but are profoundly hypothyroid (Brown, 2004; De Felice *et al.*, 2004).

2.3. Thyroid hormone metabolism and follicular cell regulation

The functional unit of the thyroid gland is the follicle, formed by a single layer of follicular cells, surrounding a lumen filled with colloid (Figure I.2). This proteinaceous substance contains mainly thyroglobulin (TG), the protein secreted by follicular cells and essential for thyroid hormones formation. The first key steps in synthesis of thyroid hormones involve active transport of iodide across the basolateral membrane into the thyrocyte,

mediated by sodium/iodide cotransporter (SLC5A5) (also known as sodium/iodide symporter, NIS) and efflux of iodide across the apical membrane, partially mediated by pendrin (SLC26A4). At the apical membrane-colloid interface, the process of iodide organification is mediated by thyroid peroxidase (TPO) in the presence of hydrogen peroxide (H_2O_2), generated by a calcium-dependent heterodimeric NADPH oxidase complex, composed of dual oxidases (DUOX1 and -2) and dual oxidase maturation factors (DUOXA1 and -2) (Grasberger, 2010). In this reaction, iodide is oxidised and incorporated into tyrosyl residues of TG and further oxidative coupling of these iodotyrosines leads to triiodothyronine (T_3) and T_4 hormones production. After TG internalization into the follicular cell and subsequent proteolysis, thyroid hormones are released into the bloodstream and iodide is recycled from retained iodotyrosines through deiodination, mediated by the enzyme iodotyrosine dehalogenase 1 (IYD), also known as DEHAL1 (Riesco-Eizaguirre and Santisteban, 2006; Bizhanova and Kopp, 2009). At responsive target cells, iodothyronine deiodinases (DIO1, DIO2 and DIO3) regulate the local bioavailability and action of thyroid hormones, by conversions between less active and active forms of the hormones (Bianco and Kim, 2006).

Production of thyroid hormones is controlled by an endocrine network known as the hypothalamic-pituitary-thyroid axis, by which thyrotropin-releasing hormone (TRH), produced by the hypothalamus, stimulates synthesis and release of TSH from the anterior pituitary. A negative feedback allows thyroid hormones to inhibit TRH and TSH secretion (Camacho *et al.*, 2011), and thus to regulate the system. TSH stimulation of the respective receptor is regarded as the main physiologic regulator of thyroid function. TSH and/or its correspondent signalling cascades transcriptionally regulates the genes necessary for thyroid hormone synthesis, like Slc5a5 (Riedel *et al.*, 2001), Slc26a4 (Pesce *et al.*, 2012), Tpo (Gerard *et al.*, 1988), and Tg (Van Heuverswyn *et al.*, 1984), and induces Slc5a5 membrane localization (Riedel *et al.*, 2001), the H_2O_2 generation (Grasberger, 2010), iodide uptake and the organification process (Marians *et al.*, 2002).

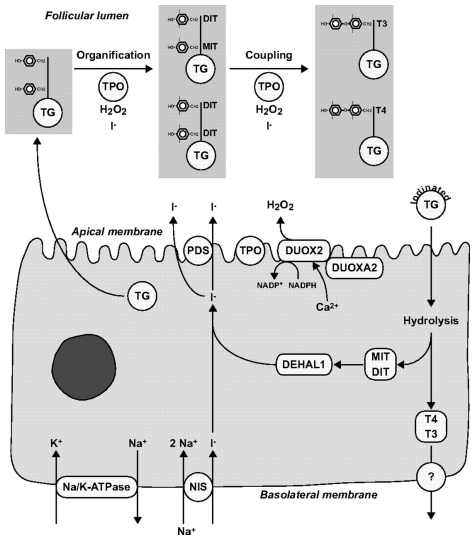

Figure I.2 - Main steps in thyroid hormones biosynthesis. The iodide is transported from the basolateral membrane of thyroid follicular cells, to the apical membrane-colloid interface, where it is oxidized by thyroid peroxidase (TPO) in the presence of hydrogen peroxide. Iodination of selected tyrosyl residues of thyroglobulin originates mono- (MIT) and di-iodotyrosines (DIT) that are coupled to form either T4 or T3 hormones. For hormones secretion, iodinated thyroglobulin (TG) stored in the follicular lumen is internalized and digested in lysosomes, allowing T4 and T3 to be released into the bloodstream. Iodide is recycled by deiodination of unused mono- and di-iodotyrosines (from Bizhanova and Kopp, 2009). NIS - sodium/iodide cotransporter (SLC5A5); DEHAL1 - iodotyrosine dehalogenase 1 (IYD); PDS - pendrin (SLC26A4); DUOX2 - dual oxidase 2; DUOXA2 - dual oxidase maturation factor; $NADP^+$ - nicotinamide adenine dinucleotide phosphate; NADPH - nicotinamide adenine dinucleotide phosphate reduced.

TSH, through Gsα/adenylyl cyclase/cAMP cascade and activation of protein kinase A, is the main inducer of cell proliferation in thyrocyte model systems from different species, including human (Kimura *et al.*, 2001; De Felice *et al.*, 2004). Indeed, activating mutations of *TSHR* are the cause of hyperfunctioning lesions (Hébrant *et al.*, 2011). In human cells, TSH by stimulation of Gq/phospholipase C cascade, can also activate intracellular calcium and protein kinase C, activators of the H_2O_2 generation system (Grasberger, 2010). Nevertheless, exogenous or autocrine insulin-like growth factor I/insulin signalling, which mostly activates phosphatidylinositol 3-kinase (PI3K) pathway, not only is potentiated by TSH, but is absolutely required for the TSH action in human thyroid cells (Kimura *et al.*, 2001). In addition, another distinct mitogenic signal for human thyroid cells is epidermal growth factor, which through activation of its receptor tyrosine kinase, strongly induces the mitogen-activated protein kinase (MAPK) pathway (Roger *et al.*, 2010). According to the transmitted signals and induced mechanisms by these mitogens, TSH is able to trigger proliferation and sustain follicular cells differentiation, whereas the other pathways stimulate proliferation but induce loss of differentiation. Appropriately, most genetic alterations found in thyroid carcinomas lead to constitutive activation of MAPK and PI3K signalling pathways (Roger *et al.*, 2010).

3. Thyroid cancer

3.1. Incidence and mortality

Thyroid cancer represents the most frequent malignancy of the endocrine system (van der Zwan *et al.*, 2012). In 40 European countries, 49 600 thyroid cancer cases were estimated in 2008, with 11 600 cases (23%) and 38 000 cases (77%) diagnosed in men and women, respectively (Ferlay *et al.*, 2010a). In Portugal, age-adjusted estimated rates in men were 4 per 100 000 persons and in women 7.5 per 100 000 persons. Thyroid cancer represented in men about 1%, and in women about 3%, of all estimated cancer cases in Portuguese (Ferlay *et al.*, 2010a) and worldwide (Ferlay *et al.*, 2010b) population. The incidence of this type of cancer has been steadily rising worldwide in the last decades (Sant *et al.*, 2003; Leenhardt *et al.*, 2004; Davies and Welch, 2006; McNally *et al.*, 2012), mainly related to improvement in diagnostic tools, which also led to increased detection of common thyroid lesions in the population, i.e. thyroid nodules and occult thyroid tumours (Ross, 2002). Nevertheless, a true increase of cancer cases and/or increased risk factors (some associated with industrialised countries) might also be involved (Burgess and Tucker, 2006; Zhu *et al.*, 2009; Cramer *et al.*, 2010; Gursoy, 2010; Morris and Myssiorek, 2010). From 2000-2004 (the most recent updated period), average annual number of deaths associated with thyroid cancer in Portugal, was 27 in men (compared to 2434 for lung and 1715 for prostate) and 44 in women (compared to 1571 for breast and 1468 for intestines) (La Vecchia *et al.*, 2010). In the European Union countries, including Portugal, and contrary to incidence, thyroid cancer mortality has declined from early 1990s to early 2000s (especially for women), a tendency maintained since the 1980s (Levi *et al.*, 2004; Bosetti *et al.*, 2008) that is probably related to improved diagnosis and treatment (La Vecchia *et al.*, 2010).

3.2. Risk factors

One of the most recognized risk factors for thyroid tumours, specially if during childhood, is radiation exposure, including medical applied (Sinnott *et al.*, 2010) and nuclear fallouts, such as from atomic bombs and Chernobyl accident (Nagataki and Nystrom, 2002).

Due to its function in iodine concentration, thyroid gland is susceptible not only to the iodine radioisotope ^{131}I (radioiodine), but also to differences in dietary iodine intake (Feldt-

Rasmussen, 2001). Iodine deficient areas, for example, are known by increased frequency of goitre cases and follicular thyroid carcinomas.

The distinct gender difference, which is less pronounced in carcinomas of older patients, suggests that oestrogens are also involved in increased female susceptibility to thyroid cancer (Santin and Furlanetto, 2011).

Most thyroid tumours are sporadic forms but a familial predisposition may account, and is well established, for 25% of the carcinomas arising from the parafollicular cells. 5 to 10% of the tumours arising from follicular cells have a hereditary origin and can occur isolated or as a phenotype of some tumour familial syndromes (Nose, 2011).

3.3. Characterisation of follicular cell-derived tumours

Thyroid tumours may arise from the two main types of epithelial thyroid cells. Parafollicular-derived tumours represent 3 to 5% of cases and are designated as medullary thyroid carcinomas (Nikiforov and Nikiforova, 2011).

Tumours arising from follicular thyroid cells may be benign forms designated as follicular thyroid adenomas (FTA), which are usually distinguished from hyperplastic nodules by presence of a thin fibrous capsule, and by a distinct growth pattern from the surrounding normal tissue (Eszlinger *et al.*, 2008). Somatic activating mutations of TSHR or Gsα can originate a type of encapsulated hyperfunctional tumour called autonomous adenoma (Corvilain *et al.*, 2001; Hébrant *et al.*, 2011). Malignant tumours are subdivided, based on morphological and clinical features, into well-differentiated thyroid carcinomas (WDTC), poorly differentiated carcinomas and anaplastic carcinomas. Thus, follicular thyroid tumours represent a classical tumorigenesis model, where a unique epithelial cell may originate several types of tumours, each with distinctive clinico-pathological features.

3.3.1. Well-differentiated thyroid carcinomas

Most thyroid carcinomas show evident follicular differentiation and are indolent lesions with 10 years survivals greater than 90% (DeLellis *et al.*, 2004).

Papillary thyroid carcinoma (PTC) is the most frequent thyroid tumour, representing 80 to 90% of cases (Kondo *et al.*, 2006; Nikiforov and Nikiforova, 2011) and is the histology

associated with childhood and radiation exposure (DeLellis *et al.*, 2004; Sinnott *et al.*, 2010). This tumour is mainly characterized by the distinctive nuclei, which are overlapped, larger than normal, present inclusions or grooves and have an empty appearance. Metastases are commonly spread to lymph nodes and less frequently disseminated through the blood (Muro-Cacho and Ku, 2000). Some histopathological variants are distinguished from the conventional or classical papillary carcinoma (cPTC). The most prevalent papillary variant in the population is papillary microcarcinoma, which due to the small size (1 cm or less in diameter) has mostly been found incidentally (Muro-Cacho and Ku, 2000; DeLellis *et al.*, 2004). Another important group is the follicular variant (fvPTC), which usually resembles encapsulated follicular adenomas/carcinoma but display the characteristic papillary nuclei (DeLellis *et al.*, 2004). This variant, especially if encapsulated, presents many genetic, histological, and clinical features more similar to follicular carcinomas (Sobrinho-Simões *et al.*, 2005; Rivera *et al.*, 2010).

Follicular thyroid carcinoma (FTC) is a malignant tumour with a follicular pattern, with no distinctive criteria for diagnosis. FTC is distinguished from FTA by presence of vascular and/or capsular invasion (DeLellis *et al.*, 2004), and is differentially diagnosed by exclusion of typical features of the fvPTC and poorly differentiated carcinoma (Muro-Cacho and Ku, 2000). FTA are referred as possible precursor lesions of the FTC (DeLellis *et al.*, 2004). Contrary to PTC, distant metastases mostly occur through haematogenous dissemination. Two main groups of FTC have been defined on the basis of the degree of invasion. In minimally invasive follicular carcinoma, despite displaying similar appearance to FTA, neoplastic cells have penetrated the capsule and/or have invaded the blood vessels. Widely invasive follicular carcinoma presents extensive infiltration of the surrounding tissue and/or vasculature, exhibits malignant features such as solid areas, high mitotic activity and necrotic areas and frequently metastasizes to lung and bones (Muro-Cacho and Ku, 2000). Due to these high-grade features, mortality rates are about 50%, higher than in PTC and minimally invasive FTC (DeLellis *et al.*, 2004).

3.3.2. Poorly differentiated and anaplastic thyroid carcinomas

Anaplastic (or undifferentiated) thyroid carcinoma (ATC) is a highly malignant tumour composed by undifferentiated cells and represents 1 to 2% of thyroid malignancies (Kondo *et al.*, 2006; Nikiforov and Nikiforova, 2011). Nevertheless, ATC may contribute between 14 to

50% of the deaths attributable to thyroid cancer and represents one of the most lethal human malignancies, with a median survival of 3 to 5 months after diagnosis (DeLellis *et al.*, 2004; Nagaiah *et al.*, 2011). ATC is typically diagnosed after 60 years of age, presenting as a rapidly growing neck mass that frequently causes difficulty in swallowing (dysphagia) and voice changes (dysphonia). Tumours are very infiltrative, spreading into surrounding lymph nodes, muscles and tissues (e.g. trachea, larynx or oesophagus), and are frequently metastasized at diagnosis, into the lungs, bones or brain (Muro-Cacho and Ku, 2000; DeLellis *et al.*, 2004). Histologically, ATC are neoplasms with extensive haemorrhagic and necrotic areas, presenting a spindle cell, giant cell, or squamoid patterns.

Contrarily to the other main types of thyroid carcinoma, poorly differentiated thyroid carcinoma (PDTC) has only been clearly defined as a separate histotype more recently. Initially, the term poorly differentiated "insular" carcinoma was applied to characterize a tumour presenting solid clusters or nests of neoplastic cells, with mitotic activity, frequent necrotic foci, and life-threatening metastases (Tallini, 2011). These heterogeneous group could also encompass papillary/follicular carcinomas with loss of differentiation and poorer prognosis (Nambiar *et al.*, 2011). The 2004 thyroid cancer classification by World Health Organization designated, for the first time, PDTC as a distinct group of neoplasms with limited evidence of follicular cell differentiation that are, both morphologically and behaviourally, placed as intermediate between WDTC and ATC (DeLellis *et al.*, 2004). In 2006, a consensus diagnostic criteria was proposed: presence of a solid, trabecular or insular pattern of growth; absence of the PTC nuclear features; and presence of convoluted nuclei or increased mitotic activity or tumour necrosis (Nambiar *et al.*, 2011; Soares *et al.*, 2011; Tallini, 2011). Several studies demonstrated that aggressive behaviour, prognosis and age at diagnosis of PDTC are midway between WDTC and ATC (Lam *et al.*, 2000; Volante *et al.*, 2004; Sanders *et al.*, 2007; Nambiar *et al.*, 2011). Mean five-year survival rate of PDTC patients is about 50% and death is mostly caused, not by extra-thyroidal extension (more common in ATC), but by the common metastases to regional lymph nodes, lungs and bones (DeLellis *et al.*, 2004; Nambiar *et al.*, 2011).

3.4. Multi-step model of thyroid tumours progression

The clinical and histological features of thyroid carcinomas, point to a continuum loss of follicular cell differentiation (a process of dedifferentiation), which leads to progressive

increase of aggressiveness and ultimately to a fatal outcome. The PDTC and ATC are believed to have a *de novo* origin or from pre-existing tumours. The origin from pre-existing tumours is demonstrated by detection of well-differentiated areas or foci (more frequently of papillary than follicular pattern) in PDTC and ATC cases (Nikiforova *et al.*, 2003a; Begum *et al.*, 2004; DeLellis *et al.*, 2004; Garcia-Rostan *et al.*, 2005; Quiros *et al.*, 2005; Takano *et al.*, 2007a; Wang *et al.*, 2007a; Costa *et al.*, 2008; Santarpia *et al.*, 2008; Ricarte-Filho *et al.*, 2009).

Several molecular evidences suggest also a step-wise progression from indolent WDTC to PDTC and to highly malignant ATC. Comparative genomic hybridisation analysis has shown that chromosomal alterations increase from WDTC to PDTC and from the latter to ATC (DeLellis *et al.*, 2004). Furthermore, the pattern and the frequency of the alterations between these carcinomas support the sequential acquisition of specific DNA gains/losses through the dedifferentiation process (Wreesmann *et al.*, 2002; Hunt *et al.*, 2003; Rodrigues *et al.*, 2004). In addition to chromosomal imbalances, gene expressions and genetic/epigenetic alterations are not randomly distributed among thyroid carcinomas. Several events are clearly associated with early tumorigenesis (involved in follicular cell transition to WDTC), are specifically involved in PDTC and ATC development or are shared between both WDTC, PDTC and ATC components (pointing to a common origin).

3.4.1. The RAS-RAF-MEK-ERK and PI3K-AKT signalling pathways

Transformation of thyroid follicular cells frequently occurs via somatic point mutations or chromosomal rearrangements involving, similarly to most human cancers, effectors of the MAPK-ERK pathway and the PI3K-AKT pathway (Figure I.3).

The MAPK-ERK (extracellular signal-regulated kinase) pathway is a kinase cascade critically involved in cell homeostasis, in response to extracellular signals (hormones, cytokines and growth factors). These, by interacting with their respective receptors, activate the RAS GTPase family. Active RAS allows recruitment of the serine/threonine-protein kinases RAF to the cell membrane, where they are activated. The most potent member of the RAF family is BRAF (Cantwell-Dorris *et al.*, 2011). Active BRAF phosphorylates and activates dual specificity mitogen-activated protein kinase kinase 1 and 2 (MAP2K1/2, also known as MEK1/2), which in turn, phosphorylates and activates mitogen-activated protein kinase 3 and 1 (MAPK3/1, also known as ERK1/2), regulators of downstream effectors of the

cascade. These effectors include the transcription factor AP-1 (JUN), proto-oncogene c-Fos (FOS), Myc proto-oncogene protein (MYC), nuclear factor NF-kappa-B (NFKB), ribosomal protein S6 kinases, Eukaryotic translation initiation factor 4E (EIF4E), histone acetyltransferases, Bcl2 antagonist of cell death (BAD), cyclin-dependent kinase inhibitor 2A (CDKN2A, also known as $p16^{INK4A}$), cyclin-dependent kinase inhibitor 1 (CDKN1A, also known as $p21^{CIP1}$) and many other proteins (Pearson *et al.*, 2001; McCubrey *et al.*, 2007). In conclusion, MAPK-ERK pathway is a master regulator of cell differentiation, proliferation and apoptosis.

The PI3K-AKT pathway is involved in regulation of essential functions for cell survival. The PI3K family is divided into three main classes, being class I, the main one involved in cancer (Engelman *et al.*, 2006). Class I of PI3K, which are activated by G-protein-coupled receptors and growth factor receptor tyrosine kinases, are composed by an 85 kDa regulatory subunit and a 110 kDa catalytic subunit. RAS family members can also interact with the catalytic subunit and thus activate PI3K-AKT signalling. Upon activation, the catalytic subunit generates the lipid second messenger phosphatidylinositol-3,4,5-trisphosphate (PIP3). Binding to this molecule, allows the localization of the RAC-alpha serine/threonine-protein kinase (AKT1, also know as protein kinase B) to the membrane, subsequent phosphorylation and activation by 3-phosphoinositide-dependent protein kinase 1 (PDPK1). Activated AKT1 regulates several downstream protein effectors, such as transcription factors of the forkhead (FOXO) family, glycogen synthase kinase 3 beta (GSK3B), BAD, serine/threonine-protein kinase mTOR (MTOR), ribosomal protein S6 kinases, p53 and protein kinase C. Thus, PI3K and AKT1 are involved in several cellular functions, including glucose metabolism, promotion of cell proliferation, inhibition of apoptosis and increased cell motility (Engelman *et al.*, 2006; Saji and Ringel, 2010).

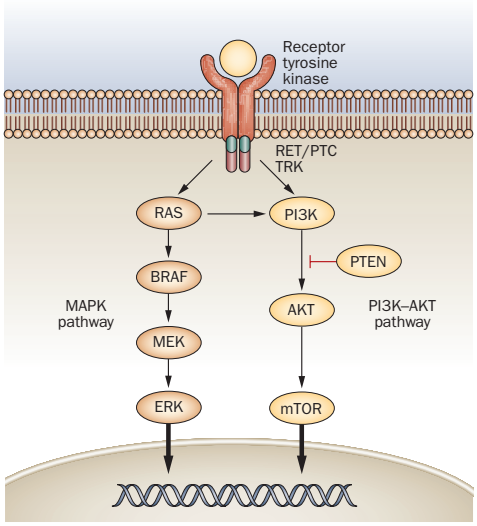

Figure I.3 - The MAPK-ERK and PI3K-AKT signalling pathways. Both pathways are involved in the response to extracellular signals from cell membrane receptor tyrosine kinases. Through successive activation of downstream proteins, these pathways regulate the gene transcription at the nucleus, and control cell proliferation, differentiation and survival. Oncogenic alterations found in thyroid tumours, include receptor tyrosine kinases rearrangements (RET/PTC and TRK) and mutations in *BRAF*, *RAS*, *PIK3CA* and *PTEN* genes (from Nikiforov and Nikiforova, 2011). MAPK - mitogen-activated protein kinase; MEK - mitogen-activated, extracellular signal-regulated kinase; ERK - extracellular signal-regulated kinase; PI3K - phosphatidylinositol 3-kinase.

3.4.2. Molecular alterations involved in thyroid carcinoma initiation

MAPK-ERK activation shows to be crucial for thyroid cancer initiation, since all mutated genes found encode membrane receptor tyrosine kinases (RET and NTRK1) and intracellular transducers (BRAF and RAS). Nevertheless RET, NTRK1 and RAS are also capable of inducing the PI3K-AKT pathway. In addition, oncogenic BRAF has also been shown to up-regulate the AKT-mTOR pathway (Faustino *et al.*, 2012; Romeo *et al.*, 2012). These are mutually exclusive activating mutations (Kimura *et al.*, 2003; Soares *et al.*, 2003; Xing, 2005) that are present in about 70% of patients with PTC (Kimura *et al.*, 2003; Nikiforov and Nikiforova, 2011).

3.4.2.a. *BRAF* mutations

The "v-raf murine sarcoma viral oncogene homolog B1" (*BRAF*) oncogene has been identified in different types of tumours, and somatic mutations are exclusively localized at the kinase domain. The missense mutation in exon 15, which substitutes glutamine for valine at residue 600 ($BRAF^{V600E}$), accounts for 80 to 90% of the *BRAF* mutations (Davies *et al.*, 2002; Cantwell-Dorris *et al.*, 2011). The $BRAF^{V600E}$ can have an increased activation by 500-fold,

leading to a constitutive self-sufficient activation of the MAPK-ERK signalling. The remaining identified mutations also activate this pathway (Wan *et al.*, 2004). Among WDTC, *BRAF* mutations are exclusively associated with PTC (Cohen *et al.*, 2003; Fukushima *et al.*, 2003; Kimura *et al.*, 2003; Xu *et al.*, 2003) and are the most common alterations in sporadic (no radiation related) PTC (Kimura *et al.*, 2003; Fugazzola *et al.*, 2006). Other less frequent *BRAF* alterations in PTC, with the same effect on MAPK-ERK pathway, include $BRAF^{K601E}$ (Trovisco *et al.*, 2004; Lupi *et al.*, 2007; Basolo *et al.*, 2010), small in-frame insertions/deletions (Trovisco *et al.*, 2005; Carta *et al.*, 2006; Hou *et al.*, 2007b; Chiosea *et al.*, 2009; Basolo *et al.*, 2010) and chromosomal rearrangement of *BRAF* with "A kinase (PRKA) anchor protein (yotiao) 9" (*AKAP9*) (Ciampi *et al.*, 2005). $BRAF^{V600E}$ is mainly associated with classic papillary pattern and tall-cell variants (Puxeddu *et al.*, 2004; Fugazzola *et al.*, 2006; Lee *et al.*, 2007) while is rarely detected in follicular variants (Nikiforova *et al.*, 2003a; Cohen *et al.*, 2004; Fugazzola *et al.*, 2006), which may instead harbour the $BRAF^{K601E}$ (Trovisco *et al.*, 2004; Castro *et al.*, 2006; Basolo *et al.*, 2010). $BRAF^{V600E}$ detection in microcarcinoma (Nikiforova *et al.*, 2003a; Lupi *et al.*, 2007; Marchetti *et al.*, 2012) suggests that it is an early event in tumorigenesis. Still, can also be associated with advanced stage, poor prognostic features and higher tumour recurrence (Xing, 2005; Riesco-Eizaguirre *et al.*, 2006; Lee *et al.*, 2007; Lupi *et al.*, 2007; Elisei *et al.*, 2008; Guerra *et al.*, 2012; Kim *et al.*, 2012).

3.4.2.b. *RET* and *NTRK1* rearrangements

Both "ret proto-oncogene" (*RET*) and "neurotrophic tyrosine kinase, receptor, type 1" (*NTRK1*) genes encode neurotrophin tyrosine kinase receptors critically involved in the nervous system (Pierotti, 2001) that are not expressed in thyroid follicular cells (Kondo *et al.*, 2006). Activation of these receptors allows the stimulation of a variety of signalling cascades, including MAPK-ERK and PI3K pathways (Kondo *et al.*, 2006; Xing, 2010). Activating mutations of RET are involved in sporadic and familial medullary thyroid carcinoma, whereas RET chimeric mutants known as RET/PTC are implicated in sporadic PTC (Santoro *et al.*, 1992). Less frequently detected, NTRK1 rearrangements with 3 different fusion partners, are known as TRK and are also restricted to PTC (Kondo *et al.*, 2006). These rearrangements are more prevalent in radiation-induced tumours and most frequently are intrachromosomal. From the fusion between the 3' portion of the receptor tyrosine kinases, coding for the kinase domain and the 5' terminal region of genes ubiquitously expressed and capable of

dimerization, results a fusion mutant protein with a protein kinase domain constitutively active and independent of ligand interaction (Pierotti, 2001). The rearrangement of *RET* was the first such event detected in thyroid cancer. Designated by *RET/PTC1*, originated from the paracentric inversion of chromosome 10q, juxtaposing *RET* with "coiled-coil domain containing 6" (*CCDC6*) (Pierotti *et al.*, 1992). *RET/PTC1* and *RET/PTC3* are the most common *RET/PTC* oncogenes and both result from paracentric inversions. Other 10 *RET/PTC* fusions have been described and represent interchromosomal translocations (Gandhi *et al.*, 2010). *RET/PTC* and *TRK* oncogenes are considered as initial events in transformation, and seem to have a low tumorigenic potential (Santoro *et al.*, 1993; Wang *et al.*, 2003). Nevertheless, transgenic mice with thyroid-specific expression of *RET/PTC* or *TRK* oncogenes develop hyperplasia and PTC (Jhiang *et al.*, 1996; Santoro *et al.*, 1996; Powell *et al.*, 1998; Russell *et al.*, 2000).

3.4.2.c. *N-, K-* and *H-RAS* mutations

RAS genes ["neuroblastoma RAS viral (v-ras) oncogene homolog" (*NRAS*), "v-Ki-ras2 Kirsten rat sarcoma viral oncogene homolog" (*KRAS*) and *HRAS*] encode highly related G-proteins, which upon stimuli through cell membrane receptors, bind GTP and activate the signalling cascades. RAS proteins have the ability to activate both MAPK-ERK and PI3K pathways and both stimulations are required for mutant RAS-induced proliferation of human primary thyroid epithelial cells (Gire *et al.*, 1999; Gire *et al.*, 2000). The normal function of RAS proteins depends on the interconversion between active (GTP-bound) and inactive (GDP-bound) states. RAS point mutations affecting the GTP-binding domain (codons 12 and 13) or the GTPase domain (codon 61) lead to a mutant protein permanently switched in the active form, constantly activating downstream pathways, even in the absence of stimuli (Nikiforov, 2008). In thyroid neoplasia, *RAS* mutations correlate with the follicular pattern, being detected in FTA, FTC, and in PTC (exclusively in follicular variants) (Namba *et al.*, 1990; Esapa *et al.*, 1999; Vasko *et al.*, 2003; Zhu *et al.*, 2003; Castro *et al.*, 2006; Di Cristofaro *et al.*, 2006). Most frequent mutations affect codon 61 of *NRAS* and *HRAS* (Nikiforov and Nikiforova, 2011). The detection in adenoma suggests the involvement of *RAS* mutations in the early transformation of follicular cells and in the susceptibility to carcinomas. Contrary to *BRAF*, *RAS* correlation with poorer outcome in WDTC has not been clearly sustained (Nikiforov, 2011).

3.4.2.d. *PAX8-PPARG* rearrangements

Besides *RAS* oncogenes, it is also frequently detected in FTC, a balanced translocation between chromosome 2 and 3, which originates the fusion between the DNA binding domain of "paired box 8" (*PAX8*) and the "peroxisome proliferator-activated receptor gamma" (*PPARG*) (Kroll *et al.*, 2000), with the resultant mutant oncogene under control of the *PAX8* promoter. This chimeric oncogene was also identified in fvPTC (Castro *et al.*, 2005; Castro *et al.*, 2006) and in FTA (Marques *et al.*, 2002; Cheung *et al.*, 2003; Lacroix *et al.*, 2004), suggesting that is also an early oncogenic event. The *PAX8-PPARG* rearrangement has been shown to modulate the expression of thyroid-specific genes, enhance cell viability (Au *et al.*, 2006; Espadinha *et al.*, 2007) and to impair wt PPARG activity (Kroll *et al.*, 2000; Gregory Powell *et al.*, 2004). PPARG is a nuclear hormone receptor transcription factor, expressed at low levels and with no known function in thyroid (Reddi *et al.*, 2007). Nevertheless, PPARG may regulate the cell cycle and apoptosis (Fajas *et al.*, 2001) and inhibit PI3K activity (Farrow and Evers, 2003). In accordance, thyroid-specific *PAX8-PPARG* expression in mice and *PAX8-PPARG*-mutated FTC, display increased AKT1 phosphorylation (Diallo-Krou *et al.*, 2009). The mice model showed that *PAX8-PPARG* is only capable of inducing thyroid hyperplasia, but combined with homozygous deletion of "phosphatase and tensin homolog" (*Pten*), the negative regulator of PI3K-AKT signalling, mice developed invasive and metastatic thyroid carcinomas (Dobson *et al.*, 2011), reasoning for the synergy of the two events in human thyroid cancer. Nevertheless, *PAX8-PPARG* and *RAS* oncogenes are usually, non-overlapping events in FTA, FTC and fvPTC (Nikiforova *et al.*, 2003b; Castro *et al.*, 2006; Banito *et al.*, 2007), similarly to the genetic alterations found in PTC.

3.4.3. Molecular alterations involved in dedifferentiation

3.4.3.a. Early involved genetic alterations

Among the genetic alterations involved in WDTC pathogenesis, *PAX8-PPARG* seems not able to induce dedifferentiation to PDTC (Marques *et al.*, 2004; Ricarte-Filho *et al.*, 2009; Volante *et al.*, 2009) nor to ATC (Tallini *et al.*, 1998; Marques *et al.*, 2002; Dwight *et al.*, 2003). The same applies to *RET/PTC*, which was reported in 0-17% of PDTC (Tallini *et al.*, 1998; Santoro *et al.*, 2002; Ricarte-Filho *et al.*, 2009; Volante *et al.*, 2009) and has not been detected in ATC (Tallini *et al.*, 1998; Quiros *et al.*, 2005; Ricarte-Filho *et al.*, 2009).

Nonetheless, copy gains of other receptor tyrosine kinases have been reported as frequent and to be concomitant in ATC cases (Liu *et al.*, 2008).

Contrarily to the fusion oncoproteins, *RAS* and *BRAF* mutations seem to be associated with further progression to PDTC and ATC. Chromosomal instability, which was induced by oncogenic *Hras* (Saavedra *et al.*, 2000; Abulaiti *et al.*, 2006), *Nras* (Vitagliano *et al.*, 2006) and $BRAF^{V600E}$ (Mitsutake *et al.*, 2005) in thyroid rat cells, is a possible major contributor for these progression (Kamata and Pritchard, 2011). Accordingly, mice with thyroid-specific $BRAF^{V600E}$ expression, developed tumours that frequently exhibited vascular invasion, extrathyroidal extension and dedifferentiated areas (although no evident metastasis were found) (Knauf *et al.*, 2005; Chakravarty *et al.*, 2011; Franco *et al.*, 2011). Oncogenic *Nras* expression in thyroid of transgenic mice was also capable of inducing invasive carcinomas with poorly differentiated areas and metastases to liver, lung and bone (Vitagliano *et al.*, 2006). Nevertheless, many factors may influence these mice models, as different phenotypic results were seen with other *Ras* members (Santelli *et al.*, 1993; Rochefort *et al.*, 1996; Charles *et al.*, 2011; Franco *et al.*, 2011) and in another $BRAF^{V600E}$ model (Charles *et al.*, 2011).

BRAF oncogene (Table I.1) is more prevalent in ATC (25%) than in PDTC (6%), and is found especially in cases with coexistent PTC areas. Presence of *BRAF* mutation in both dedifferentiated and differentiated components (Nikiforova *et al.*, 2003a; Begum *et al.*, 2004; Cohen *et al.*, 2004; Takano *et al.*, 2007a), as well as in lymph node/distant metastases (Vasko *et al.*, 2005; Costa *et al.*, 2008; Santarpia *et al.*, 2008; Ricarte-Filho *et al.*, 2009) has been confirmed, further suggesting that *BRAF* mutation is an early event that induces additional alterations and leads to dedifferentiation.

Contrary to *BRAF*, *RAS* mutations (Table I.1) seem more frequent in PDTC (31%) than in ATC (21%), and a few reports confirmed the segregation of the mutation in coexisting differentiated components (Oyama *et al.*, 1995; Costa *et al.*, 2008; Schwertheim *et al.*, 2009). Moreover, *RAS* and *BRAF* mutations have each been found in co-existence with other genetic alterations in ATC (Garcia-Rostan *et al.*, 2005; Quiros *et al.*, 2005; Hou *et al.*, 2007a; Wang *et al.*, 2007a; Liu *et al.*, 2008; Santarpia *et al.*, 2008; Ricarte-Filho *et al.*, 2009), which illustrates the accumulation/cooperation of events in dedifferentiation.

3.4.3.b. Loss of thyroid-specific functions

Dedifferentiation of thyroid epithelial cells seems to implicate the loss of the thyroid-specific and iodine metabolism markers. Contrarily to most WDTC, ATC usually do not express TPO, TG, TSHR (Brabant *et al.*, 1991; Hoang-Vu *et al.*, 1992; Elisei *et al.*, 1994; Ros *et al.*, 1999), SLC5A5 (Arturi *et al.*, 1998), NKX2-1 (Fabbro *et al.*, 1994; Katoh *et al.*, 2000; Miettinen and Franssila, 2000; Takano *et al.*, 2007b) nor FOXE1 (Zhang *et al.*, 2006; Nonaka *et al.*, 2008). PDTC may not express some of these markers or express them in a more diffuse or fainted pattern (Caillou *et al.*, 1998; Lazar *et al.*, 1999; Basolo *et al.*, 2000; DeLellis *et al.*, 2004; Nonaka *et al.*, 2008). The ability of thyroid cells to concentrate radioiodine allows the ablation of these cells in tumour patients (Schlumberger *et al.*, 2007). The loss of iodine uptake and metabolism is a critical drawback in the management and treatment of primary thyroid tumours and metastasis.

$BRAF^{V600E}$ is associated with lower iodine uptake and lower expression of SLC5A5 (Riesco-Eizaguirre *et al.*, 2006; Durante *et al.*, 2007) SLC26A4, TG (Mian *et al.*, 2008; Espadinha *et al.*, 2009) and TPO (Durante *et al.*, 2007; Romei *et al.*, 2008) in human PTC. It was shown that $BRAF^{V600E}$ impairs SLC5A5 expression and localization to the membrane (Riesco-Eizaguirre *et al.*, 2006) through stimulation of transforming growth factor beta (TGF-β) pathway (Riesco-Eizaguirre *et al.*, 2009). Thyroid-specific expression of $BRAF^{V600E}$ in mice induced lower mRNA expressions of *Tpo*, *Tg* and *Slc5a5* in the gland (Knauf *et al.*, 2005). Transformation by oncogenic *Ras* in thyroid rat cells, seems to involve ERK activation (Missero *et al.*, 2000) and independence (Shirokawa *et al.*, 2000) or inhibition (Baratta *et al.*, 2009) of TSHR/cAMP pathway, and is well known to impair the expression of most thyroid-specific genes (Fusco *et al.*, 1982; Avvedimento *et al.*, 1985; Avvedimento *et al.*, 1988; Francis-Lang *et al.*, 1992b; De Vita *et al.*, 2005). Other pathways like PI3K-AKT-mTOR (Garcia and Santisteban, 2002; Kogai *et al.*, 2008; de Souza *et al.*, 2010; Liu *et al.*, 2012) have also been found to modulate SLC5A5 and/or iodine uptake.

3.4.3.c. Further alterations in PI3K-AKT pathway

Molecular alterations in PDTC and ATC seem to include other components of the PI3K-AKT pathway and in accordance, phosphorylation of AKT1, which indicates activation of the pathway, was shown to be more prevalent than MAPK-ERK activation in ATC (Liu *et al.*, 2008).

The catalytic subunit of PI3K, encoded by "phosphatidylinositol-4,5-bisphosphate 3-kinase, catalytic subunit alpha" (*PIK3CA*) is particularly involved in cancer. The *PIK3CA* gene has been shown to be amplified (Shayesteh *et al.*, 1999) and also to be mutated mostly at exons 9 and 20 (Samuels *et al.*, 2004). In thyroid cancer, mutational screening and copy number analysis revealed that *PIK3CA* mutations and amplifications are present in 14 and 41% of ATC, respectively (Table I.1), but are also detected in WDTC, mostly in FTC (Garcia-Rostan *et al.*, 2005; Wu *et al.*, 2005; Wang *et al.*, 2007b; Liu *et al.*, 2008). Nevertheless, contrary to ATC, these events tend to be mutually exclusive with other genetic alterations in FTC (Hou *et al.*, 2007a; Wang *et al.*, 2007b). Furthermore, *PIK3CA* mutations/amplifications were not present in differentiated components coexisting in ATC cases, suggesting a specific association with progression (Garcia-Rostan *et al.*, 2005; Santarpia *et al.*, 2008). Alterations in other members that positively regulate PI3K-AKT pathway have been searched in few series. No mutations were detected in "v-akt murine thymoma viral oncogene homolog 1" (*AKT1*) in a total of 65 ATC (Liu *et al.*, 2008; Ricarte-Filho *et al.*, 2009), in "v-akt murine thymoma viral oncogene homolog 2" (*AKT2*) or in *PDPK1* in 47 ATC (Liu *et al.*, 2008). Among these three genes, copy number gain was seen for *AKT1* (9 in 48 samples) and *PDPK1* (8 in 40), as well as for "phosphatidylinositol-4,5-bisphosphate 3-kinase, catalytic subunit beta" (*PIK3CB*) gene (16 in 42) (Liu *et al.*, 2008). The prevalence and role of mutations/amplifications of PI3K-AKT signalling components, in PDTC, is mainly unknown. Only Ricarte-Filho and collaborators (Ricarte-Filho *et al.*, 2009) have analysed *PIK3CA* (Table I.1) and *AKT1* (mutations present in 6 of 32 recurrent cases but absent in 34 primary PDTC).

The *PTEN* gene encodes a phosphatase that dephosphorylates PIP3 and subsequently counteracts PI3K-AKT signalling. Nevertheless, PTEN seems to regulate other proteins, and thus has been involved in cell adhesion, migration, growth-arrest and apoptosis (Dahia, 2000). Somatic inactivating mutations of this gene were found in several types of tumours (Li *et al.*, 1997; Steck *et al.*, 1997). In addition, germ-line *PTEN* mutations are implicated in cases of Cowden syndrome (Liaw *et al.*, 1997), a multiple hamartomatous syndrome, whose features includes benign and malignant thyroid tumours, mostly of follicular pattern. Among sporadic thyroid tumours, the greatest downregulation or loss of PTEN expression has been associated with ATC (Bruni *et al.*, 2000; Gimm *et al.*, 2000; Frisk *et al.*, 2002) and accordingly, *PTEN* promoter methylation was found to be frequent (in 69% of cases) and highest in ATC (Hou *et al.*, 2008). This may be the most prevalent inactivating mechanism, because loss of

heterozygosity was found in 11 of 29 cases (38%) (Dahia *et al.*, 1997; Gimm *et al.*, 2000; Frisk *et al.*, 2002) and mutations were found in 10 of 98 analysed cases (10%) (Dahia *et al.*, 1997; Frisk *et al.*, 2002; Hou *et al.*, 2007a; Santarpia *et al.*, 2008). To our knowledge, PTEN alterations have not been assessed in PDTC.

3.4.3.d. Alterations in cell cycle and in tumour suppressor p53 function

Progression through the cell cycle is mainly controlled by complexes between cyclin-dependent kinases (CDK) and their regulatory subunits, cyclins. The main substrate of CDK is RB1, whose activity is repressed by sequential phosphorylation, allowing activation of E2F transcription factors and induction of genes for further cell cycle progression. Mitogens are major inducers of D-type cyclins, which in association with CDK4 and CDK6 are mostly involved in early G1 phase. CDK2 is activated by E-type cyclins during G1/S transition and activated by A-type cyclins during S phase (Malumbres and Barbacid, 2001). CDK inhibitors (CDKN) are known to counteract the activity of CDK, and based on sequence homology and CDK specificity, CDKN are divided into two distinct families: INK4 members (CDKN2A or $p16^{INK4A}$, CDKN2B or $p15^{INK4B}$, CDKN2C or $p18^{INK4C}$ and CDKN2D or $p19^{INK4D}$), which bind to CDK4 and CDK6; and CIP/KIP members (CDKN1A or $p21^{CIP1}$, CDKN1B or $p27^{KIP1}$ and CDKN1C or $p57^{KIP2}$), which affect cyclin D-, E-, and A-dependent kinases (Sherr and Roberts, 1999). The *CDKN2A* gene encodes another tumour suppressor protein ($p14^{ARF}$) that shares the second and third exons with $p16^{INK4A}$. Due to different first exons, these common exons have alternative reading frames, originating distinct proteins with no sequence homology. Therefore, $p14^{ARF}$ have no direct interaction with CDK, and is mainly involved in p53 positive regulation through the repression of the E3 ubiquitin-protein ligase MDM2, which mediates the ubiquitination and subsequent proteasomal degradation of p53 (Gil and Peters, 2006).

CDKN2A decreased expression and/or hypermethylation have been frequently found in PDTC and mostly in ATC (Schagdarsurengin *et al.*, 2002; Boltze *et al.*, 2003; Ball *et al.*, 2007; Lee *et al.*, 2008), but mutations were not studied in PDTC or were assessed in very small ATC series (Calabrò *et al.*, 1996; Tung *et al.*, 1996; Yane *et al.*, 1996). To the best of our knowledge, only one report (Calabrò *et al.*, 1996), found *CDKN2B* mRNA expression to be normal in 5 ATC and except for the role of the CDKN2C in medullary thyroid carcinoma, *CDKN2C* gene or protein has never been studied in thyroid tumours. Downregulation of

CDKN1B expression is more pronounced in PDTC and ATC cases (Lloyd *et al.*, 1997; Erickson *et al.*, 1998; Resnick *et al.*, 1998; Tallini *et al.*, 1999) but mutational analyses are not available. CDKN1B has been found to be regulated by PI3K-AKT pathway in thyroid tumours including ATC, such that PTEN and CDKN1B expressions are positively correlated (Bruni *et al.*, 2000) and cytosolic CDKN1B [which does not have growth-arrest properties as nucleus-localized CDKN1B (Baldassarre *et al.*, 1999)] is associated with AKT activation (Motti *et al.*, 2005b). In thyroid cancer cell lines, growth-arrest induced by cadherin-1 (CDH1, known as E-cadherin) is also mediated through CDKN1B (Motti *et al.*, 2005a).

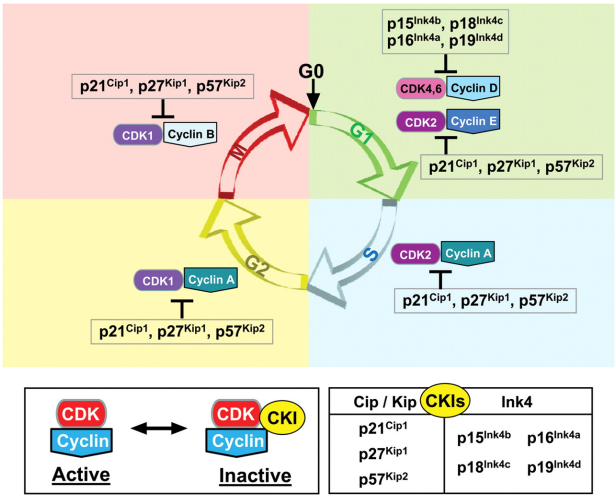

Figure I.4 - Cell cycle regulation by cyclins, CDK and CDK inhibitors. Progression through the four phases of cell cycle is regulated by the activation of protein complexes formed between cyclins (D-, E-, A- and B-type) and cyclin-dependent kinases (CDK4, -6, -2 and -1). Activated CDK are responsible for the phosphorylation of multiple targets involved in cell division. Two families of cyclin-dependent kinases inhibitors (CKI) are known to impair CDK activities (from Fuster *et al.*, 2010).

TP53 gene encodes the tumour suppressor protein p53, extensively studied due to the highly frequent detection of mutations or loss of expression in human cancer. One of the main functions of this protein is as transcription factor of genes involved in negative regulation of cell cycle, in senescence, apoptosis and DNA damage repair. One well-known effector of p53 is CDKN1A (Vousden and Lane, 2007). Interestingly, p53 is a unique tumour suppressor gene, because is frequently affected by monoallelic missense mutations that confer a dominant-negative action over wt forms, and have new oncogenic functions, including drug resistance, inhibition of apoptosis or induction of proliferation (Brosh and Rotter, 2009). Contrary to wt, p53 mutants are stabilised forms that can be readily detected in the nucleus and thus, alterations in p53 have been mostly studied by immunohistochemistry. Despite the variability in the frequency obtained using different techniques, these mutations represent the

most frequent alteration in ATC (50-65%) (Table I.1). The detection of mutations by preliminary screening techniques is smaller (38%), which shows that many mutated samples are not correctly identified. Alterations of p53 seem to be involved in about 20% of PDTC, staining is not as strong as in ATC and can be restricted only to areas of active invasion (Pilotti *et al.*, 1994a; Pollina *et al.*, 1996). Most importantly, authors have rarely detected mutations or p53-stained nuclei in WDTC, and positive staining or *TP53* genetic alterations are restricted to the ATC component in cases with concomitant differentiated areas (Nakamura *et al.*, 1992; Donghi *et al.*, 1993; Ito *et al.*, 1993; Matias-Guiu *et al.*, 1994; Pilotti *et al.*, 1994b; Matias-Guiu *et al.*, 1996; Lam *et al.*, 2000; Quiros *et al.*, 2005; Wiseman *et al.*, 2006).

3.4.3.e. Deregulated epithelial morphology, E-cadherin and β-catenin proteins

Cells maintain their adhesion and cell-cell or cell-matrix interaction through molecular structures localised at the plasma membrane: gap junctions, composed by connexins that allow intercellular communication; tight junctions characterised by occludin and claudins, which function as apical barriers; and desmosomes and adherens junctions, which mainly through cadherins-catenins complexes (in epithelial cells, mostly by E-cadherin and β-catenin interaction), mediate cell-cell adhesion and regulate cell polarity (Potter *et al.*, 1999). Catenin beta-1 (known as β-catenin), encoded by the proto-oncogene "catenin (cadherin-associated protein), beta 1, 88kDa" (*CTNNB1*), is also co-activator of target genes from the canonical WNT pathway (Figure I.5). This pathway, in the absence of ligand, maintains low levels of cytoplasmic β-catenin, through the action of a protein complex composed by axin 1 (AXIN1), adenomatous polyposis coli protein (APC), casein kinase I and GSK3B, which phosphorylates and actively targets β-catenin for proteasome degradation (MacDonald *et al.*, 2009). Upon pathway activation, β-catenin activating mutations or mutations in components of the destruction complex, β-catenin is not efficiently targeted, which leads to protein stabilization, accumulation and translocation to the nucleus, where it forms complexes with transcription factors of TCF/LEF family to stimulate expression of WNT responsive genes, the most known examples, "cyclin D1" (*CCND1*) and *MYC* (Klaus and Birchmeier, 2008). The WNT/β-catenin signalling and the crosstalk with E-cadherin (Heuberger and Birchmeier, 2010) are important regulators of cell proliferation, differentiation, cell adhesion and invasion, and thus deregulation of these pathways has been implicated in cancer development and progression.

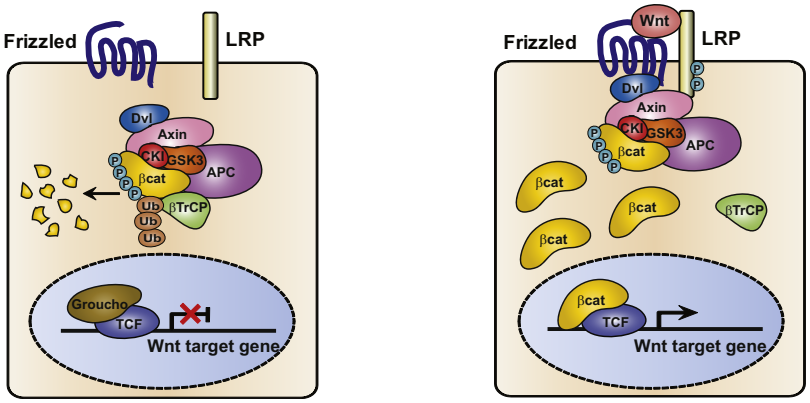

Figure I.5 - The canonical WNT/β-catenin pathway. (Left) In the absence of ligand, cytoplasmic β-catenin (βcat) forms a protein complex with axin 1 (AXIN1), adenomatous polyposis coli protein (APC), casein kinase I (CKI) and glycogen synthase kinase 3 beta (GSK3B), and becomes phosphorylated. This phosphorylation allows the β-catenin degradation by the ubiquitin-proteasome pathway and maintains groucho/TLE binding and repression of TCF/LEF transcription factors. (Right) WNT ligand activates the pathway, through frizzled receptors and low-density lipoprotein receptor-related proteins (LRP) complexes. The recruitment of Dishevelled (DVL) inactivates the destruction complex, which becomes saturated with phosphorylated β-catenin. Therefore, free cytoplasmic β-catenin translocates to the nucleus and activates WNT responsive genes (from Li *et al.*, 2012). P - phosphate group; Ub - ubiquitin; βTrCP - F-box/WD repeat-containing protein 1A (BTRC).

Immunohistochemistry analysis has revealed that decreased membranous and/or aberrant cytoplasmic staining of β-catenin may occur in WDTC (Cerrato *et al.*, 1998; Huang *et al.*, 1999; Garcia-Rostan *et al.*, 2001; Ishigaki *et al.*, 2002). In ATC, the majority of cases have exhibited a deregulated β-catenin staining, including absence of membranous expression, cytoplasmic localisation (Cerrato *et al.*, 1998; Garcia-Rostan *et al.*, 1999; Kurihara *et al.*, 2004; Wiseman *et al.*, 2007; Ralhan *et al.*, 2010) or nuclear staining (Garcia-Rostan *et al.*, 1999; Kurihara *et al.*, 2004; Ralhan *et al.*, 2010). Garcia-Rostan and collaborators showed that *CTNNB1* mutations (Table I.1), which are not found in benign tumours or WDTC (Garcia-Rostan *et al.*, 2001; Miyake *et al.*, 2001), were associated with nuclear localisation of β-catenin in 10 of the 19 mutated ATC. Other authors (Kurihara *et al.*, 2004; Hébrant *et al.*, 2012) were unable to replicate these findings. Analysis of PDTC showed that β-catenin deregulation is less marked than in ATC (Rocha *et al.*, 2003; Ralhan *et al.*, 2010) and *CTNNB1* mutations and/or nuclear immunoreactivity were only found in a minority of cases (Garcia-Rostan *et al.*, 2001). Mutations in other elements of the degradation complex, such as *APC* reported in 1 of 2 (Zeki *et al.*, 1994) and in 2 of 22 ATC (Kurihara *et al.*, 2004), and *AXIN1* reported in 18 of 22 ATC (Kurihara *et al.*, 2004), need to be further confirmed.

Loss or marked reduction of E-cadherin expression seems more relevant for PDTC and ATC, and is associated with dedifferentiation (Brabant *et al.*, 1993; Scheumman *et al.*, 1995; Soares *et al.*, 1997; Cerrato *et al.*, 1998; Naito *et al.*, 2001; Rocha *et al.*, 2003; Wiseman *et*

al., 2006; Mitselou *et al.*, 2007; Wiseman *et al.*, 2007), although no major genetic or epigenetic alterations have been reported (Graff *et al.*, 1998; Rocha *et al.*, 2003). Nonetheless, a recent study showed that histone deacetylase inhibitors were able to induce E-cadherin expression and restore membrane co-localisation of E-cadherin and β-catenin in ATC (Catalano *et al.*, 2012).

Table I.1 - Overall frequencies of the main gene alterations reported for PDTC and ATC.

Gene	ATC (%)	References	PDTC (%)	References
BRAF	**104/408 (25)**	(Garcia-Rostan *et al.*, 2005; Xing, 2005; Wang *et al.*, 2007a; Lee *et al.*, 2008; Ricarte-Filho *et al.*, 2009; Schwertheim *et al.*, 2009; Smallridge *et al.*, 2009; Sykorova *et al.*, 2010; Hébrant *et al.*, 2012; Santoro *et al.*, 2012)	**12/189 (6)**	(Nikiforova *et al.*, 2003a; Soares *et al.*, 2004; Fugazzola *et al.*, 2006; Costa *et al.*, 2008; Ricarte-Filho *et al.*, 2009; Schwertheim *et al.*, 2009; Volante *et al.*, 2009; Sykorova *et al.*, 2010)
N-, H-, KRAS	**64/307 (21)**	(Lemoine *et al.*, 1989; Manenti *et al.*, 1994; Oyama *et al.*, 1995; Capella *et al.*, 1996; Salvatore *et al.*, 1996; Bartolone *et al.*, 1998; Bouras *et al.*, 1998; Esapa *et al.*, 1999; Basolo *et al.*, 2000; Liu *et al.*, 2004; Garcia-Rostan *et al.*, 2005; Banito *et al.*, 2007; Wang *et al.*, 2007a; Ricarte-Filho *et al.*, 2009; Schwertheim *et al.*, 2009; Smallridge *et al.*, 2009; Hébrant *et al.*, 2012)	**79/252 (31)**	(Manenti *et al.*, 1994; Salvatore *et al.*, 1996; Pilotti *et al.*, 1997; Basolo *et al.*, 2000; Garcia-Rostan *et al.*, 2003; Banito *et al.*, 2007; Costa *et al.*, 2008; Ricarte-Filho *et al.*, 2009; Schwertheim *et al.*, 2009; Volante *et al.*, 2009)
TP53	**IHC 182/282 (65)**	(Dobashi *et al.*, 1993; Holm and Nesland, 1994; Matias-Guiu *et al.*, 1994; Pacini *et al.*, 1994; Pilotti *et al.*, 1994a; Soares *et al.*, 1994; Cameselle-Teijeiro *et al.*, 1995; Ito *et al.*, 1996; Pollina *et al.*, 1996; Basolo *et al.*, 1997; Moore *et al.*, 1998; Lam *et al.*, 2000; Garcia-Rostan *et al.*, 2005; Quiros *et al.*, 2005; Saltman *et al.*, 2006; Wiseman *et al.*, 2007; Gauchotte *et al.*, 2011)	**IHC 36/185 (19)**	(Dobashi *et al.*, 1993; Pilotti *et al.*, 1994a; Soares *et al.*, 1994; Ito *et al.*, 1996; Pollina *et al.*, 1996; Basolo *et al.*, 1997; Moore *et al.*, 1998; Lam *et al.*, 2000; Saltman *et al.*, 2006)
	Screening* 26/77 (34)	(Wright *et al.*, 1991; Ito *et al.*, 1992; Nakamura *et al.*, 1992; Yoshimoto *et al.*, 1992; Donghi *et al.*, 1993; Fagin *et al.*, 1993; Zou *et al.*, 1993; Dobashi *et al.*, 1994; Ho *et al.*, 1996; Jossart *et al.*, 1996; Salvatore *et al.*, 1996; Yane *et al.*, 1996; Zedenius *et al.*, 1996)	**Screening* 23/91 (25)**	(Donghi *et al.*, 1993; Dobashi *et al.*, 1994; Ho *et al.*, 1996; Salvatore *et al.*, 1996; Takeuchi *et al.*, 1999)
	Direct sequencing 14/28 (50)	(Matias-Guiu *et al.*, 1996; Wang *et al.*, 2007a; Hébrant *et al.*, 2012)	–	–
***PIK3CA* mutation**	**29/214 (14)**	(Garcia-Rostan *et al.*, 2005; Wu *et al.*, 2005; Hou *et al.*, 2007a; Wang *et al.*, 2007a; Santarpia *et al.*, 2008; Ricarte-Filho *et al.*, 2009; Hébrant *et al.*, 2012)	**Primary: 2/34 (6) Recurrent: 2/32 (6)**	(Ricarte-Filho *et al.*, 2009)
***PIK3CA* amplification§**	**39/96 (41)**	(Liu *et al.*, 2005; Hou *et al.*, 2007a; Santarpia *et al.*, 2008)	–	–
CTNNB1	**20/64 (31)**	(Garcia-Rostan *et al.*, 1999; Kurihara *et al.*, 2004; Hébrant *et al.*, 2012)	**7/39 (18)**	(Garcia-Rostan *et al.*, 2001; Rocha *et al.*, 2003)

*****Prior to sequencing, samples were screened by one of the following techniques: RNAse protection analysis; Single-strand conformational polymorphism; p53 over-expression by immunohistochemistry (IHC); Restriction-fragment length polymorphism; Denaturing gradient gel electrophoresis. §Copy number ≥ 4

4. References

Abate EG, Smallridge RC (2011). Managing anaplastic thyroid carcinoma. *Expert Rev Endocrinol Metab* **6:** 793-809.

Abulaiti A, Fikaris AJ, Tsygankova OM, Meinkoth JL (2006). Ras induces chromosome instability and abrogation of the DNA damage response. *Cancer Res* **66:** 10505-10512.

Anderson K, Lutz C, van Delft FW, Bateman CM, Guo Y, Colman SM *et al* (2011). Genetic variegation of clonal architecture and propagating cells in leukaemia. *Nature* **469:** 356-361.

Arturi F, Russo D, Schlumberger M, du Villard JA, Caillou B, Vigneri P *et al* (1998). Iodide symporter gene expression in human thyroid tumors. *J Clin Endocrinol Metab* **83:** 2493-2496.

Au AY, McBride C, Wilhelm KG, Jr., Koenig RJ, Speller B, Cheung L *et al* (2006). PAX8-peroxisome proliferator-activated receptor gamma (PPARgamma) disrupts normal PAX8 or PPARgamma transcriptional function and stimulates follicular thyroid cell growth. *Endocrinology* **147:** 367-376.

Avvedimento VE, Monticelli A, Tramontano D, Polistina C, Nitsch L, Di Lauro R (1985). Differential expression of thyroglobulin gene in normal and transformed thyroid cells. *Eur J Biochem* **149:** 467-472.

Avvedimento VE, Musti A, Fusco A, Bonapace MJ, Di Lauro R (1988). Neoplastic transformation inactivates specific trans-acting factor(s) required for the expression of the thyroglobulin gene. *Proc Natl Acad Sci U S A* **85:** 1744-1748.

Baker SJ, Fearon ER, Nigro JM, Hamilton SR, Preisinger AC, Jessup JM *et al* (1989). Chromosome 17 deletions and p53 gene mutations in colorectal carcinomas. *Science* **244:** 217-221.

Baker SJ, Markowitz S, Fearon ER, Willson JK, Vogelstein B (1990). Suppression of human colorectal carcinoma cell growth by wild-type p53. *Science* **249:** 912-915.

Baldassarre G, Belletti B, Bruni P, Boccia A, Trapasso F, Pentimalli F *et al* (1999). Overexpressed cyclin D3 contributes to retaining the growth inhibitor p27 in the cytoplasm of thyroid tumor cells. *J Clin Invest* **104:** 865-874.

Ball E, Bond J, Franc B, Demicco C, Wynford-Thomas D (2007). An immunohistochemical study of p16(INK4a) expression in multistep thyroid tumourigenesis. *Eur J Cancer* **43:** 194-201.

Banito A, Pinto AE, Espadinha C, Marques AR, Leite V (2007). Aneuploidy and RAS mutations are mutually exclusive events in the development of well-differentiated thyroid follicular tumours. *Clin Endocrinol (Oxf)* **67:** 706-711.

Baratta MG, Porreca I, Di Lauro R (2009). Oncogenic ras blocks the cAMP pathway and dedifferentiates thyroid cells via an impairment of pax8 transcriptional activity. *Mol Endocrinol* **23:** 838-848.

Bartolone L, Vermiglio F, Finocchiaro MD, Violi MA, French D, Pontecorvi A *et al* (1998). Thyroid follicular oncogenesis in iodine-deficient and iodine-sufficient areas: search for alterations of the ras, met and bFGF oncogenes and of the Rb anti-oncogene. *J Endocrinol Invest* **21:** 680-687.

Basolo F, Pollina L, Fontanini G, Fiore L, Pacini F, Baldanzi A (1997). Apoptosis and proliferation in thyroid carcinoma: correlation with bcl-2 and p53 protein expression. *Br J Cancer* **75:** 537-541.

Basolo F, Pisaturo F, Pollina LE, Fontanini G, Elisei R, Molinaro E *et al* (2000). N-ras mutation in poorly differentiated thyroid carcinomas: correlation with bone metastases and inverse correlation to thyroglobulin expression. *Thyroid* **10:** 19-23.

Basolo F, Torregrossa L, Giannini R, Miccoli M, Lupi C, Sensi E *et al* (2010). Correlation between the BRAF V600E mutation and tumor invasiveness in papillary thyroid carcinomas smaller than 20 millimeters: analysis of 1060 cases. *J Clin Endocrinol Metab* **95:** 4197-4205.

Bedford FK, Ashworth A, Enver T, Wiedemann LM (1993). HEX: a novel homeobox gene expressed during haematopoiesis and conserved between mouse and human. *Nucleic Acids Res* **21:** 1245-1249.

Begum S, Rosenbaum E, Henrique R, Cohen Y, Sidransky D, Westra WH (2004). BRAF mutations in anaplastic thyroid carcinoma: implications for tumor origin, diagnosis and treatment. *Mod Pathol* **17:** 1359-1363.

Bernstein A, MacCormick R, Martin GS (1976). Transformation-defective mutants of avian sarcoma viruses: The genetic relationship between conditional and nonconditional mutants. *Virology* **70:** 206-209.

Bianco AC, Kim BW (2006). Deiodinases: implications of the local control of thyroid hormone action. *J Clin Invest* **116:** 2571-2579.

Bizhanova A, Kopp P (2009). Minireview: The sodium-iodide symporter NIS and pendrin in iodide homeostasis of the thyroid. *Endocrinology* **150:** 1084-1090.

Boisvert FM, Ahmad Y, Gierlinski M, Charriere F, Lamont D, Scott M *et al* (2012). A quantitative spatial proteomics analysis of proteome turnover in human cells. *Mol Cell Proteomics* **11:** M111 011429.

Boltze C, Zack S, Quednow C, Bettge S, Roessner A, Schneider-Stock R (2003). Hypermethylation of the CDKN2/p16INK4A promotor in thyroid carcinogenesis. *Pathol Res Pract* **199:** 399-404.

Bosetti C, Bertuccio P, Levi F, Lucchini F, Negri E, La Vecchia C (2008). Cancer mortality in the European Union, 1970-2003, with a joinpoint analysis. *Ann Oncol* **19:** 631-640.

Bouras M, Bertholon J, Dutrieux-Berger N, Parvaz P, Paulin C, Revol A (1998). Variability of Ha-ras (codon 12) proto-oncogene mutations in diverse thyroid cancers. *Eur J Endocrinol* **139:** 209-216.

Boveri T (2008). Concerning the origin of malignant tumours by Theodor Boveri. Translated and annotated by Henry Harris. *J Cell Sci* **121 Suppl 1:** 1-84. (Original work published 1914).

Brabant G, Maenhaut C, Kohrle J, Scheumann G, Dralle H, Hoang-Vu C *et al* (1991). Human thyrotropin receptor gene: expression in thyroid tumors and correlation to markers of thyroid differentiation and dedifferentiation. *Mol Cell Endocrinol* **82:** R7-12.

Brabant G, Hoang-Vu C, Cetin Y, Dralle H, Scheumann G, Molne J *et al* (1993). E-cadherin: a differentiation marker in thyroid malignancies. *Cancer Res* **53:** 4987-4993.

Braverman LE, Cooper D (2012). *Werner & Ingbar's The Thyroid: A Fundamental and Clinical Text*. Wolters Kluwer Health.

Brosh R, Rotter V (2009). When mutants gain new powers: news from the mutant p53 field. *Nat Rev Cancer* **9:** 701-713.

Brown RS (2004). Minireview: developmental regulation of thyrotropin receptor gene expression in the fetal and newborn thyroid. *Endocrinology* **145:** 4058-4061.

Bruni P, Boccia A, Baldassarre G, Trapasso F, Santoro M, Chiappetta G *et al* (2000). PTEN expression is reduced in a subset of sporadic thyroid carcinomas: evidence that PTEN-growth suppressing activity in thyroid cancer cells mediated by p27kip1. *Oncogene* **19:** 3146-3155.

Burgess JR, Tucker P (2006). Incidence trends for papillary thyroid carcinoma and their correlation with thyroid surgery and thyroid fine-needle aspirate cytology. *Thyroid* **16:** 47-53.

Caillou B, Troalen F, Baudin E, Talbot M, Filetti S, Schlumberger M *et al* (1998). Na+/I- symporter distribution in human thyroid tissues: an immunohistochemical study. *J Clin Endocrinol Metab* **83:** 4102-4106.

Calabrò V, Strazzullo M, La Mantia G, Fedele M, Paulin C, Fusco A *et al* (1996). Status and expression of the p16INK4 gene in human thyroid tumors and thyroid-tumor cell lines. *Int J Cancer* **67:** 29-34.

Calin GA, Croce CM (2006). MicroRNA signatures in human cancers. *Nat Rev Cancer* **6:** 857-866.

Camacho PM, Almeda F, Cobin R, Cosma M, Dayal A, Emmanuele M *et al* (2011). *Clinical Endocrinology and Metabolism*. Manson Publishing Limited.

Cameselle-Teijeiro J, Febles-Perez C, Sobrinho-Simões M (1995). Papillary and mucoepidermoid carcinoma of the thyroid with anaplastic transformation: a case report with histologic and immunohistochemical findings that support a provocative histogenetic hypothesis. *Pathol Res Pract* **191:** 1214-1221.

Campbell PJ, Pleasance ED, Stephens PJ, Dicks E, Rance R, Goodhead I *et al* (2008). Subclonal phylogenetic structures in cancer revealed by ultra-deep sequencing. *Proc Natl Acad Sci U S A* **105:** 13081-13086.

Campbell PJ, Yachida S, Mudie LJ, Stephens PJ, Pleasance ED, Stebbings LA *et al* (2010). The patterns and dynamics of genomic instability in metastatic pancreatic cancer. *Nature* **467:** 1109-1113.

Cantwell-Dorris ER, O'Leary JJ, Sheils OM (2011). BRAFV600E: implications for carcinogenesis and molecular therapy. *Mol Cancer Ther* **10:** 385-394.

Capella G, Matias-Guiu X, Ampudia X, de Leiva A, Perucho M, Prat J (1996). Ras oncogene mutations in thyroid tumors: polymerase chain reaction-restriction-fragment-length polymorphism analysis from paraffin-embedded tissues. *Diagn Mol Pathol* **5:** 45-52.

Carta C, Moretti S, Passeri L, Barbi F, Avenia N, Cavaliere A *et al* (2006). Genotyping of an Italian papillary thyroid carcinoma cohort revealed high prevalence of BRAF mutations, absence of RAS mutations and allowed the detection of a new mutation of BRAF oncoprotein (BRAF(V599lns)). *Clin Endocrinol (Oxf)* **64:** 105-109.

Carthew RW, Sontheimer EJ (2009). Origins and Mechanisms of miRNAs and siRNAs. *Cell* **136:** 642-655.

Castro P, Roque L, Magalhães J, Sobrinho-Simões M (2005). A subset of the follicular variant of papillary thyroid carcinoma harbors the PAX8-PPARgamma translocation. *Int J Surg Pathol* **13:** 235-238.

Castro P, Rebocho AP, Soares RJ, Magalhães J, Roque L, Trovisco V *et al* (2006). PAX8-PPARgamma rearrangement is frequently detected in the follicular variant of papillary thyroid carcinoma. *J Clin Endocrinol Metab* **91:** 213-220.

Catalano MG, Fortunati N, Pugliese M, Marano F, Ortoleva L, Poli R *et al* (2012). Histone deacetylase inhibition modulates E-cadherin expression and suppresses migration and invasion of anaplastic thyroid cancer cells. *J Clin Endocrinol Metab* **97:** E1150-1159.

Cavenee WK, Dryja TP, Phillips RA, Benedict WF, Godbout R, Gallie BL *et al* (1983). Expression of recessive alleles by chromosomal mechanisms in retinoblastoma. *Nature* **305:** 779-784.

Cerrato A, Fulciniti F, Avallone A, Benincasa G, Palombini L, Grieco M (1998). Beta- and gamma-catenin expression in thyroid carcinomas. *J Pathol* **185:** 267-272.

Chakravarty D, Santos E, Ryder M, Knauf JA, Liao XH, West BL *et al* (2011). Small-molecule MAPK inhibitors restore radioiodine incorporation in mouse thyroid cancers with conditional BRAF activation. *J Clin Invest* **121:** 4700-4711.

Charles RP, Iezza G, Amendola E, Dankort D, McMahon M (2011). Mutationally activated BRAF(V600E) elicits papillary thyroid cancer in the adult mouse. *Cancer Res* **71:** 3863-3871.

Cheung L, Messina M, Gill A, Clarkson A, Learoyd D, Delbridge L *et al* (2003). Detection of the PAX8-PPAR gamma fusion oncogene in both follicular thyroid carcinomas and adenomas. *J Clin Endocrinol Metab* **88:** 354-357.

Chiosea S, Nikiforova M, Zuo H, Ogilvie J, Gandhi M, Seethala RR *et al* (2009). A novel complex BRAF mutation detected in a solid variant of papillary thyroid carcinoma. *Endocr Pathol* **20:** 122-126.

Chung CH, Bernard PS, Perou CM (2002). Molecular portraits and the family tree of cancer. *Nat Genet* **32 Suppl:** 533-540.

Ciampi R, Knauf JA, Kerler R, Gandhi M, Zhu Z, Nikiforova MN *et al* (2005). Oncogenic AKAP9-BRAF fusion is a novel mechanism of MAPK pathway activation in thyroid cancer. *J Clin Invest* **115:** 94-101.

Civitareale D, Lonigro R, Sinclair AJ, Di Lauro R (1989). A thyroid-specific nuclear protein essential for tissue-specific expression of the thyroglobulin promoter. *EMBO J* **8:** 2537-2542.

Cohen Y, Xing M, Mambo E, Guo Z, Wu G, Trink B *et al* (2003). BRAF mutation in papillary thyroid carcinoma. *J Natl Cancer Inst* **95:** 625-627.

Cohen Y, Rosenbaum E, Clark DP, Zeiger MA, Umbricht CB, Tufano RP *et al* (2004). Mutational analysis of BRAF in fine needle aspiration biopsies of the thyroid: a potential application for the preoperative assessment of thyroid nodules. *Clin Cancer Res* **10:** 2761-2765.

Collett MS, Erikson E, Purchio AF, Brugge JS, Erikson RL (1979). A normal cell protein similar in structure and function to the avian sarcoma virus transforming gene product. *Proc Natl Acad Sci U S A* **76:** 3159-3163.

Corvilain B, Van Sande J, Dumont JE, Vassart G (2001). Somatic and germline mutations of the TSH receptor and thyroid diseases. *Clin Endocrinol (Oxf)* **55:** 143-158.

Costa AM, Herrero A, Fresno MF, Heymann J, Alvarez JA, Cameselle-Teijeiro J *et al* (2008). BRAF mutation associated with other genetic events identifies a subset of aggressive papillary thyroid carcinoma. *Clin Endocrinol (Oxf)* **68:** 618-634.

Cramer JD, Fu P, Harth KC, Margevicius S, Wilhelm SM (2010). Analysis of the rising incidence of thyroid cancer using the Surveillance, Epidemiology and End Results national cancer data registry. *Surgery* **148:** 1147-1152; discussion 1152-1143.

Cullen BR (2006). Viruses and microRNAs. *Nat Genet* **38 Suppl:** S25-30.

Dahia PL, Marsh DJ, Zheng Z, Zedenius J, Komminoth P, Frisk T *et al* (1997). Somatic deletions and mutations in the Cowden disease gene, PTEN, in sporadic thyroid tumors. *Cancer Res* **57:** 4710-4713.

Dahia PL (2000). PTEN, a unique tumor suppressor gene. *Endocr Relat Cancer* **7:** 115-129.

Damante G, Di Lauro R (1994). Thyroid-specific gene expression. *Biochim Biophys Acta* **1218:** 255-266.

Davies H, Bignell GR, Cox C, Stephens P, Edkins S, Clegg S *et al* (2002). Mutations of the BRAF gene in human cancer. *Nature* **417:** 949-954.

Davies H, Hunter C, Smith R, Stephens P, Greenman C, Bignell G *et al* (2005). Somatic mutations of the protein kinase gene family in human lung cancer. *Cancer Res* **65:** 7591-7595.

Davies L, Welch HG (2006). Increasing incidence of thyroid cancer in the United States, 1973-2002. *JAMA* **295:** 2164-2167.

De Felice M, Di Lauro R (2004). Thyroid development and its disorders: genetics and molecular mechanisms. *Endocr Rev* **25:** 722-746.

De Felice M, Postiglione MP, Di Lauro R (2004). Minireview: thyrotropin receptor signaling in development and differentiation of the thyroid gland: insights from mouse models and human diseases. *Endocrinology* **145:** 4062-4067.

De Felice M, Di Lauro R (2011). Minireview: Intrinsic and extrinsic factors in thyroid gland development: an update. *Endocrinology* **152:** 2948-2956.

de Souza EC, Padron AS, Braga WM, de Andrade BM, Vaisman M, Nasciutti LE *et al* (2010). MTOR downregulates iodide uptake in thyrocytes. *J Endocrinol* **206:** 113-120.

De Vita G, Bauer L, da Costa VM, De Felice M, Baratta MG, De Menna M *et al* (2005). Dose-dependent inhibition of thyroid differentiation by RAS oncogenes. *Mol Endocrinol* **19:** 76-89.

DeLellis RA, Lloyd RV, Heitz PU, Eng C (2004). *World Health Organization Classification of Tumours. Pathology and Genetics of Tumours of Endocrine Organs*. IARC Press: Lyon, France.

Der CJ, Krontiris TG, Cooper GM (1982). Transforming genes of human bladder and lung carcinoma cell lines are homologous to the ras genes of Harvey and Kirsten sarcoma viruses. *Proc Natl Acad Sci U S A* **79:** 3637-3640.

Di Cristofaro J, Marcy M, Vasko V, Sebag F, Fakhry N, Wynford-Thomas D *et al* (2006). Molecular genetic study comparing follicular variant versus classic papillary thyroid carcinomas: association of N-ras mutation in codon 61 with follicular variant. *Hum Pathol* **37:** 824-830.

Diallo-Krou E, Yu J, Colby LA, Inoki K, Wilkinson JE, Thomas DG *et al* (2009). Paired box gene 8-peroxisome proliferator-activated receptor-gamma fusion protein and loss of phosphatase and tensin homolog synergistically cause thyroid hyperplasia in transgenic mice. *Endocrinology* **150:** 5181-5190.

Diaz LA, Jr., Williams RT, Wu J, Kinde I, Hecht JR, Berlin J *et al* (2012). The molecular evolution of acquired resistance to targeted EGFR blockade in colorectal cancers. *Nature* **486:** 537-540.

Ding L, Ellis MJ, Li S, Larson DE, Chen K, Wallis JW *et al* (2010). Genome remodelling in a basal-like breast cancer metastasis and xenograft. *Nature* **464:** 999-1005.

Ding L, Ley TJ, Larson DE, Miller CA, Koboldt DC, Welch JS *et al* (2012). Clonal evolution in relapsed acute myeloid leukaemia revealed by whole-genome sequencing. *Nature* **481:** 506-510.

Dobashi Y, Sakamoto A, Sugimura H, Mernyei M, Mori M, Oyama T *et al* (1993). Overexpression of p53 as a possible prognostic factor in human thyroid carcinoma. *Am J Surg Pathol* **17:** 375-381.

Dobashi Y, Sugimura H, Sakamoto A, Mernyei M, Mori M, Oyama T *et al* (1994). Stepwise participation of p53 gene mutation during dedifferentiation of human thyroid carcinomas. *Diagn Mol Pathol* **3:** 9-14.

Dobson ME, Diallo-Krou E, Grachtchouk V, Yu J, Colby LA, Wilkinson JE *et al* (2011). Pioglitazone induces a proadipogenic antitumor response in mice with PAX8-PPARgamma fusion protein thyroid carcinoma. *Endocrinology* **152:** 4455-4465.

Donghi R, Longoni A, Pilotti S, Michieli P, Della Porta G, Pierotti MA (1993). Gene p53 mutations are restricted to poorly differentiated and undifferentiated carcinomas of the thyroid gland. *J Clin Invest* **91:** 1753-1760.

Durante C, Puxeddu E, Ferretti E, Morisi R, Moretti S, Bruno R *et al* (2007). BRAF mutations in papillary thyroid carcinomas inhibit genes involved in iodine metabolism. *J Clin Endocrinol Metab* **92:** 2840-2843.

Dwight T, Thoppe SR, Foukakis T, Lui WO, Wallin G, Hoog A *et al* (2003). Involvement of the PAX8/peroxisome proliferator-activated receptor gamma rearrangement in follicular thyroid tumors. *J Clin Endocrinol Metab* **88:** 4440-4445.

Elisei R, Pinchera A, Romei C, Gryczynska M, Pohl V, Maenhaut C *et al* (1994). Expression of thyrotropin receptor (TSH-R), thyroglobulin, thyroperoxidase, and calcitonin messenger ribonucleic acids in thyroid carcinomas: evidence of TSH-R gene transcript in medullary histotype. *J Clin Endocrinol Metab* **78:** 867-871.

Elisei R, Ugolini C, Viola D, Lupi C, Biagini A, Giannini R *et al* (2008). BRAF(V600E) mutation and outcome of patients with papillary thyroid carcinoma: a 15-year median follow-up study. *J Clin Endocrinol Metab* **93:** 3943-3949.

Engelman JA, Luo J, Cantley LC (2006). The evolution of phosphatidylinositol 3-kinases as regulators of growth and metabolism. *Nat Rev Genet* **7:** 606-619.

Erickson LA, Jin L, Wollan PC, Thompson GB, van Heerden J, Lloyd RV (1998). Expression of p27kip1 and Ki-67 in benign and malignant thyroid tumors. *Mod Pathol* **11:** 169-174.

Esapa CT, Johnson SJ, Kendall-Taylor P, Lennard TW, Harris PE (1999). Prevalence of Ras mutations in thyroid neoplasia. *Clin Endocrinol (Oxf)* **50:** 529-535.

Espadinha C, Cavaco BM, Leite V (2007). PAX8PPARgamma stimulates cell viability and modulates expression of thyroid-specific genes in a human thyroid cell line. *Thyroid* **17:** 497-509.

Espadinha C, Santos JR, Sobrinho LG, Bugalho MJ (2009). Expression of iodine metabolism genes in human thyroid tissues: evidence for age and BRAFV600E mutation dependency. *Clin Endocrinol (Oxf)* **70:** 629-635.

Eszlinger M, Krohn K, Hauptmann S, Dralle H, Giordano TJ, Paschke R (2008). Perspectives for improved and more accurate classification of thyroid epithelial tumors. *J Clin Endocrinol Metab* **93:** 3286-3294.

Fabbro D, Di Loreto C, Beltrami CA, Belfiore A, Di Lauro R, Damante G (1994). Expression of thyroid-specific transcription factors TTF-1 and PAX-8 in human thyroid neoplasms. *Cancer Res* **54:** 4744-4749.

Fagin JA, Matsuo K, Karmakar A, Chen DL, Tang SH, Koeffler HP (1993). High prevalence of mutations of the p53 gene in poorly differentiated human thyroid carcinomas. *J Clin Invest* **91:** 179-184.

Fagman H, Nilsson M (2010). Morphogenesis of the thyroid gland. *Mol Cell Endocrinol* **323:** 35-54.

Fagman H, Amendola E, Parrillo L, Zoppoli P, Marotta P, Scarfo M *et al* (2011). Gene expression profiling at early organogenesis reveals both common and diverse mechanisms in foregut patterning. *Dev Biol* **359:** 163-175.

Fajas L, Debril M, Auwerx J (2001). Peroxisome proliferator-activated receptor-gamma: from adipogenesis to carcinogenesis. *J Mol Endocrinol* **27:** 1-9.

Farrow B, Evers BM (2003). Activation of PPARgamma increases PTEN expression in pancreatic cancer cells. *Biochem Biophys Res Commun* **301:** 50-53.

Faustino A, Couto JP, Populo H, Rocha AS, Pardal F, Cameselle-Teijeiro JM *et al* (2012). mTOR pathway overactivation in BRAF mutated papillary thyroid carcinoma. *J Clin Endocrinol Metab* **97:** E1139-1149.

Fearon ER, Vogelstein B (1990). A genetic model for colorectal tumorigenesis. *Cell* **61:** 759-767.

Feldt-Rasmussen U (2001). Iodine and cancer. *Thyroid* **11:** 483-486.

Ferlay J, Parkin DM, Steliarova-Foucher E (2010a). Estimates of cancer incidence and mortality in Europe in 2008. *Eur J Cancer* **46:** 765-781.

Ferlay J, Shin HR, Bray F, Forman D, Mathers C, Parkin DM (2010b). Estimates of worldwide burden of cancer in 2008: GLOBOCAN 2008. *Int J Cancer* **127:** 2893-2917.

Finlay CA, Hinds PW, Levine AJ (1989). The p53 proto-oncogene can act as a suppressor of transformation. *Cell* **57:** 1083-1093.

Floor SL, Dumont JE, Maenhaut C, Raspe E (2012). Hallmarks of cancer: of all cancer cells, all the time? *Trends Mol Med* **18:** 509-515.

Francis-Lang H, Price M, Martin U, Di Lauro R (1990). The thyroid specific nuclear factor, TTF-1, binds to the rat thyroperoxidase promoter. In: Carayon P, Ruf J (eds). *Thyroperoxidase and thyroid autoimmunity*. John Libbey Eurotext Ltd. pp 25-32.

Francis-Lang H, Price M, Polycarpou-Schwarz M, Di Lauro R (1992a). Cell-type-specific expression of the rat thyroperoxidase promoter indicates common mechanisms for thyroid-specific gene expression. *Mol Cell Biol* **12:** 576-588.

Francis-Lang H, Zannini M, De Felice M, Berlingieri MT, Fusco A, Di Lauro R (1992b). Multiple mechanisms of interference between transformation and differentiation in thyroid cells. *Mol Cell Biol* **12:** 5793-5800.

Franco AT, Malaguarnera R, Refetoff S, Liao XH, Lundsmith E, Kimura S *et al* (2011). Thyrotrophin receptor signaling dependence of Braf-induced thyroid tumor initiation in mice. *Proc Natl Acad Sci U S A* **108:** 1615-1620.

Friedel CC, Dolken L, Ruzsics Z, Koszinowski UH, Zimmer R (2009). Conserved principles of mammalian transcriptional regulation revealed by RNA half-life. *Nucleic Acids Res* **37:** e115.

Friend SH, Bernards R, Rogelj S, Weinberg RA, Rapaport JM, Albert DM *et al* (1986). A human DNA segment with properties of the gene that predisposes to retinoblastoma and osteosarcoma. *Nature* **323:** 643-646.

Frisk T, Foukakis T, Dwight T, Lundberg J, Hoog A, Wallin G *et al* (2002). Silencing of the PTEN tumor-suppressor gene in anaplastic thyroid cancer. *Genes Chromosomes Cancer* **35:** 74-80.

Fugazzola L, Puxeddu E, Avenia N, Romei C, Cirello V, Cavaliere A *et al* (2006). Correlation between B-RAFV600E mutation and clinico-pathologic parameters in papillary thyroid carcinoma: data from a multicentric Italian study and review of the literature. *Endocr Relat Cancer* **13:** 455-464.

Fukushima T, Suzuki S, Mashiko M, Ohtake T, Endo Y, Takebayashi Y *et al* (2003). BRAF mutations in papillary carcinomas of the thyroid. *Oncogene* **22:** 6455-6457.

Fung YK, Murphree AL, T'Ang A, Qian J, Hinrichs SH, Benedict WF (1987). Structural evidence for the authenticity of the human retinoblastoma gene. *Science* **236:** 1657-1661.

Fusco A, Pinto A, Tramontano D, Tajana G, Vecchio G, Tsuchida N (1982). Block in the expression of differentiation markers of rat thyroid epithelial cells by transformation with Kirsten murine sarcoma virus. *Cancer Res* **42:** 618-626.

Fuster JJ, Fernandez P, Gonzalez-Navarro H, Silvestre C, Nabah YN, Andres V (2010). Control of cell proliferation in atherosclerosis: insights from animal models and human studies. *Cardiovasc Res* **86:** 254-264.

Gandhi M, Evdokimova V, Nikiforov YE (2010). Mechanisms of chromosomal rearrangements in solid tumors: the model of papillary thyroid carcinoma. *Mol Cell Endocrinol* **321:** 36-43.

Garcia B, Santisteban P (2002). PI3K is involved in the IGF-I inhibition of TSH-induced sodium/iodide symporter gene expression. *Mol Endocrinol* **16:** 342-352.

Garcia-Rostan G, Tallini G, Herrero A, D'Aquila TG, Carcangiu ML, Rimm DL (1999). Frequent mutation and nuclear localization of beta-catenin in anaplastic thyroid carcinoma. *Cancer Res* **59:** 1811-1815.

Garcia-Rostan G, Camp RL, Herrero A, Carcangiu ML, Rimm DL, Tallini G (2001). Beta-catenin dysregulation in thyroid neoplasms: down-regulation, aberrant nuclear expression, and CTNNB1 exon 3 mutations are markers for aggressive tumor phenotypes and poor prognosis. *Am J Pathol* **158:** 987-996.

Garcia-Rostan G, Zhao H, Camp RL, Pollan M, Herrero A, Pardo J *et al* (2003). ras mutations are associated with aggressive tumor phenotypes and poor prognosis in thyroid cancer. *J Clin Oncol* **21:** 3226-3235.

Garcia-Rostan G, Costa AM, Pereira-Castro I, Salvatore G, Hernandez R, Hermsem MJ *et al* (2005). Mutation of the PIK3CA gene in anaplastic thyroid cancer. *Cancer Res* **65:** 10199-10207.

Gauchotte G, Philippe C, Lacomme S, Leotard B, Wissler MP, Allou L *et al* (2011). BRAF, p53 and SOX2 in anaplastic thyroid carcinoma: evidence for multistep carcinogenesis. *Pathology* **43:** 447-452.

Gerard CM, Lefort A, Libert F, Christophe D, Dumont JE, Vassart G (1988). Transcriptional regulation of the thyroperoxydase gene by thyrotropin and forskolin. *Mol Cell Endocrinol* **60:** 239-242.

Gerlinger M, Rowan AJ, Horswell S, Larkin J, Endesfelder D, Gronroos E *et al* (2012). Intratumor heterogeneity and branched evolution revealed by multiregion sequencing. *N Engl J Med* **366:** 883-892.

Gil J, Peters G (2006). Regulation of the INK4b-ARF-INK4a tumour suppressor locus: all for one or one for all. *Nat Rev Mol Cell Biol* **7:** 667-677.

Gilbert SF (2000). *Developmental Biology*. Sinauer Associates.

Gimm O, Perren A, Weng LP, Marsh DJ, Yeh JJ, Ziebold U *et al* (2000). Differential nuclear and cytoplasmic expression of PTEN in normal thyroid tissue, and benign and malignant epithelial thyroid tumors. *Am J Pathol* **156:** 1693-1700.

Gire V, Marshall CJ, Wynford-Thomas D (1999). Activation of mitogen-activated protein kinase is necessary but not sufficient for proliferation of human thyroid epithelial cells induced by mutant Ras. *Oncogene* **18:** 4819-4832.

Gire V, Marshall C, Wynford-Thomas D (2000). PI-3-kinase is an essential anti-apoptotic effector in the proliferative response of primary human epithelial cells to mutant RAS. *Oncogene* **19:** 2269-2276.

Graff JR, Greenberg VE, Herman JG, Westra WH, Boghaert ER, Ain KB *et al* (1998). Distinct patterns of E-cadherin CpG island methylation in papillary, follicular, Hurthle's cell, and poorly differentiated human thyroid carcinoma. *Cancer Res* **58:** 2063-2066.

Grasberger H (2010). Defects of thyroidal hydrogen peroxide generation in congenital hypothyroidism. *Mol Cell Endocrinol* **322:** 99-106.

Greenman C, Stephens P, Smith R, Dalgliesh GL, Hunter C, Bignell G *et al* (2007). Patterns of somatic mutation in human cancer genomes. *Nature* **446:** 153-158.

Gregory Powell J, Wang X, Allard BL, Sahin M, Wang XL, Hay ID *et al* (2004). The PAX8/PPARgamma fusion oncoprotein transforms immortalized human thyrocytes through a mechanism probably involving wild-type PPARgamma inhibition. *Oncogene* **23:** 3634-3641.

Griffith OL, Melck A, Jones SJ, Wiseman SM (2006). Meta-analysis and meta-review of thyroid cancer gene expression profiling studies identifies important diagnostic biomarkers. *J Clin Oncol* **24:** 5043-5051.

Guazzi S, Price M, De Felice M, Damante G, Mattei MG, Di Lauro R (1990). Thyroid nuclear factor 1 (TTF-1) contains a homeodomain and displays a novel DNA binding specificity. *EMBO J* **9:** 3631-3639.

Guerra A, Fugazzola L, Marotta V, Cirillo M, Rossi S, Cirello V *et al* (2012). A high percentage of BRAFV600E alleles in papillary thyroid carcinoma predicts a poorer outcome. *J Clin Endocrinol Metab* **97:** 2333-2340.

Gursoy A (2010). Rising thyroid cancer incidence in the world might be related to insulin resistance. *Med Hypotheses* **74:** 35-36.

Hanahan D, Weinberg RA (2000). The hallmarks of cancer. *Cell* **100:** 57-70.

Hanahan D, Weinberg RA (2011). Hallmarks of cancer: the next generation. *Cell* **144:** 646-674.

Hébrant A, van Staveren WC, Maenhaut C, Dumont JE, Leclere J (2011). Genetic hyperthyroidism: hyperthyroidism due to activating TSHR mutations. *Eur J Endocrinol* **164:** 1-9.

Hébrant A, Dom G, Dewaele M, Andry G, Tresallet C, Leteurtre E *et al* (2012). mRNA expression in papillary and anaplastic thyroid carcinoma: molecular anatomy of a killing switch. *PLoS One* **7:** e37807.

Heuberger J, Birchmeier W (2010). Interplay of cadherin-mediated cell adhesion and canonical Wnt signaling. *Cold Spring Harb Perspect Biol* **2:** a002915.

Ho YS, Tseng SC, Chin TY, Hsieh LL, Lin JD (1996). p53 gene mutation in thyroid carcinoma. *Cancer Lett* **103:** 57-63.

Hoang-Vu C, Dralle H, Scheumann G, Maenhaut C, Horn R, von zur Muhlen A *et al* (1992). Gene expression of differentiation- and dedifferentiation markers in normal and malignant human thyroid tissues. *Exp Clin Endocrinol* **100:** 51-56.

Holm R, Nesland JM (1994). Retinoblastoma and p53 tumour suppressor gene protein expression in carcinomas of the thyroid gland. *J Pathol* **172:** 267-272.

Hou P, Liu D, Shan Y, Hu S, Studeman K, Condouris S *et al* (2007a). Genetic alterations and their relationship in the phosphatidylinositol 3-kinase/Akt pathway in thyroid cancer. *Clin Cancer Res* **13:** 1161-1170.

Hou P, Liu D, Xing M (2007b). Functional characterization of the T1799-1801del and A1799-1816ins BRAF mutations in papillary thyroid cancer. *Cell Cycle* **6:** 377-379.

Hou P, Ji M, Xing M (2008). Association of PTEN gene methylation with genetic alterations in the phosphatidylinositol 3-kinase/AKT signaling pathway in thyroid tumors. *Cancer* **113:** 2440-2447.

Huang HJ, Yee JK, Shew JY, Chen PL, Bookstein R, Friedmann T *et al* (1988). Suppression of the neoplastic phenotype by replacement of the RB gene in human cancer cells. *Science* **242:** 1563-1566.

Huang SH, Wu JC, Chang KJ, Liaw KY, Wang SM (1999). Expression of the cadherin-catenin complex in well-differentiated human thyroid neoplastic tissue. *Thyroid* **9:** 1095-1103.

Huber MA, Kraut N, Beug H (2005). Molecular requirements for epithelial-mesenchymal transition during tumor progression. *Curr Opin Cell Biol* **17:** 548-558.

Hunt JL, Tometsko M, LiVolsi VA, Swalsky P, Finkelstein SD, Barnes EL (2003). Molecular evidence of anaplastic transformation in coexisting well-differentiated and anaplastic carcinomas of the thyroid. *Am J Surg Pathol* **27:** 1559-1564.

Hunter C, Smith R, Cahill DP, Stephens P, Stevens C, Teague J *et al* (2006). A hypermutation phenotype and somatic MSH6 mutations in recurrent human malignant gliomas after alkylator chemotherapy. *Cancer Res* **66:** 3987-3991.

Ishigaki K, Namba H, Nakashima M, Nakayama T, Mitsutake N, Hayashi T *et al* (2002). Aberrant localization of beta-catenin correlates with overexpression of its target gene in human papillary thyroid cancer. *J Clin Endocrinol Metab* **87:** 3433-3440.

Ito T, Seyama T, Mizuno T, Tsuyama N, Hayashi T, Hayashi Y *et al* (1992). Unique association of p53 mutations with undifferentiated but not with differentiated carcinomas of the thyroid gland. *Cancer Res* **52:** 1369-1371.

Ito T, Seyama T, Mizuno T, Tsuyama N, Hayashi Y, Dohi K *et al* (1993). Genetic alterations in thyroid tumor progression: association with p53 gene mutations. *Jpn J Cancer Res* **84:** 526-531.

Ito Y, Kobayashi T, Takeda T, Komoike Y, Wakasugi E, Tamaki Y *et al* (1996). Expression of p21 (WAF1/CIP1) protein in clinical thyroid tissues. *Br J Cancer* **74:** 1269-1274.

Jhiang SM, Sagartz JE, Tong Q, Parker-Thornburg J, Capen CC, Cho JY *et al* (1996). Targeted expression of the ret/PTC1 oncogene induces papillary thyroid carcinomas. *Endocrinology* **137:** 375-378.

Jones PA, Laird PW (1999). Cancer epigenetics comes of age. *Nat Genet* **21:** 163-167.

Jones SJ, Laskin J, Li YY, Griffith OL, An J, Bilenky M *et al* (2010). Evolution of an adenocarcinoma in response to selection by targeted kinase inhibitors. *Genome Biol* **11:** R82.

Jossart GH, Epstein HD, Shaver JK, Weier HU, Greulich KM, Tezelman S *et al* (1996). Immunocytochemical detection of p53 in human thyroid carcinomas is associated with mutation and immortalization of cell lines. *J Clin Endocrinol Metab* **81:** 3498-3504.

Kamata T, Pritchard C (2011). Mechanisms of aneuploidy induction by RAS and RAF oncogenes. *Am J Cancer Res* **1:** 955-971.

Kan Z, Jaiswal BS, Stinson J, Janakiraman V, Bhatt D, Stern HM *et al* (2010). Diverse somatic mutation patterns and pathway alterations in human cancers. *Nature* **466:** 869-873.

Katoh R, Kawaoi A, Miyagi E, Li X, Suzuki K, Nakamura Y *et al* (2000). Thyroid transcription factor-1 in normal, hyperplastic, and neoplastic follicular thyroid cells examined by immunohistochemistry and nonradioactive in situ hybridization. *Mod Pathol* **13:** 570-576.

Kim SJ, Lee KE, Myong JP, Park JH, Jeon YK, Min HS *et al* (2012). BRAF V600E mutation is associated with tumor aggressiveness in papillary thyroid cancer. *World J Surg* **36:** 310-317.

Kimura ET, Nikiforova MN, Zhu Z, Knauf JA, Nikiforov YE, Fagin JA (2003). High prevalence of BRAF mutations in thyroid cancer: genetic evidence for constitutive activation of the RET/PTC-RAS-BRAF signaling pathway in papillary thyroid carcinoma. *Cancer Res* **63:** 1454-1457.

Kimura T, Van Keymeulen A, Golstein J, Fusco A, Dumont JE, Roger PP (2001). Regulation of thyroid cell proliferation by TSH and other factors: a critical evaluation of in vitro models. *Endocr Rev* **22:** 631-656.

Klaus A, Birchmeier W (2008). Wnt signalling and its impact on development and cancer. *Nat Rev Cancer* **8:** 387-398.

Knauf JA, Ma X, Smith EP, Zhang L, Mitsutake N, Liao XH *et al* (2005). Targeted expression of BRAFV600E in thyroid cells of transgenic mice results in papillary thyroid cancers that undergo dedifferentiation. *Cancer Res* **65:** 4238-4245.

Knudson AG (2001). Two genetic hits (more or less) to cancer. *Nat Rev Cancer* **1:** 157-162.

Knudson AG, Jr. (1971). Mutation and cancer: statistical study of retinoblastoma. *Proc Natl Acad Sci U S A* **68:** 820-823.

Kogai T, Sajid-Crockett S, Newmarch LS, Liu YY, Brent GA (2008). Phosphoinositide-3-kinase inhibition induces sodium/iodide symporter expression in rat thyroid cells and human papillary thyroid cancer cells. *J Endocrinol* **199:** 243-252.

Kondo T, Ezzat S, Asa SL (2006). Pathogenetic mechanisms in thyroid follicular-cell neoplasia. *Nat Rev Cancer* **6:** 292-306.

Kroll TG, Sarraf P, Pecciarini L, Chen CJ, Mueller E, Spiegelman BM *et al* (2000). PAX8-PPARgamma1 fusion oncogene in human thyroid carcinoma [corrected]. *Science* **289:** 1357-1360.

Kurihara T, Ikeda S, Ishizaki Y, Fujimori M, Tokumoto N, Hirata Y *et al* (2004). Immunohistochemical and sequencing analyses of the Wnt signaling components in Japanese anaplastic thyroid cancers. *Thyroid* **14:** 1020-1029.

La Vecchia C, Bosetti C, Lucchini F, Bertuccio P, Negri E, Boyle P *et al* (2010). Cancer mortality in Europe, 2000-2004, and an overview of trends since 1975. *Ann Oncol* **21:** 1323-1360.

Lacroix L, Mian C, Barrier T, Talbot M, Caillou B, Schlumberger M *et al* (2004). PAX8 and peroxisome proliferator-activated receptor gamma 1 gene expression status in benign and malignant thyroid tissues. *Eur J Endocrinol* **151:** 367-374.

Lam KY, Lo CY, Chan KW, Wan KY (2000). Insular and anaplastic carcinoma of the thyroid: a 45-year comparative study at a single institution and a review of the significance of p53 and p21. *Ann Surg* **231:** 329-338.

Lander ES, Linton LM, Birren B, Nusbaum C, Zody MC, Baldwin J *et al* (2001). Initial sequencing and analysis of the human genome. *Nature* **409:** 860-921.

Lazar V, Bidart JM, Caillou B, Mahe C, Lacroix L, Filetti S *et al* (1999). Expression of the Na+/I-symporter gene in human thyroid tumors: a comparison study with other thyroid-specific genes. *J Clin Endocrinol Metab* **84:** 3228-3234.

Lazzaro D, Price M, de Felice M, Di Lauro R (1991). The transcription factor TTF-1 is expressed at the onset of thyroid and lung morphogenesis and in restricted regions of the foetal brain. *Development* **113:** 1093-1104.

Lee JH, Lee ES, Kim YS (2007). Clinicopathologic significance of BRAF V600E mutation in papillary carcinomas of the thyroid: a meta-analysis. *Cancer* **110:** 38-46.

Lee JJ, Au AY, Foukakis T, Barbaro M, Kiss N, Clifton-Bligh R *et al* (2008). Array-CGH identifies cyclin D1 and UBCH10 amplicons in anaplastic thyroid carcinoma. *Endocr Relat Cancer* **15:** 801-815.

Lee W, Jiang Z, Liu J, Haverty PM, Guan Y, Stinson J *et al* (2010). The mutation spectrum revealed by paired genome sequences from a lung cancer patient. *Nature* **465:** 473-477.

Lee WH, Bookstein R, Hong F, Young LJ, Shew JY, Lee EY (1987). Human retinoblastoma susceptibility gene: cloning, identification, and sequence. *Science* **235:** 1394-1399.

Leenhardt L, Grosclaude P, Cherie-Challine L (2004). Increased incidence of thyroid carcinoma in france: a true epidemic or thyroid nodule management effects? Report from the French Thyroid Cancer Committee. *Thyroid* **14:** 1056-1060.

Lemoine NR, Mayall ES, Wyllie FS, Williams ED, Goyns M, Stringer B *et al* (1989). High frequency of ras oncogene activation in all stages of human thyroid tumorigenesis. *Oncogene* **4:** 159-164.

Levi F, Lucchini F, Negri E, Boyle P, La Vecchia C (2004). Cancer mortality in Europe, 1995-1999, and an overview of trends since 1960. *Int J Cancer* **110:** 155-169.

Ley TJ, Mardis ER, Ding L, Fulton B, McLellan MD, Chen K *et al* (2008). DNA sequencing of a cytogenetically normal acute myeloid leukaemia genome. *Nature* **456:** 66-72.

Li J, Yen C, Liaw D, Podsypanina K, Bose S, Wang SI *et al* (1997). PTEN, a putative protein tyrosine phosphatase gene mutated in human brain, breast, and prostate cancer. *Science* **275:** 1943-1947.

Li VS, Ng SS, Boersema PJ, Low TY, Karthaus WR, Gerlach JP *et al* (2012). Wnt signaling through inhibition of beta-catenin degradation in an intact Axin1 complex. *Cell* **149:** 1245-1256.

Liaw D, Marsh DJ, Li J, Dahia PL, Wang SI, Zheng Z *et al* (1997). Germline mutations of the PTEN gene in Cowden disease, an inherited breast and thyroid cancer syndrome. *Nat Genet* **16:** 64-67.

Liu D, Mambo E, Ladenson PW, Xing M (2005). Letter re: uncommon mutation but common amplifications of the PIK3CA gene in thyroid tumors. *J Clin Endocrinol Metab* **90:** 5509.

Liu RT, Hou CY, You HL, Huang CC, Hock L, Chou FF *et al* (2004). Selective occurrence of ras mutations in benign and malignant thyroid follicular neoplasms in Taiwan. *Thyroid* **14:** 616-621.

Liu YY, Zhang X, Ringel MD, Jhiang SM (2012). Modulation of sodium iodide symporter expression and function by LY294002, Akti-1/2 and Rapamycin in thyroid cells. *Endocr Relat Cancer* **19:** 291-304.

Liu Z, Hou P, Ji M, Guan H, Studeman K, Jensen K *et al* (2008). Highly prevalent genetic alterations in receptor tyrosine kinases and phosphatidylinositol 3-kinase/akt and mitogen-activated protein kinase pathways in anaplastic and follicular thyroid cancers. *J Clin Endocrinol Metab* **93:** 3106-3116.

Lloyd RV, Jin L, Qian X, Kulig E (1997). Aberrant p27kip1 expression in endocrine and other tumors. *Am J Pathol* **150:** 401-407.

Lujambio A, Lowe SW (2012). The microcosmos of cancer. *Nature* **482:** 347-355.

Lupi C, Giannini R, Ugolini C, Proietti A, Berti P, Minuto M *et al* (2007). Association of BRAF V600E mutation with poor clinicopathological outcomes in 500 consecutive cases of papillary thyroid carcinoma. *J Clin Endocrinol Metab* **92:** 4085-4090.

MacDonald BT, Tamai K, He X (2009). Wnt/beta-catenin signaling: components, mechanisms, and diseases. *Dev Cell* **17:** 9-26.

Malumbres M, Barbacid M (2001). To cycle or not to cycle: a critical decision in cancer. *Nat Rev Cancer* **1:** 222-231.

Malumbres M, Barbacid M (2003). RAS oncogenes: the first 30 years. *Nat Rev Cancer* **3:** 459-465.

Manenti G, Pilotti S, Re FC, Della Porta G, Pierotti MA (1994). Selective activation of ras oncogenes in follicular and undifferentiated thyroid carcinomas. *Eur J Cancer* **30A:** 987-993.

Marchetti I, Iervasi G, Mazzanti CM, Lessi F, Tomei S, Naccarato AG *et al* (2012). Detection of the BRAF(V600E) mutation in fine needle aspiration cytology of thyroid papillary microcarcinoma cells selected by manual macrodissection: an easy tool to improve the preoperative diagnosis. *Thyroid* **22:** 292-298.

Mardis ER, Ding L, Dooling DJ, Larson DE, McLellan MD, Chen K *et al* (2009). Recurring mutations found by sequencing an acute myeloid leukemia genome. *N Engl J Med* **361:** 1058-1066.

Marians RC, Ng L, Blair HC, Unger P, Graves PN, Davies TF (2002). Defining thyrotropin-dependent and -independent steps of thyroid hormone synthesis by using thyrotropin receptor-null mice. *Proc Natl Acad Sci U S A* **99:** 15776-15781.

Marques AR, Espadinha C, Catarino AL, Moniz S, Pereira T, Sobrinho LG *et al* (2002). Expression of PAX8-PPAR gamma 1 rearrangements in both follicular thyroid carcinomas and adenomas. *J Clin Endocrinol Metab* **87:** 3947-3952.

Marques AR, Espadinha C, Frias MJ, Roque L, Catarino AL, Sobrinho LG *et al* (2004). Underexpression of peroxisome proliferator-activated receptor (PPAR)gamma in PAX8/PPARgamma-negative thyroid tumours. *Br J Cancer* **91:** 732-738.

Martin GS (1970). Rous sarcoma virus: a function required for the maintenance of the transformed state. *Nature* **227:** 1021-1023.

Martin GS (2004). The road to Src. *Oncogene* **23:** 7910-7917.

Matias-Guiu X, Cuatrecasas M, Musulen E, Prat J (1994). p53 expression in anaplastic carcinomas arising from thyroid papillary carcinomas. *J Clin Pathol* **47:** 337-339.

Matias-Guiu X, Villanueva A, Cuatrecasas M, Capella G, De Leiva A, Prat J (1996). p53 in a thyroid follicular carcinoma with foci of poorly differentiated and anaplastic carcinoma. *Pathol Res Pract* **192:** 1242-1249; discussion 1250-1241.

McCubrey JA, Steelman LS, Chappell WH, Abrams SL, Wong EW, Chang F *et al* (2007). Roles of the Raf/MEK/ERK pathway in cell growth, malignant transformation and drug resistance. *Biochim Biophys Acta* **1773:** 1263-1284.

McNally RJ, Blakey K, James PW, Gomez Pozo B, Basta NO, Hale J (2012). Increasing incidence of thyroid cancer in Great Britain, 1976-2005: age-period-cohort analysis. *Eur J Epidemiol* **27:** 615-622.

Mian C, Barollo S, Pennelli G, Pavan N, Rugge M, Pelizzo MR *et al* (2008). Molecular characteristics in papillary thyroid cancers (PTCs) with no 131I uptake. *Clin Endocrinol (Oxf)* **68:** 108-116.

Miettinen M, Franssila KO (2000). Variable expression of keratins and nearly uniform lack of thyroid transcription factor 1 in thyroid anaplastic carcinoma. *Hum Pathol* **31:** 1139-1145.

Misale S, Yaeger R, Hobor S, Scala E, Janakiraman M, Liska D *et al* (2012). Emergence of KRAS mutations and acquired resistance to anti-EGFR therapy in colorectal cancer. *Nature* **486:** 532-536.

Missero C, Pirro MT, Di Lauro R (2000). Multiple ras downstream pathways mediate functional repression of the homeobox gene product TTF-1. *Mol Cell Biol* **20:** 2783-2793.

Mitselou A, Ioachim E, Peschos D, Charalabopoulos K, Michael M, Agnantis NJ *et al* (2007). E-cadherin adhesion molecule and syndecan-1 expression in various thyroid pathologies. *Exp Oncol* **29:** 54-60.

Mitsutake N, Knauf JA, Mitsutake S, Mesa C, Jr., Zhang L, Fagin JA (2005). Conditional BRAFV600E expression induces DNA synthesis, apoptosis, dedifferentiation, and chromosomal instability in thyroid PCCL3 cells. *Cancer Res* **65:** 2465-2473.

Miyake N, Maeta H, Horie S, Kitamura Y, Nanba E, Kobayashi K *et al* (2001). Absence of mutations in the beta-catenin and adenomatous polyposis coli genes in papillary and follicular thyroid carcinomas. *Pathol Int* **51:** 680-685.

Montero-Conde C, Martin-Campos JM, Lerma E, Gimenez G, Martinez-Guitarte JL, Combalia N *et al* (2008). Molecular profiling related to poor prognosis in thyroid carcinoma. Combining gene expression data and biological information. *Oncogene* **27:** 1554-1561.

Moore D, Ohene-Fianko D, Garcia B, Chakrabarti S (1998). Apoptosis in thyroid neoplasms: relationship with p53 and bcl-2 expression. *Histopathology* **32:** 35-42.

Morris LGT, Myssiorek D (2010). Improved detection does not fully explain the rising incidence of well-differentiated thyroid cancer: a population-based analysis. *Am J Surg* **200:** 454-461.

Motti ML, Califano D, Baldassarre G, Celetti A, Merolla F, Forzati F *et al* (2005a). Reduced E-cadherin expression contributes to the loss of p27kip1-mediated mechanism of contact inhibition in thyroid anaplastic carcinomas. *Carcinogenesis* **26:** 1021-1034.

Motti ML, Califano D, Troncone G, De Marco C, Migliaccio I, Palmieri E *et al* (2005b). Complex regulation of the cyclin-dependent kinase inhibitor p27kip1 in thyroid cancer cells by the PI3K/AKT pathway: regulation of p27kip1 expression and localization. *Am J Pathol* **166:** 737-749.

Mullighan CG, Phillips LA, Su X, Ma J, Miller CB, Shurtleff SA *et al* (2008). Genomic analysis of the clonal origins of relapsed acute lymphoblastic leukemia. *Science* **322:** 1377-1380.

Muro-Cacho CA, Ku NN (2000). Tumors of the thyroid gland: histologic and cytologic features--part 1. *Cancer Control* **7:** 276-287.

Nagaiah G, Hossain A, Mooney CJ, Parmentier J, Remick SC (2011). Anaplastic thyroid cancer: a review of epidemiology, pathogenesis, and treatment. *J Oncol* **2011:** 542358.

Nagataki S, Nystrom E (2002). Epidemiology and primary prevention of thyroid cancer. *Thyroid* **12:** 889-896.

Naito A, Iwase H, Kuzushima T, Nakamura T, Kobayashi S (2001). Clinical significance of E-cadherin expression in thyroid neoplasms. *J Surg Oncol* **76:** 176-180.

Nakamura T, Yana I, Kobayashi T, Shin E, Karakawa K, Fujita S *et al* (1992). p53 gene mutations associated with anaplastic transformation of human thyroid carcinomas. *Jpn J Cancer Res* **83:** 1293-1298.

Namba H, Rubin SA, Fagin JA (1990). Point mutations of ras oncogenes are an early event in thyroid tumorigenesis. *Mol Endocrinol* **4:** 1474-1479.

Nambiar A, Pv S, Susheelan V, Kuriakose MA (2011). The concepts in poorly differentiated carcinoma of the thyroid: a review article. *J Surg Oncol* **103:** 818-821.

Navin N, Krasnitz A, Rodgers L, Cook K, Meth J, Kendall J *et al* (2010). Inferring tumor progression from genomic heterogeneity. *Genome Res* **20:** 68-80.

Navin N, Kendall J, Troge J, Andrews P, Rodgers L, McIndoo J *et al* (2011). Tumour evolution inferred by single-cell sequencing. *Nature* **472:** 90-94.

Nevins JR, Potti A (2007). Mining gene expression profiles: expression signatures as cancer phenotypes. *Nat Rev Genet* **8:** 601-609.

Nik-Zainal S, Van Loo P, Wedge DC, Alexandrov LB, Greenman CD, Lau KW *et al* (2012). The life history of 21 breast cancers. *Cell* **149:** 994-1007.

Nikiforov YE (2008). Thyroid carcinoma: molecular pathways and therapeutic targets. *Mod Pathol* **21 Suppl 2:** S37-43.

Nikiforov YE (2011). Molecular analysis of thyroid tumors. *Mod Pathol* **24 Suppl 2:** S34-43.

Nikiforov YE, Nikiforova MN (2011). Molecular genetics and diagnosis of thyroid cancer. *Nat Rev Endocrinol* **7:** 569-580.

Nikiforova MN, Kimura ET, Gandhi M, Biddinger PW, Knauf JA, Basolo F *et al* (2003a). BRAF mutations in thyroid tumors are restricted to papillary carcinomas and anaplastic or poorly differentiated carcinomas arising from papillary carcinomas. *J Clin Endocrinol Metab* **88:** 5399-5404.

Nikiforova MN, Lynch RA, Biddinger PW, Alexander EK, Dorn GW, Tallini G *et al* (2003b). RAS point mutations and PAX8-PPAR gamma rearrangement in thyroid tumors: evidence for distinct molecular pathways in thyroid follicular carcinoma. *J Clin Endocrinol Metab* **88:** 2318-2326.

Nikiforova MN, Chiosea SI, Nikiforov YE (2009). MicroRNA expression profiles in thyroid tumors. *Endocr Pathol* **20:** 85-91.

Nonaka D, Tang Y, Chiriboga L, Rivera M, Ghossein R (2008). Diagnostic utility of thyroid transcription factors Pax8 and TTF-2 (FoxE1) in thyroid epithelial neoplasms. *Mod Pathol* **21:** 192-200.

Nose V (2011). Familial thyroid cancer: a review. *Mod Pathol* **24 Suppl 2:** S19-33.

Notta F, Mullighan CG, Wang JC, Poeppl A, Doulatov S, Phillips LA *et al* (2011). Evolution of human BCR-ABL1 lymphoblastic leukaemia-initiating cells. *Nature* **469:** 362-367.

Nowell PC (1976). The clonal evolution of tumor cell populations. *Science* **194:** 23-28.

Oppermann H, Levinson AD, Varmus HE, Levintow L, Bishop JM (1979). Uninfected vertebrate cells contain a protein that is closely related to the product of the avian sarcoma virus transforming gene (src). *Proc Natl Acad Sci U S A* **76:** 1804-1808.

Oyama T, Suzuki T, Hara F, Iino Y, Ishida T, Sakamoto A *et al* (1995). N-ras mutation of thyroid tumor with special reference to the follicular type. *Pathol Int* **45:** 45-50.

Pacini F, Pinchera A, Mancusi F, Pollina L, Fontanini G, Bevilacqua G *et al* (1994). Anaplastic thyroid-carcinoma - a retrospective clinical and immunohistochemical study. *Oncol Rep* **1:** 921-925.

Parada LF, Tabin CJ, Shih C, Weinberg RA (1982). Human EJ bladder carcinoma oncogene is homologue of Harvey sarcoma virus ras gene. *Nature* **297:** 474-478.

Parmentier M, Libert F, Maenhaut C, Lefort A, Gerard C, Perret J *et al* (1989). Molecular cloning of the thyrotropin receptor. *Science* **246:** 1620-1622.

Parsons DW, Jones S, Zhang X, Lin JC, Leary RJ, Angenendt P *et al* (2008). An integrated genomic analysis of human glioblastoma multiforme. *Science* **321:** 1807-1812.

Pearson G, Robinson F, Beers Gibson T, Xu BE, Karandikar M, Berman K *et al* (2001). Mitogen-activated protein (MAP) kinase pathways: regulation and physiological functions. *Endocr Rev* **22:** 153-183.

Pellizzari L, D'Elia A, Rustighi A, Manfioletti G, Tell G, Damante G (2000). Expression and function of the homeodomain-containing protein Hex in thyroid cells. *Nucleic Acids Res* **28:** 2503-2511.

Pesce L, Bizhanova A, Caraballo JC, Westphal W, Butti ML, Comellas A *et al* (2012). TSH regulates pendrin membrane abundance and enhances iodide efflux in thyroid cells. *Endocrinology* **153:** 512-521.

Pierotti MA, Santoro M, Jenkins RB, Sozzi G, Bongarzone I, Grieco M *et al* (1992). Characterization of an inversion on the long arm of chromosome 10 juxtaposing D10S170 and RET and creating the oncogenic sequence RET/PTC. *Proc Natl Acad Sci U S A* **89:** 1616-1620.

Pierotti MA (2001). Chromosomal rearrangements in thyroid carcinomas: a recombination or death dilemma. *Cancer Lett* **166:** 1-7.

Pilotti S, Collini P, Del Bo R, Cattoretti G, Pierotti MA, Rilke F (1994a). A novel panel of antibodies that segregates immunocytochemically poorly differentiated carcinoma from undifferentiated carcinoma of the thyroid gland. *Am J Surg Pathol* **18:** 1054-1064.

Pilotti S, Collini P, Rilke F, Cattoretti G, Del Bo R, Pierotti MA (1994b). Bcl-2 protein expression in carcinomas originating from the follicular epithelium of the thyroid gland. *J Pathol* **172:** 337-342.

Pilotti S, Collini P, Mariani L, Placucci M, Bongarzone I, Vigneri P *et al* (1997). Insular carcinoma: a distinct de novo entity among follicular carcinomas of the thyroid gland. *Am J Surg Pathol* **21:** 1466-1473.

Plachov D, Chowdhury K, Walther C, Simon D, Guenet JL, Gruss P (1990). Pax8, a murine paired box gene expressed in the developing excretory system and thyroid gland. *Development* **110:** 643-651.

Pleasance ED, Cheetham RK, Stephens PJ, McBride DJ, Humphray SJ, Greenman CD *et al* (2010). A comprehensive catalogue of somatic mutations from a human cancer genome. *Nature* **463:** 191-196.

Poleev A, Fickenscher H, Mundlos S, Winterpacht A, Zabel B, Fidler A *et al* (1992). PAX8, a human paired box gene: isolation and expression in developing thyroid, kidney and Wilms' tumors. *Development* **116:** 611-623.

Pollina L, Pacini F, Fontanini G, Vignati S, Bevilacqua G, Basolo F (1996). bcl-2, p53 and proliferating cell nuclear antigen expression is related to the degree of differentiation in thyroid carcinomas. *Br J Cancer* **73:** 139-143.

Potter E, Bergwitz C, Brabant G (1999). The cadherin-catenin system: implications for growth and differentiation of endocrine tissues. *Endocr Rev* **20:** 207-239.

Powell DJ, Jr., Russell J, Nibu K, Li G, Rhee E, Liao M *et al* (1998). The RET/PTC3 oncogene: metastatic solid-type papillary carcinomas in murine thyroids. *Cancer Res* **58:** 5523-5528.

Puxeddu E, Moretti S, Elisei R, Romei C, Pascucci R, Martinelli M *et al* (2004). BRAF(V599E) mutation is the leading genetic event in adult sporadic papillary thyroid carcinomas. *J Clin Endocrinol Metab* **89:** 2414-2420.

Quiros RM, Ding HG, Gattuso P, Prinz RA, Xu X (2005). Evidence that one subset of anaplastic thyroid carcinomas are derived from papillary carcinomas due to BRAF and p53 mutations. *Cancer* **103:** 2261-2268.

Ralhan R, Cao J, Lim T, Macmillan C, Freeman JL, Walfish PG (2010). EpCAM nuclear localization identifies aggressive thyroid cancer and is a marker for poor prognosis. *BMC Cancer* **10:** 331.

Reddi HV, McIver B, Grebe SK, Eberhardt NL (2007). The paired box-8/peroxisome proliferator-activated receptor-gamma oncogene in thyroid tumorigenesis. *Endocrinology* **148:** 932-935.

Reddy EP, Reynolds RK, Santos E, Barbacid M (1982). A point mutation is responsible for the acquisition of transforming properties by the T24 human bladder carcinoma oncogene. *Nature* **300:** 149-152.

Resnick MB, Schacter P, Finkelstein Y, Kellner Y, Cohen O (1998). Immunohistochemical analysis of p27/kip1 expression in thyroid carcinoma. *Mod Pathol* **11:** 735-739.

Ricarte-Filho JC, Ryder M, Chitale DA, Rivera M, Heguy A, Ladanyi M *et al* (2009). Mutational profile of advanced primary and metastatic radioactive iodine-refractory thyroid cancers reveals distinct pathogenetic roles for BRAF, PIK3CA, and AKT1. *Cancer Res* **69:** 4885-4893.

Riedel C, Levy O, Carrasco N (2001). Post-transcriptional regulation of the sodium/iodide symporter by thyrotropin. *J Biol Chem* **276:** 21458-21463.

Riesco-Eizaguirre G, Gutierrez-Martinez P, Garcia-Cabezas MA, Nistal M, Santisteban P (2006). The oncogene BRAF V600E is associated with a high risk of recurrence and less differentiated papillary thyroid carcinoma due to the impairment of Na+/I- targeting to the membrane. *Endocr Relat Cancer* **13:** 257-269.

Riesco-Eizaguirre G, Santisteban P (2006). A perspective view of sodium iodide symporter research and its clinical implications. *Eur J Endocrinol* **155:** 495-512.

Riesco-Eizaguirre G, Santisteban P (2007). New insights in thyroid follicular cell biology and its impact in thyroid cancer therapy. *Endocr Relat Cancer* **14:** 957-977.

Riesco-Eizaguirre G, Rodriguez I, De la Vieja A, Costamagna E, Carrasco N, Nistal M *et al* (2009). The BRAFV600E oncogene induces transforming growth factor beta secretion leading to sodium iodide symporter repression and increased malignancy in thyroid cancer. *Cancer Res* **69:** 8317-8325.

Rivera M, Ricarte-Filho J, Knauf J, Shaha A, Tuttle M, Fagin JA *et al* (2010). Molecular genotyping of papillary thyroid carcinoma follicular variant according to its histological subtypes (encapsulated vs infiltrative) reveals distinct BRAF and RAS mutation patterns. *Mod Pathol* **23:** 1191-1200.

Rocha AS, Soares P, Fonseca E, Cameselle-Teijeiro J, Oliveira MC, Sobrinho-Simões M (2003). E-cadherin loss rather than β-catenin alterations is a common feature of poorly differentiated thyroid carcinomas. *Histopathology* **42:** 580-587.

Rochefort P, Caillou B, Michiels FM, Ledent C, Talbot M, Schlumberger M *et al* (1996). Thyroid pathologies in transgenic mice expressing a human activated Ras gene driven by a thyroglobulin promoter. *Oncogene* **12:** 111-118.

Rodrigues RF, Roque L, Rosa-Santos J, Cid O, Soares J (2004). Chromosomal imbalances associated with anaplastic transformation of follicular thyroid carcinomas. *Br J Cancer* **90:** 492-496.

Roger PP, van Staveren WC, Coulonval K, Dumont JE, Maenhaut C (2010). Signal transduction in the human thyrocyte and its perversion in thyroid tumors. *Mol Cell Endocrinol* **321:** 3-19.

Romei C, Ciampi R, Faviana P, Agate L, Molinaro E, Bottici V *et al* (2008). BRAFV600E mutation, but not RET/PTC rearrangements, is correlated with a lower expression of both thyroperoxidase and sodium iodide symporter genes in papillary thyroid cancer. *Endocr Relat Cancer* **15:** 511-520.

Romeo Y, Moreau J, Zindy PJ, Saba-El-Leil M, Lavoie G, Dandachi F *et al* (2012). RSK regulates activated BRAF signalling to mTORC1 and promotes melanoma growth. *Oncogene*.

Ros P, Rossi DL, Acebron A, Santisteban P (1999). Thyroid-specific gene expression in the multi-step process of thyroid carcinogenesis. *Biochimie* **81:** 389-396.

Ross DS (2002). Nonpalpable thyroid nodules--managing an epidemic. *J Clin Endocrinol Metab* **87:** 1938-1940.

Russell JP, Powell DJ, Cunnane M, Greco A, Portella G, Santoro M *et al* (2000). The TRK-T1 fusion protein induces neoplastic transformation of thyroid epithelium. *Oncogene* **19:** 5729-5735.

Saavedra HI, Knauf JA, Shirokawa JM, Wang J, Ouyang B, Elisei R *et al* (2000). The RAS oncogene induces genomic instability in thyroid PCCL3 cells via the MAPK pathway. *Oncogene* **19:** 3948-3954.

Saji M, Ringel MD (2010). The PI3K-Akt-mTOR pathway in initiation and progression of thyroid tumors. *Mol Cell Endocrinol* **321:** 20-28.

Saltman B, Singh B, Hedvat CV, Wreesmann VB, Ghossein R (2006). Patterns of expression of cell cycle/apoptosis genes along the spectrum of thyroid carcinoma progression. *Surgery* **140:** 899-905; discussion 905-896.

Salvatore D, Celetti A, Fabien N, Paulin C, Martelli ML, Battaglia C *et al* (1996). Low frequency of p53 mutations in human thyroid tumours; p53 and Ras mutation in two out of fifty-six thyroid tumours. *Eur J Endocrinol* **134:** 177-183.

Salvatore G, Nappi TC, Salerno P, Jiang Y, Garbi C, Ugolini C *et al* (2007). A cell proliferation and chromosomal instability signature in anaplastic thyroid carcinoma. *Cancer Res* **67:** 10148-10158.

Samuels Y, Wang Z, Bardelli A, Silliman N, Ptak J, Szabo S *et al* (2004). High frequency of mutations of the PIK3CA gene in human cancers. *Science* **304:** 554.

Sanders EM, Jr., LiVolsi VA, Brierley J, Shin J, Randolph GW (2007). An evidence-based review of poorly differentiated thyroid cancer. *World J Surg* **31:** 934-945.

Sant M, Aareleid T, Berrino F, Bielska Lasota M, Carli PM, Faivre J *et al* (2003). EUROCARE-3: survival of cancer patients diagnosed 1990-94--results and commentary. *Ann Oncol* **14 Suppl 5:** v61-118.

Santarpia L, El-Naggar AK, Cote GJ, Myers JN, Sherman SI (2008). Phosphatidylinositol 3-kinase/akt and ras/raf-mitogen-activated protein kinase pathway mutations in anaplastic thyroid cancer. *J Clin Endocrinol Metab* **93:** 278-284.

Santelli G, de Franciscis V, Portella G, Chiappetta G, D'Alessio A, Califano D *et al* (1993). Production of transgenic mice expressing the Ki-ras oncogene under the control of a thyroglobulin promoter. *Cancer Res* **53:** 5523-5527.

Santin AP, Furlanetto TW (2011). Role of estrogen in thyroid function and growth regulation. *J Thyroid Res* **2011:** 875125.

Santoro A, Pannone G, Carosi MA, Francesconi A, Pescarmona E, Russo GM *et al* (2012). BRAF mutation and RASSF1A expression in thyroid carcinoma of southern Italy. *J Cell Biochem*.

Santoro M, Carlomagno F, Hay ID, Herrmann MA, Grieco M, Melillo R *et al* (1992). Ret oncogene activation in human thyroid neoplasms is restricted to the papillary cancer subtype. *J Clin Invest* **89:** 1517-1522.

Santoro M, Melillo RM, Grieco M, Berlingieri MT, Vecchio G, Fusco A (1993). The TRK and RET tyrosine kinase oncogenes cooperate with ras in the neoplastic transformation of a rat thyroid epithelial cell line. *Cell Growth Differ* **4:** 77-84.

Santoro M, Chiappetta G, Cerrato A, Salvatore D, Zhang L, Manzo G *et al* (1996). Development of thyroid papillary carcinomas secondary to tissue-specific expression of the RET/PTC1 oncogene in transgenic mice. *Oncogene* **12:** 1821-1826.

Santoro M, Papotti M, Chiappetta G, Garcia-Rostan G, Volante M, Johnson C *et al* (2002). RET activation and clinicopathologic features in poorly differentiated thyroid tumors. *J Clin Endocrinol Metab* **87:** 370-379.

Santos E, Tronick SR, Aaronson SA, Pulciani S, Barbacid M (1982). T24 human bladder carcinoma oncogene is an activated form of the normal human homologue of BALB- and Harvey-MSV transforming genes. *Nature* **298:** 343-347.

Schagdarsurengin U, Gimm O, Hoang-Vu C, Dralle H, Pfeifer GP, Dammann R (2002). Frequent epigenetic silencing of the CpG island promoter of RASSF1A in thyroid carcinoma. *Cancer Res* **62:** 3698-3701.

Scheumman GF, Hoang-Vu C, Cetin Y, Gimm O, Behrends J, von Wasielewski R *et al* (1995). Clinical significance of E-cadherin as a prognostic marker in thyroid carcinomas. *J Clin Endocrinol Metab* **80:** 2168-2172.

Schlumberger M, Lacroix L, Russo D, Filetti S, Bidart JM (2007). Defects in iodide metabolism in thyroid cancer and implications for the follow-up and treatment of patients. *Nat Clin Pract Endocrinol Metab* **3:** 260-269.

Schwertheim S, Sheu SY, Worm K, Grabellus F, Schmid KW (2009). Analysis of deregulated miRNAs is helpful to distinguish poorly differentiated thyroid carcinoma from papillary thyroid carcinoma. *Horm Metab Res* **41:** 475-481.

Shah SP, Morin RD, Khattra J, Prentice L, Pugh T, Burleigh A *et al* (2009). Mutational evolution in a lobular breast tumour profiled at single nucleotide resolution. *Nature* **461:** 809-813.

Shah SP, Roth A, Goya R, Oloumi A, Ha G, Zhao Y *et al* (2012). The clonal and mutational evolution spectrum of primary triple-negative breast cancers. *Nature* **486:** 395-399.

Shayesteh L, Lu Y, Kuo WL, Baldocchi R, Godfrey T, Collins C *et al* (1999). PIK3CA is implicated as an oncogene in ovarian cancer. *Nat Genet* **21:** 99-102.

Sherr CJ, Roberts JM (1999). CDK inhibitors: positive and negative regulators of G1-phase progression. *Genes Dev* **13:** 1501-1512.

Shirokawa JM, Elisei R, Knauf JA, Hara T, Wang J, Saavedra HI *et al* (2000). Conditional apoptosis induced by oncogenic ras in thyroid cells. *Mol Endocrinol* **14:** 1725-1738.

Sinclair AJ, Lonigro R, Civitareale D, Ghibelli L, Di Lauro R (1990). The tissue-specific expression of the thyroglobulin gene requires interaction between thyroid-specific and ubiquitous factors. *Eur J Biochem* **193:** 311-318.

Sinnott B, Ron E, Schneider AB (2010). Exposing the thyroid to radiation: a review of its current extent, risks, and implications. *Endocr Rev* **31:** 756-773.

Sjoblom T, Jones S, Wood LD, Parsons DW, Lin J, Barber TD *et al* (2006). The consensus coding sequences of human breast and colorectal cancers. *Science* **314:** 268-274.

Smallridge RC, Marlow LA, Copland JA (2009). Anaplastic thyroid cancer: molecular pathogenesis and emerging therapies. *Endocr Relat Cancer* **16:** 17-44.

Soares P, Cameselle-Teijeiro J, Sobrinho-Simões M (1994). Immunohistochemical detection of p53 in differentiated, poorly differentiated and undifferentiated carcinomas of the thyroid. *Histopathology* **24:** 205-210.

Soares P, Berx G, van Roy F, Sobrinho-Simões M (1997). E-cadherin gene alterations are rare events in thyroid tumors. *Int J Cancer* **70:** 32-38.

Soares P, Trovisco V, Rocha AS, Lima J, Castro P, Preto A *et al* (2003). BRAF mutations and RET/PTC rearrangements are alternative events in the etiopathogenesis of PTC. *Oncogene* **22:** 4578-4580.

Soares P, Trovisco V, Rocha AS, Feijão T, Rebocho AP, Fonseca E *et al* (2004). BRAF mutations typical of papillary thyroid carcinoma are more frequently detected in undifferentiated than in insular and insular-like poorly differentiated carcinomas. *Virchows Arch* **444:** 572-576.

Soares P, Lima J, Preto A, Castro P, Vinagre J, Celestino R *et al* (2011). Genetic alterations in poorly differentiated and undifferentiated thyroid carcinomas. *Curr Genomics* **12:** 609-617.

Sobrinho-Simões M, Preto A, Rocha AS, Castro P, Máximo V, Fonseca E *et al* (2005). Molecular pathology of well-differentiated thyroid carcinomas. *Virchows Arch* **447:** 787-793.

Spector DH, Varmus HE, Bishop JM (1978). Nucleotide sequences related to the transforming gene of avian sarcoma virus are present in DNA of uninfected vertebrates. *Proc Natl Acad Sci U S A* **75:** 4102-4106.

Steck PA, Pershouse MA, Jasser SA, Yung WK, Lin H, Ligon AH *et al* (1997). Identification of a candidate tumour suppressor gene, MMAC1, at chromosome 10q23.3 that is mutated in multiple advanced cancers. *Nat Genet* **15:** 356-362.

Stehelin D, Varmus HE, Bishop JM, Vogt PK (1976). DNA related to the transforming gene(s) of avian sarcoma viruses is present in normal avian DNA. *Nature* **260:** 170-173.

Stephens P, Edkins S, Davies H, Greenman C, Cox C, Hunter C *et al* (2005). A screen of the complete protein kinase gene family identifies diverse patterns of somatic mutations in human breast cancer. *Nat Genet* **37:** 590-592.

Stephens PJ, Tarpey PS, Davies H, Van Loo P, Greenman C, Wedge DC *et al* (2012). The landscape of cancer genes and mutational processes in breast cancer. *Nature* **486:** 400-404.

Stratton MR (2011). Exploring the genomes of cancer cells: progress and promise. *Science* **331:** 1553-1558.

Sykorova V, Dvorakova S, Ryska A, Vcelak J, Vaclavikova E, Laco J *et al* (2010). BRAFV600E mutation in the pathogenesis of a large series of papillary thyroid carcinoma in Czech Republic. *J Endocrinol Invest* **33:** 318-324.

Szinnai G, Lacroix L, Carre A, Guimiot F, Talbot M, Martinovic J *et al* (2007). Sodium/iodide symporter (NIS) gene expression is the limiting step for the onset of thyroid function in the human fetus. *J Clin Endocrinol Metab* **92:** 70-76.

Tabin CJ, Bradley SM, Bargmann CI, Weinberg RA, Papageorge AG, Scolnick EM *et al* (1982). Mechanism of activation of a human oncogene. *Nature* **300:** 143-149.

Takano T, Ito Y, Hirokawa M, Yoshida H, Miyauchi A (2007a). BRAF V600E mutation in anaplastic thyroid carcinomas and their accompanying differentiated carcinomas. *Br J Cancer* **96:** 1549-1553.

Takano T, Ito Y, Matsuzuka F, Miya A, Kobayashi K, Yoshida H *et al* (2007b). Quantitative measurement of telomerase reverse transcriptase, thyroglobulin and thyroid transcription factor 1 mRNAs in anaplastic thyroid carcinoma tissues and cell lines. *Oncol Rep* **18:** 715-720.

Takeuchi Y, Daa T, Kashima K, Yokoyama S, Nakayama I, Noguchi S (1999). Mutations of p53 in thyroid carcinoma with an insular component. *Thyroid* **9:** 377-381.

Tallini G, Santoro M, Helie M, Carlomagno F, Salvatore G, Chiappetta G *et al* (1998). RET/PTC oncogene activation defines a subset of papillary thyroid carcinomas lacking evidence of progression to poorly differentiated or undifferentiated tumor phenotypes. *Clin Cancer Res* **4:** 287-294.

Tallini G, Garcia-Rostan G, Herrero A, Zelterman D, Viale G, Bosari S *et al* (1999). Downregulation of p27KIP1 and Ki67/Mib1 labeling index support the classification of thyroid carcinoma into prognostically relevant categories. *Am J Surg Pathol* **23:** 678-685.

Tallini G (2011). Poorly differentiated thyroid carcinoma. Are we there yet? *Endocr Pathol* **22:** 190-194.

Taparowsky E, Suard Y, Fasano O, Shimizu K, Goldfarb M, Wigler M (1982). Activation of the T24 bladder carcinoma transforming gene is linked to a single amino acid change. *Nature* **300:** 762-765.

Thomas PQ, Brown A, Beddington RS (1998). Hex: a homeobox gene revealing peri-implantation asymmetry in the mouse embryo and an early transient marker of endothelial cell precursors. *Development* **125:** 85-94.

Thorpe-Beeston JG, Nicolaides KH, Felton CV, Butler J, McGregor AM (1991). Maturation of the secretion of thyroid hormone and thyroid-stimulating hormone in the fetus. *N Engl J Med* **324:** 532-536.

Trovisco V, Vieira de Castro I, Soares P, Máximo V, Silva P, Magalhães J *et al* (2004). BRAF mutations are associated with some histological types of papillary thyroid carcinoma. *J Pathol* **202:** 247-251.

Trovisco V, Soares P, Soares R, Magalhães J, Sa-Couto P, Sobrinho-Simões M (2005). A new BRAF gene mutation detected in a case of a solid variant of papillary thyroid carcinoma. *Hum Pathol* **36:** 694-697.

Tung WS, Shevlin DW, Bartsch D, Norton JA, Wells SA, Jr., Goodfellow PJ (1996). Infrequent CDKN2 mutation in human differentiated thyroid cancers. *Mol Carcinog* **15:** 5-10.

van der Zwan JM, Mallone S, van Dijk B, Bielska-Lasota M, Otter R, Foschi R *et al* (2012). Carcinoma of endocrine organs: results of the RARECARE project. *Eur J Cancer* **48:** 1923-1931.

Van Heuverswyn B, Streydio C, Brocas H, Refetoff S, Dumont J, Vassart G (1984). Thyrotropin controls transcription of the thyroglobulin gene. *Proc Natl Acad Sci U S A* **81:** 5941-5945.

Vasko V, Ferrand M, Di Cristofaro J, Carayon P, Henry JF, de Micco C (2003). Specific pattern of RAS oncogene mutations in follicular thyroid tumors. *J Clin Endocrinol Metab* **88:** 2745-2752.

Vasko V, Hu S, Wu G, Xing JC, Larin A, Savchenko V *et al* (2005). High prevalence and possible de novo formation of BRAF mutation in metastasized papillary thyroid cancer in lymph nodes. *J Clin Endocrinol Metab* **90:** 5265-5269.

Venter JC, Adams MD, Myers EW, Li PW, Mural RJ, Sutton GG *et al* (2001). The sequence of the human genome. *Science* **291:** 1304-1351.

Virchow R (1863). *Cellular pathology as based upon physiological and pathological histology*, Second edn. (Chance F, Trans.) Philadelphia: J.B. Lippincott. (Original work published 1859).

Vitagliano D, Portella G, Troncone G, Francione A, Rossi C, Bruno A *et al* (2006). Thyroid targeting of the N-ras(Gln61Lys) oncogene in transgenic mice results in follicular tumors that progress to poorly differentiated carcinomas. *Oncogene* **25:** 5467-5474.

Volante M, Landolfi S, Chiusa L, Palestini N, Motta M, Codegone A *et al* (2004). Poorly differentiated carcinomas of the thyroid with trabecular, insular, and solid patterns: a clinicopathologic study of 183 patients. *Cancer* **100:** 950-957.

Volante M, Rapa I, Gandhi M, Bussolati G, Giachino D, Papotti M *et al* (2009). RAS mutations are the predominant molecular alteration in poorly differentiated thyroid carcinomas and bear prognostic impact. *J Clin Endocrinol Metab* **94:** 4735-4741.

Vousden KH, Lane DP (2007). p53 in health and disease. *Nat Rev Mol Cell Biol* **8:** 275-283.

Wan PT, Garnett MJ, Roe SM, Lee S, Niculescu-Duvaz D, Good VM *et al* (2004). Mechanism of activation of the RAF-ERK signaling pathway by oncogenic mutations of B-RAF. *Cell* **116:** 855-867.

Wang HM, Huang YW, Huang JS, Wang CH, Kok VC, Hung CM *et al* (2007a). Anaplastic carcinoma of the thyroid arising more often from follicular carcinoma than papillary carcinoma. *Ann Surg Oncol* **14:** 3011-3018.

Wang J, Knauf JA, Basu S, Puxeddu E, Kuroda H, Santoro M *et al* (2003). Conditional expression of RET/PTC induces a weak oncogenic drive in thyroid PCCL3 cells and inhibits thyrotropin action at multiple levels. *Mol Endocrinol* **17:** 1425-1436.

Wang LH, Duesberg PH, Kawai S, Hanafusa H (1976). Location of envelope-specific and sarcoma-specific oligonucleotides on RNA of Schmidt-Ruppin Rous sarcoma virus. *Proc Natl Acad Sci U S A* **73:** 447-451.

Wang Y, Hou P, Yu H, Wang W, Ji M, Zhao S *et al* (2007b). High prevalence and mutual exclusivity of genetic alterations in the phosphatidylinositol-3-kinase/akt pathway in thyroid tumors. *J Clin Endocrinol Metab* **92:** 2387-2390.

Wiseman SM, Masoudi H, Niblock P, Turbin D, Rajput A, Hay J *et al* (2006). Derangement of the E-cadherin/catenin complex is involved in transformation of differentiated to anaplastic thyroid carcinoma. *Am J Surg* **191:** 581-587.

Wiseman SM, Masoudi H, Niblock P, Turbin D, Rajput A, Hay J *et al* (2007). Anaplastic thyroid carcinoma: expression profile of targets for therapy offers new insights for disease treatment. *Ann Surg Oncol* **14:** 719-729.

Wood LD, Parsons DW, Jones S, Lin J, Sjoblom T, Leary RJ *et al* (2007). The genomic landscapes of human breast and colorectal cancers. *Science* **318:** 1108-1113.

Wreesmann VB, Ghossein RA, Patel SG, Harris CP, Schnaser EA, Shaha AR *et al* (2002). Genome-wide appraisal of thyroid cancer progression. *Am J Pathol* **161:** 1549-1556.

Wright PA, Lemoine NR, Goretzki PE, Wyllie FS, Bond J, Hughes C *et al* (1991). Mutation of the p53 gene in a differentiated human thyroid carcinoma cell line, but not in primary thyroid tumours. *Oncogene* **6:** 1693-1697.

Wu G, Mambo E, Guo Z, Hu S, Huang X, Gollin SM *et al* (2005). Uncommon mutation, but common amplifications, of the PIK3CA gene in thyroid tumors. *J Clin Endocrinol Metab* **90:** 4688-4693.

Xing M (2005). BRAF mutation in thyroid cancer. *Endocr Relat Cancer* **12:** 245-262.

Xing M (2010). Genetic alterations in the phosphatidylinositol-3 kinase/Akt pathway in thyroid cancer. *Thyroid* **20:** 697-706.

Xu J, Lamouille S, Derynck R (2009). TGF-beta-induced epithelial to mesenchymal transition. *Cell Res* **19:** 156-172.

Xu X, Quiros RM, Gattuso P, Ain KB, Prinz RA (2003). High prevalence of BRAF gene mutation in papillary thyroid carcinomas and thyroid tumor cell lines. *Cancer Res* **63:** 4561-4567.

Yachida S, Jones S, Bozic I, Antal T, Leary R, Fu B *et al* (2010). Distant metastasis occurs late during the genetic evolution of pancreatic cancer. *Nature* **467:** 1114-1117.

Yane K, Konishi N, Kitahori Y, Naito H, Okaichi K, Ohnishi T *et al* (1996). Lack of p16/CDKN2 alterations in thyroid carcinomas. *Cancer Lett* **101:** 85-92.

Yang E, van Nimwegen E, Zavolan M, Rajewsky N, Schroeder M, Magnasco M *et al* (2003). Decay Rates of Human mRNAs: Correlation With Functional Characteristics and Sequence Attributes. *Genome Res* **13:** 1863-1872.

Yoshimoto K, Iwahana H, Fukuda A, Sano T, Saito S, Itakura M (1992). Role of p53 mutations in endocrine tumorigenesis: mutation detection by polymerase chain reaction-single strand conformation polymorphism. *Cancer Res* **52:** 5061-5064.

You JS, Jones PA (2012). Cancer genetics and epigenetics: two sides of the same coin? *Cancer Cell* **22:** 9-20.

Zannini M, Francis-Lang H, Plachov D, Di Lauro R (1992). Pax-8, a paired domain-containing protein, binds to a sequence overlapping the recognition site of a homeodomain and activates transcription from two thyroid-specific promoters. *Mol Cell Biol* **12:** 4230-4241.

Zannini M, Avantaggiato V, Biffali E, Arnone MI, Sato K, Pischetola M *et al* (1997). TTF-2, a new forkhead protein, shows a temporal expression in the developing thyroid which is consistent with a role in controlling the onset of differentiation. *EMBO J* **16:** 3185-3197.

Zedenius J, Larsson C, Wallin G, Backdahl M, Aspenblad U, Hoog A *et al* (1996). Alterations of p53 and expression of WAF1/p21 in human thyroid tumors. *Thyroid* **6:** 1-9.

Zeki K, Spambalg D, Sharifi N, Gonsky R, Fagin JA (1994). Mutations of the adenomatous polyposis coli gene in sporadic thyroid neoplasms. *J Clin Endocrinol Metab* **79:** 1317-1321.

Zhang P, Zuo H, Nakamura Y, Nakamura M, Wakasa T, Kakudo K (2006). Immunohistochemical analysis of thyroid-specific transcription factors in thyroid tumors. *Pathol Int* **56:** 240-245.

Zhu C, Zheng T, Kilfoy BA, Han X, Ma S, Ba Y *et al* (2009). A birth cohort analysis of the incidence of papillary thyroid cancer in the United States, 1973-2004. *Thyroid* **19:** 1061-1066.

Zhu Z, Gandhi M, Nikiforova MN, Fischer AH, Nikiforov YE (2003). Molecular profile and clinical-pathologic features of the follicular variant of papillary thyroid carcinoma. An unusually high prevalence of ras mutations. *Am J Clin Pathol* **120:** 71-77.

Zou M, Shi Y, Farid NR (1993). p53 mutations in all stages of thyroid carcinomas. *J Clin Endocrinol Metab* **77:** 1054-1058.

CHAPTER II

Gene expression profiling associated with the progression to poorly differentiated thyroid carcinomas

JM Pita, A Banito, BM Cavaco, V Leite

British Journal of Cancer (2009) **101:** 1782-1791

Author's note

The work was already in progress, when I joined the research group. A Banito was responsible for the samples selection and RNA extraction/preparation for the microarrays hybridisations at the Core Facility. A Banito also introduced me to the methods for microarray data analysis. I was responsible for the mutational screening, data and statistical analysis, quantitative RT-PCR and writing of the article. BM Cavaco and V Leite were both responsible for the work supervision and for the writing and revision of the article. The published article is presented with minor changes.

1. Abstract and keywords

Background: Poorly differentiated thyroid carcinomas represent a heterogeneous, aggressive entity, presenting features that suggest a progression from well-differentiated carcinomas. To elucidate the mechanisms underlying such progression and identify novel therapeutic targets, we assessed the genome-wide expression in normal and tumour thyroid tissues.

Methods: Microarray analyses of 24 thyroid carcinomas – 7 classic papillary, 8 follicular variants of papillary, 4 follicular and 5 PDTC – were performed and correlated with *RAS*, *BRAF*, *RET/PTC* and *PAX8-PPARG* alterations. Selected genes were validated by quantitative RT-PCR in an independent set of 28 thyroid tumours.

Results: Unsupervised analyses showed that gene expression similarity was higher between PDTC and fvPTC, particularly for tumours harbouring *RAS* mutations. PDTC presented molecular signatures related to cell proliferation, poor prognosis, spindle assembly checkpoint and cell adhesion. Compared with normal tissues, PTC had 307/494 (60%) genes over-expressed, FTC had 137/171 (80%) genes under-expressed, while PDTC had 92/107 (86%) genes under-expressed, suggesting that gene downregulation is involved in tumour dedifferentiation. Significant *UHRF1* and *ITIH5* deregulated gene expression in PDTC, relatively to normal tissues, was confirmed by quantitative RT-PCR.

Conclusion: Our findings suggest that fvPTC are possible precursors of PDTC. Furthermore, *UHRF1* and *ITIH5* have a potential therapeutic/prognostic value for aggressive thyroid tumours.

Keywords: dedifferentiation; genome-wide expression; oligonucleotide microarray; poorly differentiated thyroid carcinoma; molecular signatures

2. Introduction

Most thyroid neoplasias derive from follicular cells and show a wide range of biological behaviours from indolent to highly invasive cancers (DeLellis *et al.*, 2004). WDTC, such as PTC and FTC, are usually treated successfully with surgery and radioactive iodine; however, PDTC and ATC can behave aggressively with no effective form of treatment (Patel and Shaha, 2006).

Previous reports suggest a model of progression from WDTC to PDTC and to ATC. PDTC show limited follicular cell differentiation and are, both morphologically and behaviourally, positioned between well- and undifferentiated carcinomas (DeLellis *et al.*, 2004). Indeed, cases of WDTC containing areas of poor- or undifferentiation, as well as, cases of PDTC/ATC containing well-differentiated areas, have been widely detected (Lam *et al.*, 2000). Progression is further suggested by the sequential increase of chromosomal abnormalities from WDTC to PDTC and ATC (Wreesmann *et al.*, 2002; Rodrigues *et al.*, 2004). Mutations in the *RAS* and *BRAF* genes also support a model of tumour progression, since the frequency of these events in PDTC is midway between well-differentiated and undifferentiated carcinomas, rather than being randomly distributed (Garcia-Rostan *et al.*, 2003; Nikiforova *et al.*, 2003). Other alterations, such as tumour suppressor *TP53* mutations, are specifically found in PDTC and ATC, and often associated with *RAS* or *BRAF* mutations (Quiros *et al.*, 2005; Wang *et al.*, 2007), suggesting an accumulation of events during progression. Nevertheless, it is not clear if PDTC derive from either PTC or FTC, or if they arise *de novo*. In addition, the genetic and epigenetic mechanisms underlying the process remain ill defined.

Genome-wide expression analysis has been successfully used to identify molecular signatures, improving the diagnosis and prognosis of several types of tumours (Quackenbush, 2006). For thyroid neoplasias, one of the earliest reports of genome-wide expression analysis, described a consistent gene expression profile that distinguished PTC from normal cells (Huang *et al.*, 2001). Most of the genes identified in this work, were corroborated in subsequent studies. Gene expression studies have also been used to differentiate benign from malignant thyroid tumours, and correlate gene expression patterns with specific mutations or rearrangements in PTC and FTC [for review, see (Eszlinger *et al.*, 2007)].

To our knowledge, only two studies have addressed the genome-wide expression of PDTC. One of these studies compared gene expression of PDTC and ATC cell lines to normal

thyroid tissue, and showed that these cells presented largely altered expression profiles that have been associated with the cancer process (Rodrigues *et al.*, 2007). Although the authors confirmed some of the abnormal expressed genes in primary tumours, it has been shown that immortal cell lines may not fully reflect the functional aspects of the tumours, and that some molecular processes might be specifically acquired during the immortalisation step (Dairkee *et al.*, 2004). In the other study, which used WDTC, PDTC and ATC primary tumours, deregulation of different molecular pathways, such as the MAPK-ERK signalling pathway, focal adhesion and cell motility, cell proliferation and cell cycle progression, were associated with dedifferentiation in PDTC and ATC (Montero-Conde *et al.*, 2008).

In this study, we used the array platform *GeneChip Human Genome U133 Plus 2.0* (*HG-U133 Plus 2.0*) to analyse the expression of a wide range of genes (> 30 000) in well- and poorly differentiated thyroid tumours and, to correlate, for the first time, gene expression with *BRAF*, *RAS*, *RET/PTC* and *PAX8-PPARG* alterations.

3. Materials and methods

Tissue samples

Both tumour and normal thyroid tissue samples were obtained at time of surgery, and immediately frozen in liquid nitrogen. Histological classifications followed the criteria described in World Health Organization classification of thyroid tumours (DeLellis *et al.*, 2004). All samples were obtained with permission, and the project was approved by our institution ethical committee.

The microarray sample set consisted of a total of 24 tumour samples – 5 PDTC, 7 cPTC, 8 fvPTC and 4 FTC (Supplementary Table 1). A pool of human thyroid total RNA obtained from 65 Caucasian individuals with 18 to 61 years old, whom died from sudden death (BD Bioscience, Franklin Lakes, NJ, USA), and 2 normal tissue samples taken from the opposite lobe of thyroid tumours, were also processed.

An independent sample set, consisting of 5 PDTC, 7 cPTC, 7 fvPTC, 9 FTC, and 6 normal thyroid tissues taken from the opposite lobe of thyroid tumours, was used for quantitative real-time RT-PCR. Expression was also studied in two poorly differentiated thyroid cancer cell lines, T243 and T351 [described earlier by (Rodrigues *et al.*, 2007)],

kindly supplied by Dr. Lúcia Roque, from Unidade de Investigação de Patobiologia Molecular (UIPM), Instituto Português de Oncologia de Lisboa Francisco Gentil, Lisbon, Portugal.

Total RNA isolation/extraction

Total RNA was extracted and purified using the RNeasy Mini Kit (Qiagen, Hamburg, GmbH), according to the manufacturer's protocol, and quantified by UV spectrophotometry (NanoDrop ND-1000, Thermo Fisher Scientific, Wilmington, DE, USA). RNA integrity was assessed by micro capillary electrophoresis (Agilent 2100 Bioanalyzer, Santa Clara, CA, USA) and samples with RNA integrity number equal or higher than 7.7 were selected for microarray analysis.

RNA processing and hybridisation

RNA samples were processed following the one-cycle eukaryotic target labelling protocol from *Affymetrix*, and were hybridised using the *HG-U133 Plus 2.0 Array* (*Affymetrix*, Santa Clara, CA, USA). Hybridisation results were scanned using the *GeneChip Scanner 3000* and stored in the *GeneChip Operating Software*.

Microarray data analysis

Partek Genomics Suite software (Partek Inc., St. Louis, MO, USA) was used for unsupervised analyses. First, arrays data was normalised and the expression levels were determined applying the robust multi-array average method (Irizarry *et al.*, 2003), and data was corrected for non-biological factors. Samples were represented three-dimensionally, according to the expression levels of all probe-sets, by principal components analysis (PCA). Probe-sets data were also used to obtain a dendogram of the samples, by hierarchical clustering, with the Pearson correlation coefficient.

DNA-Chip Analyzer (*dChip*) 2006 software (Li and Wong, 2001) was used to obtain differentially expressed genes between groups. Arrays were normalised with the invariant set normalisation method and expression levels were calculated by model-based expression analysis with perfect match-only model. Probe-sets that were absent in all samples or that did not change across samples (coefficient of variation lower than 0.2 and higher than 10) were

eliminated from further analysis. Probe-sets were considered to be differentially expressed between two groups when the lower 90% limit of the confidence interval of the fold change (ratio of the expression level in the two groups) was equal or higher than 2-fold, with an unpaired *t*-test considered significant at $P \leq 0.01$. Onto-Express from Onto-Tools package (Khatri *et al.*, 2002) was used to classify genes differentially expressed according to their biological role.

Gene Set Enrichment Analysis (GSEA) software (Subramanian *et al.*, 2005) was used to determine whether members of defined groups of genes, which share common features (gene sets), are preferentially placed towards the top or the bottom of a list of genes. In this list, genes were ranked according to the differential expression between two sample groups. This method was applied using two catalogues of gene sets: one whose products are involved in specific pathways/functions and another defined by expression neighbourhoods, which indicates molecular signatures associated with cancer-related genes. Statistical significance was estimated by a nominal *P* value obtained by phenotype permutation. *P* values were corrected for multiple hypothesis testing using false discovery rate (FDR) and family wise-error rate (FWER). Gene sets were considered significant at $P < 0.05$ and with FWER ≤ 0.25.

First-strand cDNA synthesis

cDNA was synthesised from 1 μg of total RNA (for cDNA sequence analysis) or 2 μg of total RNA (for Quantitative RT-PCR), at 37ºC for 90 minutes, using Random Primer $p(dN)_6$ (Roche Diagnostics Corporation, Indianapolis, IN, USA) and SuperScript II Reverse Transcriptase (Invitrogen, Paisley, UK).

Mutational analysis of the *RAS*, *BRAF* genes and *PAX8-PPARG*, *RET/PTC* rearrangements

Mutational analysis was undertaken using cDNA from the tumour samples of the microarray set. PTC were screened for *BRAF* mutations and rearrangements of *RET/PTC* and, in addition, follicular variants were also analysed for *RAS* mutations and *PAX8-PPARG* rearrangements. FTC were screened for *RAS* and *PAX8-PPARG* rearrangements. PDTC were analysed for *BRAF*, *RAS* and *PAX8-PPARG* genes. Primers were designed to amplify exon 15 of the *BRAF* gene, exons 2 and 3 of the *N-*, *KRAS* genes and exons 1 and 2 of the *HRAS* gene. Primers flanking the respective fusion points were used to screen the presence of *RET/PTC1*,

RET/PTC2, *RET/PTC3* and *PAX8-PPARG* fusion transcripts, as described earlier (Marques *et al.*, 2002; Rebelo *et al.*, 2003). Sequencing analysis, to search for mutations and to confirm the rearrangements, was performed with the same primers as for PCR, using the Big Dye Terminator v1.1 Cycle Sequencing Kit (Applied Biosystems, Foster City, CA, USA), according to the manufacturer's protocol. Sequencing products were separated in an ABI Prism 310 Genetic Analyser (Applied Biosystems) and analysed with the Sequence Analysis Software version 3.4.1 (Applied Biosystems). Primer sequences are presented in Chapter VI.

Quantitative real-time RT-PCR

Real-time RT-PCR assays were performed in 96-well reaction plates (MicroAmp Optical 96-Well Reaction Plate; Applied Biosystems) on an ABI Prism 7900 HT Sequence Detection System (Applied Biosystems) with the SDS Software version 2.3 (Applied Biosystems). PCR amplifications were performed using for each gene, pre-developed primers and probe [Inventoried TaqMan Gene Expression Assays ID: Hs00218544_m1 (*PBK*); Hs00273589_m1 (*UHRF1*); Hs00228960_m1 (*ITIH5*); Applied Biosystems], and TaqMan Universal PCR Master Mix (Applied Biosystems), according to the manufacturer's protocol. In order to normalise differences in the amount of template used, "glyceraldehyde-3-phosphate dehydrogenase" (*GAPDH*) transcript was used as an endogenous control (Pre-Developed TaqMan Assay Reagents Human *GAPDH*; Applied Biosystems). Two-fold serial dilutions were used to apply the relative standard curve method. A pool of five normal thyroid tissues was used as calibrator to determine the relative expression in samples. All reactions, including a control without template, were performed in triplicate.

Quantitative RT-PCR results were analysed using the GraphPad Prism version 4.00 (GraphPad Software, Inc.). Intensity levels were calculated as mean ± standard error of the mean (SEM). Comparisons between sample groups were performed using the Kruskal-Wallis with Dunn's Multiple Comparison test, because samples distribution was not Gaussian or variances between groups were not equal. Correlations of quantitative RT-PCR data with other variables were performed using the Pearson or the Spearman correlations (for a non-Gaussian distribution). The correlations and differences between group means were considered significant at $P < 0.05$.

4. Results

Mutation screening

Tumour samples were screened for mutations in MAPK-ERK pathway effectors, which are frequently mutated in thyroid cancer (Supplementary Table II.1). The $BRAF^{V600E}$ substitution was only present in cPTC, accounting for 57.1% (4/7) of the cases. On the other hand, mutations of *N*- or *KRAS* genes were observed in 50% (4/8) of the fvPTC and in 40% (2/5) of PDTC. All FTC (n = 4) were *RAS* negative. The *PAX8-PPARG* fusion gene was found in 12.5% (1/8) of fvPTC and in 25% (1/4) of FTC. No *RET/PTC1*, *-2* or *-3* rearrangements were identified in PTC. However, since other rearrangements involving the *RET* (Ciampi *et al.*, 2007) or *NTRK1* (Pierotti and Greco, 2006) genes have also been described in PTC, we specifically analysed *RET* and *NTRK1* microarray mRNA expression in PTC negative for mutations. In one cPTC (sample 2 – Supplementary Table II.1), a 20-fold increase in *RET* expression was detected in comparison to the other samples. Fluorescence *in situ* hybridisation (FISH) confirmed the presence of a *RET/PTC* rearrangement in 37% (71/194) of these tumour cells (data not shown).

Unsupervised analyses for global gene expression profiling

We carried out unsupervised analyses to examine the relationship between gene expression, tumour histotype and mutational status. Global gene expression similarity between the 27 samples was examined using hierarchical clustering (Figure II.1). As represented on the dendrogram, distinct profiles separated FTC from the other tumours. Interestingly, a case of fvPTC diffuse (or multinodular) with a *PAX8-PPARG* rearrangement clustered with FTC. Different molecular signatures were present in the PTC sub-set: cPTC formed a separate sub-group from fvPTC and, among these PTC subtypes, samples with *RAS*/*BRAF* mutations were separated from samples without mutations. By PCA of data for all probe-sets, which represents the samples three-dimensionally according to the global gene expression profile, the FTC and the fvPTC diffuse (or multinodular) also formed a group apart from the other tumours and normal thyroid samples, which tended to cluster together (Supplementary Figure II.1 and Supplementary Movie II.1). PDTC samples, particularly those with *RAS* mutations, clustered with PTC in both representations.

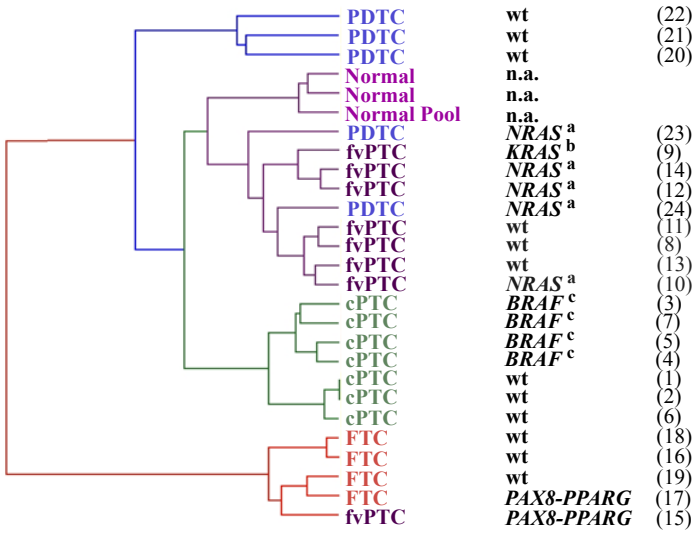

Figure II.1 - Global gene expression similarity between samples using the unsupervised hierarchical clustering method. In the dendogram, distance separating samples represents the gene expression resemblance between them. The result of mutational analysis for each tumour specimen is shown. Wild-type (wt) label denotes absence of mutation in screened genes; [a]Q61R mutant of NRAS; [b]G13R mutant of KRAS; [c]V600E mutant of BRAF; in parenthesis is indicated the sample number assigned in Supplementary Table II.1. PDTC - poorly differentiated thyroid carcinoma; fvPTC - follicular variant of papillary thyroid carcinoma; cPTC - classic papillary thyroid carcinoma; FTC - follicular thyroid carcinoma; n.a. - not applicable.

Genes differentially expressed between tumours and normal tissue

Differentially expressed genes were defined as those with an expression level equal, or higher, than 2-fold in a group relatively to another, with a *P* value ≤ 0.01. We compared each tumour group (cPTC, fvPTC, FTC and PDTC) with the three normal thyroid samples, and we found over-expression of about 60% of probe-sets for both cPTC and fvPTC, whereas in FTC and PDTC, about 80% of the probe-sets were under-expressed (Figure II.2). PDTC had 92 downregulated genes relatively to normal tissues (Supplementary Table II.2), but only 15 out of the 107 genes differentially expressed were over-expressed (Table II.1).

The biological processes mainly represented by the probe-sets differentially expressed between thyroid tumours and normal tissues, were the signal transduction, cell adhesion, regulation of transcription and cell proliferation/cell cycle (Supplementary Figure II.2). We were also able to identify 11 probe-sets that were under-expressed in all tumours comparatively to normal tissues (Table II.2).

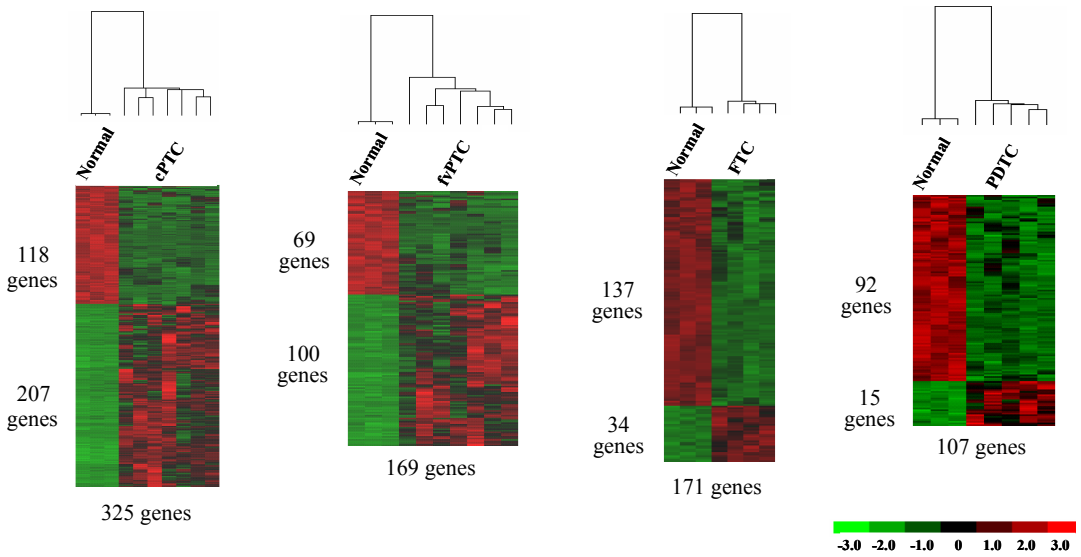

Figure II.2 - Expression profile of the genes differentially expressed between tumours and normal tissues. Each tumour histology was compared to the normal thyroid tissues and expression levels of the genes differentially expressed were represented. Expression levels are indicated by colour intensities in which green and red correspond, respectively, to a lower and a higher expression than the mean value for the gene, in all samples being compared. On the left of each profile, the number of under- and over-expressed genes in the tumour set is shown. At the bottom, the total number of differentially expressed genes is indicated. Only one probe-set was considered for each gene. PDTC - poorly differentiated thyroid carcinoma; fvPTC - follicular variant of papillary thyroid carcinoma; cPTC - classic papillary thyroid carcinoma; FTC - follicular thyroid carcinoma.

Table II.1 - Main characteristics of differentially expressed genes in poorly differentiated tumours.

Probe set	Gene name in array *HG-U133 Plus 2.0*	Official symbol[a]	Accession number	Biological process[b]	LBFC	*P*-value
Genes over-expressed in PDTC versus normal thyroid tissues						
204170_s_at	CDC28 protein kinase regulatory subunit 2	*CKS2*	NM_001827	Cell cycle	5.43	4.68E-03
219148_at	PDZ binding kinase	*PBK*	NM_018492	Cell cycle	4.29	8.04E-03
202503_s_at	KIAA0101	*KIAA0101*	NM_014736	Cell cycle	3.46	5.80E-03
205034_at	Cyclin E2	*CCNE2*	NM_004702	Cell cycle	2.95	6.21E-03
202975_s_at	Rho-related BTB domain containing 3	*RHOBTB3*	N21138	-	2.94	9.42E-03
218096_at	1-acylglycerol-3-phosphate O-acyltransferase 5 (lysophosphatidic acid acyltransferase, epsilon)	*AGPAT5*	NM_018361	Phospholipid metabolism	2.76	4.23E-03
225655_at	Ubiquitin-like, containing PHD and RING finger domains, 1	*UHRF1*	AK025578	Cell cycle	2.61	8.96E-03
229551_x_at	Zinc finger protein 367	*ZNF367*	N62196	Transcription regulation	2.59	6.36E-04
220608_s_at	Homo sapiens PRO1914 protein (PRO1914)	*ZNF770*	NM_014106	Transcription regulation	2.58	2.73E-03
222848_at	Leucine zipper protein FKSG14	*CENPK*	BC005400	Transcription regulation	2.53	4.85E-04
224726_at	Mindbomb homolog 1 (Drosophila)	*MIB1*	W80418	*Notch* signaling	2.38	1.98E-04
220145_at	ASAP	*MAP9*	NM_024826	Cell cycle	2.07	6.36E-03
218819_at	DEAD/H (Asp-Glu-Ala-Asp/His) box polypeptide 26	*INTS6*	NM_012141	snRNA processing	2.05	3.30E-03
235609_at	BRCA1 interacting protein C-terminal helicase 1	*BRIP1*	BF056791	DNA DBS repair	2.05	7.46E-03
203007_x_at	Lysophospholipase I	*LYPLA1*	AF077198	Phospholipid metabolism	2.03	2.24E-03
Genes under-expressed in PDTC versus WDTC						
225119_at	Chromatin modifying protein 4B	*CHMP4B*	AW299290	Protein transport	-2.97	0.00
204524_at	3-phosphoinositide dependent protein kinase-1	*PDPK1*	NM_002613	Cell adhesion	-2.61	0.00

[a]Assigned in *EntrezGene*; [b]Information taken from Online Mendelian Inheritance in Man (OMIM) or from *EntrezGene*. *P* values for difference in mean expression between groups were calculated using an unpaired t-test. DBS - double-strand breaks; LBFC - lower bound of fold change; snRNA - small nuclear RNA.

Table II.2 - Main characteristics of differentially expressed genes in the four thyroid tumour histotypes versus normal thyroid tissues.

Probe set	Gene name in array *HG-U133 Plus 2.0*	Official symbol[a]	Accession number	Biological process[b]	LBFC	*P*-value
205382_s_at	D component of complement (adipsin)	*CFD*	NM_001928	Immune response	-9.31	4.74E-03
204606_at	Chemokine (C-C motif) ligand 21	*CCL21*	NM_002989	Inflammatory response	-7.57	5.72E-03
235849_at	Hypothetical protein MGC45780	*SCARA5*	BE787752	Immune response	-6.38	9.25E-03
205350_at	Cellular retinoic acid binding protein 1	*CRABP1*	NM_004378	Retinoic acid metabolism	-6.13	5.13E-03
203060_s_at	3'-phosphoadenosine 5'-phosphosulfate synthase 2	*PAPSS2*	AF074331	Sulfur metabolism	-5.98	8.55E-04
212713_at	Microfibrillar-associated protein 4	*MFAP4*	R72286	Cell adhesion	-4.20	3.81E-04
1556427_s_at	Similar to hypothetical protein	*LOC221091*	AL834319	-	-4.07	5.57E-03
219778_at	Zinc finger protein, multitype 2	*ZFPM2*	NM_012082	Transcription regulation	-4.03	7.60E-03
205413_at	Chromosome 11 open reading frame 8	*MPPED2*	NM_001584	Nervous system development	-3.59	9.00E-05
206201_s_at	Mesenchyme homeo box 2 (growth arrest-specific homeo box)	*MEOX2*	NM_005924	Development	-2.92	5.85E-03
217525_at	Olfactomedin-like 1	*OLFML1*	AW305097	Cell proliferation	-2.64	2.34E-04

[a]Assigned in *EntrezGene*; [b]Information taken from Online Mendelian Inheritance in Man (OMIM) or from *EntrezGene*. *P* values for difference in mean expression between tumours and normal tissues were calculated using an unpaired t-test. LBFC - lower bound of fold change.

Genes specific for PDTC

The PDTC group had 3, 8 and 1 over-expressed probe-sets and 11, 154 and 59 under-expressed probe-sets compared with FTC, cPTC and fvPTC, respectively (data not shown). Only two probe-sets were consistently under-expressed in the PDTC tumour set comparatively to the WDTC (Table II.1).

Gene Set Enrichment Analysis for PDTC

GSEA is another method for interpreting gene expression data that focus on groups of genes sharing common biological function, chromosomal location or regulation. This approach can reveal important effects on pathways, which might be missed in single-gene analysis (Subramanian *et al.*, 2005). We applied this methodology to identify pathways altered in thyroid tumour progression. There were no statistically significant functional-defined gene sets enriched in PDTC samples *versus* WDTC, still we analysed the 20 most relevant results (Table II.3). The "BUB1 mitotic checkpoint serine/threonine kinase" (*BUB1*) was the most represented gene being present in 13 of the 20 gene sets. "Cyclin-dependent kinase 1" (*CDK1* or *CDC2*) and "cyclin B2" (*CCNB2*) were represented in 12 of the 20 gene sets, and 10 gene sets contained "MAD2 mitotic arrest deficient-like 1 (yeast)" (*MAD2L1*),

"topoisomerase (DNA) II alpha 170kDa" (*TOP2A*), "cyclin-dependent kinase inhibitor 3" (*CDKN3*) and "centromere protein A" (*CENPA*). In addition, statistically significant molecular signatures of 4 deregulated genes, which are involved in the cancer process, were identified in PDTC (Table II.3 – Expression neighbourhoods-defined Gene Sets).

Table II.3 - Gene sets enriched in the poorly differentiated versus the well-differentiated groups.

Gene set name[a]	Gene set description	Nominal *P*-value	FDR	FWER	Reference
Functional-defined gene sets					
LEE_TCELLS3_UP	Enriched in both intrathymic T progenitor cells and $CD3^{int}CD4^{+}CD8^{+}$ thymocytes	1.01E-02	0.95	0.43	Lee *et al*., 2004
YU_CMYC_UP	C-Myc activated genes	6.93E-03	0.56	0.47	Yu *et al*., 2005
GREENBAUM_E2A_UP	Upregulated in E2A-deficient pre-B-cell lines	5.14E-03	0.44	0.51	Greenbaum *et al*., 2004
VANTVEER_BREAST_OUTCOME_GOOD_VS_POOR_DN	Poor prognosis marker genes in breast cancer	7.61E-03	0.38	0.55	Van't Veer *et al*., 2002
MANALO_HYPOXIA_DN	Genes downregulated in human pulmonary endothelial cells under hypoxic conditions	8.89E-03	0.31	0.55	Manalo *et al*., 2005
ADIP_DIFF_CLUSTER5	Strongly upregulated at 24 hours during differentiation of 3T3-L1 fibroblasts into adipocytes	2.40E-02	0.32	0.62	Burton *et al*., 2002
CANCER_UNDIFFERENTIATED_META_UP	Genes commonly upregulated in undifferentiated cancer relative to well-differentiated cancer	1.64E-02	0.30	0.64	Rhodes *et al*., 2004
HUMAN_TISSUE_TESTIS	Genes expressed specifically in human testis tissue	1.15E-02	0.34	0.70	Su *et al*., 2002
ZHAN_MM_CD138_PR_VS_REST	Top ranked over-expressed genes in proliferation subgroup of bone marrow plasma cells from multiple myeloma patients	9.83E-03	0.31	0.70	Zhan *et al*., 2006
CROONQUIST_IL6_STARVE_UP	Genes upregulated in multiple myeloma cells exposed to cytokine IL6 versus IL6 starved cells	7.21E-03	0.29	0.71	Croonquist *et al*., 2003
BRCA_PROGNOSIS_NEG	Negatively correlated with metastasis and poor prognosis in breast cancer	1.37E-02	0.28	0.73	Van't Veer *et al*., 2002
P21_ANY_DN	Down-regulated follwing ectopic expression of p21 (*CDKN1A*) in ovarian cancer cell line	2.12E-02	0.27	0.74	Wu *et al*., 2002
DOX_RESIST_GASTRIC_UP	Upregulated in gastric cancer cell lines resistant to doxorubicin, compared to parent chemosensitive lines	1.94E-02	0.31	0.80	Kang *et al*., 2004
CROONQUIST_IL6_RAS_DN	Genes downregulated in multiple myeloma cells exposed to IL6 versus *NRAS* activating mutations cells	1.73E-02	0.29	0.80	Croonquist *et al*., 2003
REN_E2F1_TARGETS	E2F1 targets in primary fibroblast WI-38	2.84E-02	0.28	0.81	Ren *et al*., 2002
BREAST_DUCTAL_CARCINOMA_GENES	Genes upregulated in high tumor grade breast tumours progressing from pre-invasive ductal carcinoma *in situ* to invasive ductal carcinoma	2.43E-02	0.30	0.84	a
SERUM_FIBROBLAST_CELLCYCLE	Cell-cycle dependent genes, regulated following exposure to serum in a variety of human fibroblast cell lines	5.04E-02	0.28	0.85	Chang *et al*., 2004
BRENTANI_CELL_CYCLE	Cancer related genes involved in the cell cycle	1.87E-02	0.28	0.86	Brentani *et al*., 2003
SHEPARD_CRASH_AND_BURN_MUT_VS_WT_DN	Genes upregulated in wild type zebra fish compared to the B-Myb loss-of-fuction mutants	2.13E-02	0.28	0.86	Shepard *et al*., 2005
GOLDRATH_CELLCYCLE	Cell cycle genes induced during antigen activation of $CD8^{+}$ T cells	2.50E-02	0.27	0.87	Goldrath *et al*., 2004
Expression neighbourhoods-defined gene sets					
GNF2_CKS1B	Expression neighbourhood of *CKS1B* in the GNF2 expression compendium	0.00	0.04	0.02	a
MORF_BUB1	Expression neighbourhood of *BUB1* in the MORF expression compendium	4.74E-03	0.14	0.10	a
MORF_BUB1B	Expression neighbourhood of *BUB1B* in the MORF expression compendium	0.00	0.20	0.19	a
GNF2_ESPL1	Expression neighbourhood of *ESPL1* in the GNF2 expression compendium	9.59E-03	0.18	0.21	a

[a]Assigned in Molecular Signatures Database (www.broad.mit.edu/gsea/msigdb/ index.jsp). References are supplied as supplementary data. BUB1 - BUB1 mitotic checkpoint serine/threonine kinase; BUB1B - BUB1 mitotic checkpoint serine/threonine kinase B; CD - cluster of differentiation; IL6 - interleukin 6 (interferon, beta 2); CDKN1A - cyclin-dependent kinase inhibitor 1A ($p21^{CIP1}$); CKS1B - CDC28 protein kinase regulatory subunit 1B; ESPL1 - extra spindle pole bodies homolog 1 (S. cerevisiae); FDR - false discovery rate; FWER - family wise-error rate.

Validation of microarray gene expression

Real-Time RT-PCR was performed in order to validate 3 genes differentially expressed between PDTC and normal thyroid samples: "ubiquitin-like with PHD and ring finger domains 1" (*UHRF1*), "PDZ binding kinase" (*PBK*) and "inter-alpha-trypsin inhibitor heavy chain family, member 5" (*ITIH5*). This validation was processed in an independent sample set of 28 tumours (Figure II.3). *UHRF1* and *PBK* had increased expression in all tumour samples relatively to normal tissue samples, but the highest expression levels were detected in PDTC. Differences in the *UHRF1* expression (Figure II.3B) between PDTC and normal tissue were statistically significant (11.77 ± 3.07 *versus* 1.77 ± 0.36; $P < 0.01$), even if only considering the expression in the independent set (14.30 ± 5.49 *versus* 1.77 ± 0.36; $P < 0.05$) (Figure II.3A). On the other hand, differences in the *PBK* expression were not statistically significant (Figure II.3A and D). *ITIH5* expression was decreased in all tumours samples relatively to normal tissues (Figure II.3E and F). Statistically significant differences were detected in all tumour groups relatively to normal samples, except in cPTC (PDTC: 0.22 ± 0.17, $P < 0.001$; FTC: 0.15 ± 0.05, $P < 0.001$; fvPTC: 0.22 ± 0.03, $P < 0.05$ *versus* normal: 1.00 ± 0.10). Differences were also significant when considering the independent set of samples (PDTC: 0.41 ± 0.33, $P < 0.05$; FTC: 0.14 ± 0.07, $P < 0.001$ *versus* normal: 1.00 ± 0.10). Additionally, we assessed *UHRF1* and *ITIH5* expressions in two PDTC cell lines. No significant increase in *UHRF1* expression was detected (Mean ± standard deviation: 1.86 ± 0.16 and 1.43 ± 0.16 *versus* 1.77 ± 0.36). On the other hand, *ITIH5* expression was undetectable (Ct values > 37) in both cell lines. Correlation of quantitative RT-PCR data with the expression levels obtained in the microarray analysis was statistically significant (Pearson correlation $r = 0.61$ for *UHRF1* with $P=0.0015$; Spearman correlation $r = 0.70$ for *PBK* with $P=0.0001$; Pearson correlation $r = 0.94$ for *ITIH5* with $P < 0.0001$). There was no correlation of gene expression with tumour size, gender or age, except for *ITIH5*, whose decreased expression was associated with larger tumours (Spearman correlation $r = -0.33$ with $P=0.02$).

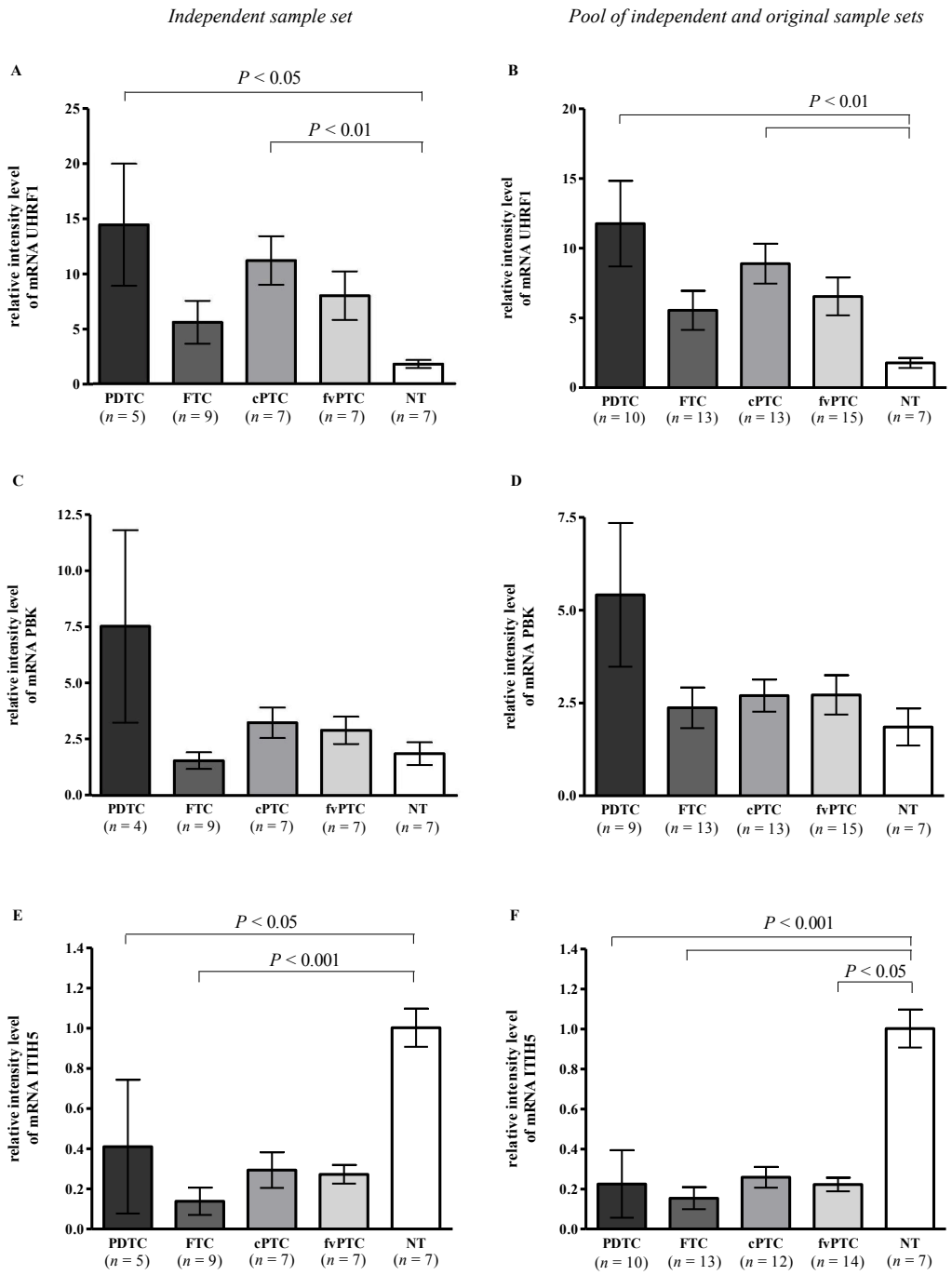

Figure II.3 - Expression of the *UHRF1*, *PBK* and *ITIH5* genes in different tumour histotypes, assessed by quantitative RT-PCR. Relative mRNA levels for *UHRF1* (A, B), *PBK* (C, D) and *ITIH5* (E, F), were assessed in an independent sample set (left panel) and in the entire sample set, comprising the microarray and the independent sample sets (right panel). Expression levels were normalised with the "glyceraldehyde-3-phosphate dehydrogenase" (*GAPDH*) expression and determined relatively to a calibrator. Error bars denote ± SEM. The *P* values for difference in mean expression between groups were performed using the Kruskal-Wallis with Dunn's Multiple Comparison test. These genes could not be assayed in one cPTC from the microarray set, *PBK* could not be evaluated in one PDTC sample, as well as, *ITIH5* in one fvPTC and one cPTC from microarray set. PDTC - poorly differentiated thyroid carcinoma; fvPTC - follicular variant of papillary thyroid carcinoma; cPTC - classic papillary thyroid carcinoma; FTC - follicular thyroid carcinoma; NT - normal thyroid tissue.

5. Discussion

The more aggressive thyroid carcinomas (PDTC and ATC) have high malignant potential and it is not yet clear if they arise from pre-existing indolent WDTC or if they arise *de novo*. Some PDTC cases bear areas of pre-existing PTC and have a significant prevalence of *BRAF* mutations (Nikiforova *et al.*, 2003). Others, instead of *BRAF*, frequently display *RAS* mutations (Garcia-Rostan *et al.*, 2003), which are typically detected in follicular thyroid adenomas, FTC and fvPTC. Comparative genomic hybridisation (CGH) studies showed that among 11 copy number changes present in PTC, 8 were also present in the PDTC set, thus suggesting common genetic pathways (Wreesmann *et al.*, 2002).

In our work, we were able to identify distinct gene expression profiles among different thyroid tumour histotypes. Our results suggest that PDTC have a gene expression profile closer to PTC, in particular to the follicular variant, than to FTC. In fact, for PDTC harbouring *RAS* mutations, a clear similarity to the gene profile of *RAS*-mutated fvPTC was observed. Interestingly, these *RAS*-mutated PDTC, presented papillary like nuclei. In keeping with our findings, it has been observed that fvPTC, in contrast to cPTC, are more frequently aneuploid (Wreesmann *et al.*, 2004), a feature common in PDTC. Therefore, fvPTC are likely to be precursors of PDTC, particularly those cases harbouring *RAS* mutations.

We also analysed the differential gene expression between tumours and normal thyroid tissues. PTC cases had slightly more over- than under-expressed probe-sets, confirming previous reports (Huang *et al.*, 2001). On the other hand, FTC and PDTC had clearly a predominance of downregulated probe-sets, which is also in accordance with others (Aldred *et al.*, 2003; Rodrigues *et al.*, 2007). Studies have shown that allelic losses are clearly more frequent in FTC and PDTC than in PTC (Ward *et al.*, 1998; Rodrigues *et al.*, 2004). This could account for the differences in gene expression since a genomic loss could, theoretically, originate under-expression of genes. Epigenetic mechanisms, such as DNA hypermethylation, are also likely to explain these expression profiles. Indeed, increased frequency of hypermethylated CpG islands is a common alteration in tumour progression.

Eleven probe-sets were simultaneously under-expressed in all tumours relatively to normal tissues, suggesting that these genes may have important suppressor activity in thyroid tumorigenesis. Among these, “metallophosphoesterase domain containing 2” (*MPPED2*) and “cellular retinoic acid binding protein 1” (*CRABP1*) under-expression have already been observed in thyroid tumours (Griffith *et al.*, 2006).

As observed earlier in other genome-wide studies, comparing clinically aggressive PTC with differentiated PTC cases (Fluge *et al.*, 2006) or comparing PDTC with normal tissue (Rodrigues *et al.*, 2007) or with WDTC (Montero-Conde *et al.*, 2008), we found that many of the genes differentially upregulated in PDTC relatively to normal tissues were associated with the cell cycle, indicating that the deregulation of this process is crucial in the progression to more aggressive thyroid tumours. In particular, we identified genes with major roles in mitosis, such as "CDC28 protein kinase regulatory subunit 2" (*CKS2*) and "cyclin E2" (*CCNE2*), which have been reported as over-expressed in various types of tumours (Gudas *et al.*, 1999; Scrideli *et al.*, 2008).

We selected 3 genes for Real-Time RT-PCR analysis, which were shown in the microarray analysis, to be differentially over-expressed (*PBK* and *UHRF1*) and under-expressed (*ITIH5*) between PDTC and normal thyroid tissues. *UHRF1* and *ITIH5* expressions were statistically different between PDTC and normal thyroid samples. Although not statistically significant, *PBK* had higher expression levels in PDTC compared with normal thyroid. Therefore, *PBK* is also a potential therapeutic target, as it encodes a mitotic protein, member of MAPK kinases family, which was found to be over-expressed in haematological (Nandi *et al.*, 2004) and breast tumours (Park *et al.*, 2006), and in PDTC cell lines (Rodrigues *et al.*, 2007). *UHRF1* over-expression has been already reported in lung (Jenkins *et al.*, 2005) and breast (Hopfner *et al.*, 2000) cancers. By conventional CGH analyses, the chromosomal *locus* 19p13.3, where *UHRF1* is located, was identified as a common region of chromosomal gains in Hürthle cell thyroid neoplasms (Wada *et al.*, 2002) and recently, using array-CGH, gains involving the 19p13 region were also found in 67% of ATC (Lee *et al.*, 2008). *UHRF1* encodes a nuclear protein that transcriptionally regulates TOP2A (Hopfner *et al.*, 2000), an enzyme that catalyses the breaking and rejoining of DNA strands, during transcription. Interestingly, *TOP2A* showed a 5-fold increase in PDTC *versus* normal tissues (P=0.02). In addition, UHRF1 is known to regulate the RB1 (Jeanblanc *et al.*, 2005) and is involved in the DNA damage response (Jenkins *et al.*, 2005). More recently, an essential role for UHRF1 in the control of DNA (cytosine-5)-methyltransferase 1 (DNMT1), the protein responsible for DNA methylation maintenance in mammalian cells, has also been reported (Bostick *et al.*, 2007; Sharif *et al.*, 2007). UHRF1 and DNMT1 interactions have been shown to be involved in vascular endothelial growth factor A (VEGFA) regulation, a major pro-angiogenic protein (Achour *et al.*, 2008).

Classification according to biological functions showed that about 8.5% of the genes

differentially expressed between PDTC and normal tissues were downregulated and all related to cell adhesion. Interestingly, by further analysis, we found that under-expressed genes were mainly related to the cell membrane, encoding receptors, transmembranar or extracelular proteins. In agreement with this, the *ITIH5* gene, which may play an essential role in cell attachment and invasion, was under-expressed in PDTC tumours. *ITIH5* is a recently discovered member of the inter-alpha-trypsin inhibitor heavy chain (ITIH) gene family (Himmelfarb *et al.*, 2004). In particular, the main function of ITIH is based on their covalent linkage to hyaluronic acid, the major component of the extracellular matrix. Therefore deregulation of ITIH proteins affects the stability of the extracellular matrix and so, may promote tumour invasion and metastasis (Bost *et al.*, 1998). Accordingly, *ITIH* genes have been shown to be downregulated in a variety of human tumours and have been proposed as tumour suppressor or metastasis repressor genes (Hamm *et al.*, 2008). *ITIH5* downregulation in breast cancer, caused by promoter hypermethylation, is associated with poorer clinical outcome, and reduced protein expression was proved to be a bad prognostic marker in invasive node-negative patients (Veeck *et al.*, 2008). In fact, we found that lower expression of *ITIH5* was statistically associated with larger tumours, as well as with more aggressive cases, such as PDTC (reaching undetectable levels in the two PDTC cell lines). Interestingly, we could also observe that extensively invasive FTC had lower *ITIH5* expression levels than minimally invasive ones.

Compared with WDTC, PDTC had enriched gene sets (represented by over-expressed genes) associated earlier with cell cycle and poor prognosis signatures. Interestingly, one of these sets corresponded to a meta-signature of genes differentially over-expressed in undifferentiated relatively to well-differentiated cancers of different tissues (Rhodes *et al.*, 2004). Among the most represented genes in these sets, were cell-cycle regulators (*CDK1*, *CCNB2*, *CDKN3* and *TOP2A*), as well as genes with a role in the structure of the kinetochore and in the mitotic spindle assembly checkpoint (*CENPA*, *BUB1* and *MAD2L1*). We also found statistically significant molecular signatures associated with the *BUB1* and "BUB1 mitotic checkpoint serine/threonine kinase B" (*BUB1B*) genes. Some of these genes were reported earlier to be over-expressed in advanced cases of thyroid tumours (Montero-Conde *et al.*, 2008; Wada *et al.*, 2008). These observations indicate that PDTC may have abnormalities in mitotic spindle assembly checkpoint or in the attachment of kinetochores, which may compromise mitotic fidelity and contribute to chromosomal instability. Accordingly, we observed earlier (Banito *et al.*, 2007) that 4 out of the 5 PDTC analysed in the present study,

were aneuploid.

In the analysis of genes differentially expressed between PDTC and WDTC, we only identified two genes. One of these, the *PDPK1* gene, encodes a protein responsible for protein kinase B or AKT activation. PI3K-AKT pathway has a central role in regulation of apoptosis, proliferation and cell cycle progression and its abnormal activation is frequently found in cancers, including thyroid tumours (Shinohara *et al.*, 2007). Unexpectedly, and contrary to other cancer types, we observed that *PDPK1* gene was under-expressed in PDTC.

The identification of molecular mechanisms involved in tumour progression is important in the design of new strategies for treating aggressive neoplasias, such as PDTC and ATC. For instance, over-expression of UHRF1 in PDTC samples, a protein that seems to be essential for DNMT1 function, indicates that UHRF1 targeting may offer a new therapeutic approach for PDTC cases. On the other hand, *ITIH5* downregulation may be an essential mechanism in thyroid tumorigenesis, especially in tumour metastasis. In addition, and similarly to breast cancer, ITIH5 may prove to be a useful prognostic marker.

6. Acknowledgements

We would like to thank Dr. Jörg D. Becker, from the Affymetrix Core Facility at Instituto Gulbenkian de Ciência (Oeiras, Portugal) for the processing of RNA samples with *HG-U133 Plus 2.0* arrays. We also thank Drs. Jorge Rosa Santos and Olimpia Cid for the surgical collection of tissue samples and Dr. Rafael Cabrera for the histological analysis. Authors are also grateful to Pedro Batista for helpful assistance. This work was supported by Fundação Calouste Gulbenkian. JM Pita is recipient of a Portuguese government (Fundação para a Ciência e Tecnologia) PhD fellowship (SFRH/BD/46096/2008).

7. References

Achour M, Jacq X, Ronde P, Alhosin M, Charlot C, Chataigneau T *et al* (2008). The interaction of the SRA domain of ICBP90 with a novel domain of DNMT1 is involved in the regulation of VEGF gene expression. *Oncogene* **27:** 2187-2197.

Aldred MA, Ginn-Pease ME, Morrison CD, Popkie AP, Gimm O, Hoang-Vu C *et al* (2003). Caveolin-1 and caveolin-2, together with three bone morphogenetic protein-related genes, may encode novel tumor suppressors down-regulated in sporadic follicular thyroid carcinogenesis. *Cancer Res* **63:** 2864-2871.

Banito A, Pinto AE, Espadinha C, Marques AR, Leite V (2007). Aneuploidy and RAS mutations are mutually exclusive events in the development of well-differentiated thyroid follicular tumours. *Clin Endocrinol (Oxf)* **67:** 706-711.

Bost F, Diarra-Mehrpour M, Martin JP (1998). Inter-alpha-trypsin inhibitor proteoglycan family--a group of proteins binding and stabilizing the extracellular matrix. *Eur J Biochem* **252:** 339-346.

Bostick M, Kim JK, Esteve PO, Clark A, Pradhan S, Jacobsen SE (2007). UHRF1 plays a role in maintaining DNA methylation in mammalian cells. *Science* **317:** 1760-1764.

Ciampi R, Giordano TJ, Wikenheiser-Brokamp K, Koenig RJ, Nikiforov YE (2007). HOOK3-RET: a novel type of RET/PTC rearrangement in papillary thyroid carcinoma. *Endocr Relat Cancer* **14:** 445-452.

Dairkee SH, Ji Y, Ben Y, Moore DH, Meng Z, Jeffrey SS (2004). A molecular 'signature' of primary breast cancer cultures; patterns resembling tumor tissue. *BMC Genomics* **5:** 47.

DeLellis RA, Lloyd RV, Heitz PU, Eng C (2004). *World Health Organization Classification of Tumours. Pathology and Genetics of Tumours of Endocrine Organs*. IARC Press: Lyon, France.

Eszlinger M, Krohn K, Kukulska A, Jarzab B, Paschke R (2007). Perspectives and limitations of microarray-based gene expression profiling of thyroid tumors. *Endocr Rev* **28:** 322-338.

Fluge O, Bruland O, Akslen LA, Lillehaug JR, Varhaug JE (2006). Gene expression in poorly differentiated papillary thyroid carcinomas. *Thyroid* **16:** 161-175.

Garcia-Rostan G, Zhao H, Camp RL, Pollan M, Herrero A, Pardo J *et al* (2003). ras mutations are associated with aggressive tumor phenotypes and poor prognosis in thyroid cancer. *J Clin Oncol* **21:** 3226-3235.

Griffith OL, Melck A, Jones SJ, Wiseman SM (2006). Meta-analysis and meta-review of thyroid cancer gene expression profiling studies identifies important diagnostic biomarkers. *J Clin Oncol* **24:** 5043-5051.

Gudas JM, Payton M, Thukral S, Chen E, Bass M, Robinson MO *et al* (1999). Cyclin E2, a novel G1 cyclin that binds Cdk2 and is aberrantly expressed in human cancers. *Mol Cell Biol* **19:** 612-622.

Hamm A, Veeck J, Bektas N, Wild PJ, Hartmann A, Heindrichs U *et al* (2008). Frequent expression loss of Inter-alpha-trypsin inhibitor heavy chain (ITIH) genes in multiple human solid tumors: a systematic expression analysis. *BMC Cancer* **8:** 25.

Himmelfarb M, Klopocki E, Grube S, Staub E, Klaman I, Hinzmann B *et al* (2004). ITIH5, a novel member of the inter-alpha-trypsin inhibitor heavy chain family is downregulated in breast cancer. *Cancer Lett* **204:** 69-77.

Hopfner R, Mousli M, Jeltsch JM, Voulgaris A, Lutz Y, Marin C *et al* (2000). ICBP90, a novel human CCAAT binding protein, involved in the regulation of topoisomerase IIalpha expression. *Cancer Res* **60:** 121-128.

Huang Y, Prasad M, Lemon WJ, Hampel H, Wright FA, Kornacker K *et al* (2001). Gene expression in papillary thyroid carcinoma reveals highly consistent profiles. *Proc Natl Acad Sci U S A* **98:** 15044-15049.

Irizarry RA, Hobbs B, Collin F, Beazer-Barclay YD, Antonellis KJ, Scherf U *et al* (2003). Exploration, normalization, and summaries of high density oligonucleotide array probe level data. *Biostatistics* **4:** 249-264.

Jeanblanc M, Mousli M, Hopfner R, Bathami K, Martinet N, Abbady AQ *et al* (2005). The retinoblastoma gene and its product are targeted by ICBP90: a key mechanism in the G1/S transition during the cell cycle. *Oncogene* **24:** 7337-7345.

Jenkins Y, Markovtsov V, Lang W, Sharma P, Pearsall D, Warner J *et al* (2005). Critical role of the ubiquitin ligase activity of UHRF1, a nuclear RING finger protein, in tumor cell growth. *Mol Biol Cell* **16:** 5621-5629.

Khatri P, Draghici S, Ostermeier GC, Krawetz SA (2002). Profiling gene expression using onto-express. *Genomics* **79:** 266-270.

Lam KY, Lo CY, Chan KW, Wan KY (2000). Insular and anaplastic carcinoma of the thyroid: a 45-year comparative study at a single institution and a review of the significance of p53 and p21. *Ann Surg* **231:** 329-338.

Lee JJ, Au AY, Foukakis T, Barbaro M, Kiss N, Clifton-Bligh R *et al* (2008). Array-CGH identifies cyclin D1 and UBCH10 amplicons in anaplastic thyroid carcinoma. *Endocr Relat Cancer* **15:** 801-815.

Li C, Wong WH (2001). Model-based analysis of oligonucleotide arrays: expression index computation and outlier detection. *Proc Natl Acad Sci U S A* **98:** 31-36.

Marques AR, Espadinha C, Catarino AL, Moniz S, Pereira T, Sobrinho LG *et al* (2002). Expression of PAX8-PPAR gamma 1 rearrangements in both follicular thyroid carcinomas and adenomas. *J Clin Endocrinol Metab* **87:** 3947-3952.

Montero-Conde C, Martin-Campos JM, Lerma E, Gimenez G, Martinez-Guitarte JL, Combalia N *et al* (2008). Molecular profiling related to poor prognosis in thyroid carcinoma. Combining gene expression data and biological information. *Oncogene* **27:** 1554-1561.

Nandi A, Tidwell M, Karp J, Rapoport AP (2004). Protein expression of PDZ-binding kinase is up-regulated in hematologic malignancies and strongly down-regulated during terminal differentiation of HL-60 leukemic cells. *Blood Cells Mol Dis* **32:** 240-245.

Nikiforova MN, Kimura ET, Gandhi M, Biddinger PW, Knauf JA, Basolo F *et al* (2003). BRAF mutations in thyroid tumors are restricted to papillary carcinomas and anaplastic or poorly differentiated carcinomas arising from papillary carcinomas. *J Clin Endocrinol Metab* **88:** 5399-5404.

Park JH, Lin ML, Nishidate T, Nakamura Y, Katagiri T (2006). PDZ-binding kinase/T-LAK cell-originated protein kinase, a putative cancer/testis antigen with an oncogenic activity in breast cancer. *Cancer Res* **66:** 9186-9195.

Patel KN, Shaha AR (2006). Poorly differentiated and anaplastic thyroid cancer. *Cancer Control* **13:** 119-128.

Pierotti MA, Greco A (2006). Oncogenic rearrangements of the NTRK1/NGF receptor. *Cancer Lett* **232:** 90-98.

Quackenbush J (2006). Microarray analysis and tumor classification. *N Engl J Med* **354:** 2463-2472.

Quiros RM, Ding HG, Gattuso P, Prinz RA, Xu X (2005). Evidence that one subset of anaplastic thyroid carcinomas are derived from papillary carcinomas due to BRAF and p53 mutations. *Cancer* **103:** 2261-2268.

Rebelo S, Domingues R, Catarino AL, Mendonca E, Santos JR, Sobrinho L *et al* (2003). Immunostaining and RT-PCR: different approaches to search for RET rearrangements in patients with papillary thyroid carcinoma. *Int J Oncol* **23:** 1025-1032.

Rhodes DR, Yu J, Shanker K, Deshpande N, Varambally R, Ghosh D *et al* (2004). Large-scale meta-analysis of cancer microarray data identifies common transcriptional profiles of neoplastic transformation and progression. *Proc Natl Acad Sci U S A* **101:** 9309-9314.

Rodrigues RF, Roque L, Rosa-Santos J, Cid O, Soares J (2004). Chromosomal imbalances associated with anaplastic transformation of follicular thyroid carcinomas. *Br J Cancer* **90:** 492-496.

Rodrigues RF, Roque L, Krug T, Leite V (2007). Poorly differentiated and anaplastic thyroid carcinomas: chromosomal and oligo-array profile of five new cell lines. *Br J Cancer* **96:** 1237-1245.

Scrideli CA, Carlotti CG, Jr., Okamoto OK, Andrade VS, Cortez MA, Motta FJ *et al* (2008). Gene expression profile analysis of primary glioblastomas and non-neoplastic brain tissue: identification of potential target genes by oligonucleotide microarray and real-time quantitative PCR. *J Neurooncol* **88:** 281-291.

Sharif J, Muto M, Takebayashi S, Suetake I, Iwamatsu A, Endo TA *et al* (2007). The SRA protein Np95 mediates epigenetic inheritance by recruiting Dnmt1 to methylated DNA. *Nature* **450:** 908-912.

Shinohara M, Chung YJ, Saji M, Ringel MD (2007). AKT in thyroid tumorigenesis and progression. *Endocrinology* **148:** 942-947.

Subramanian A, Tamayo P, Mootha VK, Mukherjee S, Ebert BL, Gillette MA *et al* (2005). Gene set enrichment analysis: a knowledge-based approach for interpreting genome-wide expression profiles. *Proc Natl Acad Sci U S A* **102:** 15545-15550.

Veeck J, Chorovicer M, Naami A, Breuer E, Zafrakas M, Bektas N *et al* (2008). The extracellular matrix protein ITIH5 is a novel prognostic marker in invasive node-negative breast cancer and its aberrant expression is caused by promoter hypermethylation. *Oncogene* **27:** 865-876.

Wada N, Duh QY, Miura D, Brunaud L, Wong MG, Clark OH (2002). Chromosomal aberrations by comparative genomic hybridization in hurthle cell thyroid carcinomas are associated with tumor recurrence. *J Clin Endocrinol Metab* **87:** 4595-4601.

Wada N, Yoshida A, Miyagi Y, Yamamoto T, Nakayama H, Suganuma N *et al* (2008). Overexpression of the mitotic spindle assembly checkpoint genes hBUB1, hBUBR1 and hMAD2 in thyroid carcinomas with aggressive nature. *Anticancer Res* **28:** 139-144.

Wang HM, Huang YW, Huang JS, Wang CH, Kok VC, Hung CM *et al* (2007). Anaplastic carcinoma of the thyroid arising more often from follicular carcinoma than papillary carcinoma. *Ann Surg Oncol* **14:** 3011-3018.

Ward LS, Brenta G, Medvedovic M, Fagin JA (1998). Studies of allelic loss in thyroid tumors reveal major differences in chromosomal instability between papillary and follicular carcinomas. *J Clin Endocrinol Metab* **83:** 525-530.

Wreesmann VB, Ghossein RA, Patel SG, Harris CP, Schnaser EA, Shaha AR *et al* (2002). Genome-wide appraisal of thyroid cancer progression. *Am J Pathol* **161:** 1549-1556.

Wreesmann VB, Ghossein RA, Hezel M, Banerjee D, Shaha AR, Tuttle RM *et al* (2004). Follicular variant of papillary thyroid carcinoma: genome-wide appraisal of a controversial entity. *Genes Chromosomes Cancer* **40:** 355-364.

CHAPTER III

Cell cycle deregulation and TP53 and RAS mutations are major events in poorly differentiated and undifferentiated thyroid carcinomas

JM Pita, IF Figueiredo, V Leite, BM Cavaco

Second phase of submission to The Journal of Clinical Endocrinology & Metabolism under preparation

Author's note

IF Figueiredo and I, are co-first authors as both contributed equally for this work. IF Figueiredo, working for her Master's degree, was responsible for the mutational analysis of samples, for quantitative RT-PCR, and assisted V Leite in the clinical-pathological revision of patients. I was responsible for the selection and preparation of samples for microarray hybridisation at the Core Facility, for data and statistical analysis, for quantitative RT-PCR and for the writing of the article. V Leite and BM Cavaco were both responsible for the work supervision and for the writing and revision of the article. The submitted manuscript is presented with some minor changes and layout modifications.

1. Abstract and keywords

Objective: Anaplastic thyroid carcinomas are among the most lethal malignancies, for which there is no effective treatment. In the present study, we aimed to elucidate the molecular alterations contributing to ATC development, and to identify novel therapeutic targets.

Design: We profiled the global gene expression of 5 ATC, and validated differentially expressed genes by quantitative RT-PCR in an independent set of tumours. In a series of 26 ATC, we searched for pathogenic alterations in genes involved in the most deregulated cellular processes, including the hot-spot regions of *RAS*, *BRAF*, *TP53*, *CTNNB1* (β-catenin) and *PIK3CA* genes, and, for the first time, a comprehensive analysis of components involved in cell cycle [*CDKN1A* ($p21^{CIP1}$); *CDKN1B* ($p27^{KIP1}$); *CDKN2A* ($p14^{ARF}$, $p16^{INK4A}$); *CDKN2B* ($p15^{INK4B}$); *CDKN2C* ($p18^{INK4C}$)], and in epithelial-to-mesenchymal transition (*AXIN1*). Mutational analysis was also performed in 22 PDTC.

Results: Expression profiling revealed that ATC were characterised by under-expression of epithelial components, upregulation of mesenchymal markers and genes from TGF-β pathway, as well as, over-expression of cell cycle-related genes. In accordance, upregulation of the *SNAI2* gene, a TGF-β-responsive mesenchymal factor, was validated. *CDKN3*, which prevents G1/S transition, was significantly upregulated in ATC and PDTC, and aberrantly spliced in ATC.

Mutational analysis showed that most mutations were present in *TP53* (42% of ATC; 27% of PDTC) or *RAS* (31% of ATC; 18% of PDTC). *TP53* and *RAS* alterations showed evidence of mutual exclusivity (P=0.0354), and were associated with significant lower survival (P=0.0383). *PIK3CA*, *CDKN2A* and *CDKN2B* mutations were present in nearly 25% of PDTC, and in less than 5% of ATC. *BRAF*, *CTNNB1* and *AXIN1* mutations were rarely detected.

Conclusion: Overall, this study identified crucial roles for *TP53*, *RAS*, CDK inhibitors, and TGF-β pathway, which may represent feasible therapeutic targets for ATC and PDTC treatment.

Keywords: poorly differentiated thyroid carcinoma; anaplastic thyroid carcinoma; genome-wide expression; somatic mutations; cell cycle; epithelial-to-mesenchymal transition

2. Introduction

The majority of thyroid neoplasias, arising from follicular cells, are well-differentiated tumours, namely PTC and FTC, which can be successfully treated with surgery and radioiodine. On the other hand, PDTC and ATC are dedifferentiated tumours, and present a more aggressive behaviour. In particular, ATC rapid onset, extensive invasion and distant metastases, contribute to be one of the most lethal malignancies, with a median survival of 3-4 months (Smallridge *et al.*, 2009). In addition, most current therapeutic options have been ineffective.

PDTC and ATC have been identified in co-existence with well-differentiated areas, suggesting that these tumours can arise from pre-existing PTC and/or FTC cases (Quiros *et al.*, 2005; Wang *et al.*, 2007; Santarpia *et al.*, 2008). This process of dedifferentiation is supported by the detection, in PDTC and ATC, of *BRAF* and *RAS* genes mutations (commonly found in WDTC) in association with later acquired alterations in *TP53*, *CTNNB1* (β-catenin) and *PIK3CA* genes (Garcia-Rostan *et al.*, 2001; Garcia-Rostan *et al.*, 2005; Quiros *et al.*, 2005; Wang *et al.*, 2007; Santarpia *et al.*, 2008).

Global gene expression profiling has been used to define the molecular events involved in the PDTC and ATC pathogenesis. Several authors have described that, compared with WDTC cases, PDTC and ATC exhibit deregulation of different cellular events, *e.g.*, focal adhesion, cell motility, TGF-β signalling, chromosome segregation, cell cycle and proliferation (Fluge *et al.*, 2006; Salvatore *et al.*, 2007; Montero-Conde *et al.*, 2008). We have compared the transcriptional profiles of PDTC, WDTC and normal thyroid samples, and found that PDTC presented molecular signatures mainly related to cell proliferation, poor prognosis, spindle assembly checkpoint and cell adhesion (Chapter II).

In the present study, in an attempt to further elucidate the main molecular pathways and alterations contributing to PDTC and ATC, we profiled the ATC gene expression, and analysed the mutational status of *N*-, *H*-, *KRAS*, *BRAF*, *TP53*, *CTNNB1* and *PIK3CA* genes in a series of 48 tumours (26 ATC and 22 PDTC), 4 ATC- and 2 PDTC-derived cell lines. Additionally, in accordance with the deregulated pathways found in ATC and PDTC, we sequenced the coding regions and splice sites of *CDKN1A* ($p21^{CIP1}$), *CDKN1B* ($p27^{KIP1}$), *CDKN2A* ($p14^{ARF}$, $p16^{INK4A}$), *CDKN2B* ($p15^{INK4B}$) and *CDKN2C* ($p18^{INK4C}$), which encode critical regulators of the cell cycle and proliferation. We also analysed *AXIN1* gene, which

encodes a negative regulator of WNT signalling pathway, found mutated in 81.8% of ATC from a Japanese series (Kurihara *et al.*, 2004).

3. Materials and methods

Tissue samples

WDTC cases, normal thyroid tissues samples (all taken from the opposite lobe of thyroid tumours), 12 PDTC and 15 ATC were obtained at time of surgery, and were immediately frozen in liquid nitrogen. 8 PDTC and 5 ATC were preserved as formalin-fixed paraffin embedded samples (FFPE). 2 PDTC and 7 ATC were collected during fine-needle aspiration biopsies (FNAB), being conserved in RLT buffer (RNeasy Mini Kit, Qiagen, Hamburg, GmbH, Germany) with 1% (v/v) 2-Mercaptoethanol and maintained at -70ºC. Histological classifications followed the criteria described in World Health Organization classification of thyroid tumours (DeLellis *et al.*, 2004). All samples were obtained with permission, and the project was approved by our institution ethical committee.

A pool of human thyroid RNA obtained from 65 Caucasian individuals with 18 to 61 years old, whom died from sudden death (BD Bioscience, Franklin Lakes, NJ, USA), 2 PDTC-derived (T243 and T351) and 4 ATC-derived (T235, T238, T241 and C643) cell lines were also used.

Genomic DNA isolation/extraction

Genomic DNA was extracted and purified using the Citogene DNA Tissue kit (Citomed, Lisbon, Portugal), according to the manufacturer's protocol. Extracted DNA was quantified by UV spectrophotometry (NanoDrop ND-1000, Thermo Fisher Scientific, Wilmington, DE, USA).

Genomic DNA was extracted from FFPE as previously described (Imyanitov *et al.*, 2001), with minor modifications. Briefly, after xylene treatment and tissue permeabilization with proteinase K (Promega, Mannheim, GmbH, Germany), a DNA recovery assay was applied using *Taq* DNA polymerase (Invitrogen, Paisley, UK). Obtained DNA was purified

with InstaGene Matrix (Biorad, Hercules, CA, USA) and integrity was checked by agarose gel electroforesis.

Total RNA isolation/extraction

Total RNA was extracted and purified using the RNeasy Mini kit (Qiagen) according to the manufacturer's protocol, and quantified by UV spectrophotometry (NanoDrop ND-1000). RNA integrity of microarray samples was assessed by micro capillary electrophoresis (Agilent 2100 Bioanalyzer, Santa Clara, CA, USA).

RNA processing and array hybridisation

Samples used in microarray hybridisation consisted of 5 ATC (3 fresh-frozen and 2 FNAB), 3 normal thyroid tissues and the commercial pool of RNA.

RNA samples were processed following the Whole Transcript Sense Target Labelling Assay from Affymetrix (Santa Clara, CA, USA) and were hybridised in GeneChip Gene 1.0 ST Array (Affymetrix).

Microarray data analysis

Partek Genomics Suite Software (Partek Inc, St Louis, MO, USA) was used for hierarchical clustering of the samples, applying Pearson's dissimilarity and Ward's clustering method. Robust multi-array average method (Irizarry *et al.*, 2003) was first employed for array data normalisation and expression levels determination.

DNA-Chip Analyzer (dChip) 2010.01 software (Li and Wong, 2001) was used to obtain differentially expressed genes between ATC and normal thyroid samples. Arrays were normalised with the invariant set normalisation method and gene-level expressions were determined by summarizing the multiple probes across the genes (median of 26 probes per gene) into single gene level-probe set expressions, using model-based expression analysis with perfect match-only model. Gene level-probe sets that were absent in all samples or those that did not change across samples (coefficient of variation lower than 0.2 and higher than 10) were eliminated from further analysis. Gene level-probe sets were considered to be differentially expressed, with a lower 90% limit of the confidence interval of the fold change

(ratio of the expression level in the two groups), equal or higher than two-fold, and with an unpaired t-test considered significant at $P \leq 0.001$. Onto-Express (Khatri *et al.*, 2002) and Pathway-Express (Draghici *et al.*, 2007) from Onto-Tools package were used for functional profiling according to cellular components and for pathway impact analysis of differentially expressed genes, respectively.

GSEA software (Subramanian *et al.*, 2005) was applied to the complete list of 33252 probe-sets, to determine Gene Ontology-defined gene sets associated with increased or decreased expression in ATC. Statistical significance was estimated by a nominal *P* value obtained by gene set permutation (not phenotype permutation) due to small sample set size. *P* values were corrected for multiple hypothesis testing using false discovery rate and family wise-error rate. Gene sets were considered significant at $P \leq 0.05$ and FDR≤ 0.25.

Venn diagram analysis was performed using GenePattern platform (Reich *et al.*, 2006).

First-strand cDNA synthesis

cDNA was synthesised from 1 μg of total RNA, using random primer $p(dN)_6$ (Roche Diagnostics Corporation, Indianapolis, IN, USA) and SuperScript II reverse transcriptase (Invitrogen).

Mutational analysis

Mutational analysis was performed in 22 PDTC (12 fresh-frozen, 2 FNAB and 8 FFPE), in 26 ATC (15 fresh-frozen, 6 FNAB and 5 FFPE) and in the 6 cell lines. The presence of reported variants with uncertain pathogenic effect was verified, when available, in corresponding normal FFPE or in corresponding blood lymphocytes of patients.

Primers were designed to amplify hot-spot regions of *BRAF* (exon 15), *N-*, *KRAS* (exons 2 and 3), *HRAS* (exons 1 and 2), *PIK3CA* (exons 1, 9 and 20), *CTNNB1* (exon 3) and *TP53* (exons 5 to 9) genes. The entire coding sequence and exon-intron boundaries were sequenced for *CDKN2A* (both $p14^{ARF}$ and $p16^{INK4A}$ transcripts), *CDKN2B*, *CDKN2C*, *CDKN1A*, *CDKN1B* and *AXIN1* genes. After PCR or RT-PCR amplification following *Taq* DNA Polymerase (Invitrogen) protocol, sequencing products were obtained using the Big Dye Terminator v1.1 Cycle Sequencing kit (Applied Biosystems, Foster City, CA, USA), according to the manufacturer's protocol. Chromatographic separations of products were

performed in an ABI Prism 310 Genetic Analyser (Applied Biosystems) and electropherograms were obtained with the Sequence Analysis Software version 3.4.1 (Applied Biosystems). Software Variant Reporter v1.0 (Applied Biosystems) was used for sequence analysis. Primer sequences are presented in Chapter VI.

Sequence variants information was searched in dbSNP (http://www.ncbi.nlm.nih.gov /snp), Catalogue Of Somatic Mutations In Cancer (http://www.sanger.ac.uk/genetics/CGP /cosmic/), The Human Gene Mutation Database (http://www.hgmd.org/) and Ensembl (www.ensembl.org/). For prediction of the functional impact of new reported sequence variants, Polyphen (http://genetics.bwh.harvard.edu/pph2), SIFT (http://sift.jcvi.org/www/ SIFT_enst_submit.html) and MutationTaster (http://www.mutationtaster.org) softwares were used.

CDKN3 splice variants analysis

Presence of "cyclin-dependent kinase inhibitor 3" (*CDKN3*) splice variants was searched in RNA from 5 normal thyroid tissues, commercial pool of human thyroid, 3 fresh-frozen ATC and 6 cell lines.

After cDNA synthesis, *CDKN3* transcripts were amplified using designed primers to anneal to the 5' and 3' untranslated regions of the gene. RT-PCR products were subcloned into pCR 2.1-TOPO vector using the TOPO TA cloning kit (Invitrogen), according to the manufacturer's protocol. Ten to twenty *E. coli* transformants of each RT-PCR reaction were picked, cultured overnight in Luria-Bertani (LB) medium supplied with ampicillin, and used as template in a PCR reaction containing M13 forward and reverse primers. PCR products were size-controlled on agarose gel and between 5 to 10 products containing insert, were chosen. After purification of PCR products, sequencing reactions were performed with the same M13 primers. Primer sequences are presented in Chapter VI.

Quantitative RT–PCR

CDKN3 quantitative RT-PCR analysis was performed in 8 cPTC, 8 fvPTC, 8 FTC, 7 fresh-frozen PDTC, 9 ATC (5 FNAB and 4 fresh-frozen), 6 cell lines, 6 normal thyroid tissues and commercial pool of human thyroid RNA. Assays were performed in 384-well reaction plates (LightCycler 480 Multiwell Plate 384; Roche) on a LightCycler 480 Real-time

PCR System (Roche). Two primer pairs were designed to separately amplify exons 2 to 4 and exons 7 to 8 of *CDKN3* gene. PCR amplifications were performed using 4 pmol of each primer (forward and reverse) and Power SYBR Green PCR Master Mix (Applied Biosystems), according to the manufacturer's protocol. Ten-fold serial dilutions were used, to apply the relative standard curve method. To normalise differences in the amount of template used, "hypoxanthine phosphoribosyltransferase 1" (*HPRT1*) was used as endogenous control. The commercial pool of normal thyroid RNA was used as calibrator to determine the relative expression in samples. Amplicons sizes were controlled on agarose gel, and specificity was assessed by melting curves analysis. All reactions, including a control without template, were performed in triplicate. Primer sequences are shown in Chapter VI.

Seven cPTC, 7 fvPTC, 7 FTC, 12 PDTC (1 FNAB and 11 fresh-frozen), 19 ATC (3 FNAB and 16 fresh-frozen), 6 cell lines, 7 normal samples and commercial RNA pool were used for "snail homolog 2 (Drosophila)" (*SNAI2*) quantitative analysis. Real-time RT-PCR assays were performed in 96-well reaction plates (MicroAmp Optical 96-Well Reaction Plate; Applied Biosystems) on an ABI Prism 7900 HT Sequence Detection System (Applied Biosystems). RT-PCR amplifications were performed using pre-developed primers and probe (Inventoried TaqMan Gene Expression Assays ID: Hs00950344_m1; Applied Biosystems), and TaqMan Universal PCR Master Mix (Applied Biosystems), according to the manufacturer's protocol. The endogenous control used was "actin, beta" (*ACTB*) (Inventoried TaqMan Gene Expression Assays ID: Hs01060665_g1; Applied Biosystems). Ten-fold serial dilutions were used to apply the relative standard curve method. The commercial pool of normal thyroid RNA was used as calibrator, but sample expressions were determined relatively to one of the normal thyroid tissues. All reactions, including a control without template, were performed in triplicate.

Statistical analysis

GraphPad Prism version 4.00 (GraphPad Software, Inc.) was implemented for statistical analysis and for comparison of survival distributions by logrank test. Differences were considered significant at $P \leq 0.05$. Kaplan-Meier plots for estimation of survival function, were made using GenePattern platform (Reich *et al.*, 2006).

4. Results

ATC transcriptome analyses

We determined the ATC global gene expression profile, using RNA extracted from 3 fresh-frozen tumours and 2 FNAB, and compared it with 3 normal thyroid tissues and a commercial pool of normal human thyroid RNA. Unsupervised analysis using hierarchical clustering showed that all 5 ATC samples clustered together, separated from the normal samples (Figure III.1A). GSEA identified sets of genes with increased expression in ATC, markedly related to cell cycle and division processes, checkpoints and chromosome segregation (Supplementary Table III.1). Under-expressed genes in ATC were mainly related to tight junctions, intercellular junctions and oxidoreductase activity (Supplementary Table III.2).

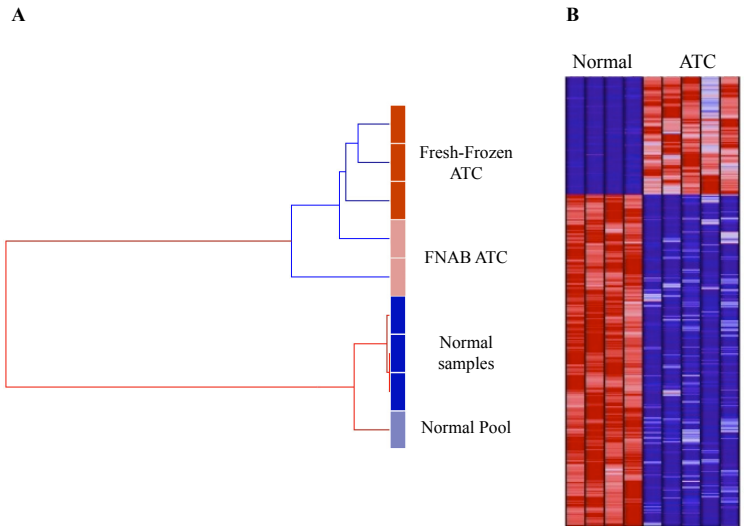

Figure III.1 - Analysis of genome-wide expression in ATC. (A) Global gene expression similarity between samples using the unsupervised hierarchical clustering method. Distance separating samples represents the gene expression resemblance between them. (B) Expression profile of the genes differentially expressed between ATC and normal thyroid tissue samples. Expression levels are indicated by colour intensities in which blue and red correspond, respectively, to a lower and a higher expression than the mean value for the gene, in all samples being compared; Only one probe set was considered for each gene. FNAB - fine-needle aspiration biopsy; ATC - anaplastic thyroid carcinoma.

Gene expression comparison analysis showed that ATC and normal thyroid samples had 1333 differentially expressed genes, defined as those with expression level (set at the lower limit of 90% confidence) equal, or higher, than two-fold between the defined two groups, with a statistical significance equal or lower than 0.001 (Figure III.1B). Among these genes, 983 (74%) were downregulated and 350 (26%) were upregulated in ATC. Pathway impact analysis pointed out several deregulated pathways in ATC (Table III.1). Adherens junction

(Supplementary Figure III.1), tight junction (Supplementary Figure III.2) and focal adhesion (Supplementary Figure III.3) pathways, comprised mainly downregulated genes, contrary to cell cycle, which was completely associated with over-expressed genes (Supplementary Figure III.4). TGF-β signalling pathway (Supplementary Figure III.5) was associated with increased expression of genes involved in TGF-β ligand reception, but to decreased expression of components from bone morphogenetic protein signalling. Functional profiling of the differentially expressed genes, revealed the involvement of different cell components, such as cytoskeleton, spindle, microtubules, chromosomes and the aforementioned cell junctions (Table III.2).

Table III.1 - Pathway impact analysis of differentially expressed genes between ATC and normal tissues.

Pathway	Impact factor	Pathway genes	Input genes	*P*-value[1]
Leukocyte transendothelial migration	940.353	119	14	0.00
Cell adhesion molecules	529.089	134	15	3.69×10^{-226}
Phosphatidylinositol signaling system	39.521	76	5	7.78×10^{-15}
Adherens junction	32.95	78	11	3.49×10^{-12}
Systemic lupus erythematosus	24.075	144	33	1.47×10^{-8}
Tight junction	11.89	135	20	1.24×10^{-3}
Cell cycle	7.488	118	19	5.26×10^{-2}
Focal adhesion	7.358	203	26	5.26×10^{-2}
Hedgehog signaling pathway	7.294	57	4	5.26×10^{-2}
Autoimmune thyroid disease	6.275	53	4	0.11
TGF-beta signaling pathway	5.357	87	13	0.22
mTOR signaling pathway	5.277	52	3	0.22
Axon guidance	4.897	129	16	0.25
Complement and coagulation cascades	4.882	69	11	0.25
Long-term potentiation	4.865	73	4	0.25
Melanoma	4.505	71	4	0.32
Prostate cancer	3.932	90	7	0.47
Basal cell carcinoma	3.84	55	3	0.47
Type II diabetes mellitus	3.81	45	7	0.47
ECM-receptor interaction	3.443	84	11	0.58

[1]*P*-value obtained using the impact analysis and corrected for multiple comparison. TGF - transforming growth factor; ECM - extracellular matrix.

Table III.2 - Functional profiling of differentially expressed genes between ATC and normal tissues.

Cellular component	Number of genes (%)	*P*-value[1]
Tight junction	1.27	$3.00x10^{-5}$
Cytoplasm	24.4	$4.00x10^{-5}$
Extrinsic to membrane	0.75	$4.80x10^{-4}$
Plasma membrane	15.9	$1.00x10^{-3}$
Apical plasma membrane	1.34	$1.83x10^{-3}$
Cytoskeleton	3.73	$5.73x10^{-3}$
Chromosome	1.57	$8.00x10^{-3}$
Microtubule associated complex	0.90	$1.05x10^{-2}$
Proteinaceous extracellular matrix	2.09	$1.07x10^{-2}$
Chromosome centromeric region	0.67	$1.12x10^{-2}$
Integral to plasma membrane	6.34	$1.19x10^{-2}$
Nucleosome	0.90	$1.19x10^{-2}$
Cell junction	2.84	$2.24x10^{-2}$
Integral to Golgi membrane	0.67	$2.67x10^{-2}$
Microtubule	1.94	$2.67x10^{-2}$
Spindle	0.75	$5.98x10^{-2}$
Cell-cell adherens junction	0.30	$7.50x10^{-2}$
Complement component C1 complex	0.15	$8.27x10^{-2}$
Actin cytoskeleton	0.90	$9.98x10^{-2}$
Extracellular region	9.03	0.13

[1]*P*-value corrected for multiple comparison.

In the Chapter II, we analysed the gene expression of cPTC and fvPTC, FTC and PDTC. To compare the ATC gene expression with our previous work, we searched for differentially expressed genes relatively to normal thyroid that ATC had in common with each other tumour types (Supplementary Figure III.6). Of the 1333 genes in ATC, 71 were common to cPTC, 31 to fvPTC, 30 to FTC and 34 to PDTC. Six genes were shared between all tumours (Supplementary File III.1). Exclusion of all these common genes left 1216 genes that are specifically deregulated, only in ATC (Supplementary File III.2).

Validation of gene expression results

CDKN3 was the most over-expressed gene in ATC. We searched for the presence of *CDKN3* abnormal splice variants, associated with this upregulation. In 6 normal thyroid samples, we only detected *CDKN3* full-length transcript, whereas analysis of 3 ATC samples, 2 PDTC cell lines and 4 ATC cell lines, revealed the presence of full-length transcripts in combination with splice variants (Figure III.2A). Quantitative RT-PCR assays allowed the

differential analysis of the expression levels due to splice variants or due to full-length transcript, in 46 thyroid tumours and 7 normal samples (Figure III.2B). Despite a higher total *CDKN3* (full length transcript plus splice variants) expression in some WDTC, and in PDTC (P<0.05) relatively to normal samples, the majority of the tumours expressed only the full-length transcript. In ATC tumours and cell lines, we also found a statistically significant over-expression of total *CDKN3* transcription, relatively to normal tissue (P<0.01 and P<0.001, respectively), but, in these groups, total *CDKN3* quantification was significantly higher than the correspondent quantification of sole full-length transcript (P=0.0122 and P=0.0111, respectively). So, contrarily to WDTC and PDTC, *CDKN3* upregulation in ATC and cell lines was associated with expression of abnormal splice variants.

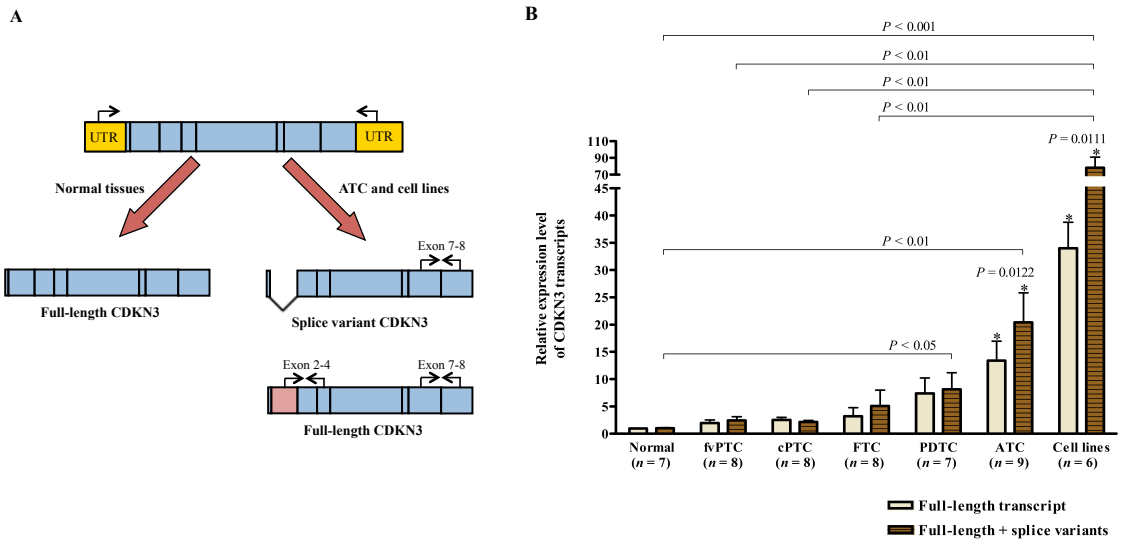

Figure III.2 - Characterisation of *CDKN3* status in thyroid tumours. (A) Schematic representation of the results obtained upon *CDKN3* transcripts analysis. Due to the lack of exon 2, expression of each transcript can be determined, using two different pairs of primers. (B) Quantitative RT-PCR analysis of *CDKN3* expression in normal thyroid tissues, in 5 thyroid tumour histotypes and in 2 PDTC- and 4 ATC-derived cell lines. Expression levels of full-length transcription and total (full-length and splice variants) transcription were both determined for each sample, normalised with the "hypoxanthine phosphoribosyltransferase 1" (*HPRT1*) expression and determined relatively to a calibrator. Error bars denote SEM. The *P*-values for difference in mean expression were performed using the Kruskal–Wallis with Dunn's multiple comparison test. **P* values calculated by paired t-test; fvPTC - follicular variant of papillary thyroid carcinoma; cPTC - classic papillary thyroid carcinoma; FTC - follicular thyroid carcinoma; PDTC - poorly differentiated thyroid carcinoma; ATC - anaplastic thyroid carcinoma.

We used TaqMan RT-PCR to further validate our microarray results for *SNAI2* gene, in a set of thyroid tumour samples and cell lines (Figure III.3). In agreement with the global gene expression, *SNAI2* was significantly more expressed in ATC than in normal tissues (P<0.01). A sub-group of 8 ATC was clearly distinguished, with relative expression levels higher than 3-fold. The ATC cell line (C643) and a minimally invasive FTC also had more than 3-fold expression. *SNAI2* expression was not correlated with age at diagnosis or tumour size in ATC (data not shown).

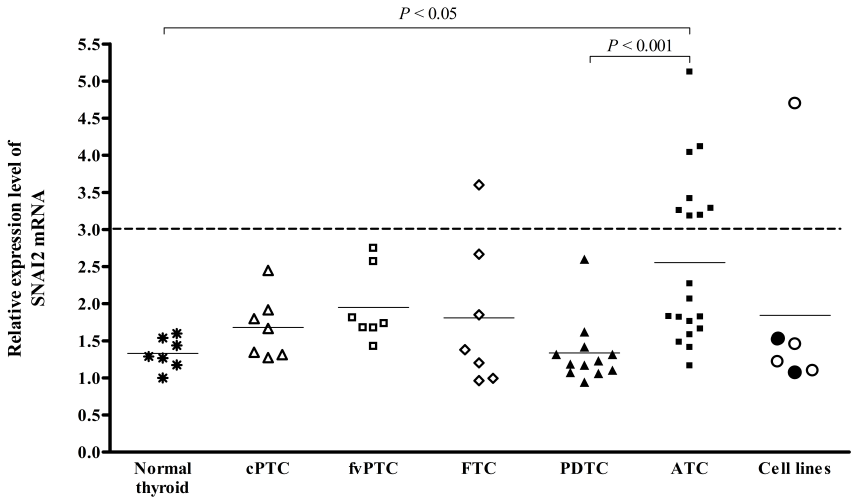

Figure III.3 - *SNAI2* expression in different thyroid tumour histotypes and in 2 PDTC- and 4 ATC-derived cell lines, assessed by quantitative RT-PCR. Expression levels were normalised with the "actin, beta" (*ACTB*) expression and determined relatively to a calibrator. Line denotes mean expression level in each group. *SNAI2* relative expression equal to 3-fold is indicated by a dashed line. For cell lines, a closed and an open mark represents PDTC and ATC cell line, respectively. *P*-values for difference in mean expression were calculated using the one-way analysis of variance with Bonferroni's multiple comparison test, after transformation of expressions values to reciprocals. cPTC - classic papillary thyroid carcinoma; fvPTC - follicular variant of papillary thyroid carcinoma; FTC - follicular thyroid carcinoma; PDTC - poorly differentiated thyroid carcinoma; ATC - anaplastic thyroid carcinoma.

ATC and PDTC mutational analysis

A total of 22 PDTC, 26 ATC, 2 PDTC- and 4 ATC-cell lines were screened for sequence variations in 13 genes. Overall, 49 different alterations, totalising 66 mutated sequences, were identified (Supplementary Table III.3) and were present in 12 PDTC (55%), 19 ATC (73%) and 3 ATC cell lines. From these, only two variants, both identified in the *AXIN1* gene, were not considered pathogenic, since were present in the corresponding normal tissue, and were predicted *in silico* to be benign. *RAS*, *TP53*, *CDKN2A*, *CDKN2B* and *PIK3CA* genes were mutated at similar frequencies (14-27%) in PDTC (Table III.3 and Supplementary Table III.4). In ATC (Table III.3 and Supplementary Table III.5), *CDKN2A*, *CDKN2B* and *PIK3CA* mutations were rare (≤ 5%), contrasting with *TP53* and *RAS* alterations, which were the

most frequent (42% and 31%, respectively). None of the mutations had a significant association with ATC or PDTC (Table III.3). In 48 screened tumours, only one ATC, out of seventeen *TP53* mutated samples and out of twelve *RAS* mutated samples, had both mutations in coexistence, suggesting that these events were mutually exclusive (*P*=0.0354, Fisher's exact test).

Table III.3 - Frequency of mutated genes and association with histotype.

Gene	PDTC (%)	ATC (%)	*P* value[1]
TP53	6/22 (27)	11/26 (42)	0.3681
RAS	4/22 (18)[2]	8/26 (31)[2]	0.5048
CDKN2A	3/20 (15)	1/22 (5)	0.3327
PIK3CA	3/22 (14)	1/26 (4)	0.3202
CDKN2B	4/20 (20)	0/20 (0)[3]	0.1060
BRAF	1/22 (5)	2/26 (8)	1.0000
CTNNB1	1/22 (5)	0/26 (0)	0.4583
AXIN1	0/12 (0)	1/17 (6)	1.0000
CDKN2C	0/12 (0)	1/17 (6)	1.0000

[1]*P* values calculated with Fisher's exact test; [2]2 samples could not be assessed for *KRAS*; [3]2 samples could not be totally assessed; Mutations were not detected in *CDKN1A* and *CDKN1B*; PDTC - poorly differentiated thyroid carcinoma; ATC - anaplastic thyroid carcinoma.

Correlation with clinical-pathological features and patients survival

Comparisons between PDTC and ATC groups showed that ATC patients had higher age at presentation (*P*=0.0009) and considerably lower median survival (*P*=0.0001) (Supplementary Table III.6). We attempted to correlate the clinical-pathological characteristic (Supplementary Table III.7) with the expressional and mutational results. No significant associations were found between the clinical-pathological features (gender, age at diagnosis, size of the tumour and presence of metastasis) and *SNAI2* over-expression, presence of *TP53* or *RAS* mutations, or number of mutated genes (data not shown). It should be noted that tumour size information was very limited for ATC samples.

No differences in survival were detected in *SNAI2* over-expressed ATC patients (data not shown). Survival analysis of patients, according to the mutational data (Table III.4), revealed that the group of patients with *TP53* and/or *RAS* mutations was significantly associated with a lower survival (*P*=0.0383) (Figure III.4A). Presence of *TP53* mutations alone was also significantly associated with a lower patients survival (*P*=0.0454) (Figure III.4B).

Table III.4 - Comparison of survival distribution by logrank test.

	PDTC and ATC
Median survival (months)	
TP53 and *RAS* wt	35 (*n* =19)
RAS mut	6 (*n* = 11)
Hazard Ratio	1.627
95% CI of ratio	0.6936 - 4.781
Chi square	1.481
P value	0.2236
Median survival (months)	
TP53 and *RAS* wt	35 (*n* = 19)
TP53 mut	6.5 (*n* = 16)
Hazard Ratio	2.099
95% CI of ratio	1.017 - 5.286
Chi square	4.004
P value	0.0454
Median survival (months)	
TP53 and *RAS* wt	35 (*n* = 19)
TP53 and/or *RAS* mut	6 (*n* = 28)
Hazard Ratio	1.992
95% CI of ratio	1.040 - 4.095
Chi square	4.290
P value	0.0383
Median survival (months)	
no mutations	35 (*n* = 16)
1 or more mutations	6 (*n* = 31)
Hazard Ratio	1.439
95% CI of ratio	0.7172 - 3.118
Chi square	1.152
P value	0.2832

wt - wild-type; mut - mutated; CI - confidence interval; PDTC - poorly differentiated thyroid carcinoma; ATC - anaplastic thyroid carcinoma.

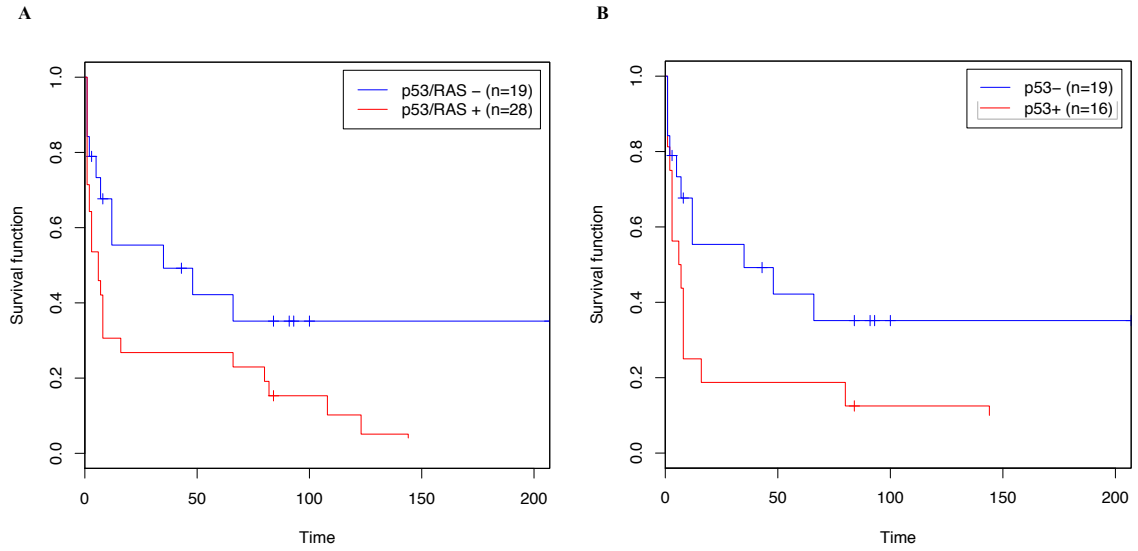

Figure III.6 - Kaplan-Meier estimator for comparison of patients according to the mutational results. (A) Survival curves of poorly differentiated and anaplastic thyroid carcinomas patients, with *TP53* and/or *RAS* mutations (p53/RAS+) comparatively to patients with neither *TP53* nor *RAS* mutation (p53/RAS-). (B) Survival curves of poorly differentiated and anaplastic thyroid carcinomas patients, with *TP53* mutations and no *RAS* mutations (p53+) comparatively to patients with neither *TP53* nor *RAS* mutation (p53-).

5. Discussion

Although representing a minority of thyroid malignancies, PDTC and particularly ATC, may contribute for more than half of the deaths attributable to thyroid cancer. ATC are associated with elderly patients, presenting as a rapidly growing mass with widespread invasion of soft tissues, and extensive haemorrhagic and necrotic areas (DeLellis *et al.*, 2004). Contrariwise, PDTC definition has not been clear, and a definite designation as a separate entity, intermediate between WDTC and ATC (DeLellis *et al.*, 2004), was only obtained in 2004. Subsequent studies demonstrated that PDTC patients had distinctive older age, more aggressive features and poorer prognosis relatively to WDTC cases (Nambiar *et al.*, 2011). In agreement with others (Lam *et al.*, 2000; Volante *et al.*, 2004), in this study we found ATC patients had statistically significant older age and lower survival than PDTC patients.

Due to the high risks of recurrence and metastasis, unfeasible surgical resection and failure of conventional chemotherapy and radiotherapy, novel treatment strategies against PDTC and ATC are particularly needed. Therefore, complete molecular profiling of these tumours is considerably important. Previously, we analysed the genome-wide expression of PDTC. In the present study, we expanded our analysis to ATC and, in addition, searched for

genetic alterations potentially driving the aberrant expression and aggressiveness of PDTC and ATC.

Analysing ATC differentially expressed genes relatively to normal thyroid tissue, we found, in accordance with others (Onda *et al.*, 2004; Rodrigues *et al.*, 2007; Salvatore *et al.*, 2007), that the majority were under-expressed, a pattern also present in PDTC and FTC (Aldred *et al.*, 2003; Rodrigues *et al.*, 2007; Pita *et al.*, 2009). From the comparison of differentially expressed genes relatively to normal tissues, between ATC and our previous studied tumours (Chapter II), we observed 1216 genes that were only associated with ATC, and thus represent specific pathways involved in ATC progression.

As previously observed (Onda *et al.*, 2004; Rodrigues *et al.*, 2007; Montero-Conde *et al.*, 2008; Hébrant *et al.*, 2012), loss of thyroid follicular cell identity in ATC was notably represented by downregulation of genes encoding critical thyroid transcription factors and proteins important for thyroid hormones metabolism. Furthermore, deregulated gene sets were related to different cell junctions, to cell-cell adhesion and to actin cytoskeleton, reflecting the loss of the epithelial morphology and transition to a mesenchymal state. Loss of epithelial phenotype is a key process in activation of epithelial-to-mesenchymal transition (EMT), whereby epithelial cells lose contact, undergo cytoskeleton remodelling and manifest a higher migratory phenotype (Thiery and Sleeman, 2006). In our gene expression analysis, ATC presented defining features of EMT such as the downregulation of "cadherin 1, type 1, E-cadherin (epithelial)" (*CDH1*) gene (Wiseman *et al.*, 2006; Montero-Conde *et al.*, 2008; Hébrant *et al.*, 2012) and gain of mesenchymal markers, like "fibronectin 1" (*FN1*) (Prasad *et al.*, 2005; Takano *et al.*, 2007) and "wingless-type MMTV integration site family, member 5A" (*WNT5A*) genes. Moreover, as described before (Montero-Conde *et al.*, 2008; Hébrant *et al.*, 2012), we detected over-expression of TGF-β signalling components ["transforming growth factor, beta-induced, 68kDa" (*TGFBI*), "transforming growth factor, beta 1" (*TGFB1*), "transforming growth factor, beta receptor 1" (*TGFBR1*) and "latent transforming growth factor beta binding protein 1" (*LTBP1*)], which suggests an autocrine pathway, potentially relevant due to its role in the promotion of EMT (Huber *et al.*, 2005). A recent report described the activation of EMT program in mammary cells, by combined autocrine loops of TGF-β signalling and WNT signalling (through WNT5A). Most interesting, induction of EMT had to be accompanied by reduced levels of inhibitors of these pathways, such as bone morphogenetic proteins (Scheel *et al.*, 2011), which we also found to be downregulated in ATC. In PTC samples, increased TGFB1 staining was present at the invasive fronts (Riesco-

Eizaguirre *et al.*, 2009), where an EMT-like expression profile was found (Vasko *et al.*, 2007). Interestingly, despite the low detection of *BRAF* mutations (2 in 26), and presenting mostly under-expressed genes (similarly to PDTC and FTC), ATC shared more common differentially expressed genes (relatively to normal thyroid) with cPTC. This observation is in agreement with recent work (Hébrant *et al.*, 2012), reporting that 43% of the genes deregulated in PTC were similarly regulated in 11 ATC (2 with mutated *BRAF*) and suggests that ATC could derive from PTC through a progressive transition to an undifferentiated and more mesenchymal state. In our PDTC analysis (Chapter II), similarity with cPTC was not evident and genes related to EMT were not found, probably because the series did not include PDTC with associated classical papillary components. Nevertheless, analysis of paired PDTC-PTC foci from *BRAF* mutant mice, did reveal a characteristically EMT gene profile in PDTC, which was driven by concomitant MAPK-ERK and TGF-β signalling (Knauf *et al.*, 2011). So, upon MAPK-ERK constitutive activation, TGF-β may be the key promoter of invasion and metastasis in ATC and papillary-associated PDTC. We confirmed that *SNAI2*, which is induced in response to TGF-β (Xu *et al.*, 2009), was one of the genes specifically over-expressed only in ATC, a finding very recently corroborated by immunohistochemistry (Buehler *et al.*, 2013). *SNAI2* gene encodes a zinc-finger transcription factor that represses not only the expression of the epithelial marker, E-cadherin but also, occludin, claudins, and cytokeratins (Peinado *et al.*, 2007). A sub-group of tumours clearly had higher *SNAI2* expression, representing 42% of ATC with a significant TGF-β activation (assuming *SNAI2* expression as proportional). Among these samples, 3 had *RAS* mutations, 3 had *TP53* mutations and one was mutated for both genes, indicating as previously seen for other tumours, that both *RAS* (Wang *et al.*, 2010) and *TP53* (Zhang *et al.*, 2011) mutants may promote *SNAI2* expression. Another pathway contributing to EMT (Huber *et al.*, 2005) and shown to be involved in thyroid cancer is WNT/β-catenin signalling. Prior results showed that decreased β-catenin expression (Wiseman *et al.*, 2006) or aberrant nuclear expression (42-48%) and *CTNNB1* exon 3 mutations (61-65%) are involved in ATC (Garcia-Rostan *et al.*, 1999; Garcia-Rostan *et al.*, 2001). However, Kurihara and collaborators found *CTNNB1* mutations only in 4.5% and *APC* mutations in 9% of ATC, pointing out *AXIN1* gene (mutated in 82%) as the main altered component of WNT pathway (Kurihara *et al.*, 2004). Hébrant *et al*. also found no *CTNNB1* mutations in 11 ATC (Hébrant *et al.*, 2012). In PDTC, β-catenin mutations and nuclear expression were present in 25% and 21% of cases, respectively (Garcia-Rostan *et al.*, 2001), whereas in other 17 cases, no alterations were found (Rocha *et al.*, 2003). Unexpectedly, our mutational analysis only revealed three different germ-line

AXIN1 variants (2 benign and 1 pathogenic), and a single *CTNNB1* mutation in a PDTC that also harboured mutations in other genes, undermining a major role for this pathway. More mutational analyses are required to elucidate the observed discrepancies and to verify the importance of this pathway in thyroid progression.

The present study showed ATC gene expression was deregulated for gene sets related to cell cycle regulation and checkpoints, chromosome segregation and spindle structure. Thus, similarly to PDTC (Chapter II), ATC have upregulation of genes related to proliferation, cell cycle (Hébrant *et al.*, 2012) and chromosomal instability (Salvatore *et al.*, 2007). Progression through the cell cycle may be controlled by the interaction of CDK and cyclins complexes, with CDKN. Based on sequence homology and CDK specificity, CDKN are divided into two distinct families (Sherr and Roberts, 1999), INK4 members ($p16^{INK4A}$, $p15^{INK4B}$, $p18^{INK4C}$ and $p19^{INK4D}$) and CIP/KIP members ($p21^{CIP1}$, $p27^{KIP1}$ and $p57^{KIP2}$). In addition, all CIP/KIP may be involved in actin dynamics and cell migration. Upon cytoplasmic mislocalisation, CIP/KIP proteins regulate, at distinct levels, the Rho pathway, promoting cell motility and invasion (Besson *et al.*, 2008). This suggests that rather than being inactivated, CIP/KIP members are subverted for increased tumorigenesis, justifying, the absence of *CDKN1A* ($p21^{CIP1}$) and *CDKN1B* ($p27^{KIP1}$) mutations in ATC and PDTC. On the contrary, mutations in INK4 members were found in 5 PDTC [3 with *CDKN2A* ($p16^{INK4A}$) and 4 with *CDKN2B* ($p15^{INK4B}$) mutations] and in 2 ATC [one with *CDKN2A* and one with *CDKN2C* ($p18^{INK4C}$) mutations]. To our knowledge, only one report (Calabrò *et al.*, 1996), found *CDKN2B* mRNA expression to be normal in 5 ATC, and except for the role of the $p18^{INK4C}$ in medullary thyroid carcinoma, *CDKN2C* gene (or $p18^{INK4C}$ protein) has never been studied in thyroid tumours. *CDKN2A* decreased expression and/or hypermethylation have been frequently found in ATC and PDTC (Schagdarsurengin *et al.*, 2002; Boltze *et al.*, 2003; Ball *et al.*, 2007; Lee *et al.*, 2008) but, in agreement with our results, mutations were uncommon in ATC (Calabrò *et al.*, 1996; Tung *et al.*, 1996). In PDTC, to our knowledge, we demonstrated for the first time that *CDKN2A* and *CDKN2B* mutations might be involved in up to 25% of PDTC. Interestingly, the most over-expressed gene found in ATC (*CDKN3*) is also a CDKN. This gene encodes a dual-specificity phosphatase that blocks G1/S phase progression through CDK2 kinase dephosphorylation (Hannon *et al.*, 1994). However, *CDKN3* was found to be over-expressed, and to increase neoplastic transformation, in breast and prostate cancer (Lee *et al.*, 2000). These contradictory observations were clarified upon the findings in glioblastoma, in which upregulation was associated with increased aberrant splicing and loss of full-length protein

(Yu *et al.*, 2007). We showed that *CDKN3* is also aberrantly spliced, specifically in ATC. The splice variants found lacked exon 2, which is predicted to originate a truncated protein of only 23 amino acids. It remains to clarify if these variants could inhibit the full-length *CDKN3* transcription or if an abnormal peptide may be translated and affect the CDKN3 functions.

We found that *PIK3CA* mutations were more prevalent in PDTC (3/22) than in ATC (1/26), coexisting with *CDKN2A* mutations in PDTC, and with *BRAF* mutations. Indeed, prior studies in ATC, found *PIK3CA* mutations/copy number gains to be overlapped with *BRAF*, *RAS* mutations or p53 increased expression (Garcia-Rostan *et al.*, 2005; Hou *et al.*, 2007; Liu *et al.*, 2008; Santarpia *et al.*, 2008), suggesting that *PIK3CA* alterations often cooperate with other oncogenic events in these type of tumours. Unexpectedly, the frequency of *PIK3CA* mutations in our ATC samples (4%) is lower than the reported in the literature (12-23%).

Our results corroborated p53 inactivation, rather than *CTNNB1* and *PIK3CA* mutations, as the main event in ATC and PDTC progression (Nikiforov and Nikiforova, 2011). In addition and confirming prior results (Lam *et al.*, 2000), PDTC and ATC patients presenting *TP53* mutation had decreased survival, stressing its major influence in tumorigenesis. *RAS* was the second most mutated gene, whereas *BRAF* mutations were present in only 3 samples, as expected for a series with no histological evidence of PTC derivation (Nikiforova *et al.*, 2003; Begum *et al.*, 2004; Soares *et al.*, 2004). Our detection of mutated *RAS* is in agreement with other PDTC (Volante *et al.*, 2009) and ATC (Garcia-Rostan *et al.*, 2003; Wang *et al.*, 2007) studies, in which it has been associated with decreased survival. From progression point of view (Figure III.5), it may be suggested that these dedifferentiated tumours derive from *RAS*-mutated WDTC, that is, FTC and/or fvPTC. In Chapter II, based on the similarity of gene expression profile, we suggested fvPTC as plausible precursors of *RAS*-mutated PDTC. Interestingly, in Costa and collaborators work (Costa *et al.*, 2008), 6 out of 13 *RAS*-mutated PDTC, exhibited fvPTC microscopic foci. In contrast, our and others (Hébrant *et al.*, 2012) expression analysis suggested that ATC were molecularly more similar to cPTC. Rather than a common origin, this may suggest a molecular mechanism affecting both cPTC and ATC (for example TGF-β activation). In either case, our work suggests that *RAS* and *TP53* mutations are alternative events, rather than progressively accumulated events, during PDTC and ATC progression (Wang *et al.*, 2007).

In conclusion, 10 PDTC (45%) and 7 ATC (27%) harboured no mutations in the 13 genes profiled. Other mechanisms may be driving progression in these tumours, and further molecular characterisation is required, especially for PDTC. For the mutated cases found,

different therapeutic approaches are available depending on the alteration uncovered. Most novel treatments tested for thyroid cancer are tyrosine kinase inhibitors (Kapiteijn *et al.*, 2012). The present work, points out additional targets that may be used, alone or in combination. The detection of *TP53* mutations in 27% PDTC and 42% ATC allows the use of molecules for reactivation of the p53 functions (Selivanova, 2010). The deregulated profile related to proliferation, *CDKN2A*/*CDKN2B* mutations (in 25% PDTC and 5% ATC) and *CDKN3* abnormal splicing in ATC, suggest that inhibitors of CDK, for example roscovitine and flavopiridol, may be efficient in such cases (Cicenas and Valius, 2011). *SNAI2* over-expression in 42% of cases and the likely influence of TGF-β signalling in ATC, suggest that TGF-β inhibitors, which some are already in clinical trials (Meulmeester and Ten Dijke, 2011), represent also a reasonable therapeutic option.

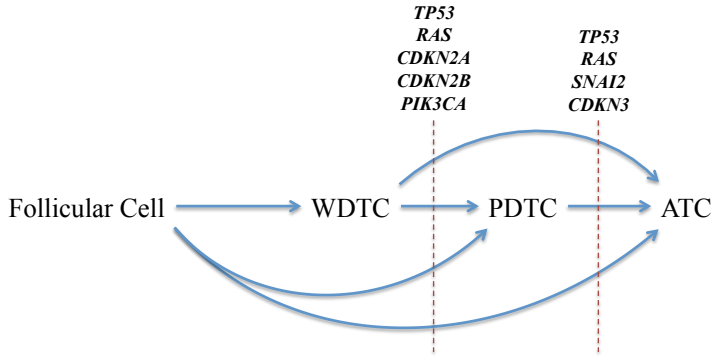

Figure III.7 - Molecular alterations involved in the development of PDTC and ATC. Genes, for which mutations, over-expression or aberrant splicing were found in more than 10% of cases are represented. WDTC - well-differentiated thyroid carcinoma; PDTC - poorly differentiated thyroid carcinoma; ATC - anaplastic thyroid carcinoma

6. Acknowledgements

The authors gratefully acknowledge Dr. Rita Santos from Departamento de Endocrinologia, from Instituto Português de Oncologia de Lisboa, for the identification of PDTC and ATC cases. We are also grateful to Serviço de Cirurgia de Cabeça e Pescoço, and Serviço de Anatomia Patológica, for the supply and histological analysis of thyroid tumours.

J.M. Pita is recipient of a Portuguese government (Fundação para a Ciência e Tecnologia) PhD fellowship (SFRH/BD/46096/2008).

This work was funded by Sociedade Portuguesa de Endocrinologia, Diabetes e Metabolismo (SPEDM), and received the award "Prémio Nacional de Endocrinologia - SPEDM/Novartis Oncology 2012".

7. References

Aldred MA, Ginn-Pease ME, Morrison CD, Popkie AP, Gimm O, Hoang-Vu C *et al* (2003). Caveolin-1 and caveolin-2, together with three bone morphogenetic protein-related genes, may encode novel tumor suppressors down-regulated in sporadic follicular thyroid carcinogenesis. *Cancer Res* **63:** 2864-2871.

Ball E, Bond J, Franc B, Demicco C, Wynford-Thomas D (2007). An immunohistochemical study of p16(INK4a) expression in multistep thyroid tumourigenesis. *Eur J Cancer* **43:** 194-201.

Begum S, Rosenbaum E, Henrique R, Cohen Y, Sidransky D, Westra WH (2004). BRAF mutations in anaplastic thyroid carcinoma: implications for tumor origin, diagnosis and treatment. *Mod Pathol* **17:** 1359-1363.

Besson A, Dowdy SF, Roberts JM (2008). CDK inhibitors: cell cycle regulators and beyond. *Dev Cell* **14:** 159-169.

Boltze C, Zack S, Quednow C, Bettge S, Roessner A, Schneider-Stock R (2003). Hypermethylation of the CDKN2/p16INK4A promotor in thyroid carcinogenesis. *Pathol Res Pract* **199:** 399-404.

Buehler D, Hardin H, Shan W, Montemayor-Garcia C, Rush PS, Asioli S *et al* (2013). Expression of epithelial-mesenchymal transition regulators SNAI2 and TWIST1 in thyroid carcinomas. *Mod Pathol* **26:** 54-61.

Calabrò V, Strazzullo M, La Mantia G, Fedele M, Paulin C, Fusco A *et al* (1996). Status and expression of the p16INK4 gene in human thyroid tumors and thyroid-tumor cell lines. *Int J Cancer* **67:** 29-34.

Cicenas J, Valius M (2011). The CDK inhibitors in cancer research and therapy. *J Cancer Res Clin Oncol* **137:** 1409-1418.

Costa AM, Herrero A, Fresno MF, Heymann J, Alvarez JA, Cameselle-Teijeiro J *et al* (2008). BRAF mutation associated with other genetic events identifies a subset of aggressive papillary thyroid carcinoma. *Clin Endocrinol (Oxf)* **68:** 618-634.

DeLellis RA, Lloyd RV, Heitz PU, Eng C (2004). *World Health Organization Classification of Tumours. Pathology and Genetics of Tumours of Endocrine Organs*. IARC Press: Lyon, France.

Draghici S, Khatri P, Tarca AL, Amin K, Done A, Voichita C *et al* (2007). A systems biology approach for pathway level analysis. *Genome Res* **17:** 1537-1545.

Fluge O, Bruland O, Akslen LA, Lillehaug JR, Varhaug JE (2006). Gene expression in poorly differentiated papillary thyroid carcinomas. *Thyroid* **16:** 161-175.

Garcia-Rostan G, Tallini G, Herrero A, D'Aquila TG, Carcangiu ML, Rimm DL (1999). Frequent mutation and nuclear localization of beta-catenin in anaplastic thyroid carcinoma. *Cancer Res* **59:** 1811-1815.

Garcia-Rostan G, Camp RL, Herrero A, Carcangiu ML, Rimm DL, Tallini G (2001). Beta-catenin dysregulation in thyroid neoplasms: down-regulation, aberrant nuclear expression, and CTNNB1 exon 3 mutations are markers for aggressive tumor phenotypes and poor prognosis. *Am J Pathol* **158:** 987-996.

Garcia-Rostan G, Zhao H, Camp RL, Pollan M, Herrero A, Pardo J *et al* (2003). ras mutations are associated with aggressive tumor phenotypes and poor prognosis in thyroid cancer. *J Clin Oncol* **21:** 3226-3235.

Garcia-Rostan G, Costa AM, Pereira-Castro I, Salvatore G, Hernandez R, Hermsem MJ *et al* (2005). Mutation of the PIK3CA gene in anaplastic thyroid cancer. *Cancer Res* **65:** 10199-10207.

Hannon GJ, Casso D, Beach D (1994). KAP: a dual specificity phosphatase that interacts with cyclin-dependent kinases. *Proc Natl Acad Sci U S A* **91:** 1731-1735.

Hébrant A, Dom G, Dewaele M, Andry G, Tresallet C, Leteurtre E *et al* (2012). mRNA expression in papillary and anaplastic thyroid carcinoma: molecular anatomy of a killing switch. *PLoS One* **7:** e37807.

Hou P, Liu D, Shan Y, Hu S, Studeman K, Condouris S *et al* (2007). Genetic alterations and their relationship in the phosphatidylinositol 3-kinase/Akt pathway in thyroid cancer. *Clin Cancer Res* **13:** 1161-1170.

Huber MA, Kraut N, Beug H (2005). Molecular requirements for epithelial-mesenchymal transition during tumor progression. *Curr Opin Cell Biol* **17:** 548-558.

Imyanitov EN, Grigoriev MY, Gorodinskaya VM, Kuligina ES, Pozharisski KM, Togo AV *et al* (2001). Partial restoration of degraded DNA from archival paraffin-embedded tissues. *Biotechniques* **31:** 1000, 1002.

Irizarry RA, Hobbs B, Collin F, Beazer-Barclay YD, Antonellis KJ, Scherf U *et al* (2003). Exploration, normalization, and summaries of high density oligonucleotide array probe level data. *Biostatistics* **4:** 249-264.

Kapiteijn E, Schneider TC, Morreau H, Gelderblom H, Nortier JW, Smit JW (2012). New treatment modalities in advanced thyroid cancer. *Ann Oncol* **23:** 10-18.

Khatri P, Draghici S, Ostermeier GC, Krawetz SA (2002). Profiling gene expression using onto-express. *Genomics* **79:** 266-270.

Knauf JA, Sartor MA, Medvedovic M, Lundsmith E, Ryder M, Salzano M *et al* (2011). Progression of BRAF-induced thyroid cancer is associated with epithelial-mesenchymal transition requiring concomitant MAP kinase and TGFbeta signaling. *Oncogene* **30:** 3153-3162.

Kurihara T, Ikeda S, Ishizaki Y, Fujimori M, Tokumoto N, Hirata Y *et al* (2004). Immunohistochemical and sequencing analyses of the Wnt signaling components in Japanese anaplastic thyroid cancers. *Thyroid* **14:** 1020-1029.

Lam KY, Lo CY, Chan KW, Wan KY (2000). Insular and anaplastic carcinoma of the thyroid: a 45-year comparative study at a single institution and a review of the significance of p53 and p21. *Ann Surg* **231:** 329-338.

Lee JJ, Au AY, Foukakis T, Barbaro M, Kiss N, Clifton-Bligh R *et al* (2008). Array-CGH identifies cyclin D1 and UBCH10 amplicons in anaplastic thyroid carcinoma. *Endocr Relat Cancer* **15:** 801-815.

Lee SW, Reimer CL, Fang L, Iruela-Arispe ML, Aaronson SA (2000). Overexpression of kinase-associated phosphatase (KAP) in breast and prostate cancer and inhibition of the transformed phenotype by antisense KAP expression. *Mol Cell Biol* **20:** 1723-1732.

Li C, Wong WH (2001). Model-based analysis of oligonucleotide arrays: expression index computation and outlier detection. *Proc Natl Acad Sci U S A* **98:** 31-36.

Liu Z, Hou P, Ji M, Guan H, Studeman K, Jensen K *et al* (2008). Highly prevalent genetic alterations in receptor tyrosine kinases and phosphatidylinositol 3-kinase/akt and mitogen-activated protein kinase pathways in anaplastic and follicular thyroid cancers. *J Clin Endocrinol Metab* **93:** 3106-3116.

Meulmeester E, Ten Dijke P (2011). The dynamic roles of TGF-beta in cancer. *J Pathol* **223:** 205-218.

Montero-Conde C, Martin-Campos JM, Lerma E, Gimenez G, Martinez-Guitarte JL, Combalia N *et al* (2008). Molecular profiling related to poor prognosis in thyroid carcinoma. Combining gene expression data and biological information. *Oncogene* **27:** 1554-1561.

Nambiar A, Pv S, Susheelan V, Kuriakose MA (2011). The concepts in poorly differentiated carcinoma of the thyroid: a review article. *J Surg Oncol* **103:** 818-821.

Nikiforov YE, Nikiforova MN (2011). Molecular genetics and diagnosis of thyroid cancer. *Nat Rev Endocrinol* **7:** 569-580.

Nikiforova MN, Kimura ET, Gandhi M, Biddinger PW, Knauf JA, Basolo F *et al* (2003). BRAF mutations in thyroid tumors are restricted to papillary carcinomas and anaplastic or poorly differentiated carcinomas arising from papillary carcinomas. *J Clin Endocrinol Metab* **88:** 5399-5404.

Onda M, Emi M, Yoshida A, Miyamoto S, Akaishi J, Asaka S *et al* (2004). Comprehensive gene expression profiling of anaplastic thyroid cancers with cDNA microarray of 25 344 genes. *Endocr Relat Cancer* **11:** 843-854.

Peinado H, Olmeda D, Cano A (2007). Snail, Zeb and bHLH factors in tumour progression: an alliance against the epithelial phenotype? *Nat Rev Cancer* **7:** 415-428.

Pita JM, Banito A, Cavaco BM, Leite V (2009). Gene expression profiling associated with the progression to poorly differentiated thyroid carcinomas. *Br J Cancer* **101:** 1782-1791.

Prasad ML, Pellegata NS, Huang Y, Nagaraja HN, de la Chapelle A, Kloos RT (2005). Galectin-3, fibronectin-1, CITED-1, HBME1 and cytokeratin-19 immunohistochemistry is useful for the differential diagnosis of thyroid tumors. *Mod Pathol* **18:** 48-57.

Quiros RM, Ding HG, Gattuso P, Prinz RA, Xu X (2005). Evidence that one subset of anaplastic thyroid carcinomas are derived from papillary carcinomas due to BRAF and p53 mutations. *Cancer* **103:** 2261-2268.

Reich M, Liefeld T, Gould J, Lerner J, Tamayo P, Mesirov JP (2006). GenePattern 2.0. *Nat Genet* **38:** 500-501.

Riesco-Eizaguirre G, Rodriguez I, De la Vieja A, Costamagna E, Carrasco N, Nistal M *et al* (2009). The BRAFV600E oncogene induces transforming growth factor beta secretion leading to sodium iodide symporter repression and increased malignancy in thyroid cancer. *Cancer Res* **69:** 8317-8325.

Rocha AS, Soares P, Fonseca E, Cameselle-Teijeiro J, Oliveira MC, Sobrinho-Simões M (2003). E-cadherin loss rather than β-catenin alterations is a common feature of poorly differentiated thyroid carcinomas. *Histopathology* **42:** 580-587.

Rodrigues RF, Roque L, Krug T, Leite V (2007). Poorly differentiated and anaplastic thyroid carcinomas: chromosomal and oligo-array profile of five new cell lines. *Br J Cancer* **96:** 1237-1245.

Salvatore G, Nappi TC, Salerno P, Jiang Y, Garbi C, Ugolini C *et al* (2007). A cell proliferation and chromosomal instability signature in anaplastic thyroid carcinoma. *Cancer Res* **67:** 10148-10158.

Santarpia L, El-Naggar AK, Cote GJ, Myers JN, Sherman SI (2008). Phosphatidylinositol 3-kinase/akt and ras/raf-mitogen-activated protein kinase pathway mutations in anaplastic thyroid cancer. *J Clin Endocrinol Metab* **93:** 278-284.

Schagdarsurengin U, Gimm O, Hoang-Vu C, Dralle H, Pfeifer GP, Dammann R (2002). Frequent epigenetic silencing of the CpG island promoter of RASSF1A in thyroid carcinoma. *Cancer Res* **62:** 3698-3701.

Scheel C, Eaton Elinor N, Li Sophia H-J, Chaffer Christine L, Reinhardt F, Kah K-J *et al* (2011). Paracrine and Autocrine Signals Induce and Maintain Mesenchymal and Stem Cell States in the Breast. *Cell* **145:** 926-940.

Selivanova G (2010). Therapeutic targeting of p53 by small molecules. *Semin Cancer Biol* **20:** 46-56.

Sherr CJ, Roberts JM (1999). CDK inhibitors: positive and negative regulators of G1-phase progression. *Genes Dev* **13:** 1501-1512.

Smallridge RC, Marlow LA, Copland JA (2009). Anaplastic thyroid cancer: molecular pathogenesis and emerging therapies. *Endocr Relat Cancer* **16:** 17-44.

Soares P, Trovisco V, Rocha AS, Feijão T, Rebocho AP, Fonseca E *et al* (2004). BRAF mutations typical of papillary thyroid carcinoma are more frequently detected in undifferentiated than in insular and insular-like poorly differentiated carcinomas. *Virchows Arch* **444:** 572-576.

Subramanian A, Tamayo P, Mootha VK, Mukherjee S, Ebert BL, Gillette MA *et al* (2005). Gene set enrichment analysis: a knowledge-based approach for interpreting genome-wide expression profiles. *Proc Natl Acad Sci U S A* **102:** 15545-15550.

Takano T, Ito Y, Matsuzuka F, Miya A, Kobayashi K, Yoshida H *et al* (2007). Expression of oncofetal fibronectin mRNA in thyroid anaplastic carcinoma. *Jpn J Clin Oncol* **37:** 647-651.

Thiery JP, Sleeman JP (2006). Complex networks orchestrate epithelial-mesenchymal transitions. *Nat Rev Mol Cell Biol* **7:** 131-142.

Tung WS, Shevlin DW, Bartsch D, Norton JA, Wells SA, Jr., Goodfellow PJ (1996). Infrequent CDKN2 mutation in human differentiated thyroid cancers. *Mol Carcinog* **15:** 5-10.

Vasko V, Espinosa AV, Scouten W, He H, Auer H, Liyanarachchi S *et al* (2007). Gene expression and functional evidence of epithelial-to-mesenchymal transition in papillary thyroid carcinoma invasion. *Proc Natl Acad Sci U S A* **104:** 2803-2808.

Volante M, Landolfi S, Chiusa L, Palestini N, Motta M, Codegone A *et al* (2004). Poorly differentiated carcinomas of the thyroid with trabecular, insular, and solid patterns: a clinicopathologic study of 183 patients. *Cancer* **100:** 950-957.

Volante M, Rapa I, Gandhi M, Bussolati G, Giachino D, Papotti M *et al* (2009). RAS mutations are the predominant molecular alteration in poorly differentiated thyroid carcinomas and bear prognostic impact. *J Clin Endocrinol Metab* **94:** 4735-4741.

Wang HM, Huang YW, Huang JS, Wang CH, Kok VC, Hung CM *et al* (2007). Anaplastic carcinoma of the thyroid arising more often from follicular carcinoma than papillary carcinoma. *Ann Surg Oncol* **14:** 3011-3018.

Wang Y, Ngo VN, Marani M, Yang Y, Wright G, Staudt LM *et al* (2010). Critical role for transcriptional repressor Snail2 in transformation by oncogenic RAS in colorectal carcinoma cells. *Oncogene* **29:** 4658-4670.

Wiseman SM, Masoudi H, Niblock P, Turbin D, Rajput A, Hay J *et al* (2006). Derangement of the E-cadherin/catenin complex is involved in transformation of differentiated to anaplastic thyroid carcinoma. *Am J Surg* **191:** 581-587.

Xu J, Lamouille S, Derynck R (2009). TGF-beta-induced epithelial to mesenchymal transition. *Cell Res* **19:** 156-172.

Yu Y, Jiang X, Schoch BS, Carroll RS, Black PM, Johnson MD (2007). Aberrant splicing of cyclin-dependent kinase-associated protein phosphatase KAP increases proliferation and migration in glioblastoma. *Cancer Res* **67:** 130-138.

Zhang Y, Yan W, Chen X (2011). Mutant p53 Disrupts MCF-10A Cell Polarity in Three-dimensional Culture via Epithelial-to-mesenchymal Transitions. *J Biol Chem* **286:** 16218-16228.

CHAPTER IV

Study of microRNA stability in thyroid cancer cells

Author's note

The research work presented in this chapter was developed at Professors Jacques Dumont and Carine Maenhaut's lab at the "Institut de Recherche Interdisciplinaire en Biologie Humaine et Moléculaire" in the "Université Libre de Bruxelles". I worked in collaboration with a PhD student, Sébastien Floor, who was responsible for the hybridisations of microRNA in the arrays and for the bioinformatic analyses. The work is still ongoing and data obtained so far is presented in the manuscript format.

1. Abstract and keywords

MicroRNA (miRNA) are small non-coding RNA capable of simultaneously regulating hundreds of targets, and thus, have crucial roles in different molecular processes. As such, deregulated expression of miRNA has been found in several diseases, including cancer. Contrary to the mechanisms of biogenesis, the degradation of miRNA is still poorly understood. Nevertheless, miRNA turnover rate is a dynamic process, which is dependent on targets availability and important for the maintenance of miRNA levels.

In order to determine a complete atlas of human miRNA half-lives in an *in vitro* model of dedifferentiated thyroid cells, miRNA expression in the BCPAP thyroid cell line was analysed along the time, after transcription shutoff induced by α-amanitin. We applied a method of pulse-labelling with 4-thiouridine, which has been used to study RNA turnover, and optimized it to analyse miRNA decay. The decrease in labelled miRNA expression over time was determined by dual-colour arrays.

Despite an effective transcription blockage with α-amanitin, decreased expression of miR-494, miR-1280, miR-21 or miR-589 was not observed, upon treatment of cells for up to 72 hours. To analyse the miRNA decay for longer periods of time and in more physiological conditions, a non-disruptive labelling of newly synthesised transcripts with 4-thiouridine was applied, for the first time, to miRNA detection. We showed that incubation of cells with 200 µM of 4-thiouridine for 24 hours was not toxic for the cells, did not affect the miRNA expression and miRNA could be efficiently labelled, purified and accurately quantified. Our analysis revealed an average half-life of 2.5 days for 249 miRNA, ranging from 22 hours (miR-208a and miR-107) to more than 5.5 days (miR-1321 and miR-320d).

These results showed that miRNA are more stables than messenger RNA, exhibiting half-lives more comparable to their final targets, *i.e.*, the proteins. The comparison of these data with decay rates determined in normal cells will probably reveal that deregulation of miRNA stability is also involved in carcinogenesis and will allow the identification of more miRNA that can function as potential therapeutic targets.

Keywords: Thyroid cancer cell line; microRNA turnover; microRNA expression array; 4-thiouridine pulse-labelling

2. Introduction

MicroRNA (miRNA) are a class of small non-coding RNA, from 15 to 27 ribonucleotides long, crucially involved in post-transcriptional and translational regulation. There are presently 25 141 mature sequences distributed in 193 species, 2042 of which were found in humans (miRBase 19.0 - www.mirbase.org) (Kozomara and Griffiths-Jones, 2011).

miRNA act on the stability and translation efficiency of their target mRNA, mediating gene silencing through transcripts degradation or translational repression (Carthew and Sontheimer, 2009). Each miRNA can influence the expression of several genes, and consequently regulate development, differentiation, apoptosis and proliferation. As such, deregulated miRNA expression (Calin and Croce, 2006) and genetic alterations in miRNA biogenesis components (Ryan *et al.*, 2010; van Kouwenhove *et al.*, 2011), have been found in several types of human cancers, including thyroid tumours (Nikiforova *et al.*, 2009), suggesting an important role as oncogenes or tumour suppressor genes. More interesting, since miRNA are capable of targeting hundreds of genes, they may be potential therapeutic agents, affecting several pathways simultaneously, and circumventing the compensatory mechanisms of cancer cells (Lujambio and Lowe, 2012).

The miRNA expression profile of ATC has been investigated by a few authors (Table IV.1). For PDTC (Table IV.2), in the few studies performed, the miRNA involved seem to be identical to ATC. These analyses have shown that the majority of miRNA are downregulated in ATC suggesting that they act mainly as tumour suppressor genes. This is in contrast to PTC, in which most miRNA are found significantly over-expressed (He *et al.*, 2005; Pallante *et al.*, 2006). The only upregulated miRNA concordantly found in ATC studies (miR-221, miR-222 and miR-21) are also reported as over-expressed in PTC. These miRNA have been linked to impaired expression of mast/stem cell growth factor receptor Kit (KIT) (He *et al.*, 2005), CDKN1B ($p27^{KIP1}$) (Visone *et al.*, 2007b) and thyroid hormone receptor beta (THRB) (Jazdzewski *et al.*, 2011), and were shown to be induced by several oncogenes, to stimulate proliferation and cell cycle progression (Pallante *et al.*, 2006; Visone *et al.*, 2007b; Frezzetti *et al.*, 2011). Five miRNA (miR-30a-5p, miR-30d, miR-26a, miR-125b and let-7c) are found under-expressed in at least three studies. The miR-30 family members along with miR-200 family members were shown to regulate TGFβ-induced EMT and to decrease invasion of ATC cells, by repression of mothers against decapentaplegic homolog 2 (SMAD2), zinc finger E-box-binding homeobox 2 (ZEB2) and vimentin (VIM) proteins (Braun *et al.*, 2010).

In addition, miR-30d was also reported to inhibit histone-lysine N-methyltransferase EZH2-mediated growth and migration of ATC cell lines (Esposito *et al.*, 2012). The transfection of miR-125b and miR-26a in ATC cell lines reduced their proliferation, an effect probably mediated through targeting of "high mobility group AT-hook 1" and -2 (*HMGA1* and *HMGA2*) genes (Visone *et al.*, 2007a). The members of let-7 family are well-known regulators of cell differentiation and proliferation. Decreased expression was associated with undifferentiated cells and to some types of cancer, and in addition, let-7 miRNA negatively regulated the expression of oncogenes like *RAS*, *MYC* and *HMGA2* (Bussing *et al.*, 2008). In TPC-1, a PTC cell line harbouring RET/PTC1 rearrangement, induction of let-7f decreased MAPK-ERK activation and proliferation of cells, and induced *NKX2-1* and *TG* expressions (Ricarte-Filho *et al.*, 2009).

Table IV.1 - Expressions reported in the literature for miRNA differentially expressed between anaplastic thyroid carcinoma and normal thyroid tissues.

miRNA name	(Visone *et al.*, 2007a) *n* = 10	(Nikiforova *et al.*, 2008) *n* = 2	(Aherne *et al.*, 2008) *n* = 1	(Schwertheim *et al.*, 2009) *n* = 9	(Braun *et al.*, 2010) *n* = 3
miR-222	1.98	9.51	-29.62	20.80	7.27
miR-221	-	9.38	628977.41	20.10	7.74
miR-21	-	-	17.76	20.90	2.96
miR-30d	-4.50	-	-38.58	-3.33	-9.09
miR-26a	-3.32	-	-44.73	-3.33	-9.09
miR-125b	-3.13	-	-1.48	-2.50	-4.35
miR-30a-5p	-3.05	-	-66.46	-3.33	-14.29
let-7c	-1.72	-	-0.89	-10.00	-5.56
miR-138	-2.31	-	-	-	-8.33
miR-29b	-1.81	-	-25.24	-	-3.45
miR-99b	-1.57	-	-3.04	-	-2.63
miR-125a-5p	-2.07	-	2.80	-	-5.88
miR-99a	-1.76	-	2.61	-	-9.09
miR-145	-1.72	-	2.26	-	-7.14

Concordant expression in at least two article are presented; Expression ratio relatively to normal thyroid tissue.

Table IV.2 - Expressions reported in the literature for miRNA differentially expressed between poorly differentiated thyroid carcinoma and normal thyroid tissues.

miRNA name	(Nikiforova *et al.*, 2008) *n* = 2	(Aherne *et al.*, 2008) *n* = 1	(Schwertheim *et al.*, 2009) *n* = 15
miR-26a	-	-26.03	-2.50
miR-125b	-	1.69	-2.50
let-7c	-	1.69	-2.50
miR-222	13.50	-24.18	-1.25
miR-221	20.60	34809.75	1.20
miR-146b-5p	12.40	1.64	1.40
miR-181b	24.70	-6.67	1.60
miR-181a	3.90	0.43	-
miR-213	4.30	13.05	-
miR-183	5.70	-6.55	-
miR-339-5p	6.10	-5.43	-
miR-129-5p	17.30	-19.15	-
miR-187	23.50	-	-

miRNA expression in at least two article are presented; Expression ratio relatively to normal thyroid tissue.

Similarly to mRNAs, miRNAs are first transcribed in long transcripts from genomic DNA, mainly by RNA Polymerase (Pol) II (Cai *et al.*, 2004; Lee *et al.*, 2004; Ozsolak *et al.*, 2008) or in some cases by Pol III (Borchert *et al.*, 2006; Ozsolak *et al.*, 2008). These long transcripts, folded into hairpin structures, may contain a single miRNA or a cluster of miRNA, and are named primary miRNA (pri-miRNA). The first step in miRNA processing involves the recognition and cleavage of pri-miRNA by the microprocessor complex (Denli *et al.*, 2004; Gregory *et al.*, 2004), constituted by the ribonuclease 3 (DROSHA) (Lee *et al.*, 2003) and a double-stranded RNA-binding protein, the microprocessor complex subunit DGCR8 (DGCR8). This generates a 60 to 70 nucleotides stem-loop known as the miRNA precursor (pre-miRNA) that is exported from the nucleus in a process involving exportin 5 (XPO5) protein (Yi *et al.*, 2003; Lund *et al.*, 2004). In the cytoplasm, pre-miRNA are further cleaved by another endoribonuclease, DICER1 (Bernstein *et al.*, 2001; Grishok *et al.*, 2001; Hutvágner *et al.*, 2001; Ketting *et al.*, 2001; Knight and Bass, 2001), in association with the cofactor RISC-loading complex subunit (TARBP2) (Chendrimada *et al.*, 2005; Haase *et al.*, 2005), which yields a 19 to 23 nucleotides miRNA duplex of strands with 3' overhangs. Finally, selection of a guided strand as mature miRNA and assembling of miRNA-induced silencing complex (miRISC), of which argonaute (EIF2C, known as AGO) family members are the key proteins, allows the targeting of transcripts, usually by imperfect base pairing

complementary to the 3' untranslated regions (Bartel, 2004; Filipowicz *et al.*, 2008).

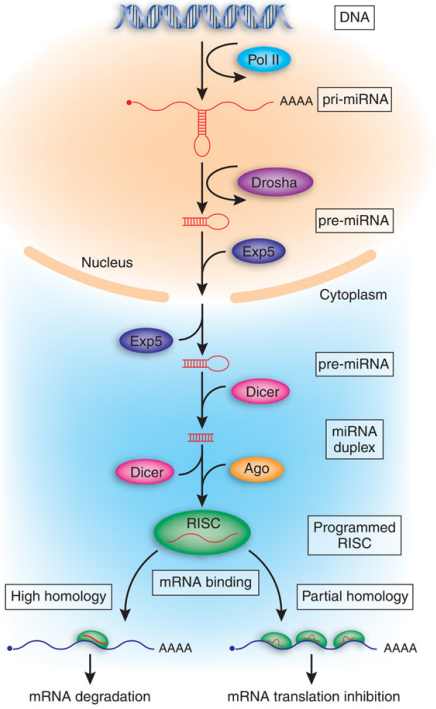

Figure IV.1 – Schematic overview of the canonical biogenesis and function of human miRNA. These non-coding RNA, 15 to 27 nucleotides long, are encoded as primary miRNA (pri-miRNA) and processed by two ribonucleases (Drosha and Dicer). In mammals, one single strand of the miRNA duplex is loaded into a RNA-induced silencing complex (RISC) which generally, base-pair imperfectly to sequences located in the 3'-untranslated region of targets mRNA (from Cullen, 2006). Pol II – RNA Polymerase II; pre-miRNA – precursor miRNA; Exp5 – Exportin 5 (XPO5); Ago – Argonaute (EIF2C).

miRNA steady-state levels is a net result from the synthesis and degradation of existent miRNA and so, the characterisation of the miRNA decay after processing is crucial to understand their biological and functional timing. Following DICER1 cleavage, mature miRNA are assumed to be highly stable molecules (Carthew and Sontheimer, 2009). A recent article described, for the first time, in mammalian cells, a global determination of miRNA turnovers after knocking out *Dicer1* in mouse embryonic fibroblasts, and reported, for a theoretically non-dividing cell population, an average miRNA half-life of 5 days, ranging from 4 days for miR-155 up to 9 days for miR-125b (Gantier *et al.*, 2011). Nevertheless, this is not always the case, and rapid miRNA turnover has been reported for instance, in retinal and cortical neurons (Krol *et al.*, 2010) and following immune cells stimulation (Ceppi *et al.*, 2009). Different post-transcriptional modifications are already known to affect miRNA stability (Kai and Pasquinelli, 2010) and degradation of mature miRNA has been attributed to members of 5'-3' exoribonuclease (XRN) and small RNA degrading nuclease (SDN) families in *C. elegans* and in *A. thaliana*, respectively (Ramachandran and Chen, 2008; Chatterjee and Grosshans, 2009; Chatterjee *et al.*, 2011).

In the present study, we proposed to determine an atlas of turnover rates of human miRNA, in the most standard conditions possible, with the hypothesis that stability differences will correlate with miRNA sequence features, with stability of corresponding targets or with the corresponding regulated pathways.

3. Materials and methods

Cell culture and reagents

Papillary thyroid carcinoma cells (BCPAP cell line) were cultured in RPMI medium 1640 with 25 mM HEPES buffer and 2 mM L-Glutamine (Invitrogen, Paisley, UK), supplemented with 10% fetal bovine serum (Invitrogen), 100 U/ml Penicillin, 100 μg/ml Streptomycin and 0.25 μg/ml Amphotericin B (Invitrogen) at 37ºC in a humidified atmosphere of 5% CO_2 (NUAIRE US Autoflow Incubator, Plymouth, MN, USA). For transcription inhibition, we used α-amanitin (Sigma-Aldrich, St. Louis, MO, USA) 1 mg/ml dissolved in Dulbecco's phosphate-buffered saline (PBS) and for RNA labelling, we used 4-thiouridine (Sigma-Aldrich) 50 mM dissolved in PBS.

MTS colorimetric assay

After cells incubation in 48-wells culture plates, cell medium was added, containing 20% of 2 mg/ml 3-(4,5-dimethylthiazol-2-yl)-5-(3-carboxymethoxyphenyl)-2-(4-sulfophenyl)-2H-tetrazolium (MTS) (Promega, Madison, WI, USA) and 1% of 0.92 mg/ml phenazine methosulfate (PMS) (Sigma-Aldrich) both dissolved in PBS. Following 2 hours at 37ºC, solution was transferred to a 96-wells microtiter plate for spectrophotometer reading at 490 nm. For each assay, cell incubation with 0.5% Triton X-100 solution was done as positive control. Incubation of reaction medium in empty wells was used for background correction. All conditions were performed in triplicate. Viability was calculated relatively to control non-treated cells.

Total RNA extraction

Total RNA, containing both mRNA and miRNA, was extracted using a TRIzol Reagent kit (Invitrogen) followed by purification with the miRNeasy mini kit (Qiagen, Hamburg, GmbH, Germany) according to the manufacturer's protocol. The RNA concentration was quantified by UV spectrophotometry (NanoDrop ND-1000, Thermo Fisher Scientific, Wilmington, DE, USA), and its integrity was verified using an automated micro capillary electrophoresis (Experion, Bio-Rad, Hercules, CA, USA).

Qualitative RT-PCR and mRNA quantitative RT-PCR

After a deoxyribonuclease treatment using DNAse I amplification Grade (Invitrogen), reverse transcription was performed using Superscript II RNase H Reverse Transcriptase (Invitrogen) following the manufacturer's protocol. Qualitative PCR reactions were performed using Taq DNA Polymerase (Invitrogen) following the manufacturer's protocol and amplicons were analysed on agarose gel. Oligonucleotide sequences corresponding to pri-miR-21 and *GAPDH*, "transfer RNA tyrosine" ($tRNA^{tyr}$) and "45S ribosomal RNA" (*45S rRNA*) precursors were previously described (Lee *et al.*, 2004). Pri-miR-494 and pri-miR-1280 were designed using Primer Express software (Applied Biosystems, Foster City, CA, USA).

Quantitative RT-PCR amplifications were run on an Applied Biosystems 7500 Fast Real Time PCR using Power SYBR Green PCR Master Mix (Applied Biosystems), according to the manufacturer's protocol. Oligonucleotide sequences corresponding to *GAPDH*, *ACTB* and *MYC* transcripts were designed using Primer Express software (Applied Biosystems). All reactions, including a control without template, were performed in triplicate. All primers sequences are shown in Chapter VI.

Quantitative RT-PCR for miRNA

Expression levels of miR-1280, miR-21, miR-494, miR-589 and miR-29a were quantified using TaqMan MicroRNA Assay kits according to the manufacturer's protocol (Applied Biosystems). miRNA-specific cDNA was generated from 10 ng of total RNA using the TaqMan microRNA RT Kit and the gene-specific RT primers from TaqMan microRNA Assays (Applied Biosystems) according to the manufacturer's instructions. All reactions, including a control without template, were performed in triplicate.

Thiol-specific biotinylation and streptavidin beads purification

After extraction from the cells, the entire total RNA was processed. Thiol-specific biotinylation was performed using EZ-Link Biotin-HPDP (Thermo Fisher Scientific) dissolved in dimethylformamide (DMF) at 1 mg/ml. Biotinylation was done for 2 hours in room temperature with rotation, in 1 mM EDTA, 10 mM Tris (pH 7.5) with 2 µl Biotin-HPDP per µg RNA used. Unbound Biotin-HPDP was removed by phenol/chloroform extraction and

RNA was isopropanol-precipitated and resuspended in RNAse-free water. The purification of the biotinylated RNA was performed using the μMACS Streptavidin kit (Miltenyi Biotec, Leiden, The Netherlands). After denaturation of RNA at 65ºC for 10 minutes followed by rapid cooling on ice for 5 minutes, RNA were incubated with 2 μl μMACS Streptavidin MicroBeads per μg RNA, for 15 minutes with rotation at room temperature. Beads were transferred and magnetically fixed to μColumns, already rinsed with 100 μl Nucleic Acid Equilibration Buffer (Miltenyi Biotec) and 1 ml washing buffer (100 mM Tris pH 7.5, 10 mM EDTA, 1 M sodium chloride, 1% Tween20, 1% sodium dodecyl sulfate). Columns were washed three times with 1 ml 70ºC washing buffer and three times with 1 ml washing buffer at room temperature. Labelled RNA was eluted by 2 elution rounds with 100 mM dithiothreitol and recovered using the miRNeasy columns (Qiagen).

miRNA microarray and bioinformatics analysis

The entire RNA obtained, after 4-thiouridine-specific purification, was engaged for the hybridisation reaction and each sample used was spiked-in with 52 synthetic 5'-phosphorylated microRNAs (Exiqon). Briefly, total RNA was labelled using the miRCURY LNA microRNA Power Labelling Kit (Hy3/Hy5) (Exiqon, Vedbaek, Denmark), according to the manufacturer's protocol. Samples were hybridized using Corning Pronto! Microarray Hybridisation Kit onto in-house-printed slides with the mercury LNA microRNA ready-to-spot probes set (V11.0 according to Mirbase 11.0) from Exiqon. All hybridisations were performed in duplicates with dyes swapped. After overnight hybridisation, microarray slides were washed under stringent conditions: twice during 60 seconds at 60°C with 2X saline-sodium citrate (SSC) and 2% sodium dodecyl sulphate; twice during 60 seconds at 60°C with 2X SSC; and twice during 60 seconds at room temperature with 0.2X SSC. Then, the slides were scanned using a GenePix 4000B scanner (Axon) and expression levels were quantified with GenePix Pro 6.0 (Axon). Treatment of the raw data was carried out by using the LIMMA 3.4.5 package for the R 2.8.1 language. A Normex + offset background correction and Loess normalisation or spike-ins based normalisation were performed. Data points were removed when intensity values for both dyes were below 200% of the background, and absent calls were removed.

miRNA half-lives determination

A total of 4 cell culture experiments were performed. In each, different time-points were assessed in order to determine the miRNA half-lives. RNA from time-points, labelled with Hy5 dye (red channel), were hybridised against control RNA labelled with Hy3 dye (green channel), and miRNA quantifications were calculated as log2 of the ratio between red and green channels intensities (R/G). Assuming that miRNA degradation follows a first-order kinetics, quantifications obtained in the arrays from each culture, were plotted as a function of time (t) (equation 1).

$$\log_2\left(\frac{R}{G}\right) = -\kappa.t \qquad \text{(Equation 1)}$$

The miRNA half-lives (time taken for half of the labelled miRNA to be degraded) ($t_{1/2}$), for each culture experiment, were then calculated, following equation 2.

$$t_{1/2} = \frac{1}{\kappa} \qquad \text{(Equation 2)}$$

The final half-lives were determined as the mean value of the half-lives obtained, in at least 2 cell culture experiments.

Assuming that during a cell division the miRNA amounts are divided into each cell, the miRNA half-lives are affected by the cell proliferation. However, our miRNA decay measurements are not impacted because, for every condition used, the entire RNA extracted from the cells was processed and analysed.

4. Results and discussion

Attempted determination of half-lives by transcription blockage

Initially, we considered inhibiting miRNA transcription, and determine the expression of mature transcripts along the time, in order to analyse the miRNA decays. To inhibit transcription, we treated the PTC cell line BCPAP with the transcriptional inhibitor α-amanitin. Evaluation of cell toxicity, upon incubation at 3 different α-amanitin concentrations, showed that more than 80% of cells are still viable up to 30 hours (Figure IV.2).

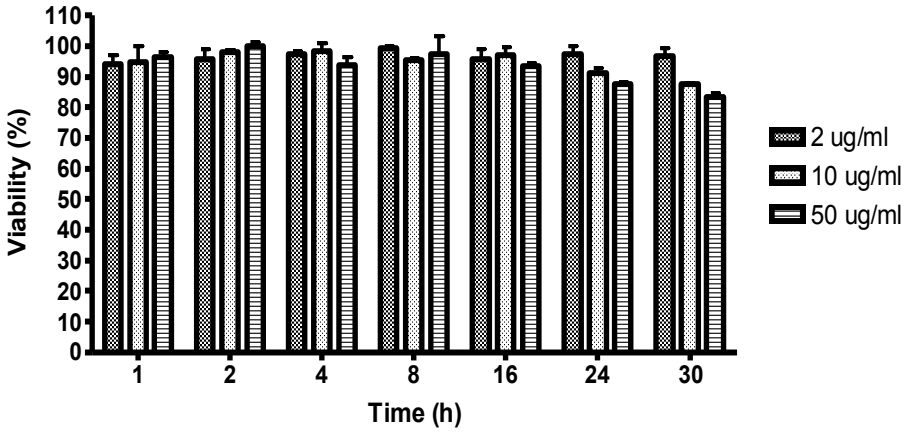

Figure IV.2 – Cell viability upon treatment with α-amanitin. BCPAP thyroid cells were treated with 2, 10 and 50 µg/ml of α-amanitin during different incubation times (1 hour to 30 hours). Error bars denote mean ± SEM of two independent experiments.

To verify the transcriptional blockage, we assessed the primary transcripts levels of 3 miRNA, as well as, Pol III (*tRNA^{tyr}* precursor) and Pol I (*45S rRNA* precursor) transcripts (Figure IV.3). RNA polymerases have different sensitivities to α-amanitin and, while Pol II is highly affected, Pol III is moderately affected and Pol I is insensitive to the toxin. In accordance, while the pri-miRNA levels decreased along the treatment time and were dependent on α-amanitin concentrations, *tRNA^{tyr}* and *45S rRNA* precursors were unaffected. As positive control, *GAPDH* precursor levels were also assessed. These results demonstrated that an efficient inhibition of the miRNA transcription was obtained after 16 to 24 hours of incubation with α-amanitin.

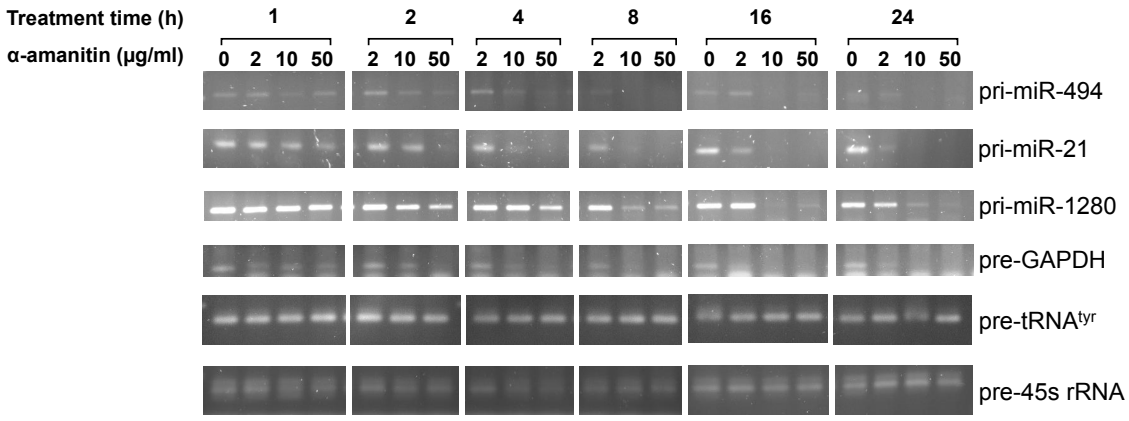

Figure IV.3 – Qualitative analysis of primary miRNA expression levels after transcription shutoff. Expression of three primary miRNA (pri-miR-494, -21 and -1280) were assessed, by RT-PCR amplification, in cells incubated with α-amanitin during the indicated times and concentrations. Expression levels were also analysed for "glyceraldehyde-3-phosphate dehydrogenase" (*GAPDH*) precursor (another Pol II transcript), for "transfer RNA tyrosine" ($tRNA^{tyr}$) precursor (Pol III transcript) and "45S ribosomal RNA" (*45s rRNA*) precursor (Pol I transcript). Representative results of two independent experiments.

A previous global miRNA analysis showed that 95% of the miRNA expressed in Human Embryonic Kidney (HEK293) cells remained stable, following a transcriptional shutoff with actinomycin D for 8 hours (Bail *et al.*, 2010). We analysed the expression of mature miRNA by quantitative RT-PCR, in cells treated with 50 μg/ml of α-amanitin (Figure IV.4). Even after 72 hours of incubation, the 4 mature miRNA tested did not have a significant decay. However, expression levels of *ACTB*, *MYC* and *GAPDH* showed a significant and pronounced decay over time (Figure IV.5). It should be noted that these results are influenced by the stability and processing time of the primary and precursor miRNA. Nevertheless, miRNA seemed to have low degradation rates and so, longer transcription blockade was needed. However, after 72 hours of incubation, cell viability dropped below 30%, invalidating the further use of α-amanitin (data not shown).

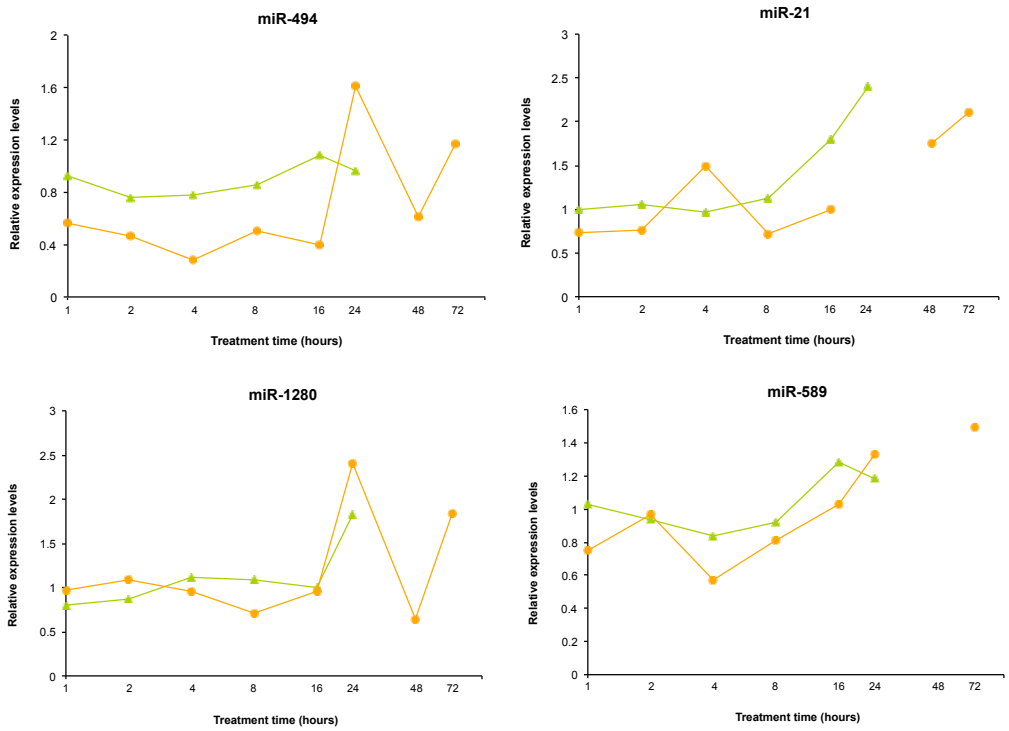

Figure IV.4 – Quantitative RT-PCR analysis of 4 mature miRNA following transcription blockage. Non-normalised expression levels in cells incubated with 50 µg/ml of α-amanitin over 72 hours and determined relatively to cells grown in control medium. Representative results of two independent experiments.

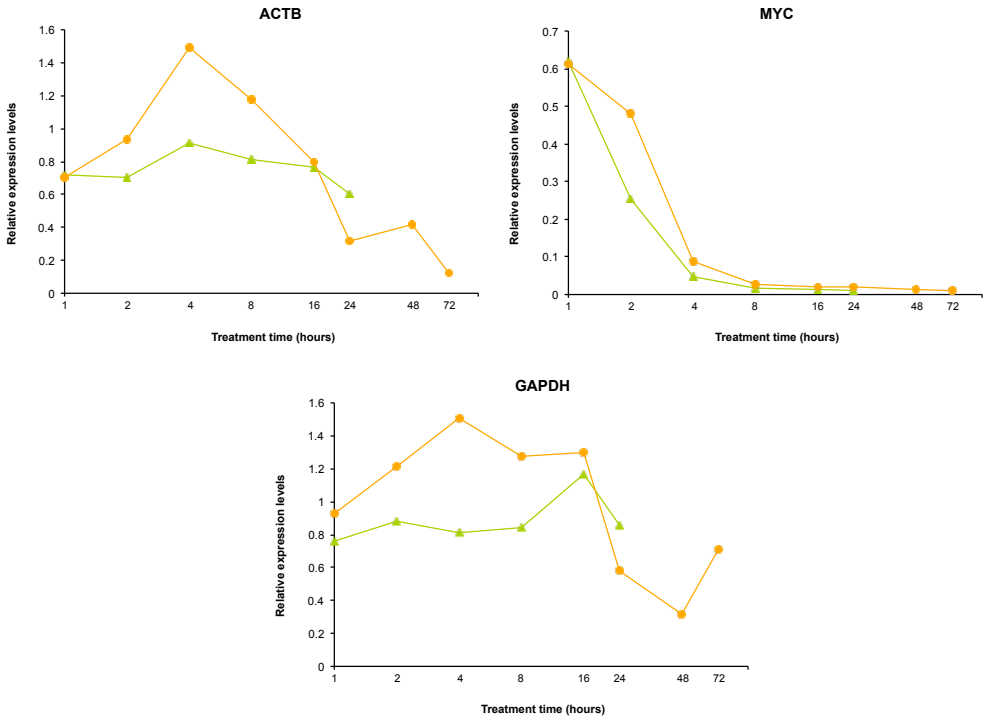

Figure IV.5 – Quantitative RT-PCR analysis of 3 mRNA transcripts following transcription blockage. Non-normalised expression levels in cells incubated with 50 µg/ml of α-amanitin over 72 hours and determined relatively to cells grown in control medium. Representative results of two independent experiments.

4-thiouridine pulse-labelling of RNA

To be able to determine miRNA half-lives for a longer period of time, we performed pulse-labelling of RNA with 4-thiouridine (4sU) (Kenzelmann *et al.*, 2007). This method does not require the use of inhibitors and takes advantage of the pyrimidine salvage pathway, by which ribonucleotides are recycled instead of being *de novo* synthesised. Therefore, thiolated analogs of nucleosides, such as 4sU, can be incorporated *in vivo* and selectively enrich newly transcribed RNA molecules. This RNA fraction can then be separated from total RNA, using thiol-specific biotinylation and subsequent purification on streptavidin-coated magnetic beads (Dolken *et al.*, 2008). Quantification of the 4sU-incorporated RNA at different time-points, after the labelling period, allows the determination of decay rates. To apply the method to miRNA quantification, we ensured an efficient labelling by increasing the time of cell exposure to 4sU to that usually used for mRNA turnover studies. Viability assays showed that cells were sensitive to this nucleoside (Figure IV.6). We also tested different modifications to the protocol (Dolken *et al.*, 2008), in order to purify more efficiently the newly synthesised miRNA. We decided to label the cells for 24 hours with 200 μM 4sU as we could obtain sufficient newly transcribed miRNA without loss of cell viability.

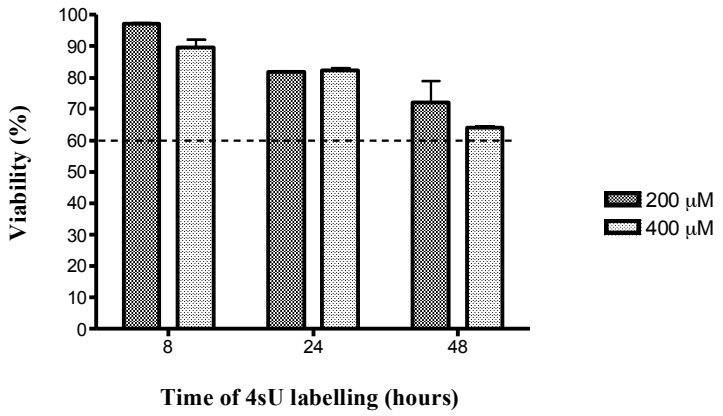

Figure IV.6 – Cell viability after incubation with 4-thiouridine. Cells were treated with medium containing 200 μM or 400 μM 4-thiouridine (4sU) for 8, 24 or 48 hours. Error bars denote mean ± SEM of two independent experiments.

Test of applicability of the method for miRNA labelling

To prove the proportional accuracy of the method, different quantities of RNA, extracted from cells treated with 4sU, were mixed with RNA extracted from non-treated control cells. This allowed us to obtain samples with different proportions of labelled RNA but still with equal quantities of total RNA. After purification of the labelled RNA fractions, we analysed

the expression of miRNA by quantitative RT-PCR (Figure IV.7). Five samples were prepared to obtain successive fractions of 4sU-containing RNA in total RNA (1, 0.5, 0.25, 0.125 and 0) and results clearly showed the expected quantity ratio, which was not due to differences in miRNA total expression between the 2 types of RNA. However, the sample with no 4sU-incorporated RNA showed that some miRNA are non-specifically purified (despite the high stringency). Therefore, we showed that the thiol-specific biotinylation and streptavidin-coated magnetic beads separation were able to accurately purify miRNA.

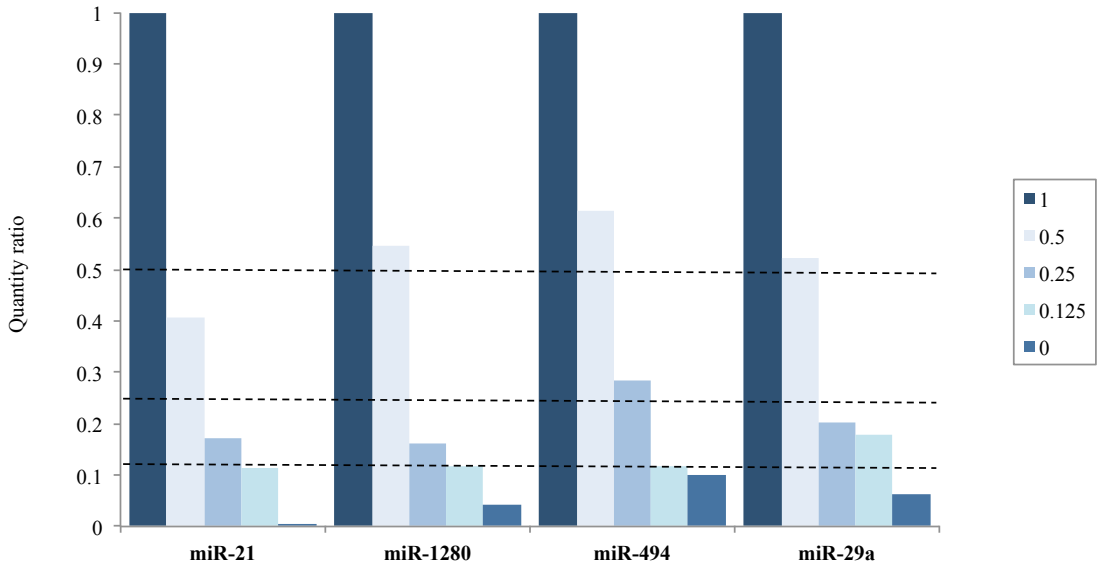

Figure IV.7 – Quantification of 4 miRNA after 4-thiouridine-specific purification of labelled RNA. Expression levels of 4 mature miRNA were analysed after 4-thiouridine-specific purification of labelled RNA in a set of test samples. These samples were obtained by mixing 4-thiouridine (4sU) labelled RNA with non-labelled RNA in 5 different proportions, in order to test different quantity ratios of 4sU-incorporated RNA (1, 0.5, 0.25, 0.125 and 0). The non-normalised expression levels were represented relatively to the expression in the pure 4sU labelled RNA. Data are representative of two independent experiments.

Determination of half-lives by miRNA arrays hybridisation

For global miRNA quantification, we performed two-colour miRNA arrays. In order to obtain the miRNA half-lives from BCPAP cells, we hybridised 4sU-specific purified RNA fractions from experimental conditions against those from control conditions. In both experimental and control conditions, cells were treated with 4sU for 24 hours (labelling time). In addition, cells from experimental conditions were incubated in standard conditions, for determined periods of time (Figure IV.8). During this time, miRNA are degraded, which will be reflected in the purification of the labelled RNA. From the representation of the miRNA

quantification along the time that cells were incubated, half-lives were determined assuming that decays follow a first-order kinetic.

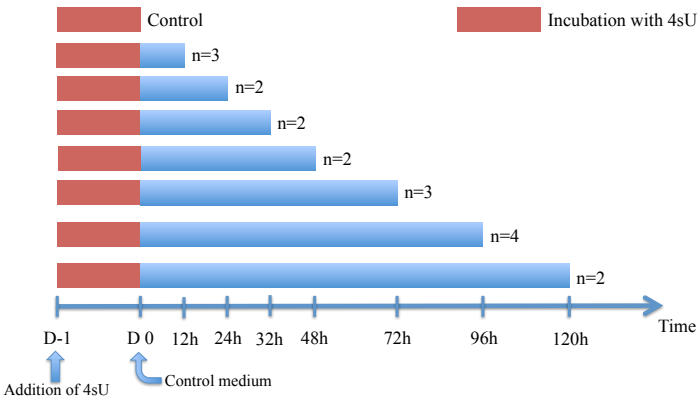

Figure IV.8 - Representative scheme of the experimental design for miRNA half-lives determination. BCPAP cells were incubated with thiouridine (4sU)-containing medium for 24 hours. After this labelling period, medium was changed for control medium and cells were grown during the represented times (number of replicates for each is shown). For each time-point, a control with the same cells was performed.

Normalisation method and thiouridine effect on miRNA quantification

Normalisation methods are applied in order to adjust the microarray data for effects arising from technical variation, which are not biologically meaningful. The usual normalisation for two-colour arrays assumes that globally, the median intensities of the two conditions being compared most be equal. But, for our purpose, we expected that the intensities in the experimental conditions were decreased relatively to the control conditions. We, then, used 52 synthetic 5'-phosphorylated miRNA, which are spiked into each RNA sample at equal quantities prior to dye labelling, allowing correction of the data. This method of normalisation was highly comparable to the Loess normalisation method, frequently used in two-colour arrays (Figure IV.9). By hybridising total RNA from 24 hours-treated cells against total RNA from non-treated cells, we also showed that 4sU metabolic labelling did not greatly affect the miRNA expression (Figure IV.9). Although we could detect 7 differentially expressed miRNA, the most affected one had an expression difference of only 1.6 fold.

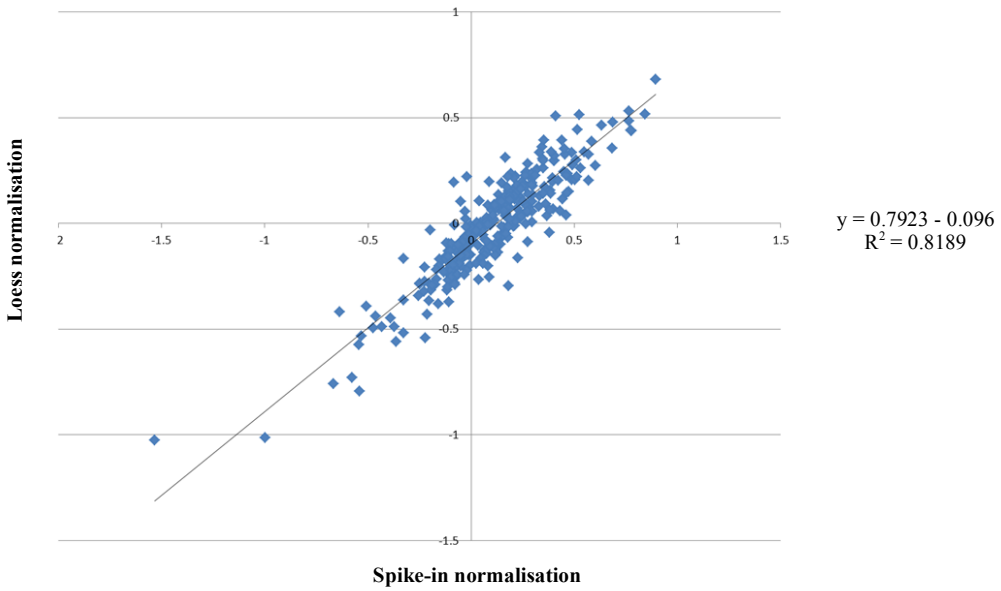

Figure IV.9 - Graphical comparison of normalisation methods and differential miRNA expression upon thiouridine labelling. miRNA expressions normalised with Loess method are represented in the vertical axis and expressions normalised using 52 synthetic spike-ins are represented in the horizontal axis. The equation and the correlation coefficient of the trend line are shown. The miRNA expressions represented were determined as log2 of the ratio between intensities from total RNA of thiouridine-treated cells and total RNA of non-treated cells.

Global miRNA decays in the BCPAP thyroid cell line

Using the BCPAP PTC cell line, we were able to determine the half-lives of 249 miRNA (Figure IV.10). The results showed that these miRNA had an average half-life of 62 hours (about 2.5 days) raging from 22 hours up to 136 hours (about 5.5 days) (Supplementary Table IV.1). The only exception was miR-320d, which had a half-life of 198 hours (8 days). In comparison to the reported half-lives, predicted for non-dividing mouse embryonic fibroblasts (ranging between 4 and 9 days) (Gantier *et al.*, 2011), our data showed that miRNA are considerably less stable. Still, miR-155 and miR-107, for example, were in each of the studies, two of the least stable miRNA. The discrepancy observed might be due to the different types of cells used (human cancer cell line versus mouse embryonic fibroblasts) or different detection methods (miRNA array versus TaqMan PCR array). Moreover, the deletion of *Dicer1* performed by Gantier and collaborators, could have led to the determination of lower turnover rates. miRNA accumulation/degradation was shown to depend on argonaute protein levels and on miRISC assembly/disassembly (Chatterjee and Grosshans, 2009; Kai and Pasquinelli, 2010). Since DICER1 associates with argonaute and is involved in loading miRNA into miRISC (Meister and Tuschl, 2004; Carthew and Sontheimer, 2009), turnover rates were probably affected by the *Dicer1* knockout.

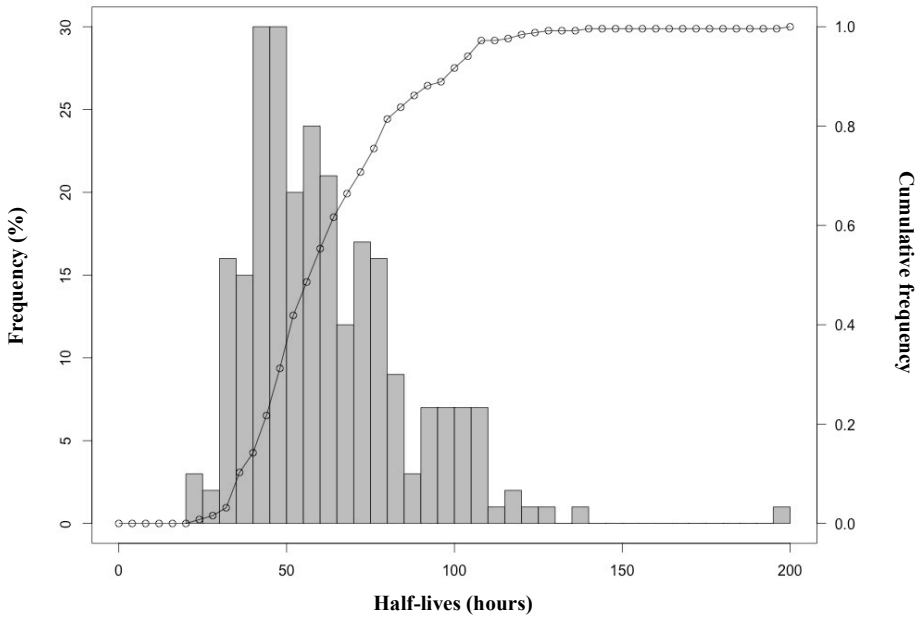

Figure IV.10 - Frequency of determined half-lives for 249 miRNA. Half-lives were grouped in bins of 5 hours and frequency/cumulative frequency over the total of the 249 miRNA detected are represented.

Our results indicate that miRNA are molecules considerably more stable than mRNA that have reported median half-lives between 315 minutes (5 hours) for human B cells (Friedel *et al.*, 2009), and 10 hours for human fibroblast and hepatocarcinoma cell line (HepG2) (Yang *et al.*, 2003). miRNA stability seems to be comparable to protein stability, which had a median half-life around 40 hours in HeLa cell line (Boisvert *et al.*, 2012).

The use of a cancer cell line allows to extrapolate the results for dedifferentiated thyroid tumours (i.e. PDTC and ATC). Thyroid cancer cell lines, including the BCPAP cell line used in this work, have been shown to exhibit expression profiles similar to ATC, both at gene (van Staveren *et al.*, 2007) and miRNA (Floor *et al.*, *submitted*) levels.

The stability of miRNA seems to be important to maintain miRNA levels, and turnover was found to be regulated by corresponding targets expression (Ameres *et al.*, 2010; Baccarini *et al.*, 2011; Chatterjee *et al.*, 2011). Since, cancer cells characteristically present deregulated gene and miRNA expressions, the determination and comparison of miRNA half-lives between cancer cells and normal cells will probably reveal miRNA stability as another deregulated mechanism. The comparison of our results with half-lives determined in primary cultures of normal thyrocytes will allow the study of the differences in miRNA stability during the oncogenic process.

5. References

Aherne ST, Smyth PC, Flavin RJ, Russell SM, Denning KM, Li JH *et al* (2008). Geographical mapping of a multifocal thyroid tumour using genetic alteration analysis & miRNA profiling. *Mol Cancer* **7:** 89.

Ameres SL, Horwich MD, Hung JH, Xu J, Ghildiyal M, Weng Z *et al* (2010). Target RNA-directed trimming and tailing of small silencing RNAs. *Science* **328:** 1534-1539.

Baccarini A, Chauhan H, Gardner TJ, Jayaprakash AD, Sachidanandam R, Brown BD (2011). Kinetic analysis reveals the fate of a microRNA following target regulation in mammalian cells. *Curr Biol* **21:** 369-376.

Bail S, Swerdel M, Liu H, Jiao X, Goff LA, Hart RP *et al* (2010). Differential regulation of microRNA stability. *RNA* **16:** 1032-1039.

Bartel DP (2004). MicroRNAs: genomics, biogenesis, mechanism, and function. *Cell* **116:** 281-297.

Bernstein E, Caudy AA, Hammond SM, Hannon GJ (2001). Role for a bidentate ribonuclease in the initiation step of RNA interference. *Nature* **409:** 363-366.

Boisvert FM, Ahmad Y, Gierlinski M, Charriere F, Lamont D, Scott M *et al* (2012). A quantitative spatial proteomics analysis of proteome turnover in human cells. *Mol Cell Proteomics* **11:** M111 011429.

Borchert GM, Lanier W, Davidson BL (2006). RNA polymerase III transcribes human microRNAs. *Nat Struct Mol Biol* **13:** 1097-1101.

Braun J, Hoang-Vu C, Dralle H, Huttelmaier S (2010). Downregulation of microRNAs directs the EMT and invasive potential of anaplastic thyroid carcinomas. *Oncogene* **29:** 4237-4244.

Bussing I, Slack FJ, Grosshans H (2008). let-7 microRNAs in development, stem cells and cancer. *Trends Mol Med* **14:** 400-409.

Cai X, Hagedorn CH, Cullen BR (2004). Human microRNAs are processed from capped, polyadenylated transcripts that can also function as mRNAs. *RNA* **10:** 1957-1966.

Calin GA, Croce CM (2006). MicroRNA signatures in human cancers. *Nat Rev Cancer* **6:** 857-866.

Carthew RW, Sontheimer EJ (2009). Origins and Mechanisms of miRNAs and siRNAs. *Cell* **136:** 642-655.

Ceppi M, Pereira PM, Dunand-Sauthier I, Barras E, Reith W, Santos MA *et al* (2009). MicroRNA-155 modulates the interleukin-1 signaling pathway in activated human monocyte-derived dendritic cells. *Proc Natl Acad Sci U S A* **106:** 2735-2740.

Chatterjee S, Grosshans H (2009). Active turnover modulates mature microRNA activity in Caenorhabditis elegans. *Nature* **461:** 546-549.

Chatterjee S, Fasler M, Bussing I, Grosshans H (2011). Target-mediated protection of endogenous microRNAs in C. elegans. *Dev Cell* **20:** 388-396.

Chendrimada TP, Gregory RI, Kumaraswamy E, Norman J, Cooch N, Nishikura K *et al* (2005). TRBP recruits the Dicer complex to Ago2 for microRNA processing and gene silencing. *Nature* **436:** 740-744.

Cullen BR (2006). Viruses and microRNAs. *Nat Genet* **38 Suppl:** S25-30.

Denli AM, Tops BB, Plasterk RH, Ketting RF, Hannon GJ (2004). Processing of primary microRNAs by the Microprocessor complex. *Nature* **432:** 231-235.

Dolken L, Ruzsics Z, Radle B, Friedel CC, Zimmer R, Mages J *et al* (2008). High-resolution gene expression profiling for simultaneous kinetic parameter analysis of RNA synthesis and decay. *RNA* **14:** 1959-1972.

Esposito F, Tornincasa M, Pallante P, Federico A, Borbone E, Pierantoni GM *et al* (2012). Down-regulation of the miR-25 and miR-30d contributes to the development of anaplastic thyroid carcinoma targeting the polycomb protein EZH2. *J Clin Endocrinol Metab* **97:** E710-718.

Filipowicz W, Bhattacharyya SN, Sonenberg N (2008). Mechanisms of post-transcriptional regulation by microRNAs: are the answers in sight? *Nat Rev Genet* **9:** 102-114.

Frezzetti D, De Menna M, Zoppoli P, Guerra C, Ferraro A, Bello AM *et al* (2011). Upregulation of miR-21 by Ras in vivo and its role in tumor growth. *Oncogene* **30:** 275-286.

Friedel CC, Dolken L, Ruzsics Z, Koszinowski UH, Zimmer R (2009). Conserved principles of mammalian transcriptional regulation revealed by RNA half-life. *Nucleic Acids Res* **37:** e115.

Gantier MP, McCoy CE, Rusinova I, Saulep D, Wang D, Xu D *et al* (2011). Analysis of microRNA turnover in mammalian cells following Dicer1 ablation. *Nucleic Acids Res* **39:** 5692-5703.

Gregory RI, Yan KP, Amuthan G, Chendrimada T, Doratotaj B, Cooch N *et al* (2004). The Microprocessor complex mediates the genesis of microRNAs. *Nature* **432:** 235-240.

Grishok A, Pasquinelli AE, Conte D, Li N, Parrish S, Ha I *et al* (2001). Genes and mechanisms related to RNA interference regulate expression of the small temporal RNAs that control C. elegans developmental timing. *Cell* **106:** 23-34.

Haase AD, Jaskiewicz L, Zhang H, Laine S, Sack R, Gatignol A *et al* (2005). TRBP, a regulator of cellular PKR and HIV-1 virus expression, interacts with Dicer and functions in RNA silencing. *EMBO Rep* **6:** 961-967.

He H, Jazdzewski K, Li W, Liyanarachchi S, Nagy R, Volinia S *et al* (2005). The role of microRNA genes in papillary thyroid carcinoma. *Proc Natl Acad Sci U S A* **102:** 19075-19080.

Hutvágner G, McLachlan J, Pasquinelli AE, Balint E, Tuschl T, Zamore PD (2001). A cellular function for the RNA-interference enzyme Dicer in the maturation of the let-7 small temporal RNA. *Science* **293:** 834-838.

Jazdzewski K, Boguslawska J, Jendrzejewski J, Liyanarachchi S, Pachucki J, Wardyn KA *et al* (2011). Thyroid hormone receptor beta (THRB) is a major target gene for microRNAs deregulated in papillary thyroid carcinoma (PTC). *J Clin Endocrinol Metab* **96:** E546-553.

Kai ZS, Pasquinelli AE (2010). MicroRNA assassins: factors that regulate the disappearance of miRNAs. *Nat Struct Mol Biol* **17:** 5-10.

Kenzelmann M, Maertens S, Hergenhahn M, Kueffer S, Hotz-Wagenblatt A, Li L *et al* (2007). Microarray analysis of newly synthesized RNA in cells and animals. *Proc Natl Acad Sci U S A* **104:** 6164-6169.

Ketting RF, Fischer SE, Bernstein E, Sijen T, Hannon GJ, Plasterk RH (2001). Dicer functions in RNA interference and in synthesis of small RNA involved in developmental timing in C. elegans. *Genes Dev* **15:** 2654-2659.

Knight SW, Bass BL (2001). A role for the RNase III enzyme DCR-1 in RNA interference and germ line development in Caenorhabditis elegans. *Science* **293:** 2269-2271.

Kozomara A, Griffiths-Jones S (2011). miRBase: integrating microRNA annotation and deep-sequencing data. *Nucleic Acids Res* **39:** D152-157.

Krol J, Busskamp V, Markiewicz I, Stadler MB, Ribi S, Richter J *et al* (2010). Characterizing light-regulated retinal microRNAs reveals rapid turnover as a common property of neuronal microRNAs. *Cell* **141:** 618-631.

Lee Y, Ahn C, Han J, Choi H, Kim J, Yim J *et al* (2003). The nuclear RNase III Drosha initiates microRNA processing. *Nature* **425:** 415-419.

Lee Y, Kim M, Han J, Yeom KH, Lee S, Baek SH *et al* (2004). MicroRNA genes are transcribed by RNA polymerase II. *EMBO J* **23:** 4051-4060.

Lujambio A, Lowe SW (2012). The microcosmos of cancer. *Nature* **482:** 347-355.

Lund E, Guttinger S, Calado A, Dahlberg JE, Kutay U (2004). Nuclear export of microRNA precursors. *Science* **303:** 95-98.

Meister G, Tuschl T (2004). Mechanisms of gene silencing by double-stranded RNA. *Nature* **431:** 343-349.

Nikiforova MN, Tseng GC, Steward D, Diorio D, Nikiforov YE (2008). MicroRNA expression profiling of thyroid tumors: biological significance and diagnostic utility. *J Clin Endocrinol Metab* **93:** 1600-1608.

Nikiforova MN, Chiosea SI, Nikiforov YE (2009). MicroRNA expression profiles in thyroid tumors. *Endocr Pathol* **20:** 85-91.

Ozsolak F, Poling LL, Wang Z, Liu H, Liu XS, Roeder RG *et al* (2008). Chromatin structure analyses identify miRNA promoters. *Genes Dev* **22:** 3172-3183.

Pallante P, Visone R, Ferracin M, Ferraro A, Berlingieri MT, Troncone G *et al* (2006). MicroRNA deregulation in human thyroid papillary carcinomas. *Endocr Relat Cancer* **13:** 497-508.

Ramachandran V, Chen X (2008). Degradation of microRNAs by a family of exoribonucleases in Arabidopsis. *Science* **321:** 1490-1492.

Ricarte-Filho JC, Fuziwara CS, Yamashita AS, Rezende E, da-Silva MJ, Kimura ET (2009). Effects of let-7 microRNA on Cell Growth and Differentiation of Papillary Thyroid Cancer. *Transl Oncol* **2:** 236-241.

Ryan BM, Robles AI, Harris CC (2010). Genetic variation in microRNA networks: the implications for cancer research. *Nat Rev Cancer* **10:** 389-402.

Schwertheim S, Sheu SY, Worm K, Grabellus F, Schmid KW (2009). Analysis of deregulated miRNAs is helpful to distinguish poorly differentiated thyroid carcinoma from papillary thyroid carcinoma. *Horm Metab Res* **41:** 475-481.

van Kouwenhove M, Kedde M, Agami R (2011). MicroRNA regulation by RNA-binding proteins and its implications for cancer. *Nat Rev Cancer* **11:** 644-656.

van Staveren WCG, Solís DW, Delys L, Duprez L, Andry G, Franc B *et al* (2007). Human Thyroid Tumor Cell Lines Derived from Different Tumor Types Present a Common Dedifferentiated Phenotype. *Cancer Res* **67:** 8113-8120.

Visone R, Pallante P, Vecchione A, Cirombella R, Ferracin M, Ferraro A *et al* (2007a). Specific microRNAs are downregulated in human thyroid anaplastic carcinomas. *Oncogene* **26:** 7590-7595.

Visone R, Russo L, Pallante P, De Martino I, Ferraro A, Leone V *et al* (2007b). MicroRNAs (miR)-221 and miR-222, both overexpressed in human thyroid papillary carcinomas, regulate p27Kip1 protein levels and cell cycle. *Endocr Relat Cancer* **14:** 791-798.

Yang E, van Nimwegen E, Zavolan M, Rajewsky N, Schroeder M, Magnasco M *et al* (2003). Decay Rates of Human mRNAs: Correlation With Functional Characteristics and Sequence Attributes. *Genome Res* **13:** 1863-1872.

Yi R, Qin Y, Macara IG, Cullen BR (2003). Exportin-5 mediates the nuclear export of pre-microRNAs and short hairpin RNAs. *Genes Dev* **17:** 3011-3016.

CHAPTER V

Conclusion

1. Final discussion

Global gene expression profiling has been widely applied to the study of cancer and has shown useful for outcome prediction, tumours classification and identification of potential therapeutic targets (Chung *et al.*, 2002; Nevins and Potti, 2007). The expression profiling of different subtypes of thyroid cancer, particularly of the WDTC subtype, has also been extensively analysed (Griffith *et al.*, 2006; Riesco-Eizaguirre and Santisteban, 2007).

The first study assessing the gene expression of ATC was obtained by comparison of 11 ATC-derived cell lines with normal thyroid tissue (Onda *et al.*, 2004). These authors identified 56 downregulated transcripts with diversified functions, and 31 over-expressed transcripts mostly related to cell growth and metabolism. However, only 3 of 15 under-expressed and 9 of 12 over-expressed genes were confirmed to be differentially expressed in primary ATC. Nevertheless, from this work, anonymous genes were selected and characterized. Suppression of "overexpressed in anaplastic thyroid carcinoma 1" (*OEATC1*) (Mizutani *et al.*, 2005) and induced expression of "transmembrane protein 184C" (*TMEM184C*, previously known as *TMEM34*) (Akaishi *et al.*, 2007), in an ATC cell line, was shown to significantly inhibit the cell growth. Moreover, "hemoglobin, beta" (*HBB*) (Onda *et al.*, 2005) and "phosphatidylethanolamine binding protein 1" (*PEBP1*, previously known as *PBP*) (Akaishi *et al.*, 2006) were confirmed to be significantly decreased in ATC relatively to both normal thyroid tissues and PTC, and in accordance, their augmented expression effectively suppressed the cell growth of an ATC cell line. Another study performed cytogenetic and transcriptional analyses of 3 ATC-derived and 2 PDTC-derived cell lines, representing the first report of PDTC cells expression profile (Rodrigues *et al.*, 2007). These 5 cell lines were screened for mutations in Chapter III of the present thesis (Supplementary Table III.4 and III.5). At the chromosomal level, multiple chromosomal imbalances were present in all cell lines, being DNA gains more frequent than losses. Interestingly, genes mapped to the highly amplified regions observed in ATC cell lines were differentially upregulated and were related to centrosome regulation and chromosome segregation. Relatively to normal thyroid, 1079 genes were over-expressed and 3159 were under-expressed in PDTC cell lines, whereas, 1039 genes were over-expressed and 2328 were under-expressed in ATC cell lines. In both types of cell lines, deregulated genes were mainly associated with cell cycle, proliferation and cell adhesion. Moreover, 140 genes mostly related to signal transduction, cell adhesion and motility, were identified as differentially expressed between PDTC and ATC cell lines. Microarray analysis of six cell lines derived

from WDTC and ATC, led to the identification of "ubiquitin-conjugating enzyme E2C" (*UBE2C* or *UBCH10*), that was upregulated 150-fold in all the cell lines tested (Pallante *et al.*, 2005) and "chromobox homolog 7" (*CBX7*), which was one of the most under-expressed genes (Pallante *et al.*, 2008). Accordingly, analysis of primary samples showed that UBE2C, a protein required for the proteolysis of mitotic cyclins by the ubiquitination pathway, was absent in normal thyroid, moderately expressed in WDTC and strongly expressed in PDTC and ATC. Knockdown of UBE2C protein through small interference RNA was able to inhibit the cell growth in 2 cell lines. Regarding the expression of CBX7, a Polycomb protein probably involved in repression of gene transcription, the normal thyroid samples were strongly stained, whereas, expression progressively decreased in WDTC to PDTC and was lost in ATC. In agreement with a tumour suppressor role, transfection with *CBX7* gene significantly inhibited the proliferation of cell lines. In summary, despite the limited validity of transcriptome analysis in cell lines, these studies have suggested that most deregulated pathways in PDTC and ATC are associated with cell proliferation and cell adhesion. In addition, several genes were identified and confirmed to contribute for tumour development.

Few studies have assessed the gene expression in primary PDTC and ATC tumours. A first work assessed the transcriptional profiles of 5 ATC, 10 PTC and 4 normal thyroid samples (Salvatore *et al.*, 2007). This analysis identified 371 upregulated and 543 downregulated genes in ATC, relatively to normal thyroid, and only 114 of these genes were differentially regulated between normal tissues and both types of carcinoma. Authors have focused their attention on 54 significantly over-expressed transcripts in ATC, not deregulated in PTC, that control cell cycle. These genes have been included in molecular signatures associated with proliferation, poor outcome and chromosomal instability in several types of cancer (Tabach *et al.*, 2005; Carter *et al.*, 2006; Whitfield *et al.*, 2006). For two of these genes, "polo-like kinase 1" (*PLK1*) and "TTK protein kinase" (*TTK*), the activity of their promoters was shown to be upregulated in ATC cell lines in comparison to normal rat thyrocytes, and to be negatively controlled by p53/CDKN1A and RB1/E2F pathways. Moreover, *PLK1* depletion in ATC cell lines, but not in normal rat thyrocytes, resulted in inhibition of cell growth and in increased apoptosis due to cytokinesis impairment. Accordingly, treatment of ATC cell lines with BI 2536, a PLK1 inhibitor, impaired their proliferation and viability in soft agar and in mice xenograft (Nappi *et al.*, 2009). More recently, Hébrant and collaborators have compared the expression profile of 11 ATC, 48 PTC and 23 normal thyroid tissues, representing the most complete study of ATC (Hébrant *et al.*,

2012). ATC showed 1051 upregulated and 1113 downregulated genes relatively to normal samples. Moreover, the possible derivation of ATC from pre-developed PTC was supported by this analysis, since 43% of the genes differentially expressed between PTC and normal tissues were similarly deregulated in ATC. Likewise, most deregulated pathways were common to both types of tumours, although more amplified in ATC. Altered molecular functions in ATC included upregulated inflammation, increased TGF-β signalling, the EMT program, increased matrix remodelling, increased proliferation, upregulation of glycolysis and repression of thyroid-associated genes. Montero-Conde and collaborators (Montero-Conde *et al.*, 2008) by comparing 7 ATC and 6 PDTC with 31 WDTC (7 FTC and 24 PTC) found 742 over-expressed and 678 under-expressed transcripts in the group of dedifferentiated tumours (ATC and PDTC). The expression profiles of this sample set was indicative of activation in the MAPK-ERK and TGF-β pathways, in focal adhesion and cell motility, in control of actin cytoskeleton, in cell cycle and in mitotic checkpoint, whereas repression was denoted for thyroid-associated functions. Only one more report performed transcriptional analysis of 7 poorly differentiated primary tumours, although these cases were actually clinically aggressive dedifferentiated PTC cases (Fluge *et al.*, 2006). Upregulation of cell motility, extracellular matrix remodeling and increased cell proliferation were identified as the main features of the less differentiated PTC, in comparison to classic PTC.

The data presented in the chapter II of this thesis represents the first study comparing well-defined PDTC, WDTC and normal thyroid profiles, as well as, the most complete gene expression data for PDTC primary tumours. As expected, the molecular signatures identified in PDTC were indicative of an increased cell proliferation, defective control on cell cycle and chromosome segregation and decreased cell adhesiveness. Moreover, the correlation with the mutational status of the samples allowed to observe that the gene expression profile of *RAS*-mutated PDTC was similar to fvPTC. In accordance, *RAS* oncogene was detected in 18% of the PDTC studied (Table III.3) and, in spite of the unclear definition of PDTC, *RAS* is the main oncogene found in the literature (Table I.1). Consequently, the exclusive detection of *RAS* mutations in WDTC of follicular pattern, *i.e.*, FTC and fvPTC, suggest these tumours as the most likely precursors of PDTC. On the other hand, ATC are more likely derived from pre-existing cPTC, due to the frequent detection of co-existing papillary components and *BRAF* mutations (Table I.1). In the present project (Chapter III), in agreement with Hébrant and collaborators (Hébrant *et al.*, 2012), ATC was shown to be more similar to cPTC, regarding the differentially expressed genes relatively to normal thyroid. Nevertheless, *RAS*

mutations were present in 31% of the profiled ATC and *BRAF* mutation was rarely present (8%). These findings suggest PDTC and ATC may have two different aetiologies from pre-existing tumours: PDTC from fvPTC and ATC from cPTC. Nevertheless, it cannot be excluded that these genes become mutated in PDTC/ATC with a *de novo* origin.

The high proliferative rate of ATC cells is explained by the extensive detection of over-expressed proteins and genes related to proliferation and mitosis functions (Smallridge *et al.*, 2009). Concerning these molecular pathways, both PDTC and ATC have a similar profile, exhibiting increased expression of genes, like *CCNE2*, *CCNB2*, *CKS2*, *TOP2A*, *CENPA*, *CENPK*, *KIAA0101*, *MAD2L1*, *BUB1*, *BUB1B*, *UHRF1* and *CDKN3*. This not only justifies the high proliferative potential but also the chromosomal instability observed in these tumours. *CDKN3* gene represented a particular case. Upregulation relatively to normal thyroid and to WDTC cases was confirmed for both ATC and PDTC. Nevertheless, and in support to the described negative control of the protein over cell cycle, ATC were distinguished from PDTC by the expression of non-functional spliced forms of *CDKN3*. The mutational analysis (Chapter III) suggested that mutations in the cell cycle regulators, *CDKN2A* and *CDKN2B*, could account for the deregulated proliferation, at least in PDTC, and represented the first time that mutations in these genes were reported for PDTC. In addition, *RAS* and *TP53* oncogenic mutations, which are frequently reported in the literature as being present in PDTC and ATC (see Table I.1) and were observed for more than 18% of PDTC and 30% of ATC in the present project (Chapter III), are also known inducers of uncontrolled proliferation.

With the exception of *TP53* and *RAS*, no other recurrent mutations were found for the genes previously described to be altered in ATC, that is *BRAF*, *PIK3CA*, *CTNNB1* and *AXIN1*. Possibly, in a similar way to *BRAF* mutations (that are associated with cases derived from PTC), these genes are altered in specific subtypes of ATC. Discrepancies in mutational analyses could also arise due to differences in the populations studied or, less likely, due to technical issues. The design of a large ATC samples cohort from different laboratories, to overcome the difficulties in establishing large sets from a single institution, would be useful to elucidate this issue.

From the performed mutational analysis, 10 PDTC and 7 ATC were identified, which harboured no mutations in the 13 genes assessed. Since alterations in other genes are probably driving progression in these tumours, these samples are suitable for next-generation sequencing. The use of this method may reveal new driver mutations with relevant roles in

PDTC and ATC. Furthermore, its higher sensitivity allows the detection of tumour subclones, which have important roles in chemoresistance and relapse. It can also be hypothesised that several genes, including those that are mutated at variable frequencies in the literature (*e.g.*, *PIK3CA*, *CTNNB1*, *AXIN1*), are altered and coexist in different subpopulations within the tumours, contributing for intra-tumour heterogeneity and for the high aggressiveness of PDTC and ATC cases.

The deregulated events that appear to be specifically associated with ATC, and not to PDTC, were the loss of epithelial and thyroid-specific functions and the gain of mesenchymal markers, which on the whole establishes the well-known EMT program. Immunohistochemical analysis of ATC has revealed the presence of the mesenchymal marker VIM in 47-90% of ATC (LiVolsi *et al.*, 1987; Venkatesh *et al.*, 1990; Ordonez *et al.*, 1991). In addition, several studies have described that ATC exhibit increased expression of the different transcription factors involved in EMT promotion, twist-related protein 1 (TWIST1) (Salerno *et al.*, 2011), zinc finger E-box-binding homeobox 1 (ZEB1), ZEB2 (Braun *et al.*, 2010) and SNAI2 (Buehler *et al.*, 2013). In the present work (Chapter III), it was confirmed that *SNAI2* gene is specifically over-expressed only in ATC. Several data indicate that this gene presents a crucial role integrating proliferation, apoptosis and differentiation signals (Moreno-Bueno *et al.*, 2006; Peinado *et al.*, 2007) from different players including, most importantly for ATC, RAS, p53 and TGF-β.

Important roles have been found for several miRNA in mediating both p53 and EMT pathways. A critical requirement for epithelial morphology maintenance is expression of miR-200 family members, which repress the mesenchymal factors ZEB1, ZEB2 (Gregory *et al.*, 2008; Park *et al.*, 2008) and SNAI2 (Liu *et al.*, 2013). These miRNA are specifically downregulated upon TGF-β induced EMT, and in several types of tumours (Mongroo and Rustgi, 2010), including ATC (Braun *et al.*, 2010). On the other hand, miR-34 family members, which can be downregulated in some kinds of cancer, have been found to be directly activated and to induce p53 responses (He *et al.*, 2007; Hermeking, 2007). Interestingly, wt and oncogenic forms of p53 have also been found to regulate cell invasion and EMT through several mechanisms (Muller *et al.*, 2011), including the modulation of the miRNA network. For instance, p53 was shown to repress EMT by activating miR-200c (Chang *et al.*, 2011) and miR-34 (Kim *et al.*, 2011; Siemens *et al.*, 2011), whereas mutant p53 forms have been reported to induce miR-155 (Neilsen *et al.*, 2012) involved in TGF-β induced EMT, and to repress miR-133b (Dong *et al.*, 2012), a repressor of ZEB1. Therefore,

miRNA represent crucial molecular players regulating simultaneously different pathways. As such, dynamic expression patterns, which depend on biosynthesis and degradation processes, are required for miRNA functions. On Chapter IV, a first catalogue of human miRNA half-lives obtained in a thyroid cancer cell line cultured under normal conditions, is presented. Further analysis of this data may reveal sequence determinants involved in the turnover differences between different miRNA. Moreover, comparison of these turnover rates with those from normal thyroyctes or from cell lines in specific conditions (*e.g.* TGF-β treated), may reveal that degradation is another level of miRNA regulation and uncover new promising miRNA to be studied.

2. Therapeutic significance

Despite improvement in diagnostic tools, patients are still diagnosed with highly aggressive thyroid carcinomas, that is, PDTC and ATC. The usual treatment modalities include surgery, radiotherapy and chemotherapy (usually, doxorubicin, paclitaxel or docetaxel). However, complete (or even partial) resection is often not possible, and combined radio- or chemo- therapies have shown only limited effects on survival (Sanders *et al.*, 2007; Smallridge *et al.*, 2009; Abate and Smallridge, 2011). So, most of the cases, typically ATC, are refractory to the common clinical management and usually represent a fatal outcome for the patients. There is a special need for new effective molecular therapies and thus, one of the major aims of the present thesis was the identification of new therapeutic targets.

Preclinical and clinical studies have shown some favourable results for the small-molecule agents known as tyrosine kinase inhibitors (erlotinib, gefitinib, vandetanib, sorafenib and imatinib) and monoclonal antibodies (cetuximab and bevacizumab) in different types of cancer, including ATC (Abate and Smallridge, 2011). These inhibitors can affect single or multiple targets, including BRAF, RET, EGFR, VEGFR and VEGFA. The data in the present thesis reasons for the targeting of additional molecules that can be combined with conventional chemotherapy agents.

RAS is a crucial signalling protein, which activates both MAPK-ERK and PI3K-AKT pathways, and was found mutated in a significant fraction of PDTC and ATC. Some developed compounds are known to inhibit RAS functions (Figure V.1). Tipifarnib is the most well-known inhibitor of farnesyltransferases, which are responsible for protein

farnesylation. This posttranslational modification is important for several cancer-related proteins, including RAS (Sebti, 2005). Patients with medullary thyroid carcinoma and PTC had significant responses, when treated with a combination of tipifarnib and the multikinase inhibitor sorafenib (Hong *et al.*, 2009; Hong *et al.*, 2011). Only one patient with ATC and one with PDTC were enrolled. ATC patient showed rapid tumour progression and PDTC patient was taken off treatment. RAS activity also depends on the proper localization at the surface of the cell membrane. Farnesylthiosalicylic acid (Salirasib), which disrupts the oncogenic RAS anchorage and potentiates its degradation (Haklai *et al.*, 1998), has shown effective growth inhibition of several types of tumours, through blockage of both RAS and mTOR signalling (Egozi *et al.*, 1999; Weisz *et al.*, 1999; McMahon *et al.*, 2005; Yue *et al.*, 2005; Charette *et al.*, 2010). In addition, Salirasib increased cell lines sensitivity to chemotherapy and cells with prolonged exposition to the drug (more than 6 months) showed no acquired resistance (Gana-Weisz *et al.*, 2002). Moreover, Salirasib inhibited the *in vitro* proliferation of an ATC cell line and the growth in xenografted mice (Levy *et al.*, 2010) [however ARO cells have been found to be cross-contaminated colon cells (Schweppe *et al.*, 2008)].

The tumour suppressor p53, which is exclusively found deregulated in PDTC and ATC, is another protein with several important roles in tumorigenesis. The majority of mutations affecting p53 are missense mutations located in the DNA-binding domain that disturbs the stability and the folding of the protein (Joerger and Fersht, 2007). Some small molecules have been identified with the capability to reactivate the normal conformation of p53 (Figure V.1). Among these compounds, CP- 31398, PRIMA-1 and MIRA have shown the most promising results (Selivanova, 2010). PRIMA-1 testing in PTC (TPC-1 and BCPAP), FTC (FTC-133) and ATC (SW1736, Hth-74, 8305-C, FF-1 and C-643) cell lines, revealed that it was able to reduce the viability and sensitize p53 mutant cells to chemotherapeutic drugs (Messina *et al.*, 2012). Other molecules, rather than restoring the mutant protein, can be used to target the interaction between wt p53 and the E3 ubiquitin-protein ligase MDM2. Thus, compounds like nutlin-3a and RITA inhibit the proteasomal degradation of p53 and have been reported to induce apoptosis and growth-inhibition. Papillary (SW579), follicular (WRO) and anaplastic (FRO) thyroid cancer cell lines have already been shown to be sensitive to nutlin-3a and a synergistic effect was observed with the proteasome inhibitor bortezomib (Ooi *et al.*, 2009).

The detection of an extensively deregulated expression profile related to cell cycle and proliferation, as well as the identification of *CDKN2A* and *CDKN2B* mutations suggest that agents with inhibitory effect over CDK may be useful for ATC and PDTC treatment (Figure

V.1). Although compounds like flavopiridol, olomoucine and R-roscovitine have shown toxicity and limited efficacy in the clinical trials, combination with cytotoxic drugs have given some promising results. Accordingly, treatment of PTC (NPA), WRO and FRO cell lines with R-roscovitine induced cell cycle arrest and sensitized cells to apoptosis (Festa *et al.*, 2009). Many other new broad-spectrum CDK inhibitors are under investigation and have shown to be effective in animal models and have advanced to clinical trials. Another kind of anticancer drugs being actively developed, repress the aurora kinases and polo-like kinases, which are essential proteins for proper spindle assembly and chromosome segregation during mitosis (Lapenna and Giordano, 2009). Previous results suggest that inhibition of these mitotic proteins have therapeutic benefits.

Finally, the gene expression data of ATC suggests that TGF-β signalling is involved in the EMT process (Figure V.1). Accordingly, TGFBR1 blockage reverted the phenotype of ATC cells, decreased VIM levels and increased *CDH1* (E-cadherin) and miR-200 expressions (Braun *et al.*, 2010). Several agents have been developed that mostly inhibit the receptors binding to TGF-β or the activation of the receptor. Despite the favorable results at pre-clinical levels, some compounds have shown toxicity and limited benefits. Nevertheless, others like Fresolimumab (a monoclonal antibody against TGF-β) have shown encouraging results and are in clinical trials of different types of cancer (Calone and Souchelnytskyi, 2012).

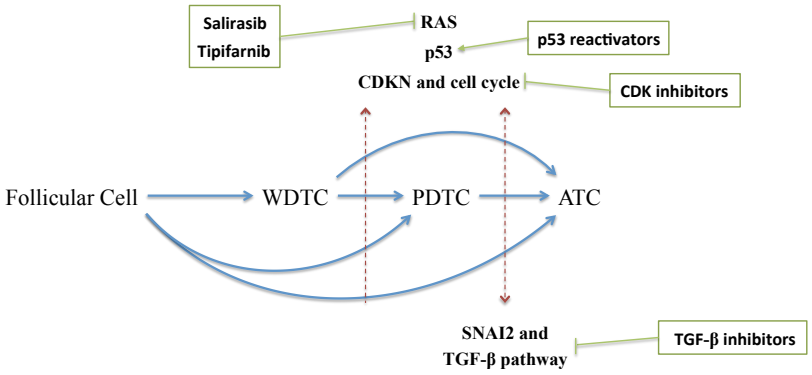

Figure V.1 - Therapeutic approaches available for the identified molecular alterations. According to the genes and pathways found to be deregulated in the progression to poorly differentiated (PDTC) and anaplastic thyroid carcinomas (ATC), different compounds are in development and are being tested as anticancer agents. CDK - cyclin-dependent kinase; WDTC - well-differentiated thyroid carcinoma.

In conclusion, the present project has elucidated the molecular mechanisms involved in the progression of the most aggressive thyroid carcinomas, PDTC and ATC. In addition, we identified several targets that may represent feasible therapeutic approaches for the treatment of these tumours.

3. References

Abate EG, Smallridge RC (2011). Managing anaplastic thyroid carcinoma. *Expert Rev Endocrinol Metab* **6:** 793-809.

Akaishi J, Onda M, Asaka S, Okamoto J, Miyamoto S, Nagahama M *et al* (2006). Growth-suppressive function of phosphatidylethanolamine-binding protein in anaplastic thyroid cancer. *Anticancer Res* **26:** 4437-4442.

Akaishi J, Onda M, Okamoto J, Miyamoto S, Nagahama M, Ito K *et al* (2007). Down-regulation of an inhibitor of cell growth, transmembrane protein 34 (TMEM34), in anaplastic thyroid cancer. *J Cancer Res Clin Oncol* **133:** 213-218.

Braun J, Hoang-Vu C, Dralle H, Huttelmaier S (2010). Downregulation of microRNAs directs the EMT and invasive potential of anaplastic thyroid carcinomas. *Oncogene* **29:** 4237-4244.

Buehler D, Hardin H, Shan W, Montemayor-Garcia C, Rush PS, Asioli S *et al* (2013). Expression of epithelial-mesenchymal transition regulators SNAI2 and TWIST1 in thyroid carcinomas. *Mod Pathol* **26:** 54-61.

Calone I, Souchelnytskyi S (2012). Inhibition of TGFbeta signaling and its implications in anticancer treatments. *Exp Oncol* **34:** 9-16.

Carter SL, Eklund AC, Kohane IS, Harris LN, Szallasi Z (2006). A signature of chromosomal instability inferred from gene expression profiles predicts clinical outcome in multiple human cancers. *Nat Genet* **38:** 1043-1048.

Chang CJ, Chao CH, Xia W, Yang JY, Xiong Y, Li CW *et al* (2011). p53 regulates epithelial-mesenchymal transition and stem cell properties through modulating miRNAs. *Nat Cell Biol* **13:** 317-323.

Charette N, De Saeger C, Lannoy V, Horsmans Y, Leclercq I, Starkel P (2010). Salirasib inhibits the growth of hepatocarcinoma cell lines in vitro and tumor growth in vivo through ras and mTOR inhibition. *Mol Cancer* **9:** 256.

Chung CH, Bernard PS, Perou CM (2002). Molecular portraits and the family tree of cancer. *Nat Genet* **32 Suppl:** 533-540.

Dong P, Karaayvaz M, Jia N, Kaneuchi M, Hamada J, Watari H *et al* (2012). Mutant p53 gain-of-function induces epithelial-mesenchymal transition through modulation of the miR-130b-ZEB1 axis. *Oncogene*.

Egozi Y, Weisz B, Gana-Weisz M, Ben-Baruch G, Kloog Y (1999). Growth inhibition of ras-dependent tumors in nude mice by a potent ras-dislodging antagonist. *Int J Cancer* **80:** 911-918.

Festa M, Petrella A, Alfano S, Parente L (2009). R-roscovitine sensitizes anaplastic thyroid carcinoma cells to TRAIL-induced apoptosis via regulation of IKK/NF-kappaB pathway. *Int J Cancer* **124:** 2728-2736.

Fluge O, Bruland O, Akslen LA, Lillehaug JR, Varhaug JE (2006). Gene expression in poorly differentiated papillary thyroid carcinomas. *Thyroid* **16:** 161-175.

Gana-Weisz M, Halaschek-Wiener J, Jansen B, Elad G, Haklai R, Kloog Y (2002). The Ras inhibitor S-trans,trans-farnesylthiosalicylic acid chemosensitizes human tumor cells without causing resistance. *Clin Cancer Res* **8:** 555-565.

Gregory PA, Bert AG, Paterson EL, Barry SC, Tsykin A, Farshid G *et al* (2008). The miR-200 family and miR-205 regulate epithelial to mesenchymal transition by targeting ZEB1 and SIP1. *Nat Cell Biol* **10:** 593-601.

Griffith OL, Melck A, Jones SJ, Wiseman SM (2006). Meta-analysis and meta-review of thyroid cancer gene expression profiling studies identifies important diagnostic biomarkers. *J Clin Oncol* **24:** 5043-5051.

Haklai R, Weisz MG, Elad G, Paz A, Marciano D, Egozi Y *et al* (1998). Dislodgment and accelerated degradation of Ras. *Biochemistry* **37:** 1306-1314.

He X, He L, Hannon GJ (2007). The guardian's little helper: microRNAs in the p53 tumor suppressor network. *Cancer Res* **67:** 11099-11101.

Hébrant A, Dom G, Dewaele M, Andry G, Tresallet C, Leteurtre E *et al* (2012). mRNA expression in papillary and anaplastic thyroid carcinoma: molecular anatomy of a killing switch. *PLoS One* **7:** e37807.

Hermeking H (2007). p53 enters the microRNA world. *Cancer Cell* **12:** 414-418.

Hong DS, Sebti SM, Newman RA, Blaskovich MA, Ye L, Gagel RF *et al* (2009). Phase I trial of a combination of the multikinase inhibitor sorafenib and the farnesyltransferase inhibitor tipifarnib in advanced malignancies. *Clin Cancer Res* **15:** 7061-7068.

Hong DS, Cabanillas ME, Wheler J, Naing A, Tsimberidou AM, Ye L *et al* (2011). Inhibition of the Ras/Raf/MEK/ERK and RET kinase pathways with the combination of the multikinase inhibitor sorafenib and the farnesyltransferase inhibitor tipifarnib in medullary and differentiated thyroid malignancies. *J Clin Endocrinol Metab* **96:** 997-1005.

Joerger AC, Fersht AR (2007). Structure-function-rescue: the diverse nature of common p53 cancer mutants. *Oncogene* **26:** 2226-2242.

Kim NH, Kim HS, Li XY, Lee I, Choi HS, Kang SE *et al* (2011). A p53/miRNA-34 axis regulates Snail1-dependent cancer cell epithelial-mesenchymal transition. *J Cell Biol* **195:** 417-433.

Lapenna S, Giordano A (2009). Cell cycle kinases as therapeutic targets for cancer. *Nat Rev Drug Discov* **8:** 547-566.

Levy R, Grafi-Cohen M, Kraiem Z, Kloog Y (2010). Galectin-3 promotes chronic activation of K-Ras and differentiation block in malignant thyroid carcinomas. *Mol Cancer Ther* **9:** 2208-2219.

Liu YN, Yin JJ, Abou-Kheir W, Hynes PG, Casey OM, Fang L *et al* (2013). MiR-1 and miR-200 inhibit EMT via Slug-dependent and tumorigenesis via Slug-independent mechanisms. *Oncogene* **32:** 296-306.

LiVolsi VA, Brooks JJ, Arendash-Durand B (1987). Anaplastic thyroid tumors. Immunohistology. *Am J Clin Pathol* **87:** 434-442.

McMahon LP, Yue W, Santen RJ, Lawrence JC, Jr. (2005). Farnesylthiosalicylic acid inhibits mammalian target of rapamycin (mTOR) activity both in cells and in vitro by promoting dissociation of the mTOR-raptor complex. *Mol Endocrinol* **19:** 175-183.

Messina RL, Sanfilippo M, Vella V, Pandini G, Vigneri P, Nicolosi ML *et al* (2012). Reactivation of p53 mutants by prima-1 [corrected] in thyroid cancer cells. *Int J Cancer* **130:** 2259-2270.

Mizutani K, Onda M, Asaka S, Akaishi J, Miyamoto S, Yoshida A *et al* (2005). Overexpressed in anaplastic thyroid carcinoma-1 (OEATC-1) as a novel gene responsible for anaplastic thyroid carcinoma. *Cancer* **103:** 1785-1790.

Mongroo PS, Rustgi AK (2010). The role of the miR-200 family in epithelial-mesenchymal transition. *Cancer Biol Ther* **10:** 219-222.

Montero-Conde C, Martin-Campos JM, Lerma E, Gimenez G, Martinez-Guitarte JL, Combalia N *et al* (2008). Molecular profiling related to poor prognosis in thyroid carcinoma. Combining gene expression data and biological information. *Oncogene* **27:** 1554-1561.

Moreno-Bueno G, Cubillo E, Sarrio D, Peinado H, Rodriguez-Pinilla SM, Villa S *et al* (2006). Genetic profiling of epithelial cells expressing E-cadherin repressors reveals a distinct role for Snail, Slug, and E47 factors in epithelial-mesenchymal transition. *Cancer Res* **66:** 9543-9556.

Muller PA, Vousden KH, Norman JC (2011). p53 and its mutants in tumor cell migration and invasion. *J Cell Biol* **192:** 209-218.

Nappi TC, Salerno P, Zitzelsberger H, Carlomagno F, Salvatore G, Santoro M (2009). Identification of Polo-like kinase 1 as a potential therapeutic target in anaplastic thyroid carcinoma. *Cancer Res* **69:** 1916-1923.

Neilsen PM, Noll JE, Mattiske S, Bracken CP, Gregory PA, Schulz RB *et al* (2012). Mutant p53 drives invasion in breast tumors through up-regulation of miR-155. *Oncogene*.

Nevins JR, Potti A (2007). Mining gene expression profiles: expression signatures as cancer phenotypes. *Nat Rev Genet* **8:** 601-609.

Onda M, Emi M, Yoshida A, Miyamoto S, Akaishi J, Asaka S *et al* (2004). Comprehensive gene expression profiling of anaplastic thyroid cancers with cDNA microarray of 25 344 genes. *Endocr Relat Cancer* **11:** 843-854.

Onda M, Akaishi J, Asaka S, Okamoto J, Miyamoto S, Mizutani K *et al* (2005). Decreased expression of haemoglobin beta (HBB) gene in anaplastic thyroid cancer and recovery of its expression inhibits cell growth. *Br J Cancer* **92:** 2216-2224.

Ooi MG, Hayden PJ, Kotoula V, McMillin DW, Charalambous E, Daskalaki E *et al* (2009). Interactions of the Hdm2/p53 and proteasome pathways may enhance the antitumor activity of bortezomib. *Clin Cancer Res* **15:** 7153-7160.

Ordonez NG, El-Naggar AK, Hickey RC, Samaan NA (1991). Anaplastic thyroid carcinoma. Immunocytochemical study of 32 cases. *Am J Clin Pathol* **96:** 15-24.

Pallante P, Berlingieri MT, Troncone G, Kruhoffer M, Orntoft TF, Viglietto G *et al* (2005). UbcH10 overexpression may represent a marker of anaplastic thyroid carcinomas. *Br J Cancer* **93:** 464-471.

Pallante P, Federico A, Berlingieri MT, Bianco M, Ferraro A, Forzati F *et al* (2008). Loss of the CBX7 gene expression correlates with a highly malignant phenotype in thyroid cancer. *Cancer Res* **68:** 6770-6778.

Park SM, Gaur AB, Lengyel E, Peter ME (2008). The miR-200 family determines the epithelial phenotype of cancer cells by targeting the E-cadherin repressors ZEB1 and ZEB2. *Genes Dev* **22:** 894-907.

Peinado H, Olmeda D, Cano A (2007). Snail, Zeb and bHLH factors in tumour progression: an alliance against the epithelial phenotype? *Nat Rev Cancer* **7:** 415-428.

Riesco-Eizaguirre G, Santisteban P (2007). New insights in thyroid follicular cell biology and its impact in thyroid cancer therapy. *Endocr Relat Cancer* **14:** 957-977.

Rodrigues RF, Roque L, Krug T, Leite V (2007). Poorly differentiated and anaplastic thyroid carcinomas: chromosomal and oligo-array profile of five new cell lines. *Br J Cancer* **96:** 1237-1245.

Salerno P, Garcia-Rostan G, Piccinin S, Bencivenga TC, Di Maro G, Doglioni C *et al* (2011). TWIST1 plays a pleiotropic role in determining the anaplastic thyroid cancer phenotype. *J Clin Endocrinol Metab* **96:** E772-781.

Salvatore G, Nappi TC, Salerno P, Jiang Y, Garbi C, Ugolini C *et al* (2007). A cell proliferation and chromosomal instability signature in anaplastic thyroid carcinoma. *Cancer Res* **67:** 10148-10158.

Sanders EM, Jr., LiVolsi VA, Brierley J, Shin J, Randolph GW (2007). An evidence-based review of poorly differentiated thyroid cancer. *World J Surg* **31:** 934-945.

Schweppe RE, Klopper JP, Korch C, Pugazhenthi U, Benezra M, Knauf JA *et al* (2008). Deoxyribonucleic acid profiling analysis of 40 human thyroid cancer cell lines reveals cross-contamination resulting in cell line redundancy and misidentification. *J Clin Endocrinol Metab* **93:** 4331-4341.

Sebti SM (2005). Protein farnesylation: implications for normal physiology, malignant transformation, and cancer therapy. *Cancer Cell* **7:** 297-300.

Selivanova G (2010). Therapeutic targeting of p53 by small molecules. *Semin Cancer Biol* **20:** 46-56.

Siemens H, Jackstadt R, Hunten S, Kaller M, Menssen A, Gotz U *et al* (2011). miR-34 and SNAIL form a double-negative feedback loop to regulate epithelial-mesenchymal transitions. *Cell Cycle* **10:** 4256-4271.

Smallridge RC, Marlow LA, Copland JA (2009). Anaplastic thyroid cancer: molecular pathogenesis and emerging therapies. *Endocr Relat Cancer* **16:** 17-44.

Tabach Y, Milyavsky M, Shats I, Brosh R, Zuk O, Yitzhaky A *et al* (2005). The promoters of human cell cycle genes integrate signals from two tumor suppressive pathways during cellular transformation. *Mol Syst Biol* **1:** 2005 0022.

Venkatesh YS, Ordonez NG, Schultz PN, Hickey RC, Goepfert H, Samaan NA (1990). Anaplastic carcinoma of the thyroid. A clinicopathologic study of 121 cases. *Cancer* **66:** 321-330.

Weisz B, Giehl K, Gana-Weisz M, Egozi Y, Ben-Baruch G, Marciano D *et al* (1999). A new functional Ras antagonist inhibits human pancreatic tumor growth in nude mice. *Oncogene* **18:** 2579-2588.

Whitfield ML, George LK, Grant GD, Perou CM (2006). Common markers of proliferation. *Nat Rev Cancer* **6:** 99-106.

Yue W, Wang J, Li Y, Fan P, Santen RJ (2005). Farnesylthiosalicylic acid blocks mammalian target of rapamycin signaling in breast cancer cells. *Int J Cancer* **117:** 746-754.

CHAPTER VI

Annexes

1. List of primers

Transcript	Template	Amplified exons	Primer	Sequence (5 '- 3')	Amplicon size
PAX8-PPARG	cDNA	*PAX8* (exon 5) *PPARG* (exon 1)	Forward Reverse	GCCACCAAGTCCCTGAGTCCC CAAAGGAGTGGGAGTGGTCT	Variable
		PAX8 (exon 7) *PPARG* (exon 1)	Forward Reverse	GCATTGACTCACAGAGCAGCA CATTACGGAGAGATCCACGG	Variable
		PAX8 (exon 8) *PPARG* (exon 1)	Forward Reverse	GCTCAACAGCACCCTGGA CATTACGGAGAGATCCACGG	Variable
RET/PTC1	cDNA	*CCDC6* (Exon 1) *RET* (Exon 13)	Forward Reverse	AGATAGAGCTGGAGACCTAC TGCAGGCCCCATACAATTTG	330
RET/PTC2	cDNA	*PRKAR1A* (Exon 7) *RET* (Exon 13)	Forward Reverse	AGGGAGCTTTGGAGAACTTG TGCAGGCCCCATACAATTTG	366
RET/PTC3	cDNA	*NCOA4* (Exon 7) *RET* (Exon 13)	Forward Reverse	CATGCCAGAGCAGAAGTCA TGCAGGCCCCATACAATTTG	404
BRAF	DNA	15	Forward Reverse	AAACTCTTCATAATGCTTGCTCTG GGCCAAAAATTTAATCAGTGGA	231
	cDNA	15	Forward Reverse	GCCAAGTCAATCATCCACAG CATCTGACTGAAAGCTGTATGGA	211
N-RAS	DNA	2	Forward Reverse	GGTTTCCAACAGGTTCTTGC CTCACCTCTATGGTGGGATCA	145
		3	Forward Reverse	CACCCCCAGGATTCTTACAG TGGCAAATACACAGAGGAAGC	148
	cDNA	2-3	Forward Reverse	TGCTGGTGTGAAATGACTGA TCGCCTGTCCTCATGTATTG	239
H-RAS	DNA	1	Forward Reverse	CAGGAGACCCTGTAGGAGGA GGGTCGTATTCGTCCACAA	148
		2	Forward Reverse	GATTCCTACCGGAAGCAGGT ATGGCAAACACACACAGGAA	140
	cDNA	1-2	Forward Reverse	CGGAATATAAGCTGGTGGT ATGGCAAACACACACAGGA	247
K-RAS	DNA	2	Forward Reverse	TTAACCTTATGTGTGACATGTTCTAAT TTGTTGGATCATATTCGTCCAC	175
		3	Forward Reverse	TCAAGTCCTTTGCCCATTTT ATGCATGGCATTAGCAAAGA	376
	cDNA	2-3	Forward Reverse	GCCTGCTGAAAATGACTGAA AAAGAAAGCCCTCCCCAGT	249
TP53	DNA	5	Forward Reverse	GCCGTCTTCCAGTTGCTTTAT GCAATCAGTGAGGAATCAGAGG	331
			Forward Reverse	GCCGTCTTCCAGTTGCTTTAT TCATGTGCTGTGACTGCTTGT	205
			Forward Reverse	CAGCTGTGGGTTGATTCCA GCAATCAGTGAGGAATCAGAGG	205
		6	Forward Reverse	GAGAGACGACAGGGCTGGTT CTGGAGGGCCACTGACAAC	240
		7	Forward Reverse	TGCTTGCCACAGGTCTCC GGTCAGAGGCAAGCAGAGG	236
		8	Forward Reverse	GGAGTAGATGGAGCCTGGTTT AGTGAATCTGAGGCATAACTGC	288
			Forward Reverse	TGCTTCTCTTTTCCTATCCTGA AGTGAATCTGAGGCATAACTGC	226
		9	Forward Reverse	TAAGCAAGCAGGACAAGAAGC CAGTCAAGAAGAAAACGGCATT	240
	cDNA	5-7	Forward Reverse	CATTCTGGGACAGCCAAGTC CCCATGCAGGAACTGTTACAC	389
		6-9	Forward Reverse	TAGTGTGGTGGTGCCCTATG AACATCTCGAAGCGCTCAC	381
PIK3CA	DNA	1	Forward Reverse	AGAATCAGAACAATGCCTCCA TCTTCCCTTTCTGCTTCTTGA	254
			Forward Reverse	AGAATCAGAACAATGCCTCCA TTCTTGCTTCTTTAAATAGTTCATGC	175
			Forward Reverse	GACTTTAGAATGCCTCCGTGA TCTTCCCTTTCTGCTTCTTGA	147
		9	Forward Reverse	TATTGAAAATGTATTTGCTTTTTC ATTTTAGCACTTACCTGTGAC	237

Continued on the next page

Transcript	Template	Amplified exons	Primer	Sequence (5 '- 3')	Amplicon size
PIK3CA	DNA	20	Forward	GCAAAGACCTGAAGGTATTAACAT	205
			Reverse	GGGTCTTTCGAATGTATGCAA	
			Forward	ATGATGCTTGGCTCTGGAAT	273
			Reverse	GGTCTTTGCCTGCTGAGAGT	
			Forward	ATGATGCTTGGCTCTGGAAT	232
			Reverse	TCCAGAGTGAGCTTTCATTTTC	
	cDNA	1	Forward	AGAATCAGAACAATGCCTCCA	254
			Reverse	TCTTCCCTTTCTGCTTCTTGA	
			Forward	GCAAGAAAATACCCCCTCCA	274
			Reverse	GAATATTTCTTCGGAAGTCCTG	
		9	Forward	TGATTGAAGAGCATGCCAAT	288
			Reverse	CCAAGCAATACATCTGGGCTA	
		20	Forward	CGTGTGCCATTTGTTTTGAC	260
			Reverse	TCCAAAGCCTCTTGCTCAGT	
			Forward	ATGATGCTTGGCTCTGGAAT	273
			Reverse	GGTCTTTTGCCTGCTGAGAGT	
CTNNB1	DNA/cDNA	3	Forward	GATTTGATGGAGTTGGACATGG	218
			Reverse	TGTTCTTGAGTGAAGGACTGAG	
AXIN1	DNA	1	Forward	AGATTGATTCACTTTGGAGCTG	241
			Reverse	CACCTTTAATGCCAACACCTT	
			Forward	CGCCAGCTACAGTTTCTGCT	243
			Reverse	GCAAACCAGAAGTCCAGCAA	
			Forward	CGACTTGCTGGACTTCTGGT	217
			Reverse	CTGGTCAAACATGGCAGGAT	
			Forward	CTGATCGATCCTGCCATGTT	236
			Reverse	TCCATGTCCTGGTCACACTTC	
			Forward	GAGGAATGGAAGTGTGACCAG	193
			Reverse	GCTCTCGGAGGTGAGTACAGA	
		2	Forward	CTGTTGGCAGGCTGTCACT	221
			Reverse	TCCGTGAGGGACTGGGTAT	
		3	Forward	CTGAGTTAACGGCTGCCTCT	150
			Reverse	ACCGCAAAGCCGGTACTTA	
		4	Forward	TTAGCCTGTGACCTTTCAACC	242
			Reverse	CAAGAAAACAGCACGACACC	
		5	Forward	AGAGGTGATGGTGCTGCTTG	220
			Reverse	TGTCCTCAGCACACGCTGTA	
			Forward	CACGAGGAGAACCCTGAGAG	230
			Reverse	ACGTGGTGGTGGACGTGT	
			Forward	CTGCACCACCACCGACAC	255
			Reverse	TCCTCACTGACAGGCGCA	
		6	Forward	AGACGAGGAAGGGGCACAG	218
			Reverse	GCCTGCTGATCTCCTTTTCC	
			Forward	CATGCAGTGGATCATTGAGG	158
			Reverse	ACTCGCCACACACACTGAAG	
		7	Forward	GCTGCCCTTGTGAGATGAG	216
			Reverse	ATGGTGGGGTCTTGGATGA	
			Forward	CTCCCACCTCTTCATCCAAG	189
			Reverse	CAGGAGTGGTGCTGTGGTAA	
		8	Forward	CTTTGACGCGGGTTGTTC	204
			Reverse	CTACGATGGGACCTGGCTTG	
		9	Forward	GTACCACCGCTGCATCTCTT	246
			Reverse	GGGCACCCACATACTCGT	
		10	Forward	GGTCATTGCACTGTTCACTGTT	239
			Reverse	TCCTCTCGAACCTCCTCAAA	
			Forward	GAGTTTGACTGTGGGGTGGT	190
			Reverse	GGCTCCTGAGTACGAGGTCA	
CDKN2A	DNA	p14-1	Forward	GCGCGCTCAGGGAAGG	444
			Reverse	GGGCTAGAGACGAATTATCTGTTTACGA	
			Forward	GCGCGCTCAGGGAAGG	196
			Reverse	AATCCGGAGGGTCACCAAG	
			Forward	GCGCAGGTTCTTGGTGAC	200
			Reverse	GGCCTTTCCTACCTGGTCTT	
			Forward	GCCCTCGTGCTGATGCTACT	152
			Reverse	GGGCTAGAGACGAATTATCTGTTTACGA	

Continued on the next page

Transcript	Template	Amplified exons	Primer	Sequence (5 '- 3')	Amplicon size
CDKN2A	DNA	p16-1	Forward	AGGAGCCCAGTCCTCCTTC	488
			Reverse	GGCCTCCGACCGTAACTATT	
			Forward	GGGTCGGGTAGAGGAGGTG	439
			Reverse	TCCCAGCACATCTTACATTTCTT	
			Forward	AGGAGCCCAGTCCTCCTTC	212
			Reverse	ACCCTGTCCCTCAAATCCTC	
			Forward	CCCCTTGCCTGGAAAGATAC	228
			Reverse	GTCAGCCGAAGGCTCCAT	
			Forward	ATGGAGCCTTCGGCTGAC	119
			Reverse	GGCCTCCGACCGTAACTATT	
			Forward	GGGTCGGGTAGAGGAGGTG	181
			Reverse	GAGAATCGAAGCGCTACCTG	
		p14/p16-2	Forward	GTGAGGGGGCTCTACACAAG	468
			Reverse	GCTGAACTTTCTGTGCTGGAA	
			Forward	GTGAGGGGGCTCTACACAAG	213
			Reverse	ACCAGCGTGTCCAGGAAG	
			Forward	GGAGGGCTTCCTGGACAC	170
			Reverse	GGGCATGGTTACTGCCTCT	
			Forward	GACCTGGCTGAGGAGCTG	194
			Reverse	GCTGAACTTTCTGTGCTGGAA	
			Forward	GAGAGGAGGGCGGGATGT	161
			Reverse	TTGTGGCCCTGTAGGACCTT	
			Forward	CCCGATTGAAAGAACCAGAG	187
			Reverse	GGTAGTGGGGGAAGGCATA	
			Forward	ATATGCCTTCCCCCACTACC	150
			Reverse	ACATGAATGTGCGCTTAGGG	
		p16-3	Forward	GCCCATACGCAACGAGATTAG	384
			Reverse	GCTCAAGCGCTCCAGGTC	
		p14/p16-3	Forward	GAGAGGAGGGCGGGATGT	396
			Reverse	ACATGAATGTGCGCTTAGGG	
CDKN2B	DNA	1	Forward	TGGGAAAGAAGGGAAGAGTGT	468
			Reverse	GAGATGGCAGAACAAAAACCA	
			Forward	TGGGAAAGAAGGGAAGAGTGT	218
			Reverse	GAAACGGTTGACTCCGTTG	
			Forward	TAGTGGAGAAGGTGCGACAG	196
			Reverse	CAACGGAGACTCCTGTACAAAT	
		2	Forward	CGGCATCTCCCATACCTG	437
			Reverse	CTTGCAGGCTTACAGGCTTT	
			Forward	CGGCATCTCCCATACCTG	191
			Reverse	ACCAGCGTGTCCAGGAAG	
			Forward	AGACCCTGCCACTCTCACC	173
			Reverse	GCAGGTACCCTGCAACGTC	
			Forward	CTTCCTGGACACGCTGGT	201
			Reverse	GGGTGGGAAATTGGGTAAGA	
CDKN2C	DNA	3	Forward	TCCTTCTGTCAGTCTCCGATG	300
			Reverse	TAGAAACCCGGGTCACGTAG	
		4	Forward	TGCACTTGAAGGATTCTACCAT	452
			Reverse	TAAAGTAGAGGCAACGTGGG	
CDKN1A	DNA	1	Forward	TGCTGCATGATCTGAGTTAGG	239
			Reverse	AAAAGGGCAACCTGATCTCC	
		2	Forward	CGGCCAGGTAACATAGTGTC	309
			Reverse	CGTGGGAAGGTAGAGCTTG	
			Forward	CACCACTGGAGGGTGACTTC	340
			Reverse	CCTTGGACCATGGATTCTGAG	
			Forward	GCGACTGTGATGCGCTAAT	240
			Reverse	CCACATGGTCTTCCTCTGCT	
			Forward	CTGGCACCTCACCTGCTCT	226
			Reverse	CCTTGGACCATGGATTCTGAG	
		3	Forward	CCCCACTGTCTTCCTCAGTT	193
			Reverse	AAGATGTAGAGCGGGCCTTT	
CDKN1B	DNA	1	Forward	CCATTTGATCAGCGGAGACT	459
			Reverse	CACCTCTTGCCACTCGTACTT	
			Forward	CGGTGGACCACGAAGAGTTA	441
			Reverse	AAGGTTAACACCCTCCAG	
		2	Forward	TGACTATGGGGCCAACTTCT	297
			Reverse	ATTTGCCAGCAACCAGTAAGA	

Continued on the next page

Transcript	Template	Amplified exons	Primer	Sequence (5 ' - 3')	Amplicon size
M13 site	DNA	-	Forward	GTAAAACGACGGCCAG	Variable
			Reverse	CAGGAAACAGCTATGAC	
CDKN3	cDNA	1-8	Forward	GAAGGACGAACCAGTGAGCTA	Variable
			Reverse	AACACTGGTGGTTTCATTTCAA	
		2-4	Forward	CCCAGTTCAATACAAACAAGTGA	144
			Reverse	ACAACCTGGAAGAGCACATAAA	
		7-8	Forward	TCACCAGAGCAAGCCATAGA	96
			Reverse	GTCCCGAAACTCATGAAGATAA	
HPRT1	cDNA	6-7	Forward	TGACACTGGCAAAACAATGCA	94
			Reverse	GGTCCTTTTCACCAGCAAGCT	
ACTB	cDNA	1-2	Forward	GCACAGAGCCTCGCCTT	93
			Reverse	GTTGTCGACGACGAGCG	
GAPDH	cDNA	1-3	Forward	ACAGTCAGCCGCATCTTCTT	102
			Reverse	CGCCCAATACGACCAAAT	
MYC	cDNA	1-2	Forward	GCTGCTTAGACGCTGGATTT	88
			Reverse	TCCTGTTGGTGAAGCTAACG	
pri-miR-21	DNA	-	Forward	GTTCGATCTTAACAGGCCAGAAATGCCTGG	302
			Reverse	ACCAGACAGAAGGACCAGAGTTTCTGATTA	
pri-miR-494	DNA	-	Forward	AACCTGGGACACGCAAATAG	416
			Reverse	AGGCCCTTCTCCAAACTCAG	
pri-miR-1280	DNA	-	Forward	GCTCTGTTGATGCCCCTAGA	374
			Reverse	TGTGTGCCCTTTTCTGTCCT	
pre-*GAPDH*	DNA	4-5	Forward	CCCATCACCATCTTCCAGGAGTGAGTGGAAGAC	178
			Reverse	CGCCCCACTTGATTTTGGAGGGATCTCGCCTACCG	
pre-$tRNA^{tyr}$	DNA	-	Forward	CCTTCGATAGCTCAGCTGGTAGAG	109
			Reverse	AAAAAACCGCACTTGTCTCCTTCG	
pre-*45S rRNA*	DNA	-	Forward	CCGTCCGTCCGTCGTCCTCCTCGC	184
			Reverse	TGTACCGGCCGTGCGTACTTAGAC	

2. Supplementary information of Chapter II

Supplementary references

Brentani H, Caballero OL, Camargo AA, da Silva AM, da Silva WA Jr, Dias Neto E *et al.* (2003) The generation and utilization of a cancer-oriented representation of the human transcriptome by using expressed sequence tags. *Proc Natl Acad Sci USA* **100**: 13418-13423.

Burton GR, Guan Y, Nagarajan R, McGehee RE Jr (2002) Microarray analysis of gene expression during early adipocyte differentiation. *Gene* **293**: 21-31.

Chang HY, Sneddon JB, Alizadeh AA, Sood R, West RB, Montgomery K *et al.* (2004) Gene expression signature of fibroblast serum response predicts human cancer progression: similarities between tumors and wounds. *PLoS Biol* **2**: E7. doi:10.1371/journal.pbio.0020007.

Croonquist PA, Linden MA, Zhao F, Van Ness BG (2003) Gene profiling of a myeloma cell line reveals similarities and unique signatures among IL-6 response, N-ras-activating mutations, and coculture with bone marrow stromal cells. *Blood* **102**: 2581-2592.

Goldrath AW, Luckey CJ, Park R, Benoist C, Mathis D (2004) The molecular program induced in T cells undergoing homeostatic proliferation. *Proc Natl Acad Sci USA* **101**: 16885-16890.

Greenbaum S, Lazorchak AS, Zhuang Y (2005) Differential functions for the transcription factor E2A in positive and negative gene regulation in pre-B lymphocytes. *J Biol Chem* **279**: 45028-45035. Erratum in: *J Biol Chem* (2005) **280**:16528.

Kang HC, Kim IJ, Park JH, Shin Y, Ku JL, Jung MS *et al.* (2004) Identification of genes with differential expression in acquired drug-resistant gastric cancer cells using high-density oligonucleotide microarrays. *Clin Cancer Res* **10**: 272-284.

Lee MS, Hanspers K, Barker CS, Korn AP, McCune JM (2004) Gene expression profiles during human CD4+ T cell differentiation. *Int Immunol* **16**: 1109-1124.

Manalo DJ, Rowan A, Lavoie T, Natarajan L, Kelly BD, Ye SQ *et al.* (2005) Transcriptional regulation of vascular endothelial cell responses to hypoxia by HIF-1. *Blood* **105**: 659-669.

Ren B, Cam H, Takahashi Y, Volkert T, Terragni J, Young RA *et al.* (2002) E2F integrates cell cycle progression with DNA repair, replication, and G(2)/M checkpoints. *Genes Dev* **16**: 245-256.

Rhodes DR, Yu J, Shanker K, Deshpande N, Varambally R, Ghosh D *et al.* (2004) Large-scale meta-analysis of cancer microarray data identifies common transcriptional profiles of neoplastic transformation and progression. *Proc Natl Acad Sci USA* **101**: 9309-9314.

Shepard JL, Amatruda JF, Stern HM, Subramanian A, Finkelstein D, Ziai J *et al.* (2005) A zebrafish bmyb mutation causes genome instability and increased cancer susceptibility. *Proc Natl Acad Sci USA* **102**: 13194-13199.

Su AI, Cooke MP, Ching KA, Hakak Y, Walker JR, Wiltshire T *et al.* (2002) Large-scale analysis of the human and mouse transcriptomes. *Proc Natl Acad Sci USA* **99**: 4465-4470.

van't Veer LJ, Dai H, van de Vijver MJ, He YD, Hart AA, Mao M *et al.* (2002) Gene expression profiling predicts clinical outcome of breast cancer. *Nature* **415**: 530-536.

Wu Q, Kirschmeier P, Hockenberry T, Yang TY, Brassard DL, Wang L *et al.* (2002) Transcriptional regulation during p21WAF1/CIP1-induced apoptosis in human ovarian cancer cells. *J Biol Chem* **277**: 36329-36337.

Yu D, Cozma D, Park A, Thomas-Tikhonenko A (2005) Functional validation of genes implicated in lymphomagenesis: an in vivo selection assay using a Myc-induced B-cell tumor. *Ann NY Acad Sci* **1059**: 145-159.

Zhan F, Huang Y, Colla S, Stewart JP, Hanamura I, Gupta S *et al.* (2006) The molecular classification of multiple myeloma. *Blood* **108**: 2020-2028.

Supplementary Table II.1 - Clinical, histological and mutational description of the 24 tumour specimens used in genome-wide expression analysis.

Sample number	Gender/Age[a]	Histology	Mutational analysis	Tumour size (mm)[b]	TNM classification[c]
1	F/14	cPTC	Negative	40	$T_{3m}N_{1b}M_1$
2	F/26	cPTC	Negative[d]	30	$T_3N_0M_0$
3	F/31	cPTC	*BRAF*^{V600E}	20	$T_{1m}N_0M_x$
4	F/35	cPTC	*BRAF*^{V600E}	30	$T_{4a}N_{1b}M_0$
5	F/38	cPTC	*BRAF*^{V600E}	10	$T_1N_0M_0$
6	F/42	cPTC	Negative	37	$T_3N_0M_0$
7	M/64	cPTC	*BRAF*^{V600E}	30	$T_2N_0M_0$
8	F/11	fvPTC	Negative	20	$T_3N_1M_1$
9	F/30	fvPTC	*KRAS*^{G13R}	25	$T_2N_0M_0$
10	F/48	fvPTC	*NRAS*^{Q61R}	50	$T_3N_0M_0$
11	F/55	fvPTC	Negative	20	$T_1N_0M_0$
12	M/28	fvPTC	*NRAS*^{Q61R}	39	$T_2N_0M_0$
13	M/38	fvPTC	Negative	40	$T_2N_0M_x$
14	M/58	fvPTC	*NRAS*^{Q61R}	90	$T_{3m}N_0M_0$
15	M/72	multinodular fvPTC	*PAX8-PPARG*	120	$T_{3m}N_{1b}M_0$
16	F/57	FTC Wi	Negative	35	$T_{4a}N_0M_0$
17	F/64	FTC Mi	*PAX8-PPARG*	35	$T_2N_0M_0$
18	F/77	FTC Wi	Negative	52	$T_4N_0M_1$
19	M/38	FTC Mi	Negative	30	$T_2N_0M_0$
20	F/38	PDTC	Negative	130	$T_4N_0M_1$
21	F/50	PDTC	Negative	33	$T_2N_1M_1$
22	F/72	PDTC	Negative	45	$T_3N_0M_0$
23	M/49	PDTC	*NRAS*^{Q61R}	40	$T_2N_0M_1$
24	M/67	PDTC	*NRAS*^{Q61R}	90	$T_{4am}N_0M_1$

[a]Age at diagnosis; [b]Tumour greatest diameter; [c]World Health Organization classification of thyroid tumours (DeLellis *et al*., 2004); [d]*RET/PTC* fusion gene was later detected using microarray data and confirmed by fluorescence *in situ* hybridisation (FISH). F - female; M - Male; PDTC - poorly differentiated thyroid carcinoma; fvPTC - follicular variant of papillary thyroid carcinoma; cPTC - classic papillary thyroid carcinoma; FTC - follicular thyroid carcinoma; Mi - minimally invasive; Wi - widely invasive.

Supplementary Table II.2 - Main characteristics of differentially under-expressed genes in poorly differentiated tumours *versus* thyroid normal tissues.

Probe set	Gene name in array *HG-U133 Plus 2.0*	Official symbol[a]	Accession number	Biological process[b]	LBFC	*P* value
205382_s_at	D component of complement (adipsin)	*CFD*	NM_001928	Immune response	-10.85	3.99E-03
229839_at	Hypothetical protein MGC45780	*SCARA5*	AI799784	Immune response	-7.40	7.07E-03
209763_at	chordin-like 1	*CHRDL1*	AL049176	Differentiation	-6.08	8.83E-03
206208_at	carbonic anhydrase IV	*CA4*	NM_000717	Bicarbonate transport	-5.96	5.79E-03
203060_s_at	3'-phosphoadenosine 5'-phosphosulfate synthase 2	*PAPSS2*	AF074331	Sulfur metabolism	-5.90	7.40E-05
204872_at	transducin-like enhancer of split 4 (E(sp1) homolog, Drosophila)	*TLE4*	NM_007005	Transcription regulation	-5.64	8.00E-06
203065_s_at	caveolin 1, caveolae protein, 22kDa	*CAV1*	NM_001753	Cell adhesion	-5.38	7.24E-03
205350_at	cellular retinoic acid binding protein 1	*CRABP1*	NM_004378	Retinoic acid metabolism	-5.03	8.79E-04
211276_at	transcription elongation factor A (SII)-like 2	*TCEAL2*	AF063606	Transcription regulation	-5.03	3.25E-03
204955_at	sushi-repeat-containing protein, X-linked	*SRPX*	NM_006307	Cell adhesion	-4.95	8.14E-03
202746_at	integral membrane protein 2A	*ITM2A*	AL021786	-	-4.93	2.10E-05
219643_at	low density lipoprotein-related protein 1B (deleted in tumors)	*LRP1B*	NM_018557	Protein transport and endocytosis	-4.69	8.33E-04
227657_at	ring finger protein 150	*RFN150*	AA722069	-	-4.40	3.87E-03
212713_at	microfibrillar-associated protein 4	*MFAP4*	R72286	Cell adhesion	-4.11	1.90E-04
218901_at	phospholipid scramblase 4	*PLSCR4*	NM_020353	Membrane phospholipid movement	-4.09	8.26E-04
219064_at	inter-alpha (globulin) inhibitor H5	*ITIH5*	NM_030569	Extracellular matrix stabilization	-3.98	2.90E-03
205158_at	ribonuclease, RNase A family, 4	*RNASE4*	NM_002937	mRNA cleavage	-3.87	1.67E-03
200696_s_at	gelsolin (amyloidosis, Finnish type)	*GSN*	NM_000177	Actin cytoskeleton regulation	-3.85	1.21E-03
226932_at	Transcribed locus, strongly similar to NP_005077.2 sarcospan; Kirsten-ras associated gene; K-ras oncogene-associated gene (sarcospan) [Homo sapiens]	-	AW467136	-	-3.63	3.66E-03
209469_at	glycoprotein M6A	*GPM6A*	BF939489	Neural cell growth	-3.60	3.70E-03
226051_at	selenoprotein M	*SELM*	BF973568	Selenium binding	-3.57	1.61E-03
227419_x_at	placenta-specific 9	*PLAC9*	AW964972	-	-3.54	2.57E-04
203571_s_at	chromosome 10 open reading frame 116	*C10ORF116*	NM_006829	-	-3.47	8.69E-04
219778_at	zinc finger protein, multitype 2	*ZFPM2*	NM_012082	Transcription regulation	-3.47	1.80E-03
202409_at	putative insulin-like growth factor II associated protein	*IGF2*	X07868	Development and growth	-3.37	6.96E-03
213451_x_at	tenascin XB	*TNXB*	BE044614	Collagen regulation	-3.34	1.60E-03
204368_at	solute carrier organic anion transporter family, member 2A1	*SLCO2A1*	NM_005630	Lipid and prostanglandin transport	-3.28	1.00E-06

Continued on the next page

Probe set	Gene name in array *HG-U133 Plus 2.0*	Official symbol[a]	Accession number	Biological process[b]	LBFC	*P* value
213800_at	complement factor H	*CFH*	X04697	Regulation of complement activation	-2.31	7.36E-03
211986_at	AHNAK nucleoprotein (desmoyokin)	*AHNAK*	BG287862	Ca^{2+} signaling	-2.30	3.60E-04
224378_x_at	microtubule-associated protein 1 light chain 3 alpha	*MAP1LC3A*	AF276658	Autophagy	-2.30	1.10E-03
228811_at	Transcribed locus, weakly similar to XP_209041.2 PREDICTED: similar to KIAA1503 protein [Homo sapiens]	-	AI493276	-	-2.30	4.22E-04
219929_s_at	zinc finger, FYVE domain containing 21	*ZFYVE21*	NM_024071	-	-2.29	2.64E-03
203729_at	epithelial membrane protein 3	*EMP3*	NM_001425	Inhibition of cell proliferation	-2.24	2.66E-04
217525_at	olfactomedin-like 1	*OLFML1*	AW305097	Cell proliferation	-2.24	1.12E-04
204249_s_at	LIM domain only 2 (rhombotin-like 1)	*LMO2*	NM_005574	Hematopoietic development	-2.20	1.77E-04
206201_s_at	mesenchyme homeo box 2 (growth arrest-specific homeo box)	*MEOX2*	NM_005924	Development	-2.20	2.02E-03
203240_at	Fc fragment of IgG binding protein	*FCGBP*	NM_003890	Cell adhesion	-2.19	3.17E-03
221529_s_at	plasmalemma vesicle associated protein	*PLVAP*	AF326591	Transendothelial transport	-2.19	8.06E-03
229168_at	collagen, type XXIII, alpha 1	*COL23A1*	AI690433	Cell adhesion	-2.19	1.06E-03
203477_at	collagen, type XV, alpha 1	*COL15A1*	NM_001855	Cell adhesion	-2.16	5.95E-04
204606_at	chemokine (C-C motif) ligand 21	*CCL21*	NM_002989	Inflammatory response	-2.16	2.10E-03
217427_s_at	HIR histone cell cycle regulation defective homolog A (S. cerevisiae)	*HIRA*	X75296	Transcription regulation	-2.16	5.68E-04
823_at	chemokine (C-X3-C motif) ligand 1	*CX3CL1*	U84487	Immune response	-2.16	3.50E-04
204802_at	Ras-related associated with diabetes	*RRAD*	NM_004165	small GTPase signal transduction	-2.15	8.51E-03
209699_x_at	aldo-keto reductase family 1, member C2 (dihydrodiol dehydrogenase 2; bile acid binding protein; 3-alpha hydroxysteroid dehydrogenase, type III)	*AKR1C2*	U05598	Prostaglandin and steroid metabolism	-2.15	1.94E-04
218110_at	XPA binding protein 2	*XAB2*	NM_020196	mRNA synthesis and transcription-coupled repair	-2.13	1.33E-03
203131_at	platelet-derived growth factor receptor, alpha polypeptide	*PDGFRA*	NM_006206	Cell proliferation and migration	-2.11	7.95E-03
204316_at	regulator of G-protein signalling 10	*RGS10*	W19676	G proteins activity regulation	-2.07	1.78E-04
213195_at	hypothetical protein LOC201229	*LOC201229*	AI625844	-	-2.07	2.24E-03
201850_at	capping protein (actin filament), gelsolin-like	*CAPG*	NM_001747	Actin cytoskeleton regulation	-2.06	6.42E-04
205413_at	chromosome 11 open reading frame 8	*MPPED2*	NM_001584	Nervous system development	-2.06	1.65E-03
202450_s_at	cathepsin K (pycnodysostosis)	*CTSK*	NM_000396	Proteolysis	-2.05	1.32E-03
208131_s_at	prostaglandin I2 (prostacyclin) synthase	*PTGIS*	NM_000961	Prostaglandin metabolism	-2.05	9.66E-03

Continued on the next page

Probe set	Gene name in array *HG-U133 Plus 2.0*	Official symbol[a]	Accession number	Biological process[b]	LBFC	*P* value
228850_s_at	gb:AI963304 /DB_XREF=gi:5756017 /DB_XREF=wt61d01.x1 /CLONE=IMAGE:2511937 /FEA=EST /CNT=18 /TID=Hs.110373.0 /TIER=Stack /STK=13 /UG=Hs.110373 /UG_TITLE=ESTs	-	AI963304	-	-2.05	5.30E-04
238999_at	Transcribed locus	-	AI610347	-	-2.05	2.90E-03
236359_at	sodium channel, voltage-gated, type IV, beta	*SCN4B*	AW026241	Sodium ion transport	-2.04	9.04E-04
204151_x_at	aldo-keto reductase family 1, member C1 (dihydrodiol dehydrogenase 1; 20-alpha (3-alpha)-hydroxysteroid dehydrogenase)	*AKR1C1*	NM_001353	Xenobiotic and bile acid metabolism	-2.03	3.14E-04
216565_x_at	similar to Interferon-induced transmembrane protein 3 (Interferon-inducible protein 1-8U)	*LOC391020*	AL121994	-	-2.03	5.86E-04
223299_at	SEC11-like 3 (S. cerevisiae)	*SEC11C*	AF212233	Proteolysis	-2.03	3.02E-04
212647_at	related RAS viral (r-ras) oncogene homolog	*RRAS*	NM_006270	Ras signal transduction	-2.02	1.07E-04
40093_at	Lutheran blood group (Auberger b antigen included)	*BCAM*	X83425	Cell adhesion	-2.02	2.55E-03
227716_at	UBX domain containing 5	*UBXN11*	AL577976	Rho GTPase activation	-2.02	3.55E-04
205668_at	lymphocyte antigen 75	*LY75*	NM_002349	Antigen endocytosis	-2.01	4.87E-03
219315_s_at	chromosome 16 open reading frame 30	*TMEM204*	NM_024600	Cell adhesion	-2.01	4.83E-04
235228_at	KIAA1912 protein	*CCDC85A*	AI376433	-	-2.00	1.98E-03

[a]Assigned in *EntrezGene*; [b]Information taken from Online Mendelian Inheritance in Man (OMIM) or from *EntrezGene*; *P* values for difference in mean expression between tumours and normal tissues were calculated using an unpaired *t*-test. LBFC - lower bound of fold change.

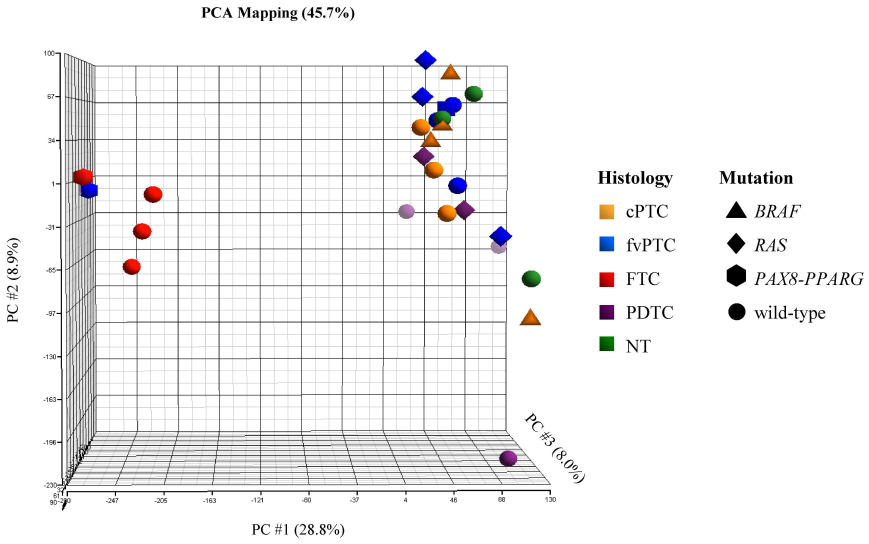

Supplementary Figure II.1 - Three-dimensional representation of gene expression resemblance between samples using the principal components analysis (PCA). In this representation, variation in probe-sets data is represented by the three principal components (PC), thus the distance between samples indicates their gene expression similarity. Numbers in percentage indicate the degree of variability corresponding to each PC. Wild-type label denotes absence of mutations in screened genes. PDTC - poorly differentiated thyroid carcinoma; fvPTC - follicular variant of papillary thyroid carcinoma; cPTC - classic papillary thyroid carcinoma; FTC - follicular thyroid carcinoma; NT - normal thyroid tissues.

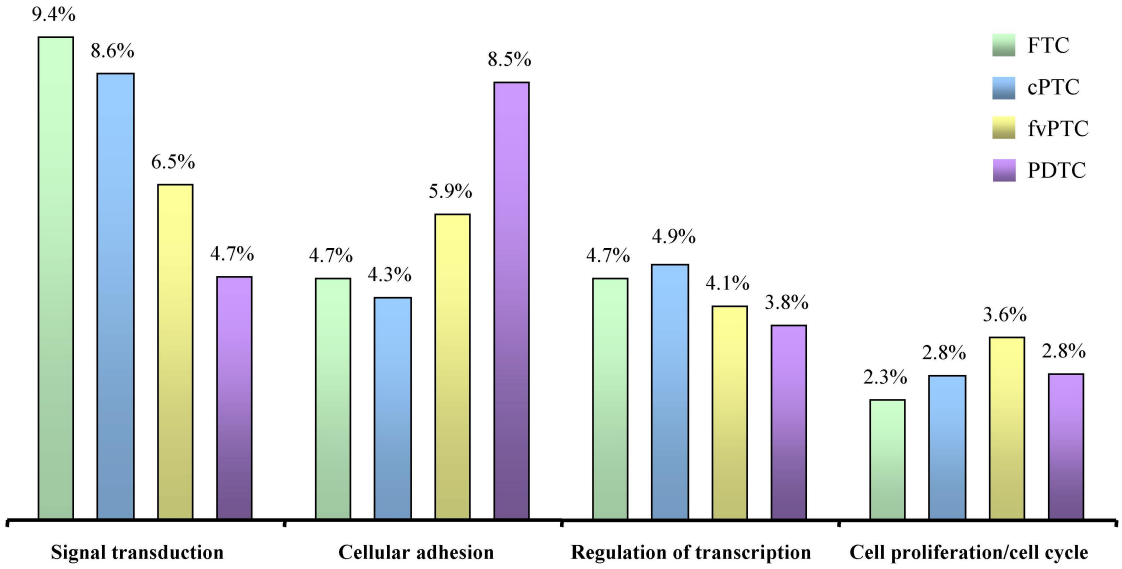

Supplementary Figure II.2 - Representation of the most deregulated biological processes, between each thyroid tumour histotype and normal thyroid tissue. Genes were classified in accordance with their biological role and the four processes represented by more differentially expressed genes, for each histotype, are indicated. Only one probe-set was considered for each gene. PDTC - poorly differentiated thyroid carcinoma; fvPTC - follicular variant of papillary thyroid carcinoma; cPTC - classic papillary thyroid carcinoma; FTC - follicular thyroid carcinoma.

3. Supplementary information of Chapter III

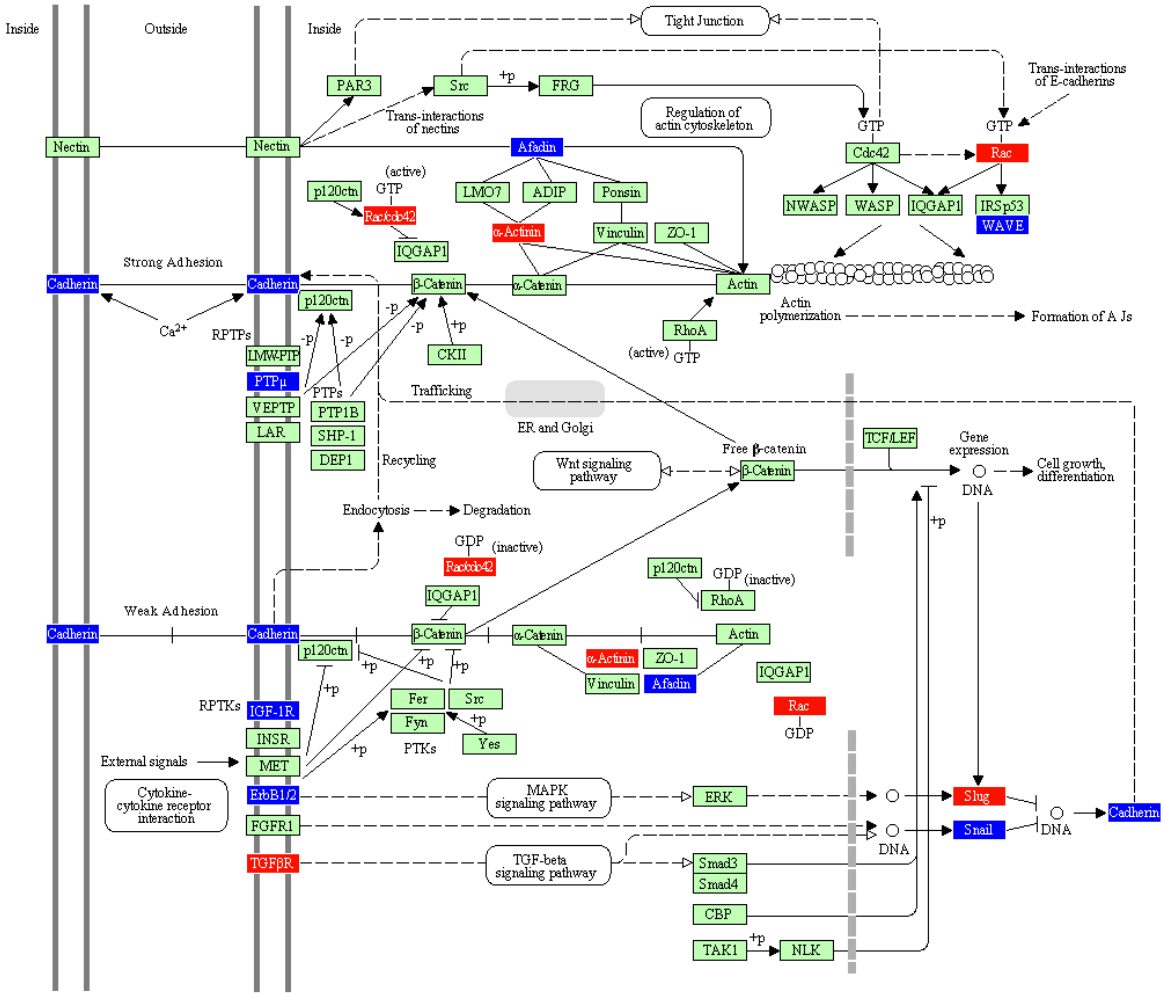

Supplementary Figure III.1 - Schematic representation of pathway impact analysis for adherens junction pathway. Blue indicates under-expressed genes and red indicates over-expressed genes, in anaplastic thyroid carcinoma comparatively to normal thyroid tissue.

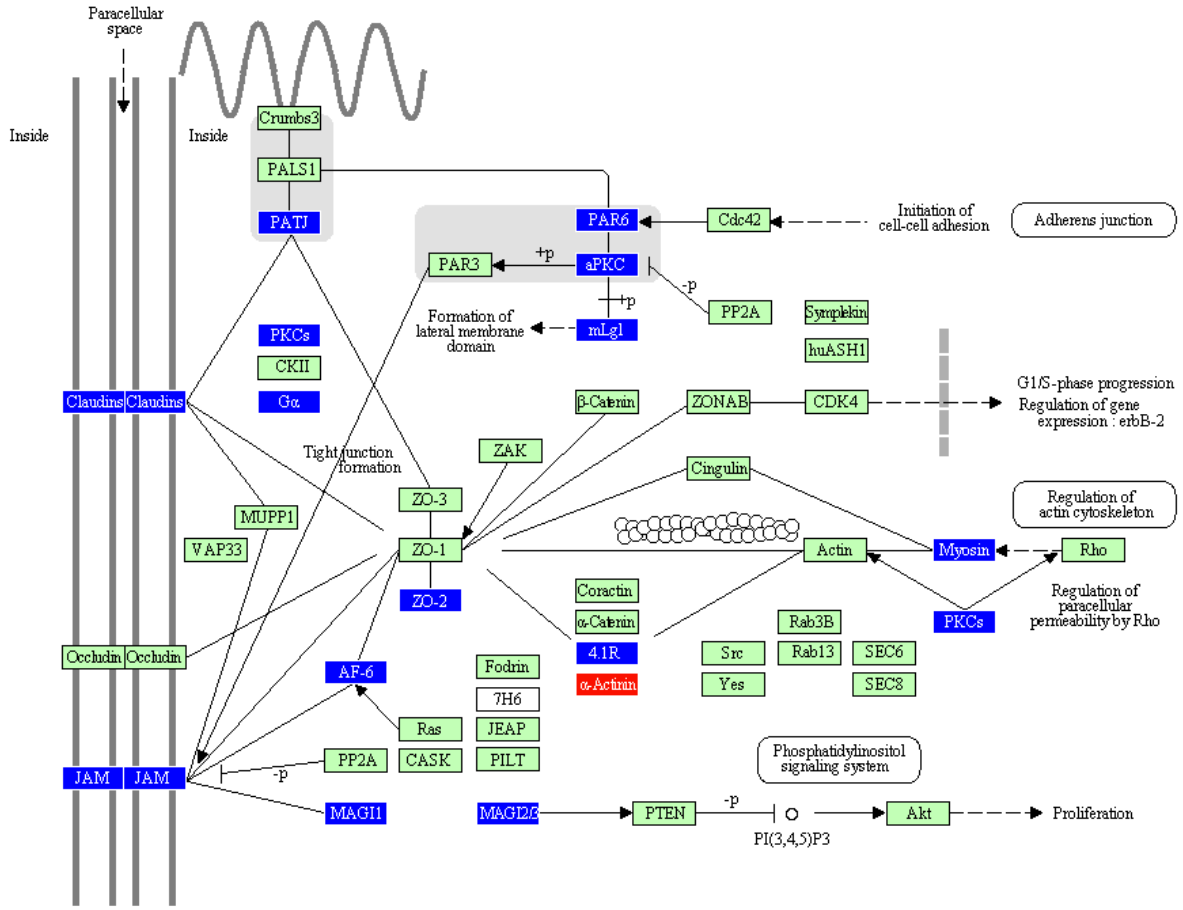

Supplementary Figure III.2 - Schematic representation of pathway impact analysis for tight junction pathway. Blue indicates under-expressed genes and red indicates over-expressed genes, in anaplastic thyroid carcinoma comparatively to normal thyroid tissue.

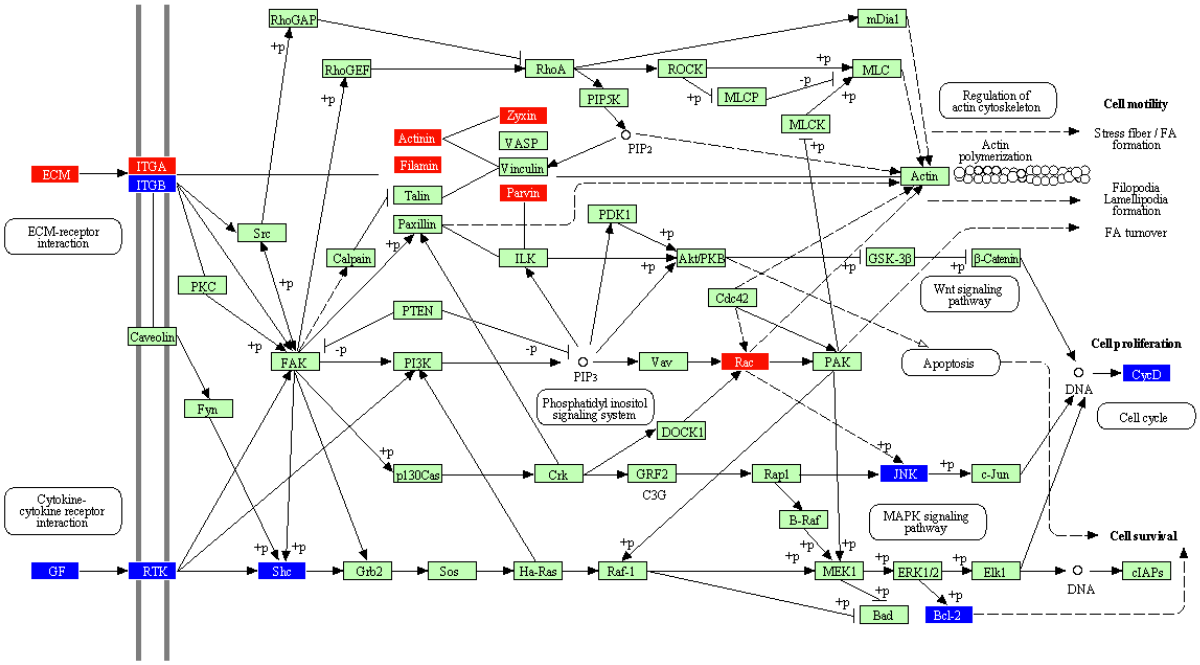

Supplementary Figure III.3 - Schematic representation of pathway impact analysis for focal adhesion. Blue indicates under-expressed genes and red indicates over-expressed genes, in anaplastic thyroid carcinoma comparatively to normal thyroid tissue.

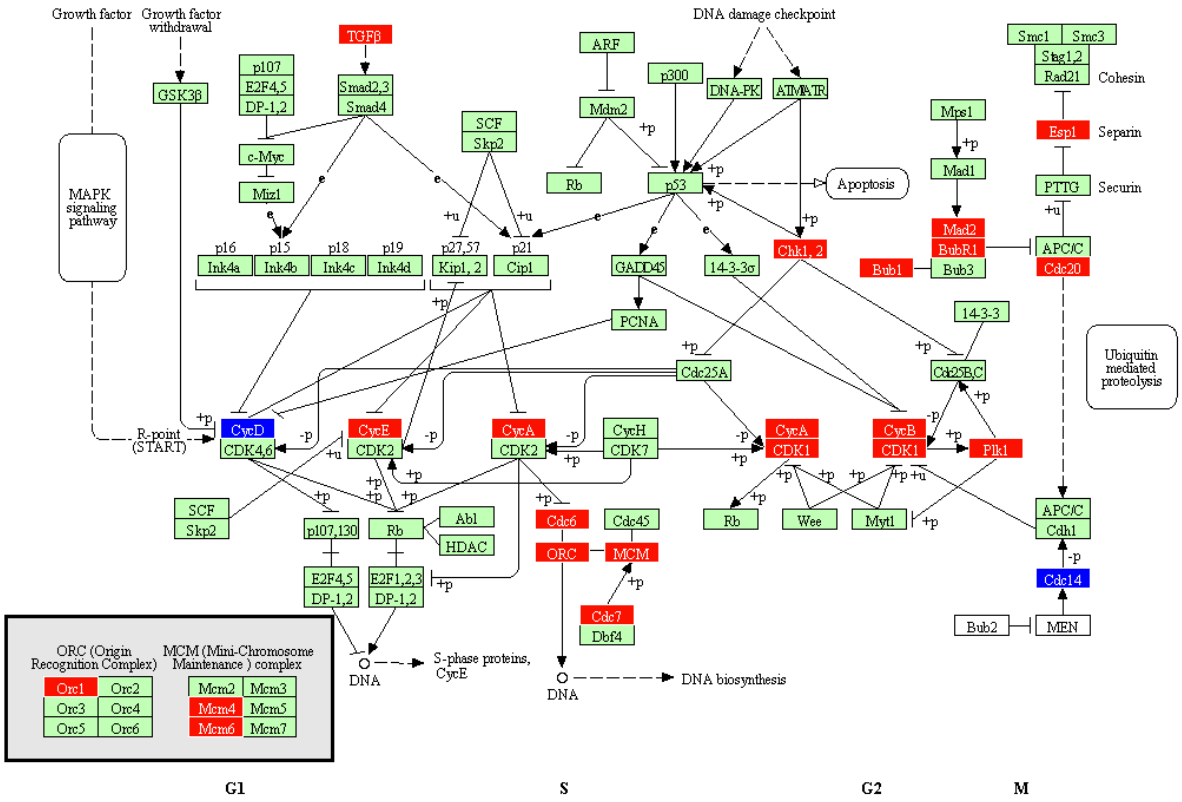

Supplementary Figure III.4 - Schematic representation of pathway impact analysis for cell cycle. Blue indicates under-expressed genes and red indicates over-expressed genes, in anaplastic thyroid carcinoma comparatively to normal thyroid tissue.

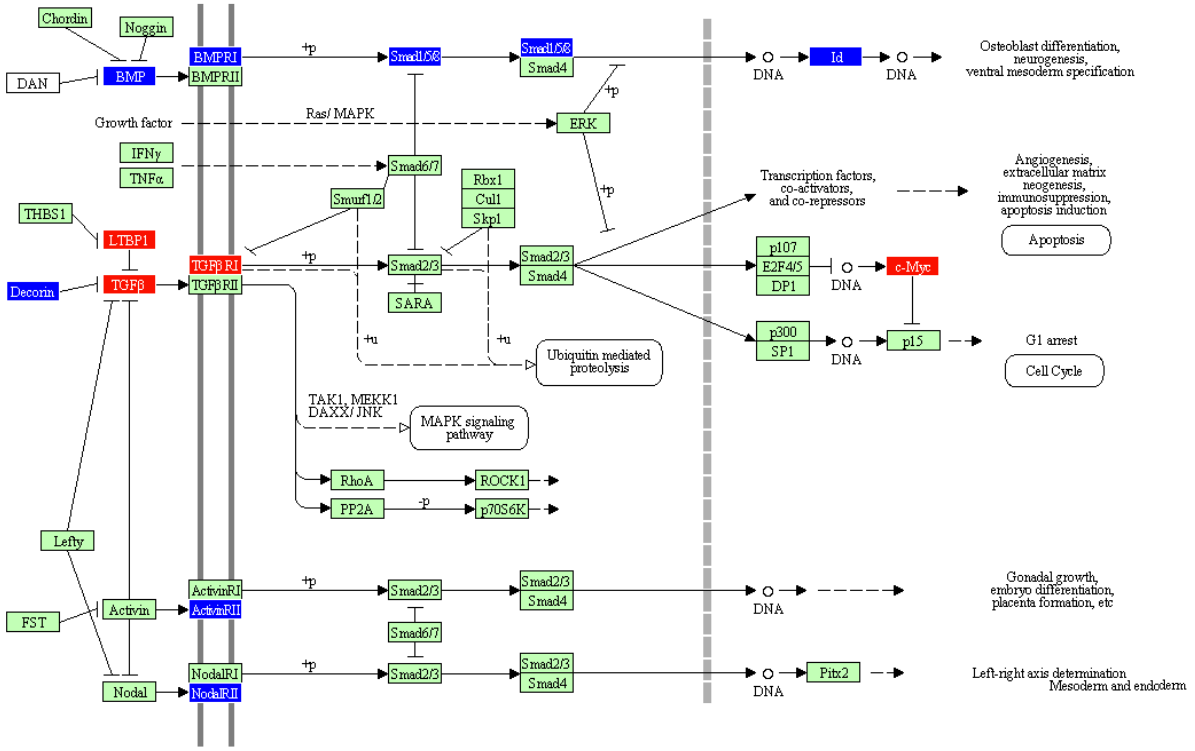

Supplementary Figure III.5 - Schematic representation of pathway impact analysis for transforming growth factor-beta signalling pathway. Blue indicates under-expressed genes and red indicates over-expressed genes, in anaplastic thyroid carcinoma comparatively to normal thyroid tissue.

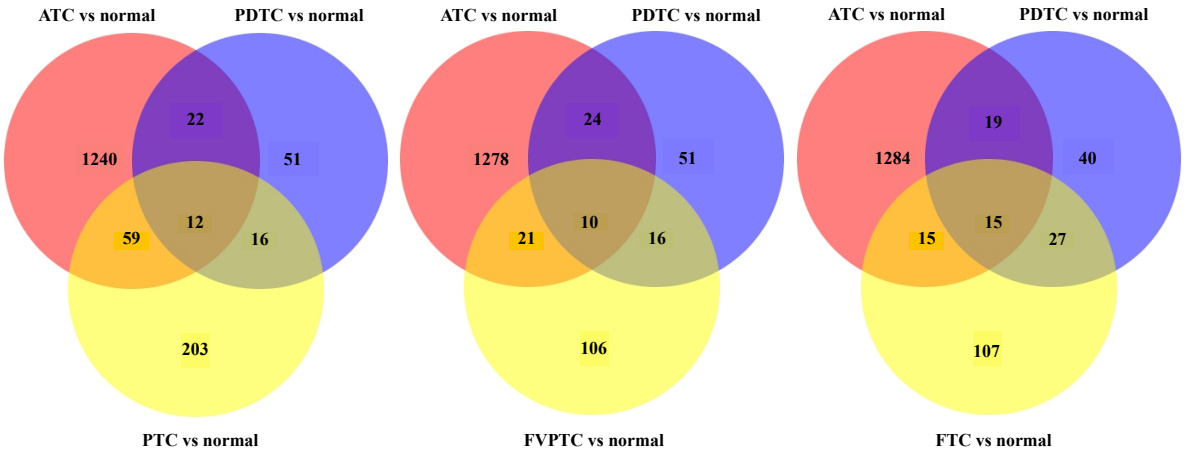

Supplementary Figure III.6 - Venn diagrams representing the common genes between differentially expressed genes in each tumour type versus normal thyroid samples. PTC - classic papillary thyroid carcinoma; fvPTC - follicular variant of papillary thyroid carcinoma; FTC - follicular thyroid carcinoma; PDTC - poorly differentiated thyroid carcinoma; ATC - anaplastic thyroid carcinoma.

Supplementary Table III.1 – Gene Set Enrichment Analysis of genes over-expressed in anaplastic thyroid carcinoma versus normal thyroid samples.

Gene set name[1]	Nominal p-val	FDR q-val	FWER p-val
M_PHASE	0.00	0.00	0.00
MITOSIS	0.00	0.00	0.00
M_PHASE_OF_MITOTIC_CELL_CYCLE	0.00	0.00	0.00
CELL_CYCLE_PHASE	0.00	0.00	0.00
CELL_CYCLE_PROCESS	0.00	0.00	0.00
MITOTIC_CELL_CYCLE	0.00	0.00	0.00
REGULATION_OF_MITOSIS	0.00	0.00	0.00
MITOTIC_CELL_CYCLE_CHECKPOINT	0.00	0.00	0.00
IMMUNE_RESPONSE	0.00	0.00	0.00
CELL_CYCLE_CHECKPOINT_GO_0000075	0.00	0.00	0.00
CHROMOSOME_SEGREGATION	0.00	0.00	0.00
IMMUNE_SYSTEM_PROCESS	0.00	0.00	0.00
CELL_CYCLE_GO_0007049	0.00	0.00	0.00
MITOTIC_SISTER_CHROMATID_SEGREGATION	0.00	1.75×10^{-4}	1.00×10^{-3}
SISTER_CHROMATID_SEGREGATION	0.00	1.63×10^{-4}	1.00×10^{-3}
SPINDLE	0.00	1.53×10^{-4}	1.00×10^{-3}
RIBONUCLEASE_ACTIVITY	0.00	1.44×10^{-4}	1.00×10^{-3}
CELL_DIVISION	0.00	1.36×10^{-4}	1.00×10^{-3}
INTERPHASE	0.00	2.64×10^{-4}	2.00×10^{-3}
ADAPTIVE_IMMUNE_RESPONSE	0.00	2.50×10^{-4}	2.00×10^{-3}

[1]Assigned in Molecular Signatures Database (www.broad.mit.edu/gsea/msigdb/ index.jsp); FDR - false discovery rate; FWER - family wise-error rate.

Supplementary Table III.2 – Gene Set Enrichment Analysis of genes under-expressed in anaplastic thyroid carcinoma versus normal thyroid samples.

Gene set name[1]	Nominal p-val	FDR q-val	FWER p-val
MICROBODY	0.00	$4.85x10^{-2}$	$7.70x10^{-2}$
PEROXISOME	0.00	$3.21x10^{-2}$	0.10
EXCRETION	0.00	0.17	0.57
OXIDOREDUCTASE_ACTIVITY__ACTING_ON_THE_ALDEHYDE_OR_OXO_GROUP_OF_DONORS	$3.12x10^{-3}$	0.17	0.67
TIGHT_JUNCTION	$2.87x10^{-3}$	0.14	0.69
CALCIUM_INDEPENDENT_CELL_CELL_ADHESION	$4.46x10^{-3}$	0.12	0.71
AMINO_ACID_DERIVATIVE_METABOLIC_PROCESS	$4.35x10^{-3}$	0.15	0.83
INTERCELLULAR_JUNCTION	0.00	0.14	0.83
APICOLATERAL_PLASMA_MEMBRANE	$6.82x10^{-3}$	0.13	0.85
APICAL_JUNCTION_COMPLEX	$5.69x10^{-3}$	0.13	0.88
CENTRAL_NERVOUS_SYSTEM_DEVELOPMENT	0.00	0.13	0.89
ELECTRON_TRANSPORT_GO_0006118	$5.33x10^{-3}$	0.12	0.90
OXIDOREDUCTASE_ACTIVITY__ACTING_ON_THE_CH_CH_ GROUP_OF_DONORS	$8.28x10^{-3}$	0.13	0.93
SODIUM_CHANNEL_ACTIVITY	$1.40x10^{-2}$	0.21	0.99

[1]Assigned in Molecular Signatures Database (www.broad.mit.edu/gsea/msigdb/ index.jsp); FDR - false discovery rate; FWER - family wise-error rate.

Supplementary Table III.3 - Alterations identified in the mutational analysis of PDTC and ATC.

Gene	Coding sequence alteration	Predicted protein alteration	Sample[1]	Somatic nature	*In silico* prediction
BRAF **(*n* = 6)**	c.1762C>T	p.Leu588Phe	ATC 23	ND	ND
	c.1792G>A	p.Ala598Thr	PDTC 19	ND	ND
	c.1799T>A	p.Val600Glu	ATC 14; T235; T238[2]	ND	ND
	c.1825C>T	p.Gln609X	PDTC 19	ND	ND
NRAS **(*n* = 11)**	c.181C>A	p.Gln61Lys	ATC 9; 11	ND	ND
	c.182A>G	p.Gln61Arg	PDTC 3; 6; 7; 8 ATC 3; 17; 7; 10; 20	ND	ND
HRAS **(*n* = 2)**	c.37G>C	p.Gly13Arg	C643	ND	ND
	c.182A>G	p.Gln61Arg	ATC 15	ND	ND
TP53 **(*n* = 24)**	c.380C>T	p.Ser127Phe	ATC 1	ND	ND
	c.404G>A	p.Cys135Tyr	ATC 7	ND	ND
	c.422G>A	p.Cys141Tyr	PDTC 22	ND	ND
	c.451C>T	p.Pro151Ser	ATC 18	ND	ND
	c.515T>A	p.Val172Asp	PDTC 22	ND	ND
	c.524G>A	p.Arg175His	PDTC 20 ATC 5	ND	ND
	c.548C>G	p.Ser183X	ATC 24 T238[2]	ND	ND
	c.583A>T	p.Ile195Phe	ATC 8	ND	ND
	c.620A>G	p.Asp207Gly	PDTC 20	ND	ND
	c.641A>G	p.His214Arg	ATC 25	ND	ND
	c.658T>A	p.Tyr220Asn	PDTC 19	ND	ND
	c.733G>C	p.Gly245Arg	ATC 8	ND	ND
	c.737T>C	p.Met246Thr	ATC 23	ND	ND

Continued on the next page

Gene	Coding sequence alteration	Predicted protein alteration	Sample[1]	Somatic nature	*In silico* prediction
TP53 **(*n* = 24)**	c.742C>T	p.Arg248Trp	PDTC 16	ND	ND
	c.743G>A	p.Arg248Gln	PDTC 5 ATC 21 C643	ND	ND
	c.817C>T	p.Arg273Cys	ATC 2; 4	ND	ND
	c.868C>T	p.Arg290Cys	PDTC 16	ND	ND
	c.873_888del	p.Lys291Asn fs*49	PDTC 1	ND	ND
	c.877G>A	p.Gly293Arg	PDTC 19	ND	ND
PIK3CA **(*n* = 7)**	c.1624G>A	p.Glu542Lys	ATC 14 T238[2]	ND	ND
	c.169C>T	p.Pro57Ser	PDTC 18	Yes	Pathogenic
	c.253G>A	p.Glu85Lys	PDTC 19	Yes	Pathogenic
	c.3032C>T	p.Pro1011Leu	PDTC 16	Yes	Pathogenic
	c.3100G>T	p.Glu1034X	PDTC 19	Yes	Pathogenic
	c.3171G>A	p.Trp1057X	PDTC 18	Yes	Pathogenic
CTNNB1 **(*n* = 1)**	c.163G>A	p.Glu55Lys	PDTC 19	ND	ND
CDKN2A **(*n* = 6)**	Homozygous gene deletion	No translation	C643[3]	ND	ND
	c.3G>A	p.Met1Ile ($p14^{ARF}$)	ATC 3	NA	Pathogenic
	c.159G>A	p.Met53Ile ($p16^{INK4A}$) p.Asp109Asn ($p14^{ARF}$)	PDTC 19	Yes	Pathogenic
	c.188T>G	p.Leu63Arg ($p16^{INK4A}$)	T238[2]	Yes	Pathogenic
	c.436G>A	p.Asp146Asn ($p16^{INK4A}$)	PDTC 18	Yes	Benign
	c.445G>A	p.Glu149Lys ($p16^{INK4A}$)	PDTC 16	Yes	Benign
CDKN2B **(*n* = 5)**	Homozygous gene deletion	No translation	C643	ND	ND
	c.24G>A	p.Met8Ile	PDTC 16	Yes	Benign
	c.62C>T	p.Ala21Val	PDTC 15	NA	Pathogenic
	c.109G>A	p.Gly37Ser	PDTC 22	Yes	Pathogenic
	c.386C>T	p.Ala129Val	PDTC 19	Yes	Benign
CDKN2C **(*n* = 1)**	c.295_297del	p.Glu99del	ATC 21	NA	Pathogenic
AXIN1 **(*n* = 3)**	c.188G>T	p.Arg63Leu	ATC 15	Germ-line	Pathogenic
	c.769G>A	p.Asp257Asn	ATC 10	Germ-line	Benign
	c.1046G>A	p.Arg349His	PDTC 12	Germ-line	Benign

[1]Sample identification according to Supplementary Tables III.4, III.5 and III.7; ND - not done due to proven oncogenic role of the mutation; NA - patient normal tissue not available; [2]mutations identified in T238 cell line were also present in tumour formalin-fixed paraffin embedded, from which the cell line was derived, but were absent in corresponding normal tissue; [3]previously identified (Schagdarsurengin *et al*., 2006); PDTC - poorly differentiated thyroid carcinoma; ATC - anaplastic thyroid carcinoma.

Supplementary reference

Schagdarsurengin U, Gimm O, Dralle H, Hoang-Vu C, Dammann R. (2006) CpG island methylation of tumor-related promoters occurs preferentially in undifferentiated carcinoma. *Thyroid* **16:** 633-642.

Supplementary Table III.4 – Mutational results for the 22 PDTC and 2 PDTC-derived cell lines.

Histotype	Sample	*BRAF*	*NRAS*	*TP53*	*PIK3CA*	*CTNNB1*	*CDKN2A*	*CDKN2B*
PDTC	**3**	NEG	**POS**	NEG	NEG	NEG	NEG	NEG
	6	NEG	**POS**	NEG	NEG	NEG	NEG	NEG
	7	NEG	**POS**	NEG	NEG	NEG	NEG	NEG
	8	NEG	**POS**	NEG	NEG	NEG	NEG	NEG
	1	NEG	NEG	**POS**	NEG	NEG	NEG	NEG
	5	NEG	NEG	**POS**	NEG	NEG	NEG	NEG
	15	NEG	NEG	NEG	NEG	NEG	NEG	**POS**
	20	NEG	NEG	**POS**	NEG	NEG	NEG	NEG
	22	NEG	NEG	**POS**	NEG	NEG	NEG	**POS**
	18	NEG	NEG	NEG	**POS**	NEG	**POS** ($p16^{INK4A}$)	NEG
	16	NEG	NEG	**POS**	**POS**	NEG	**POS** ($p16^{INK4A}$)	**POS**
	19	**POS**	NEG	**POS**	**POS**	**POS**	**POS** ($p14^{ARF}$/ $p16^{INK4A}$)	**POS**
	9	NEG	NEG	NEG	NEG	NEG	NEG	NEG
	10	NEG	NEG	NEG	NEG	NEG	NEG	NEG
	11	NEG	NEG	NEG	NEG	NEG	NEG	NEG
	12	NEG	NEG	NEG	NEG	NEG	NEG	NEG
	13	NEG	NEG	NEG	NEG	NEG	ND	ND
	14	NEG	NEG	NEG	NEG	NEG	ND	ND
	17	NEG	NEG	NEG	NEG	NEG	NEG	NEG
	21	NEG	NEG	NEG	NEG	NEG	NEG	NEG
	2	NEG	NEG	NEG	NEG	NEG	NEG	NEG
	4	NEG	NEG	NEG	NEG	NEG	NEG	NEG
Cell lines	**T243**	NEG	NEG	NEG	NEG	NEG	NEG	NEG
	T351	NEG	NEG	NEG	NEG	NEG	NEG	NEG

Genes with no detected alterations are not represented (*K-*, *HRAS*, *CDKN2C*, *CDKN1A*, *CDKN1B* and *AXIN1*); Samples identification according to Supplementary Table III.7. NEG - no mutation detected; POS - mutation detected; ND - mutational analysis not done; PDTC - poorly differentiated thyroid carcinoma.

Supplementary Table III.5 – Mutational and expressional results for the 26 ATC samples and 4 ATC-derived cell lines.

Histotype	Sample	*BRAF*	*NRAS*	*HRAS*	*TP53*	*PIK3CA*	*CDKN2A*	*CDKN2B*	*CDKN2C*	*AXIN1*	*SNAI2*[1]
ATC	**10**	NEG	**POS**	NEG	NEG	NEG	NEG	NEG	NEG	NEG	NEG
	20	NEG	**POS**	NEG	NEG	NEG	NEG	NEG	NEG	NEG	NEG
	17	NEG	**POS**	NEG	NEG	NEG	ND	ND	ND	ND	ND
	9	NEG	**POS**	NEG	NEG	NEG	NEG	NEG	NEG	NEG	**POS**
	11	NEG	**POS**	NEG	NEG	NEG	NEG	NEG	NEG	NEG	**POS**
	15	NEG	NEG	**POS**	NEG	NEG	NEG	NEG	NEG	**POS**	**POS**
	4	NEG	NEG	NEG	**POS**	NEG	NEG	NEG	NEG	NEG	NEG
	5	NEG	NEG	NEG	**POS**	NEG	NEG	NEG	NEG	NEG	NEG
	18	NEG	NEG	NEG	**POS**	NEG	ND	ND	ND	ND	NEG
	23	**POS**	NEG	NEG	**POS**	NEG	NEG	ND[2]	ND	ND	ND
	24	NEG	NEG	NEG	**POS**	NEG	NEG	NEG	ND	ND	ND
	25	NEG	NEG	NEG	**POS**	NEG	NEG	NEG	ND	ND	ND
	1	NEG	NEG	NEG	**POS**	NEG	NEG	NEG	NEG	NEG	**POS**
	2	NEG	NEG	NEG	**POS**	NEG	NEG	NEG	NEG	NEG	**POS**
	8	NEG	NEG	NEG	**POS**	NEG	NEG	NEG	NEG	NEG	**POS**
	14	**POS**	NEG	NEG	NEG	**POS**	NEG	NEG	NEG	NEG	NEG
	7	NEG	**POS**	NEG	**POS**	NEG	NEG	NEG	NEG	NEG	**POS**
	3	NEG	**POS**	NEG	NEG	NEG	**POS** ($p14^{ARF}$)	NEG	NEG	NEG	NEG
	21	NEG	NEG	NEG	**POS**	NEG	NEG	NEG	**POS**	NEG	NEG
	13	NEG	NEG	NEG	NEG	NEG	NEG	NEG	NEG	NEG	**POS**
	6	NEG	NEG	NEG	NEG	NEG	NEG	NEG	NEG	NEG	NEG
	12	NEG	NEG	NEG	NEG	NEG	NEG	NEG	NEG	NEG	NEG
	26	NEG	NEG	NEG	NEG	NEG	NEG	NEG	ND	ND	ND
	22	NEG	NEG	NEG	NEG	NEG	NEG	ND[2]	ND	ND	ND
	16	NEG	NEG	NEG	NEG	NEG	ND	ND	ND	ND	ND
	19	NEG	NEG	NEG	NEG	NEG	ND	ND	ND	ND	ND
Cell lines	**T235**	**POS**	NEG	NEG	NEG	NEG	NEG	NEG	NEG	NEG	NEG
	T238	**POS**	NEG	NEG	**POS**	**POS**	**POS** ($p16^{INK4A}$)	NEG	NEG	NEG	NEG
	C643	NEG	NEG	**POS**	**POS**	NEG	**POS**	**POS**	NEG	NEG	**POS**
	T241	NEG	NEG	NEG	NEG	NEG	NEG	NEG	NEG	NEG	NEG

Genes with no detected alterations are not represented (*KRAS*, *CTNNB1*, *CDKN1A* and *CDKN1B*). Samples identification according to Supplementary Table III.7; [1]POS - *SNAI2* expression higher than 3-fold relatively to calibrator; [2]Samples could not be totally assessed. NEG - no mutation detected; POS - mutation detected; ND - mutational analysis not done; ATC - anaplastic thyroid carcinoma.

Supplementary Table III.6 – Correlation of PDTC and ATC with clinical-pathological aspects.

	PDTC	ATC
Gender		
Female	68% (15/22)	81% (21/26)
Male	32% (7/22)	19% (5/26)
		0.3408[1]
Age at diagnosis (years) average ± SD	55.18 ± 16.97 (*n* = 22)	69.96 ± 8.53 (*n* = 26)
		0.0009[2]
Tumour size (cm) average ± SD	6.13 ± 4.12 (*n* = 20)	7.24 ± 2.68 (*n* = 8)
		0.4105[2]
Lymph node metastasis		
Present	63% (10/16)	78% (11/14)
Absent	37% (6/16)	21% (3/14)
		0.4397[1]
Distant metastasis		
Present	78% (13/17)	79% (19/24)
Absent	22% (4/17)	21% (5/24)
		1.0000[1]
Median survival (months)	66 (*n* = 22)	3 (*n* = 25)
		0.0001[3]

[1]*P* value calculated with Fisher's exact test; [2]*P* value calculated by t-test with Welch's correction; [3]*P* value calculated with Logrank test; SD - standard deviation; PDTC - poorly differentiated thyroid carcinoma; ATC - anaplastic thyroid carcinoma.

Supplementary Table III.7 – Clinical-pathological aspects of PDTC and ATC patients.

Sample nº	Sample type	Gender	Age at diagnosis[1]	Tumour size (cm)[2]	TNM stage[3]	Distant metastasis sites	Follow-up time (months)[4]	Observations
PDTC 1	Fresh-frozen	F	44	8	T4	Soft tissues, lungs	8	70% ATC
PDTC 2	Fresh-frozen	F	75	4	T4	-	12	10% ATC
PDTC 3	Fresh-frozen	M	67	9	T4	Lungs	123	Insular pattern
PDTC 4	Fresh-frozen	M	58	15	T4	Lungs	35	Multifocal tumour
PDTC 5	Fresh-frozen	F	38	13	T4	Lungs, bones	2	
PDTC 6	Fresh-frozen	M	49	4	T2	Lungs, bones	108	
PDTC 7	Fresh-frozen	F	49	n.a.	n.a.	Lungs	66	
PDTC 8	Fresh-frozen	F	73	2	T1	Bones, brain	82	
PDTC 9	Fresh-frozen	F	72	4.5	T3	Bones	12	Multifocal tumour
PDTC 10	Fresh-frozen	M	36	1.4	T1	Lungs	> 93	
PDTC 11	Fresh-frozen	F	50	3.3	T2	-	100	
PDTC 12	Fresh-frozen	F	10	2.5	T2	-	43	
PDTC 13	FNAB	F	75	6	T3	Lungs, bones	66	
PDTC 14	FNAB	M	62	n.a.	n.a.	n.e.	1	ATC areas
PDTC 15	FFPE	F	56	9	T4	Lungs	> 84	
PDTC 16	FFPE	M	74	2.5	T4	n.e.	> 84	
PDTC 17	FFPE	M	42	6	T4	n.e.	< 1	Sarcomatoid pattern
PDTC 18	FFPE	F	35	4	T4	-	> 207	10% PTC
PDTC 19	FFPE	F	69	10	T4	Lungs, bones	80	
PDTC 20	FFPE	F	45	2.8	T2	Lungs, bones, CNS	> 144	
PDTC 21	FFPE	F	67	2.5	T3	n.e.	48	
PDTC 22	FFPE	F	68	> 13	T4	n.e.	1	

Continued on the next page

Sample nº	Sample type	Gender	Age at diagnosis[1]	Tumour size (cm)[2]	TNM stage[3]	Distant metastasis sites	Follow-up time (months)[4]	Observations
ATC 1	Fresh-frozen	F	66	9	T4	Lungs, bones	6	
ATC 2	Fresh-frozen	F	77	11	T4	n.e.	3	
ATC 3	Fresh-frozen	F	62	n.a.	T4	Lungs	< 1	
ATC 4	Fresh-frozen	F	66	8	T4	Lungs, soft tissues	8	
ATC 5	Fresh-frozen	F	70	n.a.	T4	Lungs	3	
ATC 6	Fresh-frozen	M	76	5	T4	Lungs	7	
ATC 7	Fresh-frozen	M	75	n.a.	T4	Lungs	2	
ATC 8	Fresh-frozen	M	67	n.a.	T4	Bones	8	Squamous differentiation
ATC 9	Fresh-frozen	F	68	n.a.	T4	Lungs, abdomen	< 1	Giant cells
ATC 10	Fresh-frozen	F	68	n.a.	T4	Lungs, CNS, pleural cavity	6	
ATC 11	Fresh-frozen	F	70	n.a.	T4	Lungs	1	
ATC 12	Fresh-frozen	M	58	2.9	T4	Lungs	8	
ATC 13	Fresh-frozen	M	68	8	T4	Lungs	3	PTC areas
ATC 14	Fresh-frozen	F	91	n.a.	T4	n.e.	1	
ATC 15	Fresh-frozen	F	76	n.a.	n.a.	Lungs	3	
ATC 16	FNAB	F	58	n.a.	T4	Brain	5	
ATC 17	FNAB	F	58	n.a.	T4	Lungs	1	
ATC 18	FNAB	F	58	n.a.	T4	-	16	
ATC 19	FNAB	F	75	n.a.	T4	Lungs, left adrenal gland	2	
ATC 20	FNAB	F	78	n.a.	T4	Lungs, bones	< 1	
ATC 21	FNAB	F	80	n.a.	T4	-	1	
ATC 22	FFPE	F	80	n.a.	T4	-	n.d.	
ATC 23	FFPE	F	56	n.a.	T4	Lungs	3	
ATC 24	FFPE	F	75	5	T4	-	< 1	
ATC 25	FFPE	F	68	9	T4	Lungs	7	
ATC 26	FFPE	F	75	n.a.	T4	-	91	

[1]in years; [2]greatest diameter; [3]according to DeLellis *et al*., 2004; [4]from the date of presentation to the date of death or last follow-up; FNAB - fine-needle aspiration biopsy; FFPE - formalin-fixed paraffin embedded; F - female; M - male; n.a. - not available; n.e. - not evaluated; CNS - central nervous system; PDTC - poorly differentiated thyroid carcinoma; ATC - anaplastic thyroid carcinoma; PTC - papillary thyroid carcinoma.

4. Supplementary information of Chapter IV

Supplementary Table IV.1 - Half-lives for the 249 miRNA detected in BCPAP cell line.

miRNA Identification (from Exiqon)	Half-life (hours)	Standard deviation
hsa-miR-208a/mmu-miR-208a/rno-miR-208	21.54	3.66
hsa-miR-107	22.24	4.04
hsa-miR-193b	24.07	1.40
hsa-miR-125a-5p/mmu-miR-125a-5p/rno-miR-125a-5p	27.93	4.80
hsa-miR-184/mmu-miR-184/rno-miR-184	28.37	3.24
hsa-miR-34c-5p	30.06	5.98
hsa-miR-215	30.11	4.90
hsa-miR-23b	31.39	4.22
hsa-miR-155	32.03	7.11
hsa-miR-183/mmu-miR-183/rno-miR-183	32.13	6.16
hsa-miR-551a	32.34	3.42
hsa-miR-377/mmu-miR-377/rno-miR-377	32.63	4.01
hsa-miR-182/mmu-miR-182/rno-miR-182	33.21	7.42
hsa-miR-222/mmu-miR-222/rno-miR-222	33.22	5.03
hsa-miR-519e*	33.23	6.74
hsa-miR-183*/mmu-miR-183*	33.24	1.38
hsa-miR-206/mmu-miR-206/rno-miR-206	33.71	4.74
hsa-miR-518a-5p/hsa-miR-527	33.97	6.73
hsa-miR-382/mmu-miR-382/rno-miR-382	34.21	5.16
hsa-miR-335/mmu-miR-335-5p/rno-miR-335	34.60	4.41
hsa-miR-130b/mmu-miR-130b/rno-miR-130b	34.76	5.63
hsa-miR-302c*	35.23	5.29
hsa-miR-422a	35.36	7.71
hsa-miR-487b/mmu-miR-487b/rno-miR-487b	35.75	8.04
hsa-miR-516b	35.80	4.15
hsa-miR-106b/mmu-miR-106b/rno-miR-106b	35.89	6.52
hsa-miR-365/mmu-miR-365/rno-miR-365	36.63	6.16
hsa-miR-519d	36.83	4.83
hsa-miR-432	37.18	5.17
hsa-miR-616*	37.33	5.09
hsa-miR-875-3p	37.40	2.93
hsa-miR-7/mmu-miR-7a/rno-miR-7a	38.26	10.15
hsa-miR-574-3p	38.80	4.20
hsa-miR-99b/mmu-miR-99b/rno-miR-99b	39.06	5.39
hsa-miR-542-3p/mmu-miR-542-3p/rno-miR-542-3p	39.79	9.28
hsa-let-7c*	39.87	3.92
hsa-miR-93/mmu-miR-93/rno-miR-93	40.04	4.57
hsa-miR-214/mmu-miR-214/rno-miR-214	40.21	10.11
hsa-miR-583	40.32	6.04
hsa-miR-500	40.61	8.35
hsa-miR-195/mmu-miR-195/rno-miR-195	40.91	6.15
hsa-miR-553	41.54	3.54
hsa-miR-491-5p/mmu-miR-491	41.55	10.49
hsa-miR-223/mmu-miR-223/rno-miR-223	41.75	8.38
hsa-miR-518e*/hsa-miR-519a*/hsa-miR-519b-5p/ hsa-miR-519c-5p/hsa-miR-522*/hsa-miR-523*	42.32	7.50

Continued on the next page

miRNA Identification (from Exiqon)	Half-life (hours)	Standard deviation
hsa-miR-637	42.49	12.33
hsa-miR-642	42.63	15.93
hsa-miR-575	42.70	8.77
hsa-miR-425*/mmu-miR-425*	42.71	7.89
hsa-miR-381/mmu-miR-381/rno-miR-381	42.74	6.93
hsa-miR-891a	43.17	5.36
hsa-miR-525-5p	43.35	10.13
hsa-miR-200c*/mmu-miR-200c*	43.46	8.63
hsa-let-7b/mmu-let-7b/rno-let-7b	43.87	7.24
hsa-miR-520d-5p	43.96	22.01
hsa-miR-520a-5p	44.19	8.94
hsa-miR-877/mmu-miR-877/rno-miR-877	44.32	8.08
hsa-miR-890	44.35	8.20
hsa-miR-132*	44.38	5.89
hsa-miR-657	44.57	8.49
hsa-miR-491-3p	44.59	10.57
hsa-miR-934	44.90	9.57
hsa-miR-585	44.96	14.09
hsa-miR-20b*	44.99	10.77
hsa-let-7c/mmu-let-7c/rno-let-7c	44.99	17.49
hsa-miR-340	45.00	6.74
hsa-miR-337-5p	45.44	5.73
hsa-let-7a	45.48	7.33
hsa-miR-576-5p	45.57	6.10
hsa-miR-145*/mmu-miR-145*	45.94	9.49
hsa-miR-487a	46.23	8.58
hsa-miR-129-5p/mmu-miR-129-5p/rno-miR-129	46.31	5.06
hsa-miR-361-5p/mmu-miR-361/rno-miR-361	46.53	10.96
hsa-miR-518b	46.74	7.78
hsa-miR-140-3p/mmu-miR-140*/rno-miR-140*	46.74	10.79
hsa-miR-300	47.23	6.81
hsa-miR-452	47.50	11.45
hsa-miR-361-3p	47.62	3.49
hsa-miR-498	47.74	9.97
hsa-miR-622	48.03	11.95
hsa-miR-149*	48.14	5.58
hsa-miR-601	48.17	8.72
hsa-miR-765	48.24	8.37
hsa-let-7d*/mmu-let-7d*/rno-let-7d*	48.25	12.23
hsa-miR-30b/mmu-miR-30b/rno-miR-30b-5p	48.34	8.48
hsa-miR-671-3p/mmu-miR-671-3p/rno-miR-671	48.35	7.89
hsa-miR-513a-5p	48.40	8.76
hsa-miR-886-5p	48.62	9.55
hsa-miR-933	48.63	6.96
hsa-miR-635	49.09	18.38
hsa-miR-589	49.20	7.26
hsa-miR-142-5p/mmu-miR-142-5p/rno-miR-142-5p	49.22	9.02
hsa-miR-625	49.45	17.47
hsa-miR-185*	49.61	7.88
hsa-miR-552	49.65	11.38

Continued on the next page

miRNA Identification (from Exiqon)	Half-life (hours)	Standard deviation
hsa-miR-629*	49.97	9.11
hsa-miR-600	50.05	13.26
hsa-miR-198	50.06	9.89
hsa-miR-296-3p/mmu-miR-296-3p/rno-miR-296	50.09	9.48
hsa-miR-922	50.16	6.88
hsa-miR-629	50.30	7.92
hsa-miR-99b*/mmu-miR-99b*/rno-miR-99b*	50.33	8.24
hsa-miR-636	50.71	1.77
hsa-miR-630	51.12	10.59
hsa-miR-342-5p/mmu-miR-342-5p/rno-miR-342-5p	51.28	8.10
hsa-miR-122*	51.72	4.70
hsa-miR-32*	52.16	11.62
hsa-miR-490-3p/mmu-miR-490	52.28	5.80
hsa-miR-200b*/mmu-miR-200b*	52.70	9.82
hsa-miR-523	52.86	12.02
hsa-miR-766	53.30	12.52
hsa-miR-146b-3p	53.39	11.55
hsa-miR-302e	53.78	9.67
hsa-miR-486-5p	53.92	21.31
hsa-miR-602	54.46	13.46
hsa-miR-125b-1*/mmu-miR-125b-3p/rno-miR-125b-3p	54.79	21.58
hsa-miR-34a/mmu-miR-34a/rno-miR-34a	55.06	13.23
hsa-miR-24-1*/mmu-miR-24-1*/rno-miR-24-1*	55.06	13.32
hsa-miR-510	55.18	20.52
hsa-miR-938	55.32	4.45
hsa-miR-509-3-5p	55.37	18.07
hsa-miR-617	55.61	13.32
hsa-miR-937	55.74	15.30
hsa-miR-196a*/mmu-miR-196a*/rno-miR-196a*	56.09	14.70
hsa-miR-940	56.10	11.90
hsa-miR-221*	56.58	12.97
hsa-miR-887	56.80	9.30
hsa-miR-939	56.82	16.06
hsa-miR-181a-2*	56.87	21.58
hsa-miR-494/mmu-miR-494/rno-miR-494	57.00	15.29
hsa-miR-1290	57.15	0.64
hsa-miR-331-3p/mmu-miR-331-3p/rno-miR-331	57.36	6.89
hsa-miR-634	57.41	13.75
hsa-miR-139-3p/mmu-miR-139-3p/rno-miR-139-3p	57.62	16.39
hsa-miR-212/mmu-miR-212/rno-miR-212	58.07	14.34
hsa-miR-9*	58.20	11.79
hsa-miR-605	58.22	17.79
hsa-miR-576-3p	58.43	12.97
hsa-miR-412/mmu-miR-412/rno-miR-412	59.31	4.64
hsa-miR-767-5p	59.79	14.52
hsa-miR-374b*	60.15	11.60
hsa-miR-129*	60.37	18.45
hsa-miR-625*	60.44	14.20
hsa-miR-647	61.08	15.34
hsa-miR-1908	61.46	15.33

Continued on the next page

miRNA Identification (from Exiqon)	Half-life (hours)	Standard deviation
hsa-miR-22*/mmu-miR-22*/rno-miR-22*	61.69	13.57
hsa-miR-505*	61.72	18.79
hsa-miR-557	61.78	12.26
hsa-miR-220b	62.63	4.98
hsa-miR-620	62.72	12.52
hsa-miR-516a-5p	63.04	20.93
hsa-miR-483-5p	63.14	18.39
hsa-miR-208b/mmu-miR-208b	63.22	20.82
hsa-miR-34b/mmu-miR-34b-3p	63.29	16.21
hsa-miR-508-5p	63.48	15.28
hsa-miR-1255b	63.64	9.55
hsa-miR-668/mmu-miR-668	64.21	16.85
hsa-miR-220c	64.22	19.36
hsa-miR-337-3p	64.22	12.67
hsa-miR-30c/mmu-miR-30c/rno-miR-30c	64.51	3.79
hsa-miR-519a	64.84	11.33
hsa-miR-675*	66.23	9.72
hsa-miR-34c-3p	66.50	18.82
hsa-miR-542-5p/mmu-miR-542-5p/rno-miR-542-5p	66.60	11.80
hsa-miR-532-3p/mmu-miR-532-3p/rno-miR-532-3p	66.84	18.98
hsa-miR-518d-5p/hsa-miR-520c-5p/hsa-miR-526a	66.84	9.24
hsa-miR-330-5p/mmu-miR-330/rno-miR-330	67.36	10.31
hsa-miR-302b*	67.59	22.45
hsa-miR-874/mmu-miR-874/rno-miR-874	68.47	13.93
hsa-miR-720/mmu-miR-720	68.64	19.53
hsa-miR-675	69.14	19.26
hsa-miR-296-5p/mmu-miR-296-5p/rno-miR-296*	69.29	22.36
hsa-miR-520c-3p	69.33	22.60
hsa-miR-423-3p/mmu-miR-423-3p/rno-miR-423	70.65	22.84
hsa-miR-1274b	70.89	1.35
hsa-miR-551b*	71.00	18.44
hsa-miR-30d/mmu-miR-30d/rno-miR-30d	71.00	36.08
hsa-miR-671-5p/mmu-miR-671-5p	71.04	23.81
hsa-miR-125b-2*/rno-miR-125b*	71.47	15.13
hsa-miR-488	72.06	25.42
hsa-miR-597	72.47	16.96
hsa-let-7b*/mmu-let-7b*/rno-let-7b*	72.70	22.34
hsa-miR-138-1*/mmu-miR-138*/rno-miR-138*	72.89	16.28
hsa-miR-1253	74.18	14.81
hsa-miR-195*	74.22	27.17
hsa-miR-377*	74.25	16.02
hsa-miR-1273	74.65	9.38
hsa-miR-185/mmu-miR-185/rno-miR-185	74.73	14.59
hsa-miR-187*	74.83	24.32
hsa-miR-520g	75.88	23.20
hsa-miR-340*/mmu-miR-340-3p/rno-miR-340-3p	76.00	19.40
hsa-miR-513a-3p	76.08	13.86
hsa-miR-665	76.23	26.15
hsa-miR-25*	76.38	15.58
hsa-let-7a-2*	77.18	29.39

Continued on the next page

miRNA Identification (from Exiqon)	Half-life (hours)	Standard deviation
hsa-miR-549	77.24	23.01
hsa-miR-920	77.50	15.99
hsa-miR-943	77.65	22.53
hsa-miR-423-5p/mmu-miR-423-5p	77.97	28.47
hsa-miR-664	77.98	6.16
hsa-miR-150/mmu-miR-150/rno-miR-150	78.28	24.00
hsa-miR-193b*	78.41	15.48
hsa-miR-509-5p	79.17	15.87
hsa-miR-888*	79.33	23.69
hsa-miR-298	79.56	14.85
hsa-miR-628-3p	80.02	18.30
hsa-miR-659	80.97	21.74
hsa-miR-7-2*	81.67	18.54
hsa-miR-551b/mmu-miR-551b/rno-miR-551b	82.32	21.73
hsa-miR-638	82.64	26.99
hsa-miR-1300	82.75	11.74
hsa-miR-1274a/mmu-miR-1274a	84.10	17.40
hsa-miR-1272	84.35	13.37
hsa-miR-550	84.94	24.58
hsa-miR-1285	86.09	20.63
hsa-miR-130b*/mmu-miR-130b*	86.83	33.24
hsa-miR-323-3p/mmu-miR-323-3p/rno-miR-323	87.82	26.26
hsa-let-7e/mmu-let-7e/rno-let-7e	90.02	10.81
hsa-miR-424	90.28	27.08
hsa-miR-1255a	90.48	17.62
hsa-miR-1284	91.39	21.58
hsa-miR-886-3p	91.45	36.91
hsa-miR-1286	93.67	25.96
hsa-miR-1184	96.89	32.55
hsa-miR-1226	97.29	29.31
hsa-miR-1267	97.61	13.29
hsa-miR-1261	98.11	33.92
hsa-miR-1280	98.54	12.28
hsa-miR-548e	99.98	13.68
hsa-miR-1258	100.68	39.56
hsa-miR-1287	100.94	20.99
hsa-miR-921	101.22	18.24
hsa-miR-1227	101.61	3.53
hsa-miR-197/mmu-miR-197	102.60	49.17
hsa-miR-1236	103.04	18.82
hsa-miR-1264	105.12	15.81
hsa-miR-1246	105.33	22.19
hsa-miR-1827	105.62	0.40
hsa-miR-1304	106.54	25.23
hsa-miR-1265	106.55	9.67
hsa-miR-1826	106.60	3.34
hsa-miR-1275	106.72	22.86
hsa-miR-513b	113.35	11.38
hsa-miR-1260	116.74	21.44
hsa-let-7f/mmu-let-7f/rno-let-7f	119.46	43.70

Continued on the next page

miRNA Identification (from Exiqon)	Half-life (hours)	Standard deviation
hsa-miR-1308	120.93	24.00
hsa-miR-1299	127.16	25.29
hsa-miR-1321	136.24	20.88
hsa-miR-320d	197.53	13.17

Supplementary File III.1

List of 6 differentially expressed genes between ATC and normal thyroid tissues, also common to all thyroid tumours versus normal thyroid tissues

Affymetrix gene-level probe set	Gene symbol	Gene name	Accession number	Lower bound of fold change	*P* value
7985159	CRABP1	cellular retinoic acid binding protein 1	NM_004378	-24.95	6.92E-03
7947274	MPPED2	metallophosphoesterase domain containing 2	NM_001584	-17.52	0.00E+00
7938225	OLFML1	olfactomedin-like 1	NM_198474	-5.20	4.07E-03
8160889	CCL21	chemokine (C-C motif) ligand 21	NM_002989	-3.76	4.90E-05
8013341	MFAP4	microfibrillar-associated protein 4	NM_002404	-2.16	4.95E-03
8149966	SCARA5	scavenger receptor class A, member 5 (putative)	NM_173833	-2.07	1.17E-03

List of 71 differentially expressed genes between ATC and normal thyroid tissues, also common to cPTC versus normal thyroid tissues

Affymetrix gene-level probe set	Gene symbol	Gene name	Accession number	Lower bound of fold change	*P* value
8147273	SLC26A7	solute carrier family 26, member 7	NM_052832	-50.83	5.83E-03
7961580	LMO3	LIM domain only 3 (rhombotin-like 2)	NM_018640	-38.66	3.50E-05
7985159	CRABP1	cellular retinoic acid binding protein 1	NM_004378	-24.95	6.92E-03
7999291	C16orf89	chromosome 16 open reading frame 89	NM_152459	-21.94	3.42E-04
8135436	SLC26A4	solute carrier family 26, member 4	NM_000441	-18.14	1.50E-05
7947274	MPPED2	metallophosphoesterase domain containing 2	NM_001584	-17.52	0.00E+00
7980485	DIO2	deiodinase, iodothyronine, type II	NM_013989	-15.94	2.44E-03
7936734	FGFR2	fibroblast growth factor receptor 2	NM_000141	-15.27	1.41E-03
7942332	FOLR1	folate receptor 1 (adult)	NM_016730	-14.74	2.80E-03
8150419	ZMAT4	zinc finger, matrin type 4	NM_024645	-13.16	2.61E-03
8095110	KIT	v-kit Hardy-Zuckerman 4 feline sarcoma viral oncogene homolog	NM_000222	-12.38	1.40E-03
7923578	FMOD	fibromodulin	NM_002023	-11.36	2.00E-06
7909866	MOSC2	MOCO sulphurase C-terminal domain containing 2	NM_017898	-9.30	2.99E-04
8152512	TNFRSF11B	tumor necrosis factor receptor superfamily, member 11b	NM_002546	-9.19	5.27E-04
8095585	SLC4A4	solute carrier family 4, sodium bicarbonate cotransporter, member 4	NM_001098484	-9.12	1.90E-05
7956271	HSD17B6	hydroxysteroid (17-beta) dehydrogenase 6 homolog (mouse)	NM_003725	-8.94	8.91E-04
8149574	CSGALNACT1	chondroitin sulfate N-acetylgalactosaminyltransferase 1	NM_018371	-7.33	1.40E-05
8089851	HGD	homogentisate 1,2-dioxygenase (homogentisate oxidase)	NM_000187	-5.78	1.30E-03
7997593	ATP2C2	ATPase, Ca++ transporting, type 2C, member 2	NM_014861	-5.76	9.52E-04
8161892	GNA14	guanine nucleotide binding protein (G protein), alpha 14	NM_004297	-5.63	1.19E-03
7994074	SCNN1B	sodium channel, nonvoltage-gated 1, beta	NM_000336	-5.34	7.91E-04

7958352	BTBD11	BTB (POZ) domain containing 11	NM_001018072	-5.26	1.40E-04
7938225	OLFML1	olfactomedin-like 1	NM_198474	-5.20	4.07E-03
7951977	FXYD6	FXYD domain containing ion transport regulator 6	NM_022003	-5.05	1.35E-03
8147516	MATN2	matrilin 2	NM_002380	-4.90	4.00E-04
7988414	GATM	glycine amidinotransferase (L-arginine:glycine amidinotransferase)	NM_001482	-4.85	1.00E-06
8161964	FRMD3	FERM domain containing 3	NM_174938	-4.32	2.33E-03
8008321	ACSF2	acyl-CoA synthetase family member 2	NM_025149	-4.31	2.10E-05
8014349	CCL14	chemokine (C-C motif) ligand 14	NM_032962	-4.20	4.59E-04
8133983	ADAM22	ADAM metallopeptidase domain 22	NM_021723	-3.91	1.72E-03
8160889	CCL21	chemokine (C-C motif) ligand 21	NM_002989	-3.76	4.90E-05
8114300	KLHL3	kelch-like 3 (Drosophila)	NM_017415	-3.69	6.27E-04
7897132	PRDM16	PR domain containing 16	NM_022114	-3.62	1.00E-06
8161265	IGFBPL1	insulin-like growth factor binding protein-like 1	NM_001007563	-3.49	3.37E-03
7931930	PRKCQ	protein kinase C, theta	NM_006257	-3.36	2.40E-05
7953200	CCND2	cyclin D2	NM_001759	-3.13	6.00E-06
8002992	C16orf46	chromosome 16 open reading frame 46	NM_152337	-3.09	3.90E-05
8045229	ARHGEF4	Rho guanine nucleotide exchange factor (GEF) 4	NM_032995	-2.93	7.90E-05
8134036	STEAP2	six transmembrane epithelial antigen of the prostate 2	NM_152999	-2.92	5.00E-06
8020844	ASXL3	additional sex combs like 3 (Drosophila)	NM_030632	-2.86	1.96E-03
8102532	PDE5A	phosphodiesterase 5A, cGMP-specific	NM_001083	-2.72	3.93E-04
7952046	MPZL2	myelin protein zero-like 2	NM_144765	-2.63	9.95E-04
8102938	RNF150	ring finger protein 150	NM_020724	-2.62	2.12E-04
8009568	TTYH2	tweety homolog 2 (Drosophila)	NM_032646	-2.38	3.34E-03
7972021	TBC1D4	TBC1 domain family, member 4	NM_014832	-2.29	5.40E-05
8059279	EPHA4	EPH receptor A4	NM_004438	-2.26	5.61E-04
8160521	MOBKL2B	MOB1, Mps One Binder kinase activator-like 2B (yeast)	NM_024761	-2.21	6.64E-03

8115397	C5orf4	chromosome 5 open reading frame 4	NM_032385	-2.16	1.03E-03
8013341	MFAP4	microfibrillar-associated protein 4	NM_002404	-2.16	4.95E-03
7967463	RILPL1	Rab interacting lysosomal protein-like 1	NM_178314	-2.14	9.00E-06
8149966	SCARA5	scavenger receptor class A, member 5 (putative)	NM_173833	-2.07	1.17E-03
8081081	EPHA3	EPH receptor A3	NM_005233	-2.04	7.59E-04
8010983	ABR	active BCR-related gene	NM_021962	2.10	3.36E-03
8027778	FXYD5	FXYD domain containing ion transport regulator 5	NM_144779	2.26	3.96E-03
8132725	UPP1	uridine phosphorylase 1	NM_003364	2.27	4.51E-03
7978595	BAZ1A	bromodomain adjacent to zinc finger domain, 1A	NM_013448	2.36	2.07E-03
7966135	CORO1C	coronin, actin binding protein, 1C	NM_014325	2.46	2.13E-04
8167185	TIMP1	TIMP metallopeptidase inhibitor 1	NM_003254	2.53	3.22E-03
8025601	ICAM1	intercellular adhesion molecule 1	NM_000201	2.57	9.26E-03
8092552	IGF2BP2	insulin-like growth factor 2 mRNA binding protein 2	NM_006548	2.66	9.25E-03
8167449	PLP2	proteolipid protein 2 (colonic epithelium-enriched)	NM_002668	2.76	3.58E-04
7994659	MVP	major vault protein	NM_017458	2.78	4.75E-04
7930413	DUSP5	dual specificity phosphatase 5	NM_004419	2.90	5.22E-03
8058765	FN1	fibronectin 1	NM_212482	4.17	8.90E-05
7992789	TNFRSF12A	tumor necrosis factor receptor superfamily, member 12A	NM_016639	4.29	4.62E-03
8037005	TGFB1	transforming growth factor, beta 1	NM_000660	4.81	8.01E-04
8070194	RUNX1	runt-related transcription factor 1	NM_001001890	5.28	4.00E-06
8156290	CKS2	CDC28 protein kinase regulatory subunit 2	NM_001827	5.94	2.66E-03
8112376	CENPK	centromere protein K	NM_022145	6.77	6.15E-03
8037374	PLAUR	plasminogen activator, urokinase receptor	NM_002659	8.16	6.00E-05
8014974	TOP2A	topoisomerase (DNA) II alpha 170kDa	NM_001067	10.63	4.29E-03

List of 31 differentially expressed genes between ATC and normal thyroid tissues, also common to fvPTC versus normal thyroid tissues

Affymetrix gene-level probe set	Gene symbol	Gene name	Accession number	Lower bound of fold change	*P* value
7985159	CRABP1	cellular retinoic acid binding protein 1	NM_004378	-24.95	6.92E-03
7947274	MPPED2	metallophosphoesterase domain containing 2	NM_001584	-17.52	0.00E+00
8069795	CLDN8	claudin 8	NM_199328	-15.90	5.85E-03
8070567	TFF3	trefoil factor 3 (intestinal)	NM_003226	-11.90	3.00E-03
8103789	GPM6A	glycoprotein M6A	NM_005277	-11.77	3.19E-03
8105084	C7	complement component 7	NM_000587	-11.16	2.45E-03
8055496	LRP1B	low density lipoprotein-related protein 1B (deleted in tumors)	NM_018557	-9.48	1.54E-03
7908924	PRELP	proline/arginine-rich end leucine-rich repeat protein	NM_002725	-6.85	3.00E-06
7933750	SLC16A9	solute carrier family 16, member 9 (monocarboxylic acid transporter 9)	NM_194298	-6.48	3.20E-03
7938225	OLFML1	olfactomedin-like 1	NM_198474	-5.20	4.07E-03
8158431	PHYHD1	phytanoyl-CoA dioxygenase domain containing 1	NM_001100876	-5.19	1.00E-06
8147516	MATN2	matrilin 2	NM_002380	-4.90	4.00E-04
8161964	FRMD3	FERM domain containing 3	NM_174938	-4.32	2.33E-03
8014349	CCL14	chemokine (C-C motif) ligand 14	NM_032962	-4.20	4.59E-04
8160889	CCL21	chemokine (C-C motif) ligand 21	NM_002989	-3.76	4.90E-05
7915682	ZSWIM5	zinc finger, SWIM-type containing 5	NM_020883	-3.50	1.00E-05
7953200	CCND2	cyclin D2	NM_001759	-3.13	6.00E-06
7952046	MPZL2	myelin protein zero-like 2	NM_144765	-2.63	9.95E-04
8102938	RNF150	ring finger protein 150	NM_020724	-2.62	2.12E-04
8111677	LIFR	leukemia inhibitory factor receptor alpha	NM_002310	-2.43	4.06E-04

7949650	CTSF	cathepsin F	NM_003793	-2.16	3.67E-03
8013341	MFAP4	microfibrillar-associated protein 4	NM_002404	-2.16	4.95E-03
8149966	SCARA5	scavenger receptor class A, member 5 (putative)	NM_173833	-2.07	1.17E-03
8081081	EPHA3	EPH receptor A3	NM_005233	-2.04	7.59E-04
8042519	PCYOX1	prenylcysteine oxidase 1	NM_016297	-2.00	2.29E-04
8117429	HIST1H2BI	histone cluster 1, H2bi	NM_003525	2.03	5.46E-04
8152668	ATAD2	ATPase family, AAA domain containing 2	NM_014109	2.29	8.70E-04
7905079	HIST2H2AA3	histone cluster 2, H2aa3	NM_003516	2.31	3.30E-03
8117395	HIST1H2BF	histone cluster 1, H2bf	NM_003522	2.56	2.04E-04
8092552	IGF2BP2	insulin-like growth factor 2 mRNA binding protein 2	NM_006548	2.66	9.25E-03
8014974	TOP2A	topoisomerase (DNA) II alpha 170kDa	NM_001067	10.63	4.29E-03

List of 30 differentially expressed genes between ATC and normal thyroid tissues, also common to FTC versus normal thyroid tissues

Affymetrix gene-level probe set	Gene symbol	Gene name	Accession number	Lower bound of fold change	*P* value
7985159	CRABP1	cellular retinoic acid binding protein 1	NM_004378	-24.95	6.92E-03
7947274	MPPED2	metallophosphoesterase domain containing 2	NM_001584	-17.52	0.00E+00
7942332	FOLR1	folate receptor 1 (adult)	NM_016730	-14.74	2.80E-03
8105084	C7	complement component 7	NM_000587	-11.16	2.45E-03
8149629	GFRA2	GDNF family receptor alpha 2	NM_001495	-9.07	3.64E-03
8148070	COL14A1	collagen, type XIV, alpha 1	NM_021110	-8.13	5.25E-03
7908924	PRELP	proline/arginine-rich end leucine-rich repeat protein	NM_002725	-6.85	3.00E-06
7901272	CYP4X1	cytochrome P450, family 4, subfamily X, polypeptide 1	NM_178033	-6.45	1.05E-03
8105121	GHR	growth hormone receptor	NM_000163	-5.31	6.16E-04
7938225	OLFML1	olfactomedin-like 1	NM_198474	-5.20	4.07E-03
8125289	TNXA	tenascin XA pseudogene	NR_001284	-4.69	6.21E-04
8179935	TNXB	tenascin XB	NM_032470	-4.63	6.63E-04
8091600	PLCH1	phospholipase C, eta 1	NM_014996	-4.23	1.75E-03
8139680	COBL	cordon-bleu homolog (mouse)	NM_015198	-3.99	6.00E-06
8160889	CCL21	chemokine (C-C motif) ligand 21	NM_002989	-3.76	4.90E-05
8121729	PLN	phospholamban	NM_002667	-3.52	1.18E-03
7990138	GRAMD2	GRAM domain containing 2	NM_001012642	-3.01	3.86E-03
8173755	ITM2A	integral membrane protein 2A	NM_004867	-2.95	4.43E-03
8132092	INMT	indolethylamine N-methyltransferase	NM_006774	-2.84	4.34E-03
8042079	CCDC85A	coiled-coil domain containing 85A	NM_001080433	-2.82	9.00E-06

7947599	CHST1	carbohydrate (keratan sulfate Gal-6) sulfotransferase 1	NM_003654	-2.82	3.70E-03
8114249	CXCL14	chemokine (C-X-C motif) ligand 14	NM_004887	-2.72	2.42E-03
7965873	IGF1	insulin-like growth factor 1 (somatomedin C)	NM_001111283	-2.26	5.93E-03
7949650	CTSF	cathepsin F	NM_003793	-2.16	3.67E-03
8013341	MFAP4	microfibrillar-associated protein 4	NM_002404	-2.16	4.95E-03
8149966	SCARA5	scavenger receptor class A, member 5 (putative)	NM_173833	-2.07	1.17E-03
8081081	EPHA3	EPH receptor A3	NM_005233	-2.04	7.59E-04
8143441	KIAA1147	KIAA1147	BC012493	-2.03	5.60E-05
8030007	EMP3	epithelial membrane protein 3	NM_001425	2.36	1.59E-03
8059854	ARL4C	ADP-ribosylation factor-like 4C	NM_005737	7.70	8.73E-03

List of 34 differentially expressed genes between ATC and normal thyroid tissues, also common to PDTC versus normal thyroid tissues

Affymetrix gene-level probe set	Gene symbol	Gene name	Accession number	Lower bound of fold change	*P* value
7985159	CRABP1	cellular retinoic acid binding protein 1	NM_004378	-24.95	6.92E-03
8044143	C2orf40	chromosome 2 open reading frame 40	NM_032411	-24.40	1.25E-03
8135436	SLC26A4	solute carrier family 26, member 4	NM_000441	-18.14	1.50E-05
7947274	MPPED2	metallophosphoesterase domain containing 2	NM_001584	-17.52	0.00E+00
8103789	GPM6A	glycoprotein M6A	NM_005277	-11.77	3.19E-03
8055496	LRP1B	low density lipoprotein-related protein 1B (deleted in tumors)	NM_018557	-9.48	1.54E-03
8149629	GFRA2	GDNF family receptor alpha 2	NM_001495	-9.07	3.64E-03
7931977	ITIH5	inter-alpha (globulin) inhibitor H5	NM_030569	-6.54	1.56E-03
7938225	OLFML1	olfactomedin-like 1	NM_198474	-5.20	4.07E-03
8125289	TNXA	tenascin XA pseudogene	NR_001284	-4.69	6.21E-04
8179935	TNXB	tenascin XB	NM_032470	-4.63	6.63E-04
8014349	CCL14	chemokine (C-C motif) ligand 14	NM_032962	-4.20	4.59E-04
8029489	BCAM	basal cell adhesion molecule (Lutheran blood group)	NM_005581	-4.09	2.29E-04
8160889	CCL21	chemokine (C-C motif) ligand 21	NM_002989	-3.76	4.90E-05
8090823	SLCO2A1	solute carrier organic anion transporter family, member 2A1	NM_005630	-3.24	1.20E-04
8074432	HIRA	HIR histone cell cycle regulation defective homolog A (S. cerevisiae)	NM_003325	-3.12	4.83E-03
8173755	ITM2A	integral membrane protein 2A	NM_004867	-2.95	4.43E-03
8076185	CBX7	chromobox homolog 7	NM_175709	-2.87	2.81E-03
8132092	INMT	indolethylamine N-methyltransferase	NM_006774	-2.84	4.34E-03
8042079	CCDC85A	coiled-coil domain containing 85A	NM_001080433	-2.82	9.00E-06

7947599	CHST1	carbohydrate (keratan sulfate Gal-6) sulfotransferase 1	NM_003654	-2.82	3.70E-03
8114249	CXCL14	chemokine (C-X-C motif) ligand 14	NM_004887	-2.72	2.42E-03
8102938	RNF150	ring finger protein 150	NM_020724	-2.62	2.12E-04
8035297	PLVAP	plasmalemma vesicle associated protein	NM_031310	-2.35	8.30E-05
7972021	TBC1D4	TBC1 domain family, member 4	NM_014832	-2.29	5.40E-05
8013341	MFAP4	microfibrillar-associated protein 4	NM_002404	-2.16	4.95E-03
8149966	SCARA5	scavenger receptor class A, member 5 (putative)	NM_173833	-2.07	1.17E-03
8030007	EMP3	epithelial membrane protein 3	NM_001425	2.36	1.59E-03
8156290	CKS2	CDC28 protein kinase regulatory subunit 2	NM_001827	5.94	2.66E-03
8151871	CCNE2	cyclin E2	NM_057749	6.14	2.01E-03
8112376	CENPK	centromere protein K	NM_022145	6.77	6.15E-03
8024900	UHRF1	ubiquitin-like with PHD and ring finger domains 1	NM_001048201	7.79	1.24E-03
8017262	BRIP1	BRCA1 interacting protein C-terminal helicase 1	NM_032043	8.10	8.03E-03
7989647	KIAA0101	KIAA0101	NM_014736	8.64	5.67E-03

Supplementary File III.2

Complete list of 1333 differentially expressed genes between ATC and normal thyroid tissues

(Genes in common to other comparison of thyroid tumours versus normal thyroid tissue are shaded in grey)

Affymetrix gene-level probe set	Gene symbol	Gene name	Accession number	Lower bound of fold change	*P* value
8122744	IYD	iodotyrosine deiodinase	NM_203395	-55.66	9.50E-05
8147273	SLC26A7	solute carrier family 26, member 7	NM_052832	-50.83	5.83E-03
8106448	PDE8B	phosphodiesterase 8B	NM_003719	-45.08	7.10E-05
8147891	PKHD1L1	polycystic kidney and hepatic disease 1 (autosomal recessive)-like 1	NM_177531	-42.39	6.99E-04
8009493	KCNJ16	potassium inwardly-rectifying channel, subfamily J, member 16	NM_170742	-40.09	6.02E-03
8056611	LRP2	low density lipoprotein-related protein 2	NM_004525	-38.73	1.45E-04
7961580	LMO3	LIM domain only 3 (rhombotin-like 2)	NM_018640	-38.66	3.50E-05
7988350	DUOX2	dual oxidase 2	NM_014080	-37.32	5.18E-04
8148385	TG	thyroglobulin	NM_003235	-37.29	0.00E+00
8039996	TPO	thyroid peroxidase	NM_000547	-36.72	2.65E-03
7996837	CDH1	cadherin 1, type 1, E-cadherin (epithelial)	NM_004360	-31.47	1.93E-04
7976037	TSHR	thyroid stimulating hormone receptor	NM_000369	-31.02	1.64E-03
7932453	NEBL	nebulette	NM_006393	-30.05	1.34E-04
7983405	DUOXA2	dual oxidase maturation factor 2	NM_207581	-29.05	3.69E-03
8041853	TACSTD1	tumor-associated calcium signal transducer 1	NM_002354	-28.14	9.83E-03
8144712	C8orf79	chromosome 8 open reading frame 79	NM_001099677	-25.29	3.11E-04
8173825	RPS6KA6	ribosomal protein S6 kinase, 90kDa, polypeptide 6	NM_014496	-25.28	3.30E-04
7985159	CRABP1	cellular retinoic acid binding protein 1	NM_004378	-24.95	6.92E-03
7906079	RAB25	RAB25, member RAS oncogene family	NM_020387	-24.69	2.70E-05
7982070	SNORD115-32	small nucleolar RNA, C/D box 115-32	NR_003347	-24.68	1.92E-03
8044143	C2orf40	chromosome 2 open reading frame 40	NM_032411	-24.40	1.25E-03
7978676	NKX2-1	NK2 homeobox 1	NM_003317	-24.32	2.56E-04
7988990	WDR72	WD repeat domain 72	NM_182758	-23.83	9.36E-03
7965231	MGAT4C	mannosyl (alpha-1,3-)-glycoprotein beta-1,4-N-acetylglucosaminyltransferase, isozyme C (putative)	NM_013244	-23.57	9.66E-04
8068651	PCP4	Purkinje cell protein 4	NM_006198	-23.29	8.11E-04
7999291	C16orf89	chromosome 16 open reading frame 89	NM_152459	-21.94	3.42E-04
7965769	SLC5A8	solute carrier family 5 (iodide transporter), member 8	NM_145913	-20.70	6.67E-04
7968678	FREM2	FRAS1 related extracellular matrix protein 2	NM_207361	-20.67	2.25E-03

8053073	SLC4A5	solute carrier family 4, sodium bicarbonate cotransporter, member 5	NM_133478	-20.56	1.61E-03
8072436	PIB5PA	phosphatidylinositol (4,5) bisphosphate 5-phosphatase, A	NM_001002837	-19.80	3.42E-04
7983413	DUOX1	dual oxidase 1	NM_017434	-19.00	1.98E-04
8135436	SLC26A4	solute carrier family 26, member 4	NM_000441	-18.14	1.50E-05
8157193	ZNF483	zinc finger protein 483	NM_133464	-18.14	1.81E-04
8081959	STXBP5L	syntaxin binding protein 5-like	NM_014980	-17.95	1.39E-03
7947274	MPPED2	metallophosphoesterase domain containing 2	NM_001584	-17.52	0.00E+00
8140686	SEMA3D	sema domain, immunoglobulin domain (Ig), short basic domain, secreted, (semaphorin) 3D	NM_152754	-17.11	1.16E-04
8158771	C9orf58	chromosome 9 open reading frame 58	NM_031426	-17.04	8.02E-04
8156743	FOXE1	forkhead box E1 (thyroid transcription factor 2)	NM_004473	-16.46	4.88E-04
8166925	MAOA	monoamine oxidase A	NM_000240	-16.35	4.82E-04
8117120	ID4	inhibitor of DNA binding 4, dominant negative helix-loop-helix protein	NM_001546	-16.25	1.10E-05
7982052	PAR4	Prader-Willi/Angelman region gene 4	NR_022010	-16.13	9.41E-03
8133360	CLDN4	claudin 4	NM_001305	-16.10	2.76E-03
7982082	SNORD115-38	small nucleolar RNA, C/D box 115-38	NR_003353	-16.10	5.63E-03
7975238	PLEKHH1	pleckstrin homology domain containing, family H (with MyTH4 domain) member 1	NM_020715	-16.05	1.33E-04
8147351	RBM35A	RNA binding motif protein 35A	NM_017697	-15.96	2.00E-06
8126820	GPR110	G protein-coupled receptor 110	NM_153840	-15.95	6.04E-03
7980485	DIO2	deiodinase, iodothyronine, type II	NM_013989	-15.94	2.44E-03
8069795	CLDN8	claudin 8	NM_199328	-15.90	5.85E-03
8105908	OCLN	occludin	NM_002538	-15.89	1.64E-04
8058591	ACADL	acyl-Coenzyme A dehydrogenase, long chain	NM_001608	-15.74	1.08E-04
8092800	ATP13A4	ATPase type 13A4	NM_032279	-15.35	9.71E-04
7936734	FGFR2	fibroblast growth factor receptor 2	NM_000141	-15.27	1.41E-03
8017885	ABCA8	ATP-binding cassette, sub-family A (ABC1), member 8	NM_007168	-15.08	2.14E-03
8001007	PRSS8	protease, serine, 8	NM_002773	-14.79	2.66E-04
7942332	FOLR1	folate receptor 1 (adult)	NM_016730	-14.74	2.80E-03
8155734	C9orf61	chromosome 9 open reading frame 61	NM_004816	-14.69	1.43E-04
8140140	CLDN3	claudin 3	NM_001306	-14.61	9.40E-05
7903959	C1orf88	chromosome 1 open reading frame 88	NM_181643	-13.97	1.11E-03
7913385	RAP1GAP	RAP1 GTPase activating protein	NM_002885	-13.78	6.33E-04
8019541	ZNF750	zinc finger protein 750	NM_024702	-13.72	4.17E-03
8105899	MARVELD2	MARVEL domain containing 2	NM_001038603	-13.54	4.73E-04
8150419	ZMAT4	zinc finger, matrin type 4	NM_024645	-13.16	2.61E-03
8163116	EPB41L4B	erythrocyte membrane protein band 4.1 like 4B	NM_019114	-13.09	5.12E-04

7965686	ANKS1B	ankyrin repeat and sterile alpha motif domain containing 1B	NM_152788	-13.05	1.31E-03
8067185	BMP7	bone morphogenetic protein 7	NM_001719	-12.94	2.81E-03
8068383	CLIC6	chloride intracellular channel 6	NM_053277	-12.89	7.80E-04
8137485	DPP6	dipeptidyl-peptidase 6	NM_001039350	-12.81	3.21E-03
7999674	MYH11	myosin, heavy chain 11, smooth muscle	NM_022844	-12.79	4.16E-03
7945321	GLB1L2	galactosidase, beta 1-like 2	NM_138342	-12.40	6.28E-04
8095110	KIT	v-kit Hardy-Zuckerman 4 feline sarcoma viral oncogene homolog	NM_000222	-12.38	1.40E-03
8149725	PEBP4	phosphatidylethanolamine-binding protein 4	NM_144962	-12.28	4.14E-03
7961595	RERGL	RERG/RAS-like	NM_024730	-12.27	2.93E-03
7979524	TMEM30B	transmembrane protein 30B	NM_001017970	-12.21	1.66E-04
8126750	ENPP5	ectonucleotide pyrophosphatase/phosphodiesterase 5 (putative function)	NM_021572	-11.94	5.50E-05
8095907	FRAS1	Fraser syndrome 1	NM_025074	-11.92	5.39E-03
8070567	TFF3	trefoil factor 3 (intestinal)	NM_003226	-11.90	3.00E-03
8103789	GPM6A	glycoprotein M6A	NM_005277	-11.77	3.19E-03
7947548	RAG2	recombination activating gene 2	NM_000536	-11.65	8.08E-03
8016387	ATAD4	ATPase family, AAA domain containing 4	NM_024320	-11.64	3.21E-03
7924309	ESRRG	estrogen-related receptor gamma	NM_206594	-11.58	3.35E-04
7923578	FMOD	fibromodulin	NM_002023	-11.36	2.00E-06
8152506	SAMD12	sterile alpha motif domain containing 12	NM_207506	-11.21	6.44E-04
8105084	C7	complement component 7	NM_000587	-11.16	2.45E-03
8054872	TFCP2L1	transcription factor CP2-like 1	NM_014553	-10.99	5.56E-04
7924058	IRF6	interferon regulatory factor 6	NM_006147	-10.80	1.60E-05
8103494	NPY1R	neuropeptide Y receptor Y1	NM_000909	-10.72	7.42E-04
7910792	RYR2	ryanodine receptor 2 (cardiac)	NM_001035	-10.70	3.13E-03
8095751	DKFZP564O0823	DKFZP564O0823 protein	NM_015393	-10.61	7.96E-04
8117547	PRSS16	protease, serine, 16 (thymus)	NM_005865	-10.59	2.00E-06
7983393	SORD	sorbitol dehydrogenase	NM_003104	-10.54	1.00E-06
7902235	LRRC7	leucine rich repeat containing 7	NM_020794	-10.53	5.08E-03
8097829	FHDC1	FH2 domain containing 1	NM_033393	-10.42	6.39E-03
7989073	PRTG	protogenin homolog (Gallus gallus)	NM_173814	-10.28	2.72E-03
8162373	OGN	osteoglycin	NM_033014	-10.16	5.08E-03
8157300	BSPRY	B-box and SPRY domain containing	NM_017688	-9.99	1.10E-05
7988380	DUOXA1	dual oxidase maturation factor 1	NM_144565	-9.98	0.00E+00
7900340	BMP8A	bone morphogenetic protein 8a	NM_181809	-9.94	5.08E-03
8054166	TSGA10	testis specific, 10	NM_025244	-9.87	2.00E-06
8145611	FZD3	frizzled homolog 3 (Drosophila)	NM_017412	-9.70	3.18E-04
8147697	GRHL2	grainyhead-like 2 (Drosophila)	NM_024915	-9.61	8.20E-05

8055496	LRP1B	low density lipoprotein-related protein 1B (deleted in tumors)	NM_018557	-9.48	1.54E-03
8096130	CDS1	CDP-diacylglycerol synthase (phosphatidate cytidylyltransferase) 1	NM_001263	-9.42	2.00E-06
8149685	LGI3	leucine-rich repeat LGI family, member 3	NM_139278	-9.41	5.50E-04
7946340	RIC3	resistance to inhibitors of cholinesterase 3 homolog (C. elegans)	NM_024557	-9.38	9.90E-05
8142646	IQUB	IQ motif and ubiquitin domain containing	NM_178827	-9.33	2.78E-04
7909866	MOSC2	MOCO sulphurase C-terminal domain containing 2	NM_017898	-9.30	2.99E-04
8152512	TNFRSF11B	tumor necrosis factor receptor superfamily, member 11b	NM_002546	-9.19	5.27E-04
8148059	DEPDC6	DEP domain containing 6	NM_022783	-9.15	8.00E-03
8095585	SLC4A4	solute carrier family 4, sodium bicarbonate cotransporter, member 4	NM_001098484	-9.12	1.90E-05
8149629	GFRA2	GDNF family receptor alpha 2	NM_001495	-9.07	3.64E-03
8128726	PPIL6	peptidylprolyl isomerase (cyclophilin)-like 6	NM_173672	-9.05	7.43E-04
8061564	ID1	inhibitor of DNA binding 1, dominant negative helix-loop-helix protein	NM_181353	-9.02	1.11E-04
7906552	CASQ1	calsequestrin 1 (fast-twitch, skeletal muscle)	NM_001231	-8.96	7.61E-03
7956271	HSD17B6	hydroxysteroid (17-beta) dehydrogenase 6 homolog (mouse)	NM_003725	-8.94	8.91E-04
8150002	FBXO16	F-box protein 16	NM_172366	-8.93	1.36E-03
8101031	CDKL2	cyclin-dependent kinase-like 2 (CDC2-related kinase)	NM_003948	-8.87	5.99E-04
8099593	KCNIP4	Kv channel interacting protein 4	NM_147182	-8.81	9.21E-03
8097920	LRAT	lecithin retinol acyltransferase (phosphatidylcholine--retinol O-acyltransferase)	NM_004744	-8.77	4.99E-04
8148040	MAL2	mal, T-cell differentiation protein 2	NM_052886	-8.73	0.00E+00
8151056	CYP7B1	cytochrome P450, family 7, subfamily B, polypeptide 1	NM_004820	-8.72	2.74E-04
7982002	SNORD116-27	small nucleolar RNA, C/D box 116-27	NR_003341	-8.71	6.80E-05
7937709	KRTAP5-6	keratin associated protein 5-6	NM_001012416	-8.67	1.09E-03
7942453	PLEKHB1	pleckstrin homology domain containing, family B (evectins) member 1	NM_021200	-8.59	6.83E-04
8034084	AP1M2	adaptor-related protein complex 1, mu 2 subunit	NM_005498	-8.54	5.21E-04
7982098	SNORD109B	small nucleolar RNA, C/D box 109B	NR_001289	-8.47	2.71E-03
8001547	PLLP	plasma membrane proteolipid (plasmolipin)	NM_015993	-8.46	4.50E-05
8161270	ANKRD18A	ankyrin repeat domain 18A	BC152434	-8.34	4.00E-05
8086615	LRRC2	leucine rich repeat containing 2	NM_024750	-8.27	0.00E+00
7988876	MYO5C	myosin VC	NM_018728	-8.23	3.37E-04
8148070	COL14A1	collagen, type XIV, alpha 1	NM_021110	-8.13	5.25E-03
7915500	C1orf210	chromosome 1 open reading frame 210	NM_182517	-8.12	2.06E-04
8143154	DGKI	diacylglycerol kinase, iota	NM_004717	-8.04	9.36E-03
8056022	CCDC148	coiled-coil domain containing 148	NM_138803	-8.01	2.84E-03
8169603	LONRF3	LON peptidase N-terminal domain and ring finger 3	NM_001031855	-7.99	1.04E-03
7982018	SNORD115-4	small nucleolar RNA, C/D box 115-4	NR_003296	-7.95	9.95E-03
8123104	FNDC1	fibronectin type III domain containing 1	NM_032532	-7.94	4.10E-05

8028311	SPINT2	serine peptidase inhibitor, Kunitz type, 2	NM_021102	-7.92	4.00E-06
7901765	HOOK1	hook homolog 1 (Drosophila)	NM_015888	-7.89	4.50E-05
8007949	C17orf57	chromosome 17 open reading frame 57	BC036407	-7.81	1.55E-03
7961844	CASC1	cancer susceptibility candidate 1	NM_018272	-7.75	1.85E-04
7979658	GPX2	glutathione peroxidase 2 (gastrointestinal)	NM_002083	-7.74	1.00E-06
7982006	SNORD116-29	small nucleolar RNA, C/D box 116-29	NR_003360	-7.68	1.56E-03
8037103	GRIK5	glutamate receptor, ionotropic, kainate 5	NM_002088	-7.62	6.15E-04
8058462	MDH1B	malate dehydrogenase 1B, NAD (soluble)	NM_001039845	-7.60	1.22E-03
8142524	TSPAN12	tetraspanin 12	NM_012338	-7.56	1.39E-03
7982010	SNORD115-2	small nucleolar RNA, C/D box 115-2	NR_003294	-7.49	7.83E-03
8105585	RNF180	ring finger protein 180	NM_001113561	-7.46	1.66E-04
7951040	GPR83	G protein-coupled receptor 83	NM_016540	-7.43	5.94E-03
7920082	RORC	RAR-related orphan receptor C	NM_005060	-7.43	2.28E-03
8094789	LIMCH1	LIM and calponin homology domains 1	NM_014988	-7.41	4.60E-05
8106827	GPR98	G protein-coupled receptor 98	NM_032119	-7.40	6.90E-04
7970676	SHISA2	shisa homolog 2 (Xenopus laevis)	NM_001007538	-7.38	4.99E-03
7981943	PAR5	Prader-Willi/Angelman syndrome-5	NR_022008	-7.36	9.12E-03
8114354	NME5	non-metastatic cells 5, protein expressed in (nucleoside-diphosphate kinase)	NM_003551	-7.34	3.16E-04
8149574	CSGALNACT1	chondroitin sulfate N-acetylgalactosaminyltransferase 1	NM_018371	-7.33	1.40E-05
8101881	ADH1B	alcohol dehydrogenase 1B (class I), beta polypeptide	NM_000668	-7.31	3.00E-06
7934789	GRID1	glutamate receptor, ionotropic, delta 1	NM_017551	-7.31	1.20E-05
7900159	DNALI1	dynein, axonemal, light intermediate chain 1	NM_003462	-7.30	1.02E-03
8144786	SLC7A2	solute carrier family 7 (cationic amino acid transporter, y+ system), member 2	NM_003046	-7.22	3.90E-03
8039144	TMC4	transmembrane channel-like 4	NM_144686	-7.12	6.44E-04
8017927	ABCA9	ATP-binding cassette, sub-family A (ABC1), member 9	NM_080283	-7.09	5.19E-04
8057506	FRZB	frizzled-related protein	NM_001463	-7.06	4.54E-03
7981998	SNORD116-25	small nucleolar RNA, C/D box 116-25	NR_003339	-7.05	3.00E-06
8044225	SULT1C4	sulfotransferase family, cytosolic, 1C, member 4	NM_006588	-6.97	1.72E-03
7944955	PKNOX2	PBX/knotted 1 homeobox 2	NM_022062	-6.94	5.05E-03
8043835	C2orf15	chromosome 2 open reading frame 15	BC021264	-6.93	6.41E-03
7952426	VSIG2	V-set and immunoglobulin domain containing 2	NM_014312	-6.93	2.66E-04
8080511	CACNA1D	calcium channel, voltage-dependent, L type, alpha 1D subunit	NM_000720	-6.92	0.00E+00
8059878	IQCA1	IQ motif containing with AAA domain 1	NM_024726	-6.88	5.72E-04
8174119	ZMAT1	zinc finger, matrin type 1	NM_001011657	-6.88	2.18E-03
7952526	CDON	Cdon homolog (mouse)	NM_016952	-6.86	0.00E+00
7908924	PRELP	proline/arginine-rich end leucine-rich repeat protein	NM_002725	-6.85	3.00E-06

8021199	MAPK4	mitogen-activated protein kinase 4	NM_002747	-6.84	4.31E-04
8103094	NR3C2	nuclear receptor subfamily 3, group C, member 2	NM_000901	-6.84	2.80E-03
8025382	LASS4	LAG1 homolog, ceramide synthase 4	NM_024552	-6.82	0.00E+00
7982084	SNORD115-3	small nucleolar RNA, C/D box 115-3	NR_003295	-6.81	7.76E-03
8141066	PON3	paraoxonase 3	NM_000940	-6.80	4.71E-03
8143633	OR2A7	olfactory receptor, family 2, subfamily A, member 7	NM_001005328	-6.77	3.02E-03
7982000	SNORD116-26	small nucleolar RNA, C/D box 116-26	NR_003340	-6.76	2.60E-05
7958398	WSCD2	WSC domain containing 2	NM_014653	-6.75	2.26E-03
7954398	C12orf39	chromosome 12 open reading frame 39	BC004336	-6.74	5.25E-03
8129558	OR2A4	olfactory receptor, family 2, subfamily A, member 4	NM_030908	-6.70	3.03E-03
7909681	PROX1	prospero homeobox 1	NM_002763	-6.70	1.93E-03
7996185	MMP15	matrix metallopeptidase 15 (membrane-inserted)	NM_002428	-6.65	1.74E-04
7981283	SLC25A29	solute carrier family 25, member 29	NM_001039355	-6.65	2.77E-03
7981974	SNORD116-13	small nucleolar RNA, C/D box 116-13	NR_003328	-6.65	5.00E-06
8099476	PROM1	prominin 1	NM_006017	-6.62	1.88E-03
7936201	C10orf79	chromosome 10 open reading frame 79	NM_025145	-6.59	3.13E-04
7931977	ITIH5	inter-alpha (globulin) inhibitor H5	NM_030569	-6.54	1.56E-03
8100026	ATP8A1	ATPase, aminophospholipid transporter (APLT), class I, type 8A, member 1	NM_006095	-6.54	3.78E-04
8018220	GRIN2C	glutamate receptor, ionotropic, N-methyl D-aspartate 2C	NM_000835	-6.53	6.09E-03
8044212	SULT1C2	sulfotransferase family, cytosolic, 1C, member 2	NM_001056	-6.50	1.49E-03
8096704	NPNT	nephronectin	NM_001033047	-6.49	2.00E-06
7933750	SLC16A9	solute carrier family 16, member 9 (monocarboxylic acid transporter 9)	NM_194298	-6.48	3.20E-03
8161755	ALDH1A1	aldehyde dehydrogenase 1 family, member A1	NM_000689	-6.48	1.67E-03
8061013	C20orf82	chromosome 20 open reading frame 82	NM_080826	-6.48	0.00E+00
7921916	RGS5	regulator of G-protein signaling 5	NM_003617	-6.46	5.38E-04
7901272	CYP4X1	cytochrome P450, family 4, subfamily X, polypeptide 1	NM_178033	-6.45	1.05E-03
8056184	ITGB6	integrin, beta 6	NM_000888	-6.41	2.18E-04
7900555	RP4-692D3.1	hypothetical protein LOC728621	NM_001080850	-6.38	6.83E-03
7981460	PPP1R13B	protein phosphatase 1, regulatory (inhibitor) subunit 13B	NM_015316	-6.36	2.20E-05
7968577	NBEA	neurobeachin	NM_015678	-6.35	2.00E-05
7982046	SNORD115-5	small nucleolar RNA, C/D box 115-5	NR_003297	-6.34	9.66E-03
7898623	UBXN10	UBX domain protein 10	NM_152376	-6.33	4.32E-04
8088142	CHDH	choline dehydrogenase	NM_018397	-6.30	2.55E-03
7993453	MPV17L	MPV17 mitochondrial membrane protein-like	NM_173803	-6.28	4.13E-04
7929282	HHEX	hematopoietically expressed homeobox	NM_002729	-6.25	5.02E-03
8063187	EYA2	eyes absent homolog 2 (Drosophila)	NM_172111	-6.24	1.27E-04
8156134	NTRK2	neurotrophic tyrosine kinase, receptor, type 2	NM_006180	-6.21	3.00E-06

7981980	SNORD116-16	small nucleolar RNA, C/D box 116-16	NR_003331	-6.19	7.51E-04
8043043	DNHL1	dynein heavy chain-like 1	NM_173645	-6.16	8.31E-04
7899101	CNKSR1	connector enhancer of kinase suppressor of Ras 1	NM_006314	-6.10	4.00E-06
8113483	FLJ43080	hypothetical protein LOC642987	AK125070	-6.09	4.00E-06
8022817	KLHL14	kelch-like 14 (Drosophila)	NM_020805	-6.07	1.00E-05
8169235	FRMPD3	FERM and PDZ domain containing 3	ENST00000276185	-6.06	2.00E-03
7938951	ANO5	anoctamin 5	NM_213599	-5.97	7.64E-04
7943319	CNTN5	contactin 5	NM_014361	-5.96	1.29E-03
7902425	ST6GALNAC3	ST6 (alpha-N-acetyl-neuraminyl-2,3-beta-galactosyl-1,3)-N-acetylgalactosaminide alpha-2,6-sialyltransferase 3	NM_152996	-5.90	4.20E-03
8127989	SNORD50B	small nucleolar RNA, C/D box 50B	NR_003044	-5.85	1.39E-03
7901229	FAAH	fatty acid amide hydrolase	NM_001441	-5.83	2.00E-06
8020384	KIAA1772	KIAA1772	AK293321	-5.82	1.88E-03
8089851	HGD	homogentisate 1,2-dioxygenase (homogentisate oxidase)	NM_000187	-5.78	1.30E-03
8175234	GPC3	glypican 3	NM_004484	-5.78	4.88E-03
7997593	ATP2C2	ATPase, Ca++ transporting, type 2C, member 2	NM_014861	-5.76	9.52E-04
8044882	EPB41L5	erythrocyte membrane protein band 4.1 like 5	NM_020909	-5.67	1.29E-04
8005064	RICH2	Rho-type GTPase-activating protein RICH2	NM_014859	-5.65	1.93E-03
7903407	AMY2B	amylase, alpha 2B (pancreatic)	NM_020978	-5.64	6.60E-05
7934411	USP54	ubiquitin specific peptidase 54	NM_152586	-5.64	8.20E-05
8161892	GNA14	guanine nucleotide binding protein (G protein), alpha 14	NM_004297	-5.63	1.19E-03
8034227	RGL3	ral guanine nucleotide dissociation stimulator-like 3	NM_001035223	-5.63	5.19E-04
8101587	MAPK10	mitogen-activated protein kinase 10	NM_138980	-5.62	1.00E-06
7934334	TTC18	tetratricopeptide repeat domain 18	NM_145170	-5.61	7.65E-04
8027354	LOC388524	ribosomal protein SA pseudogene	NR_003662	-5.59	8.57E-04
8135544	FOXP2	forkhead box P2	NM_148898	-5.58	2.00E-06
8098549	STOX2	storkhead box 2	NM_020225	-5.53	2.96E-03
7901788	NFIA	nuclear factor I/A	NM_005595	-5.50	2.00E-06
8174201	BEX1	brain expressed, X-linked 1	NM_018476	-5.49	2.09E-03
8088397	ACOX2	acyl-Coenzyme A oxidase 2, branched chain	NM_003500	-5.48	2.79E-03
8045882	DAPL1	death associated protein-like 1	NM_001017920	-5.45	2.12E-03
8143610	FLJ43692	ARHGEF5-like	EF560743	-5.45	1.04E-04
7951351	PDGFD	platelet derived growth factor D	NM_025208	-5.45	8.68E-03
7923386	LMOD1	leiomodin 1 (smooth muscle)	NM_012134	-5.44	2.76E-04
8083546	KCNAB1	potassium voltage-gated channel, shaker-related subfamily, beta member 1	NM_003471	-5.37	1.10E-05
7971015	SMAD9	SMAD family member 9	NM_001127217	-5.37	1.00E-05
8095819	FAM47E	family with sequence similarity 47, member E	AK124936	-5.36	2.43E-04

8163548	KIF12	kinesin family member 12	NM_138424	-5.35	1.00E-06
8139622	ZPBP	zona pellucida binding protein	NM_007009	-5.35	5.85E-03
7994074	SCNN1B	sodium channel, nonvoltage-gated 1, beta	NM_000336	-5.34	7.91E-04
8139330	CAMK2B	calcium/calmodulin-dependent protein kinase (CaM kinase) II beta	NM_001220	-5.34	2.80E-05
8070097	DNAJC28	DnaJ (Hsp40) homolog, subfamily C, member 28	NM_017833	-5.34	3.81E-03
8002218	RBM35B	RNA binding motif protein 35B	NM_024939	-5.33	5.83E-04
8105121	GHR	growth hormone receptor	NM_000163	-5.31	6.16E-04
8052940	PAIP2B	poly(A) binding protein interacting protein 2B	NM_020459	-5.30	1.71E-03
7958352	BTBD11	BTB (POZ) domain containing 11	NM_001018072	-5.26	1.40E-04
8129783	MAP7	microtubule-associated protein 7	NM_003980	-5.26	2.10E-04
7964660	AVPR1A	arginine vasopressin receptor 1A	NM_000706	-5.21	1.18E-03
8113512	EPB41L4A	erythrocyte membrane protein band 4.1 like 4A	NM_022140	-5.21	1.80E-05
8097841	TRIM2	tripartite motif-containing 2	NM_015271	-5.21	2.20E-05
7938225	OLFML1	olfactomedin-like 1	NM_198474	-5.20	4.07E-03
8140620	PCLO	piccolo (presynaptic cytomatrix protein)	NM_033026	-5.20	1.00E-06
8158431	PHYHD1	phytanoyl-CoA dioxygenase domain containing 1	NM_001100876	-5.19	1.00E-06
7951565	ARHGAP20	Rho GTPase activating protein 20	NM_020809	-5.18	2.86E-03
8043071	DNAH6	dynein, axonemal, heavy chain 6	ENST00000389394	-5.17	5.77E-04
8101893	ADH1C	alcohol dehydrogenase 1C (class I), gamma polypeptide	NM_000669	-5.14	8.20E-04
8136987	ARHGEF5	Rho guanine nucleotide exchange factor (GEF) 5	NM_005435	-5.13	1.58E-04
8054439	ST6GAL2	ST6 beta-galactosamide alpha-2,6-sialyltranferase 2	NM_032528	-5.13	7.40E-05
7936050	CYP17A1	cytochrome P450, family 17, subfamily A, polypeptide 1	NM_000102	-5.11	3.66E-03
7954065	GPRC5A	G protein-coupled receptor, family C, group 5, member A	NM_003979	-5.10	5.28E-04
8067869	RBM11	RNA binding motif protein 11	NM_144770	-5.07	6.20E-05
8068363	C21orf82	chromosome 21 open reading frame 82	AF426258	-5.06	5.08E-03
7951977	FXYD6	FXYD domain containing ion transport regulator 6	NM_022003	-5.05	1.35E-03
8005289	LRRC48	leucine rich repeat containing 48	NM_031294	-5.03	6.01E-04
7959893	GPR133	G protein-coupled receptor 133	NM_198827	-5.01	7.45E-03
8140170	GTF2IRD2	GTF2I repeat domain containing 2	NM_173537	-5.01	7.90E-05
8133549	GTF2IRD2B	GTF2I repeat domain containing 2B	NM_001003795	-5.00	8.10E-05
8164853	ABO	ABO blood group (transferase A, alpha 1-3-N-acetylgalactosaminyltransferase; transferase B, alpha 1-3-galactosyltransferase)	NM_020469	-4.99	6.82E-03
7981970	SNORD116-11	small nucleolar RNA, C/D box 116-11	NR_003326	-4.99	8.47E-03
7901804	INADL	InaD-like (Drosophila)	NM_176877	-4.96	1.55E-04
8088866	CNTN3	contactin 3 (plasmacytoma associated)	NM_020872	-4.92	4.39E-04
8147516	MATN2	matrilin 2	NM_002380	-4.90	4.00E-04

8123929	HERV-FRD	HERV-FRD provirus ancestral Env polyprotein	NM_207582	-4.89	2.03E-03
7988414	GATM	glycine amidinotransferase (L-arginine:glycine amidinotransferase)	NM_001482	-4.85	1.00E-06
7994058	SCNN1G	sodium channel, nonvoltage-gated 1, gamma	NM_001039	-4.85	7.46E-03
7982088	SNORD115-41	small nucleolar RNA, C/D box 115-41	NR_003356	-4.83	6.92E-03
8136095	AHCYL2	S-adenosylhomocysteine hydrolase-like 2	NM_015328	-4.82	6.00E-06
7980908	FBLN5	fibulin 5	NM_006329	-4.82	1.43E-03
8020164	GNAL	guanine nucleotide binding protein (G protein), alpha activating activity polypeptide, olfactory type	NM_182978	-4.78	5.28E-03
8166690	CXorf59	chromosome X open reading frame 59	BC101698	-4.76	2.30E-05
8130408	PIP3-E	phosphoinositide-binding protein PIP3-E	NM_015553	-4.76	9.00E-06
7982072	SNORD115-33	small nucleolar RNA, C/D box 115-33	NR_003348	-4.76	9.51E-03
8165934	SHROOM2	shroom family member 2	NM_001649	-4.74	2.09E-03
8104035	SORBS2	sorbin and SH3 domain containing 2	NM_021069	-4.72	3.30E-04
7947156	MUC15	mucin 15, cell surface associated	NM_145650	-4.70	1.27E-03
8120833	SH3BGRL2	SH3 domain binding glutamic acid-rich protein like 2	NM_031469	-4.70	1.00E-05
8082012	SLC15A2	solute carrier family 15 (H+/peptide transporter), member 2	NM_021082	-4.70	3.61E-03
7951178	TRPC6	transient receptor potential cation channel, subfamily C, member 6	NM_004621	-4.70	1.42E-04
8125289	TNXA	tenascin XA pseudogene	NR_001284	-4.69	6.21E-04
7916789	WDR78	WD repeat domain 78	NM_024763	-4.68	1.50E-04
8179935	TNXB	tenascin XB	NM_032470	-4.63	6.63E-04
7981427	CKB	creatine kinase, brain	NM_001823	-4.63	6.49E-04
8078619	ITGA9	integrin, alpha 9	NM_002207	-4.63	2.04E-04
7958466	ACACB	acetyl-Coenzyme A carboxylase beta	NM_001093	-4.62	3.03E-03
8179399	C4A	complement component 4A (Rodgers blood group)	NM_007293	-4.62	5.49E-03
8079117	CCBP2	chemokine binding protein 2	NM_001296	-4.62	3.67E-03
8121181	FHL5	four and a half LIM domains 5	NM_020482	-4.61	5.61E-03
8080028	DOCK3	dedicator of cytokinesis 3	NM_004947	-4.60	2.55E-03
8171472	TMEM27	transmembrane protein 27	NM_020665	-4.58	4.43E-03
7897044	PRKCZ	protein kinase C, zeta	NM_002744	-4.56	7.80E-05
8088371	DNASE1L3	deoxyribonuclease I-like 3	NM_004944	-4.55	7.32E-03
8030582	MYH14	myosin, heavy chain 14	NM_001077186	-4.53	3.50E-05
8146794	DEPDC2	DEP domain containing 2	NM_024870	-4.52	4.00E-06
8112649	FAM169A	family with sequence similarity 169, member A	NM_015566	-4.52	0.00E+00
8077970	FBLN2	fibulin 2	NM_001004019	-4.51	1.05E-03
7960158	ZNF10	zinc finger protein 10	NM_015394	-4.50	1.11E-03
8134051	C7orf63	chromosome 7 open reading frame 63	NM_001039706	-4.47	1.24E-04
8177867	DDR1	discoidin domain receptor tyrosine kinase 1	NM_013993	-4.46	2.30E-05

8133770	CCDC146	coiled-coil domain containing 146	NM_020879	-4.44	1.78E-03
7975772	FAM164C	family with sequence similarity 164, member C	NM_024643	-4.42	1.89E-04
7945045	DDX25	DEAD (Asp-Glu-Ala-Asp) box polypeptide 25	NM_013264	-4.40	3.34E-03
7981968	SNORD116-10	small nucleolar RNA, C/D box 116-10	NR_003325	-4.40	1.13E-04
8168058	FAM155B	family with sequence similarity 155, member B	NM_015686	-4.38	1.86E-03
7905929	EFNA1	ephrin-A1	NM_004428	-4.36	3.10E-05
8091537	IGSF10	immunoglobulin superfamily, member 10	NM_178822	-4.35	7.31E-03
8043059	LOC200383	similar to Dynein heavy chain at 16F	BC015442	-4.35	4.30E-05
8169145	MUM1L1	melanoma associated antigen (mutated) 1-like 1	NM_152423	-4.33	4.94E-03
7951672	PIH1D2	PIH1 domain containing 2	NM_138789	-4.33	5.20E-05
8161964	FRMD3	FERM domain containing 3	NM_174938	-4.32	2.33E-03
8008321	ACSF2	acyl-CoA synthetase family member 2	NM_025149	-4.31	2.10E-05
7905283	ANXA9	annexin A9	NM_003568	-4.31	1.01E-03
8007454	RND2	Rho family GTPase 2	NM_005440	-4.29	1.43E-03
7981949	SNORD116-1	small nucleolar RNA, C/D box 116-1	NR_003316	-4.29	9.00E-06
8101874	ADH1A	alcohol dehydrogenase 1A (class I), alpha polypeptide	NM_000667	-4.28	8.30E-05
8082974	FAM62C	family with sequence similarity 62 (C2 domain containing), member C	NM_031913	-4.28	1.82E-03
8043504	MAL	mal, T-cell differentiation protein	NM_002371	-4.27	2.12E-03
8133258	WBSCR17	Williams-Beuren syndrome chromosome region 17	NM_022479	-4.27	1.63E-03
8076612	EFCAB6	EF-hand calcium binding domain 6	NM_022785	-4.25	1.00E-06
8143949	CRYGN	crystallin, gamma N	NM_144727	-4.24	3.26E-04
7982271	FAM7A1	family with sequence similarity 7, member A1	BC070492	-4.24	3.35E-04
8022145	L3MBTL4	l(3)mbt-like 4 (Drosophila)	NM_173464	-4.24	4.30E-05
8091600	PLCH1	phospholipase C, eta 1	NM_014996	-4.23	1.75E-03
8174444	IRS4	insulin receptor substrate 4	NM_003604	-4.23	8.72E-03
7981919	SNRPN	small nuclear ribonucleoprotein polypeptide N	NM_022807	-4.23	3.00E-06
7930861	CASC2	cancer susceptibility candidate 2	BC112326	-4.21	1.00E-06
8014349	CCL14	chemokine (C-C motif) ligand 14	NM_032962	-4.20	4.59E-04
8028266	ZNF540	zinc finger protein 540	NM_152606	-4.20	1.00E-05
8164766	C9orf98	chromosome 9 open reading frame 98	NM_152572	-4.18	7.38E-04
8111932	CCL28	chemokine (C-C motif) ligand 28	NM_148672	-4.18	2.85E-03
8123080	SYTL3	synaptotagmin-like 3	NM_001009991	-4.17	7.80E-05
8012830	TMEM220	transmembrane protein 220	NM_001004313	-4.17	0.00E+00
8098204	CPE	carboxypeptidase E	NM_001873	-4.16	3.00E-05
8097801	FAM160A1	family with sequence similarity 160, member A1	NM_001109977	-4.16	4.30E-05
7930311	GSTO2	glutathione S-transferase omega 2	NM_183239	-4.16	8.00E-06
7961507	ART4	ADP-ribosyltransferase 4 (Dombrock blood group)	NM_021071	-4.15	4.79E-03

8012126	CLDN7	claudin 7	NM_001307	-4.15	8.00E-06
8128837	C6orf186	chromosome 6 open reading frame 186	NM_001123364	-4.14	1.60E-03
8143629	OR2A9P	olfactory receptor, family 2, subfamily A, member 9 pseudogene	NR_002157	-4.14	1.83E-03
7968212	WASF3	WAS protein family, member 3	NM_006646	-4.14	6.00E-06
7928695	C10orf58	chromosome 10 open reading frame 58	NM_032333	-4.11	2.00E-06
8029489	BCAM	basal cell adhesion molecule (Lutheran blood group)	NM_005581	-4.09	2.29E-04
8161945	RASEF	RAS and EF-hand domain containing	NM_152573	-4.09	3.96E-03
8171313	ARHGAP6	Rho GTPase activating protein 6	NM_013427	-4.07	1.05E-04
7955441	METTL7A	methyltransferase like 7A	NM_014033	-4.07	2.00E-06
7938231	PPFIBP2	PTPRF interacting protein, binding protein 2 (liprin beta 2)	NM_003621	-4.07	0.00E+00
8097017	UGT8	UDP glycosyltransferase 8	NM_001128174	-4.05	5.68E-03
8092970	APOD	apolipoprotein D	NM_001647	-4.04	6.00E-06
8023646	BCL2	B-cell CLL/lymphoma 2	NM_000633	-4.02	4.00E-06
7985522	ADAMTSL3	ADAMTS-like 3	NM_207517	-4.01	0.00E+00
8001830	CMTM4	CKLF-like MARVEL transmembrane domain containing 4	NM_181521	-4.00	8.00E-06
8141950	RELN	reelin	NM_005045	-4.00	1.64E-03
8139680	COBL	cordon-bleu homolog (mouse)	NM_015198	-3.99	6.00E-06
7946641	GALNTL4	UDP-N-acetyl-alpha-D-galactosamine:polypeptide N-acetylgalactosaminyltransferase-like 4	NM_198516	-3.99	7.12E-03
8033190	SLC25A23	solute carrier family 25 (mitochondrial carrier; phosphate carrier), member 23	NM_024103	-3.98	6.00E-06
8031646	MGC9913	hypothetical protein MGC9913	BC008651	-3.97	2.00E-05
7898967	C1orf130	chromosome 1 open reading frame 130	NM_001010980	-3.96	2.28E-03
7981972	SNORD116-12	small nucleolar RNA, C/D box 116-12	NR_003327	-3.95	1.14E-03
8059350	AP1S3	adaptor-related protein complex 1, sigma 3 subunit	NM_001039569	-3.93	1.48E-04
8126770	CYP39A1	cytochrome P450, family 39, subfamily A, polypeptide 1	NM_016593	-3.93	3.13E-03
8133983	ADAM22	ADAM metallopeptidase domain 22	NM_021723	-3.91	1.72E-03
7981960	SNORD116-6	small nucleolar RNA, C/D box 116-6	NR_003321	-3.90	9.00E-06
8057821	DNAH7	dynein, axonemal, heavy chain 7	NM_018897	-3.87	5.62E-03
8145532	EPHX2	epoxide hydrolase 2, cytoplasmic	NM_001979	-3.87	1.00E-06
8109333	GPX3	glutathione peroxidase 3 (plasma)	NM_002084	-3.85	3.70E-05
8027793	LSR	lipolysis stimulated lipoprotein receptor	NM_205834	-3.85	8.18E-04
8167027	RGN	regucalcin (senescence marker protein-30)	NM_152869	-3.83	4.90E-05
8159501	LCN12	lipocalin 12	NM_178536	-3.82	6.76E-04
8119124	PI16	peptidase inhibitor 16	NM_153370	-3.82	3.79E-03
8018761	ST6GALNAC2	ST6 (alpha-N-acetyl-neuraminyl-2,3-beta-galactosyl-1,3)-N-acetylgalactosaminide alpha-2,6-sialyltransferase 2	NM_006456	-3.80	8.27E-03

8173059	WNK3	WNK lysine deficient protein kinase 3	NM_020922	-3.80	8.40E-05
8031632	ZNF542	zinc finger protein 542	NR_003127	-3.80	1.29E-04
8136983	OR2A20P	olfactory receptor, family 2, subfamily A, member 20 pseudogene	NR_002158	-3.79	1.99E-03
8101366	SCD5	stearoyl-CoA desaturase 5	NM_001037582	-3.79	5.60E-05
8098379	WDR17	WD repeat domain 17	NM_170710	-3.79	2.40E-05
8160889	CCL21	chemokine (C-C motif) ligand 21	NM_002989	-3.76	4.90E-05
8133938	CROT	carnitine O-octanoyltransferase	NM_021151	-3.76	2.02E-03
7936463	ABLIM1	actin binding LIM protein 1	NM_002313	-3.74	1.18E-04
7907160	ATP1B1	ATPase, Na+/K+ transporting, beta 1 polypeptide	NM_001677	-3.74	5.00E-06
7909285	PFKFB2	6-phosphofructo-2-kinase/fructose-2,6-biphosphatase 2	NM_006212	-3.74	4.80E-05
8079931	SLC38A3	solute carrier family 38, member 3	NM_006841	-3.74	1.80E-03
7947322	DCDC1	doublecortin domain containing 1	NM_181807	-3.72	5.22E-03
8013567	LOC201229	hypothetical protein LOC201229	NM_001076680	-3.72	2.41E-03
8117207	ALDH5A1	aldehyde dehydrogenase 5 family, member A1	NM_170740	-3.71	3.50E-05
7932721	LOC387646	leucine rich repeat containing 37, member A family pseudogene	NR_003525	-3.71	1.30E-05
7947147	SVIP	small VCP/p97-interacting protein	NM_148893	-3.71	1.70E-05
7977761	SALL2	sal-like 2 (Drosophila)	NM_005407	-3.70	3.37E-04
8114300	KLHL3	kelch-like 3 (Drosophila)	NM_017415	-3.69	6.27E-04
8048889	FBXO36	F-box protein 36	NM_174899	-3.69	2.80E-05
8131496	GLCCI1	glucocorticoid induced transcript 1	NM_138426	-3.69	1.46E-03
8112841	HOMER1	homer homolog 1 (Drosophila)	NM_004272	-3.69	3.10E-05
7937823	KCNQ1	potassium voltage-gated channel, KQT-like subfamily, member 1	NM_000218	-3.69	6.20E-05
8168650	PABPC5	poly(A) binding protein, cytoplasmic 5	NM_080832	-3.69	4.03E-03
8035793	ZNF737	zinc finger protein 737	XR_042310	-3.68	8.00E-06
8094184	C1QTNF7	C1q and tumor necrosis factor related protein 7	NM_031911	-3.67	5.27E-03
8099760	CENTD1	centaurin, delta 1	NM_015230	-3.67	2.01E-04
8176193	F8	coagulation factor VIII, procoagulant component	NM_000132	-3.67	4.99E-03
8088458	FHIT	fragile histidine triad gene	NM_002012	-3.67	7.55E-04
7988625	C15orf33	chromosome 15 open reading frame 33	NM_152647	-3.66	3.40E-05
8154043	DMRT3	doublesex and mab-3 related transcription factor 3	NM_021240	-3.66	3.48E-03
8168968	GPRASP1	G protein-coupled receptor associated sorting protein 1	NM_014710	-3.66	8.48E-04
8059955	RAB17	RAB17, member RAS oncogene family	NM_022449	-3.66	1.00E-06
8038213	HSD17B14	hydroxysteroid (17-beta) dehydrogenase 14	NM_016246	-3.65	6.96E-03
8023212	ZBTB7C	zinc finger and BTB domain containing 7C	NM_001039360	-3.63	1.05E-04
7897132	PRDM16	PR domain containing 16	NM_022114	-3.62	1.00E-06
7993126	ABAT	4-aminobutyrate aminotransferase	NM_020686	-3.61	2.80E-05
8113691	DTWD2	DTW domain containing 2	NM_173666	-3.61	5.80E-05

7993713	IQCK	IQ motif containing K	NM_153208	-3.60	1.00E-06
8149485	MTMR7	myotubularin related protein 7	NM_004686	-3.60	7.47E-03
8047577	ALS2CR8	amyotrophic lateral sclerosis 2 (juvenile) chromosome region, candidate 8	NM_024744	-3.59	1.00E-06
7998784	ABCA3	ATP-binding cassette, sub-family A (ABC1), member 3	NM_001089	-3.58	4.00E-06
7917612	HFM1	HFM1, ATP-dependent DNA helicase homolog (S. cerevisiae)	NM_001017975	-3.58	1.22E-04
8018264	C17orf28	chromosome 17 open reading frame 28	NM_030630	-3.57	1.07E-04
8004081	ZFP3	zinc finger protein 3 homolog (mouse)	NM_153018	-3.57	9.00E-06
8036079	DMKN	dermokine	NM_033317	-3.56	3.00E-06
7981951	SNORD116-2	small nucleolar RNA, C/D box 116-2	NR_003317	-3.56	1.53E-04
7913655	ID3	inhibitor of DNA binding 3, dominant negative helix-loop-helix protein	NM_002167	-3.55	7.00E-06
7946365	STK33	serine/threonine kinase 33	NM_030906	-3.55	1.00E-05
8065683	SNTA1	syntrophin, alpha 1 (dystrophin-associated protein A1, 59kDa, acidic component)	NM_003098	-3.54	2.90E-05
8118622	HSD17B8	hydroxysteroid (17-beta) dehydrogenase 8	NM_014234	-3.53	3.51E-03
8157949	RALGPS1	Ral GEF with PH domain and SH3 binding motif 1	NM_014636	-3.53	1.92E-03
8121729	PLN	phospholamban	NM_002667	-3.52	1.18E-03
8163202	SVEP1	sushi, von Willebrand factor type A, EGF and pentraxin domain containing 1	NM_153366	-3.52	1.40E-05
8027241	ZNF253	zinc finger protein 253	NM_021047	-3.52	1.67E-04
8123303	PACRG	PARK2 co-regulated	NM_152410	-3.51	7.60E-05
7915682	ZSWIM5	zinc finger, SWIM-type containing 5	NM_020883	-3.50	1.00E-05
8161265	IGFBPL1	insulin-like growth factor binding protein-like 1	NM_001007563	-3.49	3.37E-03
8017964	ABCA6	ATP-binding cassette, sub-family A (ABC1), member 6	NM_080284	-3.49	1.20E-05
8113666	SEMA6A	sema domain, transmembrane domain (TM), and cytoplasmic domain, (semaphorin) 6A	NM_020796	-3.49	9.56E-03
7986838	OCA2	oculocutaneous albinism II	NM_000275	-3.48	5.69E-03
8146967	CRISPLD1	cysteine-rich secretory protein LCCL domain containing 1	NM_031461	-3.47	2.09E-03
7909768	SPATA17	spermatogenesis associated 17	NM_138796	-3.47	1.47E-03
8124211	GPLD1	glycosylphosphatidylinositol specific phospholipase D1	NM_001503	-3.46	1.10E-05
8130645	PARK2	Parkinson disease (autosomal recessive, juvenile) 2, parkin	NM_004562	-3.46	5.06E-04
7980636	EML5	echinoderm microtubule associated protein like 5	NM_183387	-3.45	1.36E-03
8021966	ENOSF1	enolase superfamily member 1	NM_017512	-3.44	1.45E-03
8100393	KDR	kinase insert domain receptor (a type III receptor tyrosine kinase)	NM_002253	-3.43	4.99E-03
7959070	PEBP1	phosphatidylethanolamine binding protein 1	NM_002567	-3.43	1.39E-04
7936439	AFAP1L2	actin filament associated protein 1-like 2	NM_001001936	-3.42	5.10E-05
7944603	GRIK4	glutamate receptor, ionotropic, kainate 4	NM_014619	-3.42	9.29E-03
8146687	ADHFE1	alcohol dehydrogenase, iron containing, 1	NM_144650	-3.41	3.02E-04

7957386	ACSS3	acyl-CoA synthetase short-chain family member 3	NM_024560	-3.39	7.10E-05
8165334	CLIC3	chloride intracellular channel 3	NM_004669	-3.39	1.41E-03
8094759	NSUN7	NOL1/NOP2/Sun domain family, member 7	NM_024677	-3.38	8.00E-06
8171359	GPM6B	glycoprotein M6B	NM_001001995	-3.37	3.54E-04
7915425	ZMYND12	zinc finger, MYND-type containing 12	NM_032257	-3.37	1.35E-03
7931930	PRKCQ	protein kinase C, theta	NM_006257	-3.36	2.40E-05
7932118	C10orf30	chromosome 10 open reading frame 30	NM_152751	-3.36	1.39E-04
7982206	GOLGA9P	golgi autoantigen, golgin subfamily a, 9 pseudogene	ENST00000342314	-3.36	2.80E-03
7912537	DHRS3	dehydrogenase/reductase (SDR family) member 3	NM_004753	-3.34	3.00E-06
8156770	GALNT12	UDP-N-acetyl-alpha-D-galactosamine:polypeptide N-acetylgalactosaminyltransferase 12 (GalNAc-T12)	NM_024642	-3.34	8.00E-06
8122660	UST	uronyl-2-sulfotransferase	NM_005715	-3.33	5.10E-05
7899029	MAN1C1	mannosidase, alpha, class 1C, member 1	NM_020379	-3.32	4.58E-03
8003814	ASPA	aspartoacylase (Canavan disease)	NM_000049	-3.31	4.09E-03
8077299	CNTN6	contactin 6	NM_014461	-3.31	4.84E-03
8167690	RP11-114H20.1	hypothetical LOC401589	AK096379	-3.31	1.63E-04
8031650	ZNF471	zinc finger protein 471	NM_020813	-3.31	3.66E-04
8023267	MYO5B	myosin VB	NM_001080467	-3.29	1.09E-04
8098041	TMEM144	transmembrane protein 144	NM_018342	-3.29	1.51E-04
7957404	C12orf26	chromosome 12 open reading frame 26	BC029120	-3.28	5.00E-06
8099817	FLJ13197	hypothetical FLJ13197	AK023259	-3.28	2.20E-03
8128123	RRAGD	Ras-related GTP binding D	NM_021244	-3.27	5.00E-06
7920297	S100A14	S100 calcium binding protein A14	NM_020672	-3.27	2.33E-03
8058570	C2orf67	chromosome 2 open reading frame 67	NM_152519	-3.25	8.00E-06
8043393	THNSL2	threonine synthase-like 2 (S. cerevisiae)	NM_018271	-3.25	6.38E-04
8090823	SLCO2A1	solute carrier organic anion transporter family, member 2A1	NM_005630	-3.24	1.20E-04
7922130	DPT	dermatopontin	NM_001937	-3.24	3.89E-03
7961798	SOX5	SRY (sex determining region Y)-box 5	NM_152989	-3.24	9.20E-05
8091629	C3orf33	chromosome 3 open reading frame 33	AK289890	-3.23	8.80E-05
8027312	ZNF429	zinc finger protein 429	NM_001001415	-3.23	5.56E-03
7911096	EFCAB2	EF-hand calcium binding domain 2	NM_032328	-3.22	1.80E-05
7902565	LPHN2	latrophilin 2	NM_012302	-3.22	1.09E-04
8007493	ARL4D	ADP-ribosylation factor-like 4D	NM_001661	-3.21	3.93E-04
8101957	EMCN	endomucin	NM_016242	-3.21	7.98E-04
7996081	GPR56	G protein-coupled receptor 56	NM_201524	-3.21	2.86E-04
8138258	VWDE	von Willebrand factor D and EGF domains	AK027618	-3.21	1.16E-04
7917875	F3	coagulation factor III (thromboplastin, tissue factor)	NM_001993	-3.20	1.52E-03

8097307	INTU	inturned planar cell polarity effector homolog (Drosophila)	NM_015693	-3.20	9.00E-06
7981994	SNORD116-23	small nucleolar RNA, C/D box 116-23	NR_003337	-3.20	8.80E-05
8027254	ZNF90	zinc finger protein 90	AK298173	-3.19	5.75E-04
7971590	CAB39L	calcium binding protein 39-like	NM_030925	-3.18	2.67E-04
7977621	NDRG2	NDRG family member 2	NM_201540	-3.17	1.91E-04
7966690	TBX3	T-box 3	NM_016569	-3.17	4.50E-05
7901993	CACHD1	cache domain containing 1	NM_020925	-3.16	3.00E-06
7973875	NPAS3	neuronal PAS domain protein 3	NM_022123	-3.16	1.70E-05
8054740	PAX8	paired box 8	NM_003466	-3.16	1.14E-03
7981996	SNORD116-24	small nucleolar RNA, C/D box 116-24	NR_003338	-3.15	1.89E-04
7953200	CCND2	cyclin D2	NM_001759	-3.13	6.00E-06
8167930	FAAH2	fatty acid amide hydrolase 2	NM_174912	-3.13	6.40E-05
8099612	GPR125	G protein-coupled receptor 125	NM_145290	-3.13	2.00E-06
7984626	SENP8	SUMO/sentrin specific peptidase family member 8	NM_145204	-3.13	3.33E-03
8074432	HIRA	HIR histone cell cycle regulation defective homolog A (S. cerevisiae)	NM_003325	-3.12	4.83E-03
8125149	SLC44A4	solute carrier family 44, member 4	NM_025257	-3.12	1.64E-04
7975779	FOS	v-fos FBJ murine osteosarcoma viral oncogene homolog	NM_005252	-3.11	9.02E-03
8163149	PTPN3	protein tyrosine phosphatase, non-receptor type 3	NM_002829	-3.10	8.80E-05
8002992	C16orf46	chromosome 16 open reading frame 46	NM_152337	-3.09	3.90E-05
8084880	HES1	hairy and enhancer of split 1, (Drosophila)	NM_005524	-3.09	4.50E-05
7916493	PPAP2B	phosphatidic acid phosphatase type 2B	NM_003713	-3.09	5.90E-05
7901256	CYP4B1	cytochrome P450, family 4, subfamily B, polypeptide 1	NM_001099772	-3.08	2.00E-06
7902617	SAMD13	sterile alpha motif domain containing 13	NM_001010971	-3.07	6.57E-03
8104856	SPEF2	sperm flagellar 2	NM_024867	-3.07	9.20E-05
8157976	GARNL3	GTPase activating Rap/RanGAP domain-like 3	NM_032293	-3.06	3.83E-04
8146391	LOC644334	similar to hCG2040198	XM_001714497	-3.06	7.13E-04
8067932	C21orf34	chromosome 21 open reading frame 34	NM_001005732	-3.04	3.80E-03
8177222	CD24	CD24 molecule	NM_013230	-3.04	1.25E-03
7939620	GYLTL1B	glycosyltransferase-like 1B	NM_152312	-3.04	2.70E-05
7982299	LOC390561	similar to hect domain and RLD 2	ENST00000220188	-3.04	2.26E-03
7939411	C11orf74	chromosome 11 open reading frame 74	AK290833	-3.03	1.51E-03
8057004	PDE11A	phosphodiesterase 11A	NM_001077197	-3.02	5.77E-03
7990138	GRAMD2	GRAM domain containing 2	NM_001012642	-3.01	3.86E-03
7906954	PBX1	pre-B-cell leukemia homeobox 1	NM_002585	-3.01	1.55E-04
8035782	ZNF682	zinc finger protein 682	NM_033196	-3.01	9.42E-03
8081903	C3orf15	chromosome 3 open reading frame 15	NM_033364	-2.99	1.02E-03
7976084	SPATA7	spermatogenesis associated 7	NM_018418	-2.99	4.46E-03

7949570	GAL3ST3	galactose-3-O-sulfotransferase 3	NM_033036	-2.98	8.00E-06
8044813	TMEM37	transmembrane protein 37	NM_183240	-2.98	1.76E-03
8039044	ZNF415	zinc finger protein 415	NM_018355	-2.98	1.00E-04
8013331	B9D1	B9 protein domain 1	NM_015681	-2.97	5.00E-05
8174527	CAPN6	calpain 6	NM_014289	-2.97	3.65E-03
7952436	ESAM	endothelial cell adhesion molecule	NM_138961	-2.96	8.40E-05
7964759	GRIP1	glutamate receptor interacting protein 1	NM_021150	-2.96	1.69E-03
7966046	MTERFD3	MTERF domain containing 3	NM_001033050	-2.96	7.20E-03
8173755	ITM2A	integral membrane protein 2A	NM_004867	-2.95	4.43E-03
8174239	BEX2	brain expressed X-linked 2	NM_032621	-2.95	1.42E-03
7925342	ERO1LB	ERO1-like beta (S. cerevisiae)	NM_019891	-2.95	2.06E-03
8090872	KY	kyphoscoliosis peptidase	NM_178554	-2.94	2.18E-04
7899407	SMPDL3B	sphingomyelin phosphodiesterase, acid-like 3B	NM_014474	-2.94	7.23E-03
8045229	ARHGEF4	Rho guanine nucleotide exchange factor (GEF) 4	NM_032995	-2.93	7.90E-05
8134036	STEAP2	six transmembrane epithelial antigen of the prostate 2	NM_152999	-2.92	5.00E-06
8071981	CTA-221G9.4	KIAA1671 protein	AB051458	-2.92	5.90E-05
8056376	SCN3A	sodium channel, voltage-gated, type III, alpha subunit	NM_006922	-2.92	7.01E-03
8167957	ZC3H12B	zinc finger CCCH-type containing 12B	NM_001010888	-2.92	2.45E-04
8173647	ZDHHC15	zinc finger, DHHC-type containing 15	NM_144969	-2.92	5.26E-04
8121193	KLHL32	kelch-like 32 (Drosophila)	NM_052904	-2.91	9.70E-03
8135211	MGC35361	hypothetical MGC35361	AK298753	-2.91	2.09E-03
7930454	PDCD4	programmed cell death 4 (neoplastic transformation inhibitor)	NM_145341	-2.90	3.00E-06
8035773	ZNF506	zinc finger protein 506	NM_001099269	-2.90	1.00E-06
8134351	PPP1R9A	protein phosphatase 1, regulatory (inhibitor) subunit 9A	NM_017650	-2.89	1.79E-03
7945169	TMEM45B	transmembrane protein 45B	NM_138788	-2.89	1.75E-03
8066745	ZNF334	zinc finger protein 334	NM_199441	-2.89	6.00E-06
7999909	GPRC5B	G protein-coupled receptor, family C, group 5, member B	NM_016235	-2.88	1.00E-04
8076185	CBX7	chromobox homolog 7	NM_175709	-2.87	2.81E-03
8006906	ERBB2	v-erb-b2 erythroblastic leukemia viral oncogene homolog 2, neuro/glioblastoma derived oncogene homolog (avian)	NM_001005862	-2.87	1.63E-04
8168976	GPRASP2	G protein-coupled receptor associated sorting protein 2	NM_001004051	-2.87	5.90E-05
8089970	ILDR1	immunoglobulin-like domain containing receptor 1	NM_175924	-2.87	7.97E-04
7962455	NELL2	NEL-like 2 (chicken)	NM_006159	-2.87	8.47E-03
8020844	ASXL3	additional sex combs like 3 (Drosophila)	NM_030632	-2.86	1.96E-03
8081171	DKFZp667G2110	hypothetical protein DKFZp667G2110	NM_153605	-2.85	6.31E-03
8077198	FLJ43315	similar to Asparagine synthetase [glutamine-hydrolyzing] (Glutamine-dependent asparagine synthetase) (TS11 cell cycle control protein)	BC057848	-2.85	7.17E-03

8071036	S100B	S100 calcium binding protein B	NM_006272	-2.85	4.20E-05
8013243	SHMT1	serine hydroxymethyltransferase 1 (soluble)	NM_004169	-2.85	1.57E-04
8132092	INMT	indolethylamine N-methyltransferase	NM_006774	-2.84	4.34E-03
8179762	ATP6V1G2	ATPase, H+ transporting, lysosomal 13kDa, V1 subunit G2	NM_130463	-2.84	1.19E-04
7984380	IQCH	IQ motif containing H	NM_001031715	-2.84	2.00E-06
7997332	NUDT7	nudix (nucleoside diphosphate linked moiety X)-type motif 7	NM_001105663	-2.84	1.00E-06
8027260	ZNF486	zinc finger protein 486	NM_052852	-2.84	3.69E-03
7999079	ADCY9	adenylate cyclase 9	NM_001116	-2.83	5.19E-03
7951781	C11orf71	chromosome 11 open reading frame 71	BC071695	-2.83	7.79E-04
7964997	CAPS2	calcyphosine 2	NM_032606	-2.83	1.31E-03
8042079	CCDC85A	coiled-coil domain containing 85A	NM_001080433	-2.82	9.00E-06
7947599	CHST1	carbohydrate (keratan sulfate Gal-6) sulfotransferase 1	NM_003654	-2.82	3.70E-03
7967933	IFT88	intraflagellar transport 88 homolog (Chlamydomonas)	NM_175605	-2.82	4.11E-03
8122222	PDE7B	phosphodiesterase 7B	NM_018945	-2.82	2.63E-03
8071676	RAB36	RAB36, member RAS oncogene family	NM_004914	-2.82	1.70E-05
8098856	RNF212	ring finger protein 212	NM_194439	-2.82	5.91E-03
8112740	ZBED3	zinc finger, BED-type containing 3	NM_032367	-2.82	3.27E-04
8022338	DISP2	dispatched homolog 2 (Drosophila)	AL359580	-2.81	5.10E-05
8025984	ZNF844	zinc finger protein 844	BC125186	-2.81	1.70E-05
8058350	ICA1L	islet cell autoantigen 1,69kDa-like	NM_138468	-2.80	2.60E-05
8018038	ABCA5	ATP-binding cassette, sub-family A (ABC1), member 5	NM_018672	-2.79	4.80E-03
8008172	B4GALNT2	beta-1,4-N-acetyl-galactosaminyl transferase 2	NM_153446	-2.79	6.90E-05
8108753	PCDHB15	protocadherin beta 15	NM_018935	-2.79	8.30E-03
7972157	EDNRB	endothelin receptor type B	NM_001122659	-2.78	7.98E-04
8146533	FAM110B	family with sequence similarity 110, member B	NM_147189	-2.78	3.04E-03
8077376	ITPR1	inositol 1,4,5-triphosphate receptor, type 1	NM_001099952	-2.78	3.50E-05
7953765	FAM80B	family with sequence similarity 80, member B	NM_020734	-2.76	2.52E-03
8056151	PLA2R1	phospholipase A2 receptor 1, 180kDa	NM_007366	-2.76	7.83E-03
7969414	KLF5	Kruppel-like factor 5 (intestinal)	NM_001730	-2.74	1.56E-04
8164008	C9orf45	chromosome 9 open reading frame 45	AF251293	-2.73	4.58E-03
7983828	TEX9	testis expressed 9	NM_198524	-2.73	7.30E-05
8114249	CXCL14	chemokine (C-X-C motif) ligand 14	NM_004887	-2.72	2.42E-03
8102532	PDE5A	phosphodiesterase 5A, cGMP-specific	NM_001083	-2.72	3.93E-04
8021150	IER3IP1	immediate early response 3 interacting protein 1	AF119875	-2.72	3.90E-05
7922717	RGS16	regulator of G-protein signaling 16	NM_002928	-2.72	6.97E-03
7951521	C11orf65	chromosome 11 open reading frame 65	NM_152587	-2.71	2.47E-03
7916229	ECHDC2	enoyl Coenzyme A hydratase domain containing 2	NM_018281	-2.71	7.50E-05

7971335	CCDC122	coiled-coil domain containing 122	NM_144974	-2.70	9.18E-03
8015412	JUP	junction plakoglobin	NM_002230	-2.70	3.27E-03
7982054	SNORD115-24	small nucleolar RNA, C/D box 115-24	NR_003495	-2.70	9.73E-03
8120826	IRAK1BP1	interleukin-1 receptor-associated kinase 1 binding protein 1	NM_001010844	-2.69	2.15E-04
7914923	C1orf102	chromosome 1 open reading frame 102	NM_145047	-2.68	3.26E-04
7936144	COL17A1	collagen, type XVII, alpha 1	NM_000494	-2.68	9.62E-03
8111136	FAM134B	family with sequence similarity 134, member B	NM_001034850	-2.68	2.34E-04
8091087	NMNAT3	nicotinamide nucleotide adenylyltransferase 3	NM_178177	-2.68	9.50E-05
8021275	POLI	polymerase (DNA directed) iota	NM_007195	-2.68	1.25E-04
7930170	C10orf32	chromosome 10 open reading frame 32	BC015994	-2.67	1.44E-03
8117572	ZNF391	zinc finger protein 391	NM_001076781	-2.67	1.59E-03
7998542	IFT140	intraflagellar transport 140 homolog (Chlamydomonas)	NM_014714	-2.66	1.20E-05
8035765	ZNF14	zinc finger protein 14	NM_021030	-2.66	5.05E-03
7970763	FLT1	fms-related tyrosine kinase 1 (vascular endothelial growth factor/vascular permeability factor receptor)	NM_002019	-2.65	5.12E-04
8081758	GRAMD1C	GRAM domain containing 1C	NM_017577	-2.65	2.92E-03
7982723	IVD	isovaleryl Coenzyme A dehydrogenase	NM_002225	-2.65	6.43E-04
7997352	WWOX	WW domain containing oxidoreductase	NM_016373	-2.65	1.08E-04
7952046	MPZL2	myelin protein zero-like 2	NM_144765	-2.63	9.95E-04
8148580	C8orf31	chromosome 8 open reading frame 31	BC073830	-2.63	8.57E-04
7989055	DYX1C1	dyslexia susceptibility 1 candidate 1	NM_130810	-2.63	3.98E-04
8101728	FAM13A1	family with sequence similarity 13, member A1	NM_014883	-2.63	2.42E-04
8086908	PLXNB1	plexin B1	NM_002673	-2.63	4.44E-04
8102567	PRDM5	PR domain containing 5	NM_018699	-2.63	4.02E-04
7905299	PRUNE	prune homolog (Drosophila)	NM_021222	-2.63	1.10E-05
8102938	RNF150	ring finger protein 150	NM_020724	-2.62	2.12E-04
7947649	CHRM4	cholinergic receptor, muscarinic 4	NM_000741	-2.62	5.40E-05
8144701	LOC100131581	hypothetical LOC100131581	AK092544	-2.62	4.40E-03
8141872	NAPEPLD	N-acyl phosphatidylethanolamine phospholipase D	NM_001122838	-2.62	3.50E-05
8032553	TLE2	transducin-like enhancer of split 2 (E(sp1) homolog, Drosophila)	NM_003260	-2.62	5.90E-05
8027368	ZNF254	zinc finger protein 254	NM_203282	-2.62	3.43E-03
7957688	C12orf63	chromosome 12 open reading frame 63	NM_198520	-2.61	5.90E-03
8081657	CD200	CD200 molecule	NM_001004196	-2.61	4.91E-03
7969488	CLN5	ceroid-lipofuscinosis, neuronal 5	NM_006493	-2.61	2.02E-04
8100507	HOPX	HOP homeobox	NM_032495	-2.61	1.05E-03
8083471	SGEF	Src homology 3 domain-containing guanine nucleotide exchange factor	NM_015595	-2.61	1.65E-04
8169009	BEX4	BEX family member 4	NM_001080425	-2.60	4.10E-04

8154295	IL33	interleukin 33	NM_033439	-2.60	1.94E-03
8002029	ZDHHC1	zinc finger, DHHC-type containing 1	NM_013304	-2.60	2.40E-03
8122860	MYCT1	myc target 1	NM_025107	-2.59	1.38E-04
8085164	SRGAP3	SLIT-ROBO Rho GTPase activating protein 3	NM_014850	-2.59	7.63E-03
7935011	CPEB3	cytoplasmic polyadenylation element binding protein 3	NM_014912	-2.58	4.28E-03
8076025	PLA2G6	phospholipase A2, group VI (cytosolic, calcium-independent)	NM_003560	-2.58	1.33E-04
8028206	ZNF345	zinc finger protein 345	NM_003419	-2.58	1.00E-06
8030931	ZNF528	zinc finger protein 528	NM_032423	-2.58	8.10E-05
7995825	MT1F	metallothionein 1F	NM_005949	-2.57	7.60E-05
7974920	SYNE2	spectrin repeat containing, nuclear envelope 2	NM_182914	-2.57	1.25E-03
8170602	ZNF185	zinc finger protein 185 (LIM domain)	NM_007150	-2.57	6.70E-05
7941639	BBS1	Bardet-Biedl syndrome 1	NM_024649	-2.56	1.30E-05
8099302	MIR95	microRNA 95	NR_029511	-2.56	6.61E-03
8039645	ZNF772	zinc finger protein 772	NM_001024596	-2.56	2.00E-06
8126729	CLIC5	chloride intracellular channel 5	NM_001114086	-2.55	4.26E-04
7974270	SPG3A	spastic paraplegia 3A (autosomal dominant)	NM_015915	-2.55	6.91E-03
8152962	LRRC6	leucine rich repeat containing 6	NM_012472	-2.54	1.58E-04
8008263	PDK2	pyruvate dehydrogenase kinase, isozyme 2	NM_002611	-2.54	9.00E-06
8044849	PTPN4	protein tyrosine phosphatase, non-receptor type 4 (megakaryocyte)	NM_002830	-2.54	9.11E-03
7915955	SPATA6	spermatogenesis associated 6	NM_019073	-2.54	7.60E-05
8172022	TMEM47	transmembrane protein 47	NM_031442	-2.54	2.77E-04
7959751	ZNF664	zinc finger protein 664	NM_152437	-2.54	1.20E-05
8047006	ANKAR	ankyrin and armadillo repeat containing	NM_144708	-2.53	9.60E-05
8103079	LOC90826	hypothetical protein BC004337	AK292904	-2.53	3.69E-03
8121015	C6orf165	chromosome 6 open reading frame 165	BC035083	-2.52	2.06E-04
8050846	DTNB	dystrobrevin, beta	NM_021907	-2.52	3.50E-05
7964602	LRIG3	leucine-rich repeats and immunoglobulin-like domains 3	NM_153377	-2.52	3.17E-04
8047248	PLCL1	phospholipase C-like 1	NM_001114661	-2.52	8.13E-04
7930148	SFXN2	sideroflexin 2	NM_178858	-2.52	8.10E-05
7927915	STOX1	storkhead box 1	NM_152709	-2.52	5.49E-03
8138202	ICA1	islet cell autoantigen 1, 69kDa	NM_004968	-2.51	7.06E-03
8121632	KPNA5	karyopherin alpha 5 (importin alpha 6)	NM_002269	-2.51	3.00E-05
7909877	MOSC1	MOCO sulphurase C-terminal domain containing 1	NM_022746	-2.51	1.22E-03
8162696	XPA	xeroderma pigmentosum, complementation group A	NM_000380	-2.51	1.25E-04
8133860	GNAI1	guanine nucleotide binding protein (G protein), alpha inhibiting activity polypeptide 1	NM_002069	-2.50	3.51E-03
8077958	HDAC11	histone deacetylase 11	NM_024827	-2.49	6.92E-03

8036304	ZFP14	zinc finger protein 14 homolog (mouse)	NM_020917	-2.49	1.08E-04
8038904	ZNF577	zinc finger protein 577	NM_032679	-2.49	2.40E-05
7907297	FMO4	flavin containing monooxygenase 4	NM_002022	-2.48	4.00E-06
8089659	KIAA1407	KIAA1407	AK302488	-2.48	2.00E-06
8141882	DPY19L2P2	dpy-19-like 2 pseudogene 2 (C. elegans)	NR_003561	-2.47	9.05E-04
8014871	PERLD1	per1-like domain containing 1	NM_033419	-2.47	1.30E-05
7981976	SNORD116-14	small nucleolar RNA, C/D box 116-14	NR_003329	-2.47	8.13E-04
8044450	ZC3H6	zinc finger CCCH-type containing 6	NM_198581	-2.47	1.11E-03
7933139	ZNF33B	zinc finger protein 33B	NM_006955	-2.47	9.89E-03
8088602	MAGI1	membrane associated guanylate kinase, WW and PDZ domain containing 1	NM_015520	-2.46	3.60E-05
8142663	NDUFA5	NADH dehydrogenase (ubiquinone) 1 alpha subcomplex, 5, 13kDa	NM_005000	-2.46	4.10E-05
8132917	ZNF713	zinc finger protein 713	NM_182633	-2.46	2.20E-05
8065444	ACSS1	acyl-CoA synthetase short-chain family member 1	NM_032501	-2.45	5.99E-03
8065280	C20orf74	chromosome 20 open reading frame 74	NM_020343	-2.45	6.40E-05
7902965	BTBD8	BTB (POZ) domain containing 8	NM_183242	-2.44	7.08E-04
7918426	SLC16A4	solute carrier family 16, member 4 (monocarboxylic acid transporter 5)	NM_004696	-2.44	1.18E-03
8056995	TTC30B	tetratricopeptide repeat domain 30B	NM_152517	-2.44	5.96E-03
8111677	LIFR	leukemia inhibitory factor receptor alpha	NM_002310	-2.43	4.06E-04
8147469	PGCP	plasma glutamate carboxypeptidase	NM_016134	-2.43	0.00E+00
8096176	PTPN13	protein tyrosine phosphatase, non-receptor type 13 (APO-1/CD95 (Fas)-associated phosphatase)	NM_080683	-2.43	1.60E-03
7966448	TMEM116	transmembrane protein 116	NM_138341	-2.43	8.19E-04
7933092	ZNF248	zinc finger protein 248	NM_021045	-2.43	4.00E-06
8025978	ZNF763	zinc finger protein 763	NM_001012753	-2.43	6.02E-03
8100578	EPHA5	EPH receptor A5	NM_004439	-2.42	1.11E-03
7966760	FBXO21	F-box protein 21	NM_033624	-2.42	1.00E-05
7981895	GOLGA8E	golgi autoantigen, golgin subfamily a, 8E	NM_001012423	-2.42	1.55E-03
7909841	MARK1	MAP/microtubule affinity-regulating kinase 1	NM_018650	-2.42	1.40E-05
8046099	NOSTRIN	nitric oxide synthase trafficker	NM_001039724	-2.42	4.15E-03
7980891	TC2N	tandem C2 domains, nuclear	NM_001128596	-2.42	7.67E-04
7901613	ACOT11	acyl-CoA thioesterase 11	NM_147161	-2.41	6.87E-03
7951077	SESN3	sestrin 3	NM_144665	-2.41	6.00E-04
7936835	CPXM2	carboxypeptidase X (M14 family), member 2	NM_198148	-2.40	9.40E-05
8078386	GPD1L	glycerol-3-phosphate dehydrogenase 1-like	NM_015141	-2.40	4.08E-04
8057719	HIBCH	3-hydroxyisobutyryl-Coenzyme A hydrolase	NM_014362	-2.40	2.68E-03
7942007	LRP5	low density lipoprotein receptor-related protein 5	NM_002335	-2.40	2.29E-04
7911263	OR2M5	olfactory receptor, family 2, subfamily M, member 5	NM_001004690	-2.40	2.70E-05

7939569	PRDM11	PR domain containing 11	NM_020229	-2.40	8.84E-04
8031857	ZNF135	zinc finger protein 135	NM_003436	-2.40	9.70E-05
8039730	ZSCAN18	zinc finger and SCAN domain containing 18	NM_023926	-2.40	2.60E-05
8165974	CLCN4	chloride channel 4	NM_001830	-2.39	2.17E-03
8123407	MLLT4	myeloid/lymphoid or mixed-lineage leukemia (trithorax homolog, Drosophila); translocated to, 4	NM_001040001	-2.39	4.18E-04
8140915	PEX1	peroxisomal biogenesis factor 1	NM_000466	-2.39	1.10E-05
8049969	SH3YL1	SH3 domain containing, Ysc84-like 1 (S. cerevisiae)	NM_015677	-2.39	3.27E-03
7958692	TCTN1	tectonic family member 1	NM_001082538	-2.39	1.63E-04
8013159	TOM1L2	target of myb1-like 2 (chicken)	NM_001082968	-2.39	9.00E-06
8133062	ZNF273	zinc finger protein 273	NR_003099	-2.39	9.40E-05
8009568	TTYH2	tweety homolog 2 (Drosophila)	NM_032646	-2.38	3.34E-03
8174576	AMOT	angiomotin	NM_133265	-2.38	3.24E-04
8008629	DGKE	diacylglycerol kinase, epsilon 64kDa	NM_003647	-2.38	1.22E-04
7966839	FLJ20674	hypothetical protein FLJ20674	BC034471	-2.38	4.96E-04
8068024	JAM2	junctional adhesion molecule 2	NM_021219	-2.38	1.08E-04
8171229	PNPLA4	patatin-like phospholipase domain containing 4	NM_004650	-2.38	5.78E-03
8089701	ZBTB20	zinc finger and BTB domain containing 20	NM_015642	-2.38	5.19E-04
8027292	ZNF431	zinc finger protein 431	NM_133473	-2.38	3.99E-03
8140129	ABHD11	abhydrolase domain containing 11	NM_148912	-2.37	1.25E-04
8102247	FLJ37673	hypothetical protein FLJ37673	AK298931	-2.37	9.21E-03
7898957	RCAN3	RCAN family member 3	NM_013441	-2.37	1.50E-05
8070083	TMEM50B	transmembrane protein 50B	NM_006134	-2.37	5.07E-03
8163086	C9orf5	chromosome 9 open reading frame 5	NM_032012	-2.36	3.80E-05
8103622	CBR4	carbonyl reductase 4	NM_032783	-2.36	7.03E-03
8081503	DZIP3	DAZ interacting protein 3, zinc finger	NM_014648	-2.36	3.60E-05
8113413	NUDT12	nudix (nucleoside diphosphate linked moiety X)-type motif 12	NM_031438	-2.36	5.40E-04
8124134	TPMT	thiopurine S-methyltransferase	NM_000367	-2.36	3.00E-06
8035297	PLVAP	plasmalemma vesicle associated protein	NM_031310	-2.35	8.30E-05
7951545	EXPH5	exophilin 5	NM_015065	-2.35	2.36E-04
8133504	GTF2I	general transcription factor II, i	NM_032999	-2.35	1.10E-05
8117020	MYLIP	myosin regulatory light chain interacting protein	NM_013262	-2.35	2.73E-04
8136580	RAB19	RAB19, member RAS oncogene family	NM_001008749	-2.35	4.54E-04
7977965	SLC22A17	solute carrier family 22, member 17	NM_016609	-2.35	5.25E-04
7973850	AKAP6	A kinase (PRKA) anchor protein 6	NM_004274	-2.34	4.89E-04
7903777	GSTM5	glutathione S-transferase M5	NM_000851	-2.34	4.76E-03
7942400	P2RY2	purinergic receptor P2Y, G-protein coupled, 2	NM_176072	-2.34	1.82E-04

8043522	PROM2	prominin 2	NM_144707	-2.34	9.73E-04
8164013	STRBP	spermatid perinuclear RNA binding protein	NM_018387	-2.34	9.20E-05
8005638	ALDH3A2	aldehyde dehydrogenase 3 family, member A2	NM_001031806	-2.33	2.27E-04
8095986	ANXA3	annexin A3	NM_005139	-2.33	2.92E-03
8162610	CDC14B	CDC14 cell division cycle 14 homolog B (S. cerevisiae)	NM_033331	-2.33	1.20E-05
7909164	CTSE	cathepsin E	NM_001910	-2.33	6.47E-03
8058498	FZD5	frizzled homolog 5 (Drosophila)	NM_003468	-2.33	3.03E-04
7954077	KIAA1467	KIAA1467	NM_020853	-2.33	1.22E-04
8066161	C20orf132	chromosome 20 open reading frame 132	NM_152503	-2.32	9.20E-05
7910047	DNAH14	dynein, axonemal, heavy chain 14	ENST00000330118	-2.32	2.52E-03
7937039	EBF3	early B-cell factor 3	NM_001005463	-2.32	8.00E-06
8139057	ELMO1	engulfment and cell motility 1	NM_014800	-2.32	1.39E-04
7985221	LOC646934	similar to golgin-like protein	XR_018310	-2.32	1.29E-04
7920744	PKLR	pyruvate kinase, liver and RBC	NM_000298	-2.32	1.84E-04
8056999	TTC30A	tetratricopeptide repeat domain 30A	NM_152275	-2.32	1.49E-03
8151496	ZNF704	zinc finger protein 704	NM_001033723	-2.32	2.53E-03
7913694	FUCA1	fucosidase, alpha-L- 1, tissue	NM_000147	-2.31	1.30E-04
8002481	HYDIN	hydrocephalus inducing homolog (mouse)	NM_032821	-2.31	6.32E-03
8058670	IKZF2	IKAROS family zinc finger 2 (Helios)	NM_016260	-2.31	2.39E-03
8142332	IMMP2L	IMP2 inner mitochondrial membrane peptidase-like (S. cerevisiae)	NM_032549	-2.31	5.57E-04
8046186	KLHL23	kelch-like 23 (Drosophila)	NM_144711	-2.31	2.34E-03
8109490	SGCD	sarcoglycan, delta (35kDa dystrophin-associated glycoprotein)	NM_000337	-2.31	1.24E-03
8007799	CRHR1	corticotropin releasing hormone receptor 1	AK295559	-2.30	2.11E-04
7935882	FBXW4	F-box and WD repeat domain containing 4	NM_022039	-2.30	4.55E-03
8114778	GCSH	glycine cleavage system protein H (aminomethyl carrier)	NM_004483	-2.30	1.80E-05
7972021	TBC1D4	TBC1 domain family, member 4	NM_014832	-2.29	5.40E-05
8122827	C6orf97	chromosome 6 open reading frame 97	NM_025059	-2.29	6.62E-03
8016159	DCAKD	dephospho-CoA kinase domain containing	NM_024819	-2.29	2.46E-04
8159373	FAM69B	family with sequence similarity 69, member B	BC032097	-2.29	3.64E-04
8164087	NR6A1	nuclear receptor subfamily 6, group A, member 1	NM_033334	-2.29	7.00E-06
8158671	ASS1	argininosuccinate synthetase 1	NM_000050	-2.28	1.69E-03
8164742	DDX31	DEAD (Asp-Glu-Ala-Asp) box polypeptide 31	NM_022779	-2.28	3.14E-03
8060196	MTERFD2	MTERF domain containing 2	NM_182501	-2.28	1.78E-03
7932094	PHYH	phytanoyl-CoA 2-hydroxylase	NM_006214	-2.28	4.28E-04
7989069	PYGO1	pygopus homolog 1 (Drosophila)	NM_015617	-2.28	1.30E-03
7919984	SELENBP1	selenium binding protein 1	NM_003944	-2.28	5.99E-04
7903144	SLC44A3	solute carrier family 44, member 3	NM_001114106	-2.28	5.10E-05

8130211	SYNE1	spectrin repeat containing, nuclear envelope 1	NM_182961	-2.28	3.40E-04
8109773	WWC1	WW and C2 domain containing 1	NM_015238	-2.28	7.65E-04
8013026	ZNF287	zinc finger protein 287	NM_020653	-2.28	2.06E-04
8057578	CALCRL	calcitonin receptor-like	NM_005795	-2.27	8.39E-03
7986359	IGF1R	insulin-like growth factor 1 receptor	NM_000875	-2.27	6.05E-04
8009844	LLGL2	lethal giant larvae homolog 2 (Drosophila)	NM_001031803	-2.27	1.40E-03
8059279	EPHA4	EPH receptor A4	NM_004438	-2.26	5.61E-04
7965873	IGF1	insulin-like growth factor 1 (somatomedin C)	NM_001111283	-2.26	5.93E-03
8060949	ANKRD5	ankyrin repeat domain 5	NM_022096	-2.26	8.91E-03
8079719	CCDC36	coiled-coil domain containing 36	NM_178173	-2.26	4.50E-05
8004694	CYB5D1	cytochrome b5 domain containing 1	NM_144607	-2.26	5.19E-04
7955211	DNAJC22	DnaJ (Hsp40) homolog, subfamily C, member 22	NM_024902	-2.26	6.64E-04
8140709	KIAA1324L	KIAA1324-like	NM_152748	-2.26	7.83E-04
8015445	NT5C3L	5'-nucleotidase, cytosolic III-like	NM_052935	-2.26	6.80E-05
8145669	RBPMS	RNA binding protein with multiple splicing	NM_001008711	-2.26	1.73E-04
8150565	RNF170	ring finger protein 170	NM_030954	-2.26	1.54E-04
8075569	SLC5A4	solute carrier family 5 (low affinity glucose cotransporter), member 4	NM_014227	-2.26	8.00E-05
8036406	ZNF571	zinc finger protein 571	NM_016536	-2.26	1.05E-04
8006237	LOC400590	hypothetical LOC400590	BC062632	-2.25	1.12E-03
8133670	POR	P450 (cytochrome) oxidoreductase	NM_000941	-2.25	3.42E-03
8005865	SARM1	sterile alpha and TIR motif containing 1	NM_015077	-2.25	1.00E-05
8150537	SLC20A2	solute carrier family 20 (phosphate transporter), member 2	NM_006749	-2.25	9.08E-04
7969341	TDRD3	tudor domain containing 3	NM_030794	-2.25	5.00E-05
8007420	AOC3	amine oxidase, copper containing 3 (vascular adhesion protein 1)	NM_003734	-2.24	6.91E-04
8081810	GAP43	growth associated protein 43	NM_002045	-2.24	8.10E-05
7971602	RCBTB1	regulator of chromosome condensation (RCC1) and BTB (POZ) domain containing protein 1	NM_018191	-2.24	3.19E-03
8070489	RIPK4	receptor-interacting serine-threonine kinase 4	NM_020639	-2.24	9.20E-05
8046048	FAM130A2	family with sequence similarity 130, member A2	NM_024969	-2.23	4.43E-03
8082643	NEK11	NIMA (never in mitosis gene a)- related kinase 11	NM_024800	-2.23	1.84E-04
7898939	NPAL3	NIPA-like domain containing 3	NM_020448	-2.23	1.42E-03
7984276	SLC24A1	solute carrier family 24 (sodium/potassium/calcium exchanger), member 1	NM_004727	-2.23	9.14E-04
7943919	TTC12	tetratricopeptide repeat domain 12	NM_017868	-2.23	2.75E-04
8058857	IGFBP5	insulin-like growth factor binding protein 5	NM_000599	-2.22	1.12E-04
8068583	KCNJ15	potassium inwardly-rectifying channel, subfamily J, member 15	NM_002243	-2.22	5.21E-03
7920575	PBXIP1	pre-B-cell leukemia homeobox interacting protein 1	NM_020524	-2.22	3.21E-03
8032037	SHC2	SHC (Src homology 2 domain containing) transforming protein 2	NM_012435	-2.22	2.80E-05

7981988	SNORD116@	small nucleolar RNA, C/D box 116 cluster	AF241255	-2.22	1.18E-03
8160521	MOBKL2B	MOB1, Mps One Binder kinase activator-like 2B (yeast)	NM_024761	-2.21	6.64E-03
8046792	DUSP19	dual specificity phosphatase 19	NM_080876	-2.21	8.30E-03
8152812	FAM84B	family with sequence similarity 84, member B	NM_174911	-2.21	1.44E-04
7959002	SDSL	serine dehydratase-like	NM_138432	-2.21	3.23E-04
7969533	SLAIN1	SLAIN motif family, member 1	NM_001040153	-2.21	2.77E-03
8101659	SPARCL1	SPARC-like 1 (hevin)	NM_001128310	-2.21	2.98E-03
7959638	TCTN2	tectonic family member 2	NM_024809	-2.21	3.48E-04
7901175	TSPAN1	tetraspanin 1	NM_005727	-2.21	3.18E-03
8061305	C20orf19	chromosome 20 open reading frame 19	NM_018474	-2.20	1.54E-04
8088745	FRMD4B	FERM domain containing 4B	NM_015123	-2.20	1.50E-04
8034521	HOOK2	hook homolog 2 (Drosophila)	NM_013312	-2.20	1.30E-05
8013616	SLC46A1	solute carrier family 46 (folate transporter), member 1	NM_080669	-2.20	1.40E-03
8172379	ZNF630	zinc finger protein 630	NM_001037735	-2.20	1.35E-03
8046318	C2orf37	chromosome 2 open reading frame 37	NM_025000	-2.19	1.32E-03
8160332	MLLT3	myeloid/lymphoid or mixed-lineage leukemia (trithorax homolog, Drosophila); translocated to, 3	NM_004529	-2.19	6.26E-03
8085797	THRB	thyroid hormone receptor, beta (erythroblastic leukemia viral (v-erb-a) oncogene homolog 2, avian)	NM_001128176	-2.19	4.02E-03
8134318	CASD1	CAS1 domain containing 1	NM_022900	-2.18	1.06E-04
8060505	EBF4	early B-cell factor 4	NM_001110514	-2.18	3.47E-04
7903092	FNBP1L	formin binding protein 1-like	NM_001024948	-2.18	4.56E-04
7946781	PLEKHA7	pleckstrin homology domain containing, family A member 7	NM_175058	-2.18	6.60E-05
7931281	FANK1	fibronectin type III and ankyrin repeat domains 1	NM_145235	-2.17	9.10E-05
8084895	MUC20	mucin 20, cell surface associated	NM_152673	-2.17	1.23E-03
8010903	RPH3AL	rabphilin 3A-like (without C2 domains)	NM_006987	-2.17	6.82E-03
7941148	TM7SF2	transmembrane 7 superfamily member 2	NM_003273	-2.17	1.64E-04
8023871	ZADH2	zinc binding alcohol dehydrogenase domain containing 2	NM_175907	-2.17	6.99E-04
8115397	C5orf4	chromosome 5 open reading frame 4	NM_032385	-2.16	1.03E-03
7949650	CTSF	cathepsin F	NM_003793	-2.16	3.67E-03
8013341	MFAP4	microfibrillar-associated protein 4	NM_002404	-2.16	4.95E-03
8166671	CXorf22	chromosome X open reading frame 22	NM_152632	-2.16	3.18E-03
7923596	ETNK2	ethanolamine kinase 2	NM_018208	-2.16	8.93E-04
8161458	KGFLP2	keratinocyte growth factor-like protein 2	NR_003670	-2.16	6.47E-03
7994308	KIAA0556	KIAA0556	ENST00000261588	-2.16	6.40E-05
7904106	MAGI3	membrane associated guanylate kinase, WW and PDZ domain containing 3	NM_152900	-2.16	2.21E-03
8023926	PARD6G	par-6 partitioning defective 6 homolog gamma (C. elegans)	NM_032510	-2.16	1.27E-03

7949400	SLC25A45	solute carrier family 25, member 45	NM_182556	-2.16	6.00E-06
7919326	ACP6	acid phosphatase 6, lysophosphatidic	NM_016361	-2.15	3.43E-04
8024238	CIRBP	cold inducible RNA binding protein	NM_001280	-2.15	4.30E-05
8023165	HDHD2	haloacid dehalogenase-like hydrolase domain containing 2	NM_032124	-2.15	3.30E-05
7952305	LOC283155	hypothetical LOC283155	XR_018777	-2.15	2.35E-04
8103986	LRP2BP	LRP2 binding protein	NM_018409	-2.15	1.00E-05
7932765	MPP7	membrane protein, palmitoylated 7 (MAGUK p55 subfamily member 7)	NM_173496	-2.15	3.48E-04
7957551	SOCS2	suppressor of cytokine signaling 2	NM_003877	-2.15	2.71E-03
8155707	TJP2	tight junction protein 2 (zona occludens 2)	NM_004817	-2.15	3.80E-05
7967463	RILPL1	Rab interacting lysosomal protein-like 1	NM_178314	-2.14	9.00E-06
8046147	BBS5	Bardet-Biedl syndrome 5	NM_152384	-2.14	2.80E-05
8147057	CHMP4C	chromatin modifying protein 4C	NM_152284	-2.14	4.84E-04
8132013	CHN2	chimerin (chimaerin) 2	NM_004067	-2.14	8.41E-04
7951429	KBTBD3	kelch repeat and BTB (POZ) domain containing 3	NM_198439	-2.14	9.84E-03
7900336	MACF1	microtubule-actin crosslinking factor 1	AK023285	-2.14	6.05E-04
7969835	PCCA	propionyl Coenzyme A carboxylase, alpha polypeptide	NM_000282	-2.14	1.05E-04
8157700	RABGAP1	RAB GTPase activating protein 1	NM_012197	-2.14	5.60E-05
8122637	SASH1	SAM and SH3 domain containing 1	NM_015278	-2.14	1.59E-03
7990582	SCAPER	S phase cyclin A-associated protein in the ER	NM_020843	-2.14	6.03E-04
7953291	CD9	CD9 molecule	NM_001769	-2.13	1.55E-04
7935169	CYP2C8	cytochrome P450, family 2, subfamily C, polypeptide 8	NM_000770	-2.13	5.45E-04
8120883	DOPEY1	dopey family member 1	NM_015018	-2.13	4.30E-05
8130038	SHPRH	SNF2 histone linker PHD RING helicase	NM_001042683	-2.13	1.50E-05
7950447	XRRA1	X-ray radiation resistance associated 1	NM_182969	-2.13	1.09E-04
8027247	ZNF93	zinc finger protein 93	NM_031218	-2.13	6.10E-05
8020495	CABLES1	Cdk5 and Abl enzyme substrate 1	NM_138375	-2.12	1.97E-03
8105579	IPO11	importin 11	AY358733	-2.12	4.99E-03
8019988	PTPRM	protein tyrosine phosphatase, receptor type, M	NM_001105244	-2.12	1.80E-05
8131709	SP4	Sp4 transcription factor	NM_003112	-2.12	2.90E-05
8136516	tcag7.1228	hypothetical protein FLJ25778	NM_173569	-2.12	1.20E-05
8004201	ALOX12P2	arachidonate 12-lipoxygenase pseudogene 2	NR_002710	-2.11	1.20E-03
8096959	ANK2	ankyrin 2, neuronal	NM_001148	-2.11	1.03E-03
8126382	C6orf132	chromosome 6 open reading frame 132	ENST00000356542	-2.11	1.30E-03
8165024	C9orf116	chromosome 9 open reading frame 116	NM_001048265	-2.11	4.19E-04
7950162	PDE2A	phosphodiesterase 2A, cGMP-stimulated	NM_002599	-2.11	1.85E-04
7928855	BMPR1A	bone morphogenetic protein receptor, type IA	NM_004329	-2.10	1.31E-04
8059470	IRS1	insulin receptor substrate 1	NM_005544	-2.10	2.99E-04

7973724	KIAA1305	KIAA1305	NM_025081	-2.10	6.84E-04
8058512	PLEKHM3	pleckstrin homology domain containing, family M, member 3	NM_001080475	-2.10	5.30E-05
8090395	TXNRD3	thioredoxin reductase 3	AK299502	-2.10	7.30E-05
8086352	ULK4	unc-51-like kinase 4 (C. elegans)	NM_017886	-2.10	5.14E-03
7925691	ZNF124	zinc finger protein 124	NM_003431	-2.10	5.70E-05
8042402	C2orf13	chromosome 2 open reading frame 13	NM_173545	-2.09	1.36E-04
8116780	DSP	desmoplakin	NM_004415	-2.09	1.91E-03
8000284	GGA2	golgi associated, gamma adaptin ear containing, ARF binding protein 2	NM_015044	-2.09	3.00E-06
7909510	HHAT	hedgehog acyltransferase	NM_018194	-2.09	6.70E-05
8045860	PKP4	plakophilin 4	NM_003628	-2.09	1.71E-03
8063382	SNAI1	snail homolog 1 (Drosophila)	NM_005985	-2.09	1.19E-04
7937438	TMEM80	transmembrane protein 80	NM_174940	-2.09	4.00E-05
7957417	TMTC2	transmembrane and tetratricopeptide repeat containing 2	NM_152588	-2.09	2.15E-04
8101788	UNC5C	unc-5 homolog C (C. elegans)	NM_003728	-2.09	6.97E-03
8102065	BDH2	3-hydroxybutyrate dehydrogenase, type 2	NM_020139	-2.08	3.66E-04
7929288	EXOC6	exocyst complex component 6	NM_019053	-2.08	1.29E-04
8144699	LRLE1	liver-related low express protein 1	AY461701	-2.08	6.22E-03
7899087	PDIK1L	PDLIM1 interacting kinase 1 like	NM_152835	-2.08	3.03E-03
8008564	TOM1L1	target of myb1 (chicken)-like 1	AB065085	-2.08	3.32E-03
8094638	WDR19	WD repeat domain 19	NM_025132	-2.08	1.08E-04
7967863	ZNF605	zinc finger protein 605	NM_183238	-2.08	1.14E-03
8034395	ZNF709	zinc finger protein 709	NM_152601	-2.08	3.89E-03
8149966	SCARA5	scavenger receptor class A, member 5 (putative)	NM_173833	-2.07	1.17E-03
7933237	ANUBL1	AN1, ubiquitin-like, homolog (Xenopus laevis)	NM_174890	-2.07	9.50E-05
8059716	C2orf52	chromosome 2 open reading frame 52	BC033054	-2.07	8.00E-06
8155696	FAM122A	family with sequence similarity 122A	NM_138333	-2.07	2.50E-05
8008802	GDPD1	glycerophosphodiester phosphodiesterase domain containing 1	NM_182569	-2.07	2.70E-05
7923662	PIK3C2B	phosphoinositide-3-kinase, class 2, beta polypeptide	NM_002646	-2.07	5.92E-04
8152606	SNTB1	syntrophin, beta 1 (dystrophin-associated protein A1, 59kDa, basic component 1)	NM_021021	-2.07	1.55E-04
8006715	TADA2L	transcriptional adaptor 2 (ADA2 homolog, yeast)-like	NM_001488	-2.07	9.00E-06
8078319	ZCWPW2	zinc finger, CW type with PWWP domain 2	NM_001040432	-2.07	7.30E-05
8036232	C19orf46	chromosome 19 open reading frame 46	NM_001039876	-2.06	9.10E-05
8073578	C22orf32	chromosome 22 open reading frame 32	BC024237	-2.06	0.00E+00
7965410	DCN	decorin	NM_001920	-2.06	2.64E-03
7961702	KCNJ8	potassium inwardly-rectifying channel, subfamily J, member 8	NM_004982	-2.06	8.22E-03

8150714	PCMTD1	protein-L-isoaspartate (D-aspartate) O-methyltransferase domain containing 1	NM_052937	-2.06	4.20E-05
8099967	RBM47	RNA binding motif protein 47	NM_001098634	-2.06	9.98E-04
8078330	RBMS3	RNA binding motif, single stranded interacting protein	NM_001003793	-2.06	5.55E-04
8063444	TSHZ2	teashirt zinc finger homeobox 2	ENST00000371497	-2.06	6.81E-03
7906602	VANGL2	vang-like 2 (van gogh, Drosophila)	NM_020335	-2.06	1.66E-04
8035795	ZNF626	zinc finger protein 626	NM_145297	-2.06	4.40E-05
8162639	ZNF782	zinc finger protein 782	NM_001001662	-2.06	4.22E-03
7974473	FBXO34	F-box protein 34	NM_017943	-2.05	5.00E-06
7905581	S100A1	S100 calcium binding protein A1	NM_006271	-2.05	3.37E-03
7981978	SNORD116-15	small nucleolar RNA, C/D box 116-15	NR_003330	-2.05	1.94E-03
7932390	TRDMT1	tRNA aspartic acid methyltransferase 1	NM_004412	-2.05	1.20E-03
8017150	TUBD1	tubulin, delta 1	NM_016261	-2.05	7.10E-05
8079598	ZNF589	zinc finger protein 589	NM_016089	-2.05	1.48E-04
8039062	ZNF665	zinc finger protein 665	NM_024733	-2.05	1.70E-03
8081081	EPHA3	EPH receptor A3	NM_005233	-2.04	7.59E-04
8153405	C8orf51	chromosome 8 open reading frame 51	BC000203	-2.04	3.42E-04
8162706	C9orf156	chromosome 9 open reading frame 156	NM_016481	-2.04	1.20E-05
8081138	EPHA6	EPH receptor A6	NM_001080448	-2.04	4.46E-04
7919872	FAM63A	family with sequence similarity 63, member A	NM_018379	-2.04	1.48E-03
7952813	IGSF9B	immunoglobulin superfamily, member 9B	NM_014987	-2.04	3.29E-03
8162019	KIF27	kinesin family member 27	NM_017576	-2.04	4.70E-04
7931204	LHPP	phospholysine phosphohistidine inorganic pyrophosphate phosphatase	NM_022126	-2.04	7.28E-04
8121087	PM20D2	peptidase M20 domain containing 2	NM_001010853	-2.04	3.41E-04
7957613	VEZT	vezatin, adherens junctions transmembrane protein	NM_017599	-2.04	7.80E-05
8143441	KIAA1147	KIAA1147	BC012493	-2.03	5.60E-05
7975676	C14orf45	chromosome 14 open reading frame 45	NM_025057	-2.03	1.27E-03
8068220	C21orf49	chromosome 21 open reading frame 49	BC117397	-2.03	4.60E-04
8102135	CXXC4	CXXC finger 4	NM_025212	-2.03	1.60E-05
8047078	FLJ20160	FLJ20160 protein	NM_017694	-2.03	1.75E-04
8075493	PATZ1	POZ (BTB) and AT hook containing zinc finger 1	NM_014323	-2.03	3.70E-05
7945979	TRIM68	tripartite motif-containing 68	NM_018073	-2.03	7.90E-05
8110253	ZNF346	zinc finger protein 346	NM_012279	-2.03	1.76E-04
8045587	ACVR2A	activin A receptor, type IIA	NM_001616	-2.02	1.67E-04
7965935	LOC253724	hypothetical LOC253724	BC064342	-2.02	4.69E-04
7904751	RBM8A	RNA binding motif protein 8A	BC071577	-2.02	3.64E-04
8068810	SLC37A1	solute carrier family 37 (glycerol-3-phosphate transporter), member 1	NM_018964	-2.02	9.11E-04

8005603	SLC47A1	solute carrier family 47, member 1	NM_018242	-2.02	4.81E-03
7977075	SNORA28	small nucleolar RNA, H/ACA box 28	NR_002964	-2.02	3.88E-04
8098214	TLL1	tolloid-like 1	NM_012464	-2.02	1.70E-05
7925792	ZMYND11	zinc finger, MYND domain containing 11	NM_006624	-2.02	3.30E-05
8074845	ZNF280B	zinc finger protein 280B	NM_080764	-2.02	2.35E-03
7958784	ALDH2	aldehyde dehydrogenase 2 family (mitochondrial)	NM_000690	-2.01	2.99E-04
8096160	ARHGAP24	Rho GTPase activating protein 24	NM_001025616	-2.01	9.40E-05
7966738	C12orf49	chromosome 12 open reading frame 49	BC019843	-2.01	1.30E-04
8065202	C20orf12	chromosome 20 open reading frame 12	NM_001099407	-2.01	2.70E-05
8062251	EPB41L1	erythrocyte membrane protein band 4.1-like 1	NM_012156	-2.01	8.30E-05
8148808	KIAA1833	hypothetical protein KIAA1833	AL834145	-2.01	3.27E-03
8008646	SCPEP1	serine carboxypeptidase 1	NM_021626	-2.01	2.60E-05
7917322	SYDE2	synapse defective 1, Rho GTPase, homolog 2 (C. elegans)	NM_032184	-2.01	6.58E-04
8153920	ZNF250	zinc finger protein 250	NM_021061	-2.01	3.20E-05
8042519	PCYOX1	prenylcysteine oxidase 1	NM_016297	-2.00	2.29E-04
8005959	NEK8	NIMA (never in mitosis gene a)- related kinase 8	NM_178170	-2.00	1.46E-04
8143937	NUB1	negative regulator of ubiquitin-like proteins 1	NM_016118	-2.00	1.55E-03
8097417	PHF17	PHD finger protein 17	NM_199320	-2.00	2.71E-03
8090256	SNX4	sorting nexin 4	NM_003794	-2.00	5.11E-04
8042867	WBP1	WW domain binding protein 1	NM_012477	-2.00	1.00E-06
8125463	HLA-DQB2	major histocompatibility complex, class II, DQ beta 2	NR_003937	2.00	6.11E-03
8166797	MID1IP1	MID1 interacting protein 1 (gastrulation specific G12 homolog (zebrafish))	NM_021242	2.00	2.36E-04
8057887	STK17B	serine/threonine kinase 17b	NM_004226	2.00	4.80E-03
7944931	SLC37A2	solute carrier family 37 (glycerol-3-phosphate transporter), member 2	NM_198277	2.02	6.30E-03
8117429	HIST1H2BI	histone cluster 1, H2bi	NM_003525	2.03	5.46E-04
7903049	CCDC18	coiled-coil domain containing 18	NM_206886	2.03	3.56E-03
8177955	MICB	MHC class I polypeptide-related sequence B	NM_005931	2.03	1.44E-03
8115814	SH3PXD2B	SH3 and PX domains 2B	NM_001017995	2.03	7.52E-03
8133459	CLIP2	CAP-GLY domain containing linker protein 2	NM_003388	2.04	7.11E-03
7955045	FAM113B	family with sequence similarity 113, member B	BC008360	2.04	1.91E-03
8112807	ARSB	arylsulfatase B	NM_000046	2.05	3.71E-04
8092418	ABCC5	ATP-binding cassette, sub-family C (CFTR/MRP), member 5	NM_005688	2.06	1.60E-05
8001981	FHOD1	formin homology 2 domain containing 1	NM_013241	2.06	7.66E-03
7909175	SRGAP2	SLIT-ROBO Rho GTPase activating protein 2	NM_015326	2.07	7.36E-04
8052269	CCDC88A	coiled-coil domain containing 88A	NM_018084	2.08	4.70E-04
7898988	CLIC4	chloride intracellular channel 4	NM_013943	2.08	8.41E-03
8036252	CLIP3	CAP-GLY domain containing linker protein 3	NM_015526	2.08	4.72E-03

8041225	EHD3	EH-domain containing 3	NM_014600	2.08	1.26E-04
8101945	H2AFZ	H2A histone family, member Z	NM_002106	2.08	5.88E-03
8124510	HIST1H2BL	histone cluster 1, H2bl	NM_003519	2.08	1.46E-03
7979044	NIN	ninein (GSK3B interacting protein)	NM_020921	2.08	8.01E-03
7989277	MYO1E	myosin IE	NM_004998	2.09	1.94E-03
8010983	ABR	active BCR-related gene	NM_021962	2.10	3.36E-03
8174474	ACSL4	acyl-CoA synthetase long-chain family member 4	NM_022977	2.10	6.07E-03
8156826	TGFBR1	transforming growth factor, beta receptor 1	NM_004612	2.10	6.40E-05
8175169	RAP2C	RAP2C, member of RAS oncogene family	NM_021183	2.11	3.34E-04
7912374	SRM	spermidine synthase	NM_003132	2.11	5.89E-03
8073612	TSPO	translocator protein (18kDa)	NM_000714	2.11	2.81E-03
8088180	WNT5A	wingless-type MMTV integration site family, member 5A	NM_003392	2.11	1.78E-03
7987230	LPCAT4	lysophosphatidylcholine acyltransferase 4	NM_153613	2.13	4.70E-05
7916167	ORC1L	origin recognition complex, subunit 1-like (yeast)	NM_004153	2.13	1.31E-03
7949948	C11orf24	chromosome 11 open reading frame 24	NM_022338	2.14	4.81E-03
7935903	NPM3	nucleophosmin/nucleoplasmin, 3	NM_006993	2.14	8.71E-03
8153568	PLEC1	plectin 1, intermediate filament binding protein 500kDa	NM_201384	2.15	6.64E-03
8044462	TTL	tubulin tyrosine ligase	NM_153712	2.15	7.50E-03
7982287	ARHGAP11B	Rho GTPase activating protein 11B	NM_001039841	2.16	8.20E-03
8034420	MAN2B1	mannosidase, alpha, class 2B, member 1	NM_000528	2.16	3.20E-03
8116649	TUBB2A	tubulin, beta 2A	NM_001069	2.16	2.14E-03
8116653	TUBB2B	tubulin, beta 2B	NM_178012	2.16	2.14E-03
7963280	LOC57228	small trans-membrane and glycosylated protein	NM_001033873	2.17	6.90E-03
8081219	ST3GAL6	ST3 beta-galactoside alpha-2,3-sialyltransferase 6	NM_006100	2.17	5.14E-03
8158240	TMSB4X	thymosin beta 4, X-linked	NM_021109	2.17	2.40E-05
8136918	ZYX	zyxin	NM_003461	2.17	1.22E-04
7903719	AMPD2	adenosine monophosphate deaminase 2 (isoform L)	NM_004037	2.20	3.62E-03
7955195	TROAP	trophinin associated protein (tastin)	NM_005480	2.20	4.11E-03
8026638	MYO9B	myosin IXB	NM_004145	2.21	7.27E-03
7987636	OIP5	Opa interacting protein 5	NM_007280	2.21	5.02E-03
7958031	C12orf48	chromosome 12 open reading frame 48	AK302724	2.23	1.88E-03
7981525	CDCA4	cell division cycle associated 4	NM_017955	2.23	5.52E-03
8124540	HIST1H2AM	histone cluster 1, H2am	NM_003514	2.23	7.68E-03
8087806	PCBP4	poly(rC) binding protein 4	NM_020418	2.24	3.09E-03
8150698	SNAI2	snail homolog 2 (Drosophila)	NM_003068	2.24	1.37E-03
8066939	B4GALT5	UDP-Gal:betaGlcNAc beta 1,4- galactosyltransferase, polypeptide 5	NM_004776	2.25	3.14E-03
8032871	DPP9	dipeptidyl-peptidase 9	NM_139159	2.25	7.20E-03

8019392	FASN	fatty acid synthase	NM_004104	2.25	5.19E-03
8172266	MIR221	microRNA 221	NR_029635	2.25	9.61E-03
8022531	NPC1	Niemann-Pick disease, type C1	NM_000271	2.25	3.24E-03
8027778	FXYD5	FXYD domain containing ion transport regulator 5	NM_144779	2.26	3.96E-03
8083457	RAP2B	RAP2B, member of RAS oncogene family	NM_002886	2.26	4.26E-03
8132725	UPP1	uridine phosphorylase 1	NM_003364	2.27	4.51E-03
8032491	LMNB2	lamin B2	NM_032737	2.27	8.61E-04
8127534	C6orf150	chromosome 6 open reading frame 150	NM_138441	2.28	1.06E-03
7924150	TMEM206	transmembrane protein 206	NM_018252	2.28	2.39E-04
8152668	ATAD2	ATPase family, AAA domain containing 2	NM_014109	2.29	8.70E-04
7910950	KMO	kynurenine 3-monooxygenase (kynurenine 3-hydroxylase)	NM_003679	2.29	2.79E-03
7912481	MAD2L2	MAD2 mitotic arrest deficient-like 2 (yeast)	NM_001127325	2.29	1.96E-03
7983306	WDR76	WD repeat domain 76	NM_024908	2.29	2.76E-04
8106393	F2R	coagulation factor II (thrombin) receptor	NM_001992	2.30	4.49E-03
8117600	HIST1H2BN	histone cluster 1, H2bn	NM_003520	2.30	3.50E-03
7905079	HIST2H2AA3	histone cluster 2, H2aa3	NM_003516	2.31	3.30E-03
8033912	DNMT1	DNA (cytosine-5-)-methyltransferase 1	NM_001379	2.31	2.66E-03
8176026	FLNA	filamin A, alpha (actin binding protein 280)	NM_001456	2.31	3.46E-04
7996318	CMTM3	CKLF-like MARVEL transmembrane domain containing 3	NM_144601	2.32	5.37E-03
8003844	GSG2	germ cell associated 2 (haspin)	NM_031965	2.32	3.21E-03
8018731	RHBDF2	rhomboid 5 homolog 2 (Drosophila)	NM_024599	2.32	9.59E-04
8117614	HIST1H2BO	histone cluster 1, H2bo	NM_003527	2.33	1.93E-03
7910694	EDARADD	EDAR-associated death domain	NM_080738	2.34	1.96E-03
8157761	NEK6	NIMA (never in mitosis gene a)-related kinase 6	NM_014397	2.34	2.49E-03
7906061	SYT11	synaptotagmin XI	NM_152280	2.34	9.68E-03
8172268	MIR222	microRNA 222	NR_029636	2.35	3.82E-04
8060745	SMOX	spermine oxidase	NM_175839	2.35	3.68E-03
7978595	BAZ1A	bromodomain adjacent to zinc finger domain, 1A	NM_013448	2.36	2.07E-03
8030007	EMP3	epithelial membrane protein 3	NM_001425	2.36	1.59E-03
8021286	C18orf54	chromosome 18 open reading frame 54	NM_173529	2.36	5.38E-03
8151756	TMEM55A	transmembrane protein 55A	NM_018710	2.36	2.63E-03
8112260	DEPDC1B	DEP domain containing 1B	NM_018369	2.37	2.14E-04
7949060	PPP1R14B	protein phosphatase 1, regulatory (inhibitor) subunit 14B	NM_138689	2.37	2.75E-04
8125500	PSMB8	proteasome (prosome, macropain) subunit, beta type, 8 (large multifunctional peptidase 7)	NM_004159	2.37	1.17E-03
8055426	MCM6	minichromosome maintenance complex component 6	NM_005915	2.38	9.39E-03
8162729	TRIM14	tripartite motif-containing 14	NM_014788	2.38	3.33E-03

8104601	BASP1	brain abundant, membrane attached signal protein 1	NM_006317	2.40	5.29E-03
8016139	KIF18B	kinesin family member 18B	NM_001080443	2.40	6.17E-03
8032365	KLF16	Kruppel-like factor 16	NM_031918	2.40	1.21E-04
8066117	SAMHD1	SAM domain and HD domain 1	NM_015474	2.40	1.20E-03
8132503	STK17A	serine/threonine kinase 17a	NM_004760	2.40	5.70E-03
7955736	ESPL1	extra spindle pole bodies homolog 1 (S. cerevisiae)	NM_012291	2.41	2.41E-03
8050089	TMSL2	thymosin-like 2 (pseudogene)	BC104196	2.42	2.80E-05
8124416	HIST1H3D	histone cluster 1, H3d	NM_003530	2.43	2.35E-03
7959251	P2RX7	purinergic receptor P2X, ligand-gated ion channel, 7	NM_002562	2.43	3.50E-04
8073662	PARVB	parvin, beta	NM_001003828	2.43	2.75E-03
8104788	RAI14	retinoic acid induced 14	NM_015577	2.44	8.26E-03
7958019	DRAM	damage-regulated autophagy modulator	NM_018370	2.45	2.62E-03
8085914	SLC4A7	solute carrier family 4, sodium bicarbonate cotransporter, member 7	NM_003615	2.45	2.24E-03
7966135	CORO1C	coronin, actin binding protein, 1C	NM_014325	2.46	2.13E-04
7942372	FOLR2	folate receptor 2 (fetal)	NM_000803	2.46	4.11E-03
7959408	KNTC1	kinetochore associated 1	NM_014708	2.46	3.82E-04
8136115	FAM40B	family with sequence similarity 40, member B	AK290165	2.47	3.33E-03
8069085	TRPM2	transient receptor potential cation channel, subfamily M, member 2	NM_003307	2.47	4.19E-03
7948493	SLC15A3	solute carrier family 15, member 3	NM_016582	2.48	3.16E-03
7939365	FJX1	four jointed box 1 (Drosophila)	NM_014344	2.50	2.69E-03
7977452	FLJ39632	hypothetical LOC642477	BX248778	2.51	1.32E-04
8003298	SLC7A5	solute carrier family 7 (cationic amino acid transporter, y+ system), member 5	NM_003486	2.52	9.77E-04
8167185	TIMP1	TIMP metallopeptidase inhibitor 1	NM_003254	2.53	3.22E-03
7939376	LDLRAD3	low density lipoprotein receptor class A domain containing 3	NM_174902	2.54	4.08E-03
7929052	IFIT3	interferon-induced protein with tetratricopeptide repeats 3	NM_001031683	2.55	6.51E-03
8117395	HIST1H2BF	histone cluster 1, H2bf	NM_003522	2.56	2.04E-04
8083709	SMC4	structural maintenance of chromosomes 4	NM_005496	2.56	1.83E-03
8025601	ICAM1	intercellular adhesion molecule 1	NM_000201	2.57	9.26E-03
8026971	IFI30	interferon, gamma-inducible protein 30	NM_006332	2.57	6.70E-03
8006214	CENTA2	centaurin, alpha 2	NM_018404	2.58	7.01E-03
7914851	CLSPN	claspin homolog (Xenopus laevis)	NM_022111	2.60	8.37E-03
8105040	OSMR	oncostatin M receptor	NM_003999	2.60	6.11E-03
8032608	C19orf28	chromosome 19 open reading frame 28	NM_174983	2.62	2.03E-03
8063634	MGC4294	hypothetical protein MGC4294	BC002831	2.62	6.24E-03
8092552	IGF2BP2	insulin-like growth factor 2 mRNA binding protein 2	NM_006548	2.66	9.25E-03
8080344	STAB1	stabilin 1	NM_015136	2.69	9.51E-03

8046922	COL3A1	collagen, type III, alpha 1	NM_000090	2.72	1.55E-03
7979281	WDHD1	WD repeat and HMG-box DNA binding protein 1	NM_007086	2.73	8.10E-03
8092251	GNB4	guanine nucleotide binding protein (G protein), beta polypeptide 4	NM_021629	2.74	8.95E-04
8003503	FANCA	Fanconi anemia, complementation group A	NM_000135	2.75	4.28E-04
7914270	LAPTM5	lysosomal multispanning membrane protein 5	NM_006762	2.75	5.87E-03
8123637	LOC401233	similar to HIV TAT specific factor 1; cofactor required for Tat activation of HIV-1 transcription	AK128391	2.75	5.35E-04
8020955	MOCOS	molybdenum cofactor sulfurase	NM_017947	2.75	5.36E-03
8109350	SLC36A1	solute carrier family 36 (proton/amino acid symporter), member 1	NM_078483	2.75	1.00E-06
8167449	PLP2	proteolipid protein 2 (colonic epithelium-enriched)	NM_002668	2.76	3.58E-04
8025828	LDLR	low density lipoprotein receptor	NM_000527	2.77	8.72E-03
8146357	MCM4	minichromosome maintenance complex component 4	NM_005914	2.77	9.22E-03
7994659	MVP	major vault protein	NM_017458	2.78	4.75E-04
7906400	IFI16	interferon, gamma-inducible protein 16	NM_005531	2.78	1.00E-06
7995926	NLRC5	NLR family, CARD domain containing 5	NM_032206	2.79	7.00E-03
7919589	HIST2H3D	histone cluster 2, H3d	NM_001123375	2.81	6.41E-03
8175977	IRAK1	interleukin-1 receptor-associated kinase 1	NM_001569	2.81	4.97E-03
8170420	MAMLD1	mastermind-like domain containing 1	NM_005491	2.81	4.84E-04
8149638	DOK2	docking protein 2, 56kDa	NM_003974	2.83	7.78E-03
8007569	C17orf53	chromosome 17 open reading frame 53	AK291924	2.85	1.80E-03
8082314	PLXNA1	plexin A1	NM_032242	2.88	3.44E-03
7930413	DUSP5	dual specificity phosphatase 5	NM_004419	2.90	5.22E-03
8101260	ANTXR2	anthrax toxin receptor 2	NM_058172	2.90	1.67E-03
7915147	FHL3	four and a half LIM domains 3	NM_004468	2.93	6.33E-04
8013450	LGALS9B	lectin, galactoside-binding, soluble, 9B	NM_001042685	2.93	5.99E-03
8116070	PDLIM7	PDZ and LIM domain 7 (enigma)	NM_005451	2.93	9.79E-04
7927964	SRGN	serglycin	NM_002727	2.93	3.75E-03
8061471	GINS1	GINS complex subunit 1 (Psf1 homolog)	NM_021067	2.94	7.05E-03
8118571	PSMB9	proteasome (prosome, macropain) subunit, beta type, 9 (large multifunctional peptidase 2)	NM_002800	2.94	2.96E-03
8069269	COL6A1	collagen, type VI, alpha 1	NM_001848	2.95	3.93E-03
7954143	PTPRO	protein tyrosine phosphatase, receptor type, O	NM_030667	2.95	6.52E-03
7968484	BRCA2	breast cancer 2, early onset	NM_000059	2.97	4.24E-03
7986068	BLM	Bloom syndrome	NM_000057	2.98	1.83E-03
8089875	POLQ	polymerase (DNA directed), theta	NM_199420	2.99	1.29E-03
8069301	COL6A2	collagen, type VI, alpha 2	NM_001849	3.00	2.58E-03
8077731	FANCD2	Fanconi anemia, complementation group D2	NM_033084	3.00	2.21E-04

8131179	TTYH3	tweety homolog 3 (Drosophila)	NM_025250	3.00	2.07E-04
7929438	HELLS	helicase, lymphoid-specific	NM_018063	3.01	8.72E-03
8005458	LGALS9C	lectin, galactoside-binding, soluble, 9C	NM_001040078	3.02	5.40E-03
7902913	CDC7	cell division cycle 7 homolog (S. cerevisiae)	NM_003503	3.05	5.56E-03
8107044	ERAP2	endoplasmic reticulum aminopeptidase 2	NM_022350	3.05	8.24E-03
8117426	HIST1H2BH	histone cluster 1, H2bh	NM_003524	3.07	2.44E-03
7963786	ITGA5	integrin, alpha 5 (fibronectin receptor, alpha polypeptide)	NM_002205	3.08	5.41E-03
8051762	SLC8A1	solute carrier family 8 (sodium/calcium exchanger), member 1	NM_021097	3.08	7.13E-03
7900510	CTPS	CTP synthase	NM_001905	3.09	4.19E-03
8036224	TYROBP	TYRO protein tyrosine kinase binding protein	NM_003332	3.12	3.52E-03
7995492	ADCY7	adenylate cyclase 7	NM_001114	3.15	3.62E-03
8125512	TAP1	transporter 1, ATP-binding cassette, sub-family B (MDR/TAP)	NM_000593	3.16	3.69E-03
7900167	CDCA8	cell division cycle associated 8	NM_018101	3.17	2.79E-03
8079407	CCRL2	chemokine (C-C motif) receptor-like 2	NM_003965	3.19	3.99E-03
8121588	DSE	dermatan sulfate epimerase	NM_013352	3.19	3.09E-03
8077103	TYMP	thymidine phosphorylase	NM_001113756	3.19	6.53E-03
7947248	KIF18A	kinesin family member 18A	NM_031217	3.20	9.55E-03
8148317	MYC	v-myc myelocytomatosis viral oncogene homolog (avian)	NM_002467	3.20	1.81E-03
8107706	LMNB1	lamin B1	NM_005573	3.21	6.79E-03
8009417	KPNA2	karyopherin alpha 2 (RAG cohort 1, importin alpha 1)	NM_002266	3.22	2.96E-03
8083677	SCHIP1	schwannomin interacting protein 1	NM_014575	3.22	4.89E-03
7979824	ACTN1	actinin, alpha 1	NM_001102	3.24	7.40E-05
8012403	AURKB	aurora kinase B	NM_004217	3.24	1.97E-03
8115076	CSF1R	colony stimulating factor 1 receptor	NM_005211	3.28	1.92E-03
7963157	RACGAP1	Rac GTPase activating protein 1	NM_013277	3.28	5.99E-03
7949364	CDCA5	cell division cycle associated 5	NM_080668	3.29	3.55E-03
7973002	LOC440157	hypothetical gene supported by BC066547	BC066547	3.31	1.76E-03
8072876	LGALS1	lectin, galactoside-binding, soluble, 1	NM_002305	3.32	1.32E-04
8129763	FAM54A	family with sequence similarity 54, member A	NM_001099286	3.33	2.30E-03
8166906	GPR34	G protein-coupled receptor 34	NM_001097579	3.34	5.02E-03
7901010	KIF2C	kinesin family member 2C	NM_006845	3.35	8.42E-03
8117594	HIST1H2BM	histone cluster 1, H2bm	NM_003521	3.36	3.92E-03
7947110	E2F8	E2F transcription factor 8	NM_024680	3.38	3.34E-03
7926037	PFKFB3	6-phosphofructo-2-kinase/fructose-2,6-biphosphatase 3	NM_004566	3.41	6.00E-05
7905085	HIST2H3A	histone cluster 2, H3a	NM_001005464	3.43	7.34E-03
8091678	VEPH1	ventricular zone expressed PH domain homolog 1 (zebrafish)	NM_024621	3.43	9.61E-03
7926259	MCM10	minichromosome maintenance complex component 10	NM_182751	3.44	3.07E-03

7962487	DBX2	developing brain homeobox 2	ENST00000332700	3.48	4.73E-03
7958202	CHST11	carbohydrate (chondroitin 4) sulfotransferase 11	NM_018413	3.49	3.78E-03
8019316	PYCR1	pyrroline-5-carboxylate reductase 1	NM_006907	3.50	6.73E-03
8043363	C2orf59	chromosome 2 open reading frame 59	BC010491	3.52	1.95E-03
8039491	UBE2S	ubiquitin-conjugating enzyme E2S	NM_014501	3.54	5.11E-03
8117589	HIST1H3H	histone cluster 1, H3h	NM_003536	3.59	2.88E-04
8114612	CD14	CD14 molecule	NM_000591	3.61	1.42E-03
8051573	CDC42EP3	CDC42 effector protein (Rho GTPase binding) 3	NM_006449	3.61	2.16E-04
8062782	TOX2	TOX high mobility group box family member 2	NM_032883	3.61	3.91E-03
8117583	HIST1H2AI	histone cluster 1, H2ai	NM_003509	3.62	4.15E-04
7905116	PLEKHO1	pleckstrin homology domain containing, family O member 1	NM_016274	3.66	3.93E-03
8004510	CD68	CD68 molecule	NM_001251	3.67	1.09E-03
8043945	MAP4K4	mitogen-activated protein kinase kinase kinase kinase 4	NM_145686	3.67	1.59E-04
8019912	EMILIN2	elastin microfibril interfacer 2	NM_032048	3.72	1.93E-03
7898799	C1QC	complement component 1, q subcomponent, C chain	NM_001114101	3.76	1.62E-03
8026806	GLT25D1	glycosyltransferase 25 domain containing 1	NM_024656	3.77	2.91E-04
8018305	HN1	hematological and neurological expressed 1	NM_016185	3.77	3.13E-03
8166059	TLR7	toll-like receptor 7	NM_016562	3.78	6.04E-03
8039928	FAM72A	family with sequence similarity 72, member A	BC035696	3.79	4.64E-03
8124798	KIAA1949	KIAA1949	NM_133471	3.80	8.27E-04
7898805	C1QB	complement component 1, q subcomponent, B chain	NM_000491	3.83	4.53E-03
7940259	MS4A7	membrane-spanning 4-domains, subfamily A, member 7	NM_021201	3.83	2.25E-03
8064716	SIGLEC1	sialic acid binding Ig-like lectin 1, sialoadhesin	NM_023068	3.83	5.13E-03
8117608	HIST1H2AL	histone cluster 1, H2al	NM_003511	3.84	5.71E-03
8046695	ITGA4	integrin, alpha 4 (antigen CD49D, alpha 4 subunit of VLA-4 receptor)	NM_000885	3.87	4.03E-03
8108217	TGFBI	transforming growth factor, beta-induced, 68kDa	NM_000358	3.91	4.01E-03
7973101	RNASE6	ribonuclease, RNase A family, k6	NM_005615	3.98	6.17E-03
7973024	OR4K17	olfactory receptor, family 4, subfamily K, member 17	NM_001004715	3.99	4.01E-04
8109484	KIF4B	kinesin family member 4B	NM_001099293	4.02	8.45E-03
7958253	OCC-1	overexpressed in colon carcinoma-1	BC013920	4.02	2.24E-03
8118669	KIFC1	kinesin family member C1	NM_002263	4.12	9.63E-03
8117535	HIST1H2AG	histone cluster 1, H2ag	NM_021064	4.15	1.82E-04
8058765	FN1	fibronectin 1	NM_212482	4.17	8.90E-05
8115734	LCP2	lymphocyte cytosolic protein 2 (SH2 domain containing leukocyte protein of 76kDa)	NM_005565	4.17	7.39E-03
8072678	HMOX1	heme oxygenase (decycling) 1	NM_002133	4.18	7.78E-03
8103508	MARCH1	membrane-associated ring finger (C3HC4) 1	NM_017923	4.19	8.59E-03

8143663	EZH2	enhancer of zeste homolog 2 (Drosophila)	NM_004456	4.20	7.70E-04
8083941	ECT2	epithelial cell transforming sequence 2 oncogene	NM_018098	4.22	5.92E-03
8175039	ELF4	E74-like factor 4 (ets domain transcription factor)	NM_001421	4.23	3.04E-03
7957260	GLIPR1	GLI pathogenesis-related 1	NM_006851	4.26	1.98E-03
7948455	MS4A6A	membrane-spanning 4-domains, subfamily A, member 6A	NM_152852	4.27	9.09E-04
8152617	HAS2	hyaluronan synthase 2	NM_005328	4.28	3.19E-04
7992789	TNFRSF12A	tumor necrosis factor receptor superfamily, member 12A	NM_016639	4.29	4.62E-03
8016646	COL1A1	collagen, type I, alpha 1	NM_000088	4.35	8.05E-03
8047161	OBFC2A	oligonucleotide/oligosaccharide-binding fold containing 2A	NM_001031716	4.35	7.16E-03
7905047	FCGR1A	Fc fragment of IgG, high affinity Ia, receptor (CD64)	NM_000566	4.36	2.95E-03
8124527	HIST1H1B	histone cluster 1, H1b	NM_005322	4.36	3.22E-03
7906767	FCGR2C	Fc fragment of IgG, low affinity IIc, receptor for (CD32)	NM_201563	4.40	5.95E-04
8112428	CD180	CD180 molecule	NM_005582	4.41	7.02E-03
7921637	CD84	CD84 molecule	NM_003874	4.49	6.66E-03
8145418	CDCA2	cell division cycle associated 2	NM_152562	4.55	5.21E-03
7973336	MMP14	matrix metallopeptidase 14 (membrane-inserted)	NM_004995	4.57	4.68E-03
8115490	ADAM19	ADAM metallopeptidase domain 19 (meltrin beta)	NM_033274	4.60	6.88E-03
8059413	DOCK10	dedicator of cytokinesis 10	NM_014689	4.60	8.32E-04
8034772	ASF1B	ASF1 anti-silencing function 1 homolog B (S. cerevisiae)	NM_018154	4.70	2.75E-03
7938485	MICAL2	microtubule associated monoxygenase, calponin and LIM domain containing 2	NM_014632	4.72	1.05E-03
8146934	LY96	lymphocyte antigen 96	NM_015364	4.73	2.10E-03
8075910	RAC2	ras-related C3 botulinum toxin substrate 2 (rho family, small GTP binding protein Rac2)	NM_002872	4.73	6.43E-03
8066260	SNORA71C	small nucleolar RNA, H/ACA box 71C	NR_003017	4.76	6.20E-03
8030383	RCN3	reticulocalbin 3, EF-hand calcium binding domain	NM_020650	4.77	4.89E-03
8037005	TGFB1	transforming growth factor, beta 1	NM_000660	4.81	8.01E-04
8066619	PLTP	phospholipid transfer protein	NM_006227	4.85	6.00E-05
7898793	C1QA	complement component 1, q subcomponent, A chain	NM_015991	4.88	5.58E-03
7915926	STIL	SCL/TAL1 interrupting locus	NM_001048166	4.88	2.30E-04
8033445	CD209	CD209 molecule	NM_021155	4.93	4.00E-05
8120043	RUNX2	runt-related transcription factor 2	NM_001024630	4.93	2.94E-04
8044499	SLC20A1	solute carrier family 20 (phosphate transporter), member 1	NM_005415	4.94	8.26E-03
7942832	C11orf82	chromosome 11 open reading frame 82	ENST00000329143	4.95	8.46E-03
7982663	BUB1B	BUB1 budding uninhibited by benzimidazoles 1 homolog beta (yeast)	NM_001211	5.00	2.53E-03
8168146	KIF4A	kinesin family member 4A	NM_012310	5.02	9.60E-03
8079237	KIF15	kinesin family member 15	NM_020242	5.06	3.66E-04

7945014	CHEK1	CHK1 checkpoint homolog (S. pombe)	NM_001274	5.07	8.58E-03
8156194	LOC100130433	hypothetical protein LOC100130433	AK096255	5.07	4.74E-03
7903565	GPSM2	G-protein signaling modulator 2 (AGS3-like, C. elegans)	NM_013296	5.08	7.29E-03
8116734	LY86	lymphocyte antigen 86	NM_004271	5.11	6.37E-03
8070194	RUNX1	runt-related transcription factor 1	NM_001001890	5.28	4.00E-06
8142452	TFEC	transcription factor EC	NM_012252	5.28	7.32E-03
8062571	FAM83D	family with sequence similarity 83, member D	NM_030919	5.29	3.56E-03
8166730	CYBB	cytochrome b-245, beta polypeptide	NM_000397	5.34	1.67E-03
7985829	FANCI	Fanconi anemia, complementation group I	NM_001113378	5.34	5.00E-03
8037835	SLC1A5	solute carrier family 1 (neutral amino acid transporter), member 5	NM_005628	5.43	2.62E-03
7952341	ASAM	adipocyte-specific adhesion molecule	NM_024769	5.61	5.13E-03
8151101	MYBL1	v-myb myeloblastosis viral oncogene homolog (avian)-like 1	NM_001080416	5.65	3.85E-04
7991335	ANPEP	alanyl (membrane) aminopeptidase	NM_001150	5.71	5.08E-03
8063043	UBE2C	ubiquitin-conjugating enzyme E2C	NM_181802	5.86	4.02E-04
8104234	TRIP13	thyroid hormone receptor interactor 13	NM_004237	5.87	8.96E-03
8019857	NDC80	NDC80 homolog, kinetochore complex component (S. cerevisiae)	NM_006101	5.89	3.55E-03
7921033	IQGAP3	IQ motif containing GTPase activating protein 3	NM_178229	5.90	9.57E-03
7971866	DIAPH3	diaphanous homolog 3 (Drosophila)	NM_001042517	5.92	1.66E-03
8156290	CKS2	CDC28 protein kinase regulatory subunit 2	NM_001827	5.94	2.66E-03
8093500	TACC3	transforming, acidic coiled-coil containing protein 3	NM_006342	6.03	5.96E-03
8151871	CCNE2	cyclin E2	NM_057749	6.14	2.01E-03
7984540	KIF23	kinesin family member 23	NM_138555	6.24	3.02E-03
8117339	HIST1H3C	histone cluster 1, H3c	NM_003531	6.31	2.80E-03
8050007	PXDN	peroxidasin homolog (Drosophila)	NM_012293	6.52	3.42E-03
8124437	HIST1H3F	histone cluster 1, H3f	NM_021018	6.60	1.50E-03
7906930	NUF2	NUF2, NDC80 kinetochore complex component, homolog (S. cerevisiae)	NM_145697	6.63	9.00E-03
7982358	ARHGAP11A	Rho GTPase activating protein 11A	NM_014783	6.65	6.97E-03
7906757	FCGR2A	Fc fragment of IgG, low affinity IIa, receptor (CD32)	NM_021642	6.68	2.41E-03
8008784	PRR11	proline rich 11	NM_018304	6.73	1.63E-03
7985873	C15orf42	chromosome 15 open reading frame 42	NM_152259	6.74	9.10E-05
8112376	CENPK	centromere protein K	NM_022145	6.77	6.15E-03
8067167	AURKA	aurora kinase A	NM_198433	6.80	2.72E-03
8062766	MYBL2	v-myb myeloblastosis viral oncogene homolog (avian)-like 2	NM_002466	6.80	7.17E-03
7983969	CCNB2	cyclin B2	NM_004701	6.97	4.68E-03
7921873	FCGR3A	Fc fragment of IgG, low affinity IIIa, receptor (CD16a)	NM_000569	6.98	3.23E-03
8168794	CENPI	centromere protein I	NM_006733	7.02	5.02E-03
7961829	BCAT1	branched chain aminotransferase 1, cytosolic	NM_005504	7.04	1.85E-03

8039257	LAIR1	leukocyte-associated immunoglobulin-like receptor 1	NM_002287	7.10	2.89E-03
7940147	FAM111B	family with sequence similarity 111, member B	AY457926	7.12	7.29E-03
8067270	APCDD1L	adenomatosis polyposis coli down-regulated 1-like	NM_153360	7.20	5.30E-03
8054702	CKAP2L	cytoskeleton associated protein 2-like	NM_152515	7.21	7.80E-03
7991406	PRC1	protein regulator of cytokinesis 1	NM_003981	7.21	4.92E-03
8082035	CD86	CD86 molecule	NM_175862	7.37	1.03E-03
8007071	CDC6	cell division cycle 6 homolog (S. cerevisiae)	NM_001254	7.50	1.95E-03
8085754	SGOL1	shugoshin-like 1 (S. pombe)	NM_001012410	7.56	5.89E-03
8041383	LTBP1	latent transforming growth factor beta binding protein 1	NM_206943	7.61	5.07E-03
7906720	FCER1G	Fc fragment of IgE, high affinity I, receptor for; gamma polypeptide	NM_004106	7.69	3.17E-03
8059854	ARL4C	ADP-ribosylation factor-like 4C	NM_005737	7.70	8.73E-03
7927710	CDC2	cell division cycle 2, G1 to S and G2 to M	NM_001786	7.75	8.46E-03
8024900	UHRF1	ubiquitin-like with PHD and ring finger domains 1	NM_001048201	7.79	1.24E-03
7900699	CDC20	cell division cycle 20 homolog (S. cerevisiae)	NM_001255	8.01	5.42E-03
8017262	BRIP1	BRCA1 interacting protein C-terminal helicase 1	NM_032043	8.10	8.03E-03
8179331	C2	complement component 2	NM_000063	8.11	4.26E-03
7965094	E2F7	E2F transcription factor 7	NM_203394	8.15	1.03E-03
8037374	PLAUR	plasminogen activator, urokinase receptor	NM_002659	8.16	6.00E-05
8056257	FAP	fibroblast activation protein, alpha	NM_004460	8.17	4.69E-03
8043602	NCAPH	non-SMC condensin I complex, subunit H	NM_015341	8.32	2.69E-03
7960874	C3AR1	complement component 3a receptor 1	NM_004054	8.40	1.31E-04
7989647	KIAA0101	KIAA0101	NM_014736	8.64	5.67E-03
7994109	PLK1	polo-like kinase 1 (Drosophila)	NM_005030	8.88	4.74E-03
8102643	CCNA2	cyclin A2	NM_001237	8.96	9.88E-03
8108301	KIF20A	kinesin family member 20A	NM_005733	9.00	9.34E-03
7982889	NUSAP1	nucleolar and spindle associated protein 1	NM_016359	9.10	5.85E-04
7929334	CEP55	centrosomal protein 55kDa	NM_018131	9.21	5.34E-03
8045688	TNFAIP6	tumor necrosis factor, alpha-induced protein 6	NM_007115	9.38	5.91E-03
8155214	MELK	maternal embryonic leucine zipper kinase	NM_014791	9.57	2.21E-03
8086600	CCR1	chemokine (C-C motif) receptor 1	NM_001295	9.75	1.70E-03
8054580	BUB1	BUB1 budding uninhibited by benzimidazoles 1 homolog (yeast)	NM_004336	9.81	2.25E-03
8106743	VCAN	versican	NM_004385	9.82	1.36E-03
7982757	CASC5	cancer susceptibility candidate 5	NM_170589	10.08	3.79E-04
8014974	TOP2A	topoisomerase (DNA) II alpha 170kDa	NM_001067	10.63	4.29E-03
8168749	SRPX2	sushi-repeat-containing protein, X-linked 2	NM_014467	10.65	6.77E-03
8124388	HIST1H3B	histone cluster 1, H3b	NM_003537	11.79	1.82E-03
7990345	SEMA7A	semaphorin 7A, GPI membrane anchor (John Milton Hagen blood group)	NM_003612	12.12	4.17E-03

8124440	HIST1H3G	histone cluster 1, H3g	NM_003534	12.20	3.02E-03
7923086	ASPM	asp (abnormal spindle) homolog, microcephaly associated (Drosophila)	NM_018136	14.94	8.38E-03
8061579	TPX2	TPX2, microtubule-associated, homolog (Xenopus laevis)	NM_012112	15.24	3.25E-03
7937020	MKI67	antigen identified by monoclonal antibody Ki-67	NM_002417	15.75	4.12E-03
7979307	DLGAP5	discs, large (Drosophila) homolog-associated protein 5	NM_014750	16.78	2.65E-03
8040223	RRM2	ribonucleotide reductase M2 polypeptide	NM_001034	18.56	2.09E-03
7974404	CDKN3	cyclin-dependent kinase inhibitor 3	NM_005192	21.50	8.28E-03